中图分类号：TE341　　单位代码：10425

学　号：LS1202004

中国石油大学

# 硕士学位论文

China University of Petroleum Master Degree Thesis

# 低渗油藏注气提高采收率技术筛选：以辽河油田齐 131 块为例

# Screening of Gas Injection Techniques for IOR in Low Permeability Reservoirs: Case Study of Q131 block in Liaohe Oilfield, China


学科专业：油气田开发工程

研究方向：油气田开发理论与系统工程

作者姓名：EZEKIEL, JUSTIN CHIMA

指导教师：任韶然 教授


二〇一四年十二月

# Screening of Gas Injection Techniques for IOR in Low Permeability Reservoirs: Case Study of Q131 block in Liaohe Oilfield

A Thesis Submitted for the Degree of Master

**Candidate: Ezekiel, Justin Chima**

**Supervisor: Prof. Ren Shaoran**

College of Petroleum Engineering
China University of Petroleum (East China)

# 关于学位论文的独创性声明

本人郑重声明：所呈交的论文是本人在指导教师指导下独立进行研究工作所取得的成果，论文中有关资料和数据是实事求是的。尽我所知，除文中已经加以标注和致谢外，本论文不包含其他人已经发表或撰写的研究成果，也不包含本人或他人为获得中国石油大学（华东）或其它教育机构的学位或学历证书而使用过的材料。与我一同工作的同志对研究所做的任何贡献均已在论文中作出了明确的说明。

若有不实之处，本人愿意承担相关法律责任。

学位论文作者签名：_____ 日期： 年 月 日

# 学位论文使用授权书

本人完全同意中国石油大学（华东）有权使用本学位论文（包括但不限于其印刷版和电子版），使用方式包括但不限于：保留学位论文，按规定向国家有关部门（机构）送交学位论文，以学术交流为目的赠送和交换学位论文，允许学位论文被查阅、借阅和复印，将学位论文的全部或部分内容编入有关数据库进行检索，采用影印、缩印或其他复制手段保存学位论文。

保密学位论文在解密后的使用授权同上。

学位论文作者签名：_____ 日期： 年 月 日

指导教师签名：_____ 日期： 年 月 日

# 摘 要

辽河油田 Q131 区块属于低渗水敏轻质油藏，原始地层压力 33.4 MPa， 油藏温度 98-112℃，地质储量（OOIP）253 万 $m^3$， 地层原油粘度 0.5 mPa.s。其特征是油层较厚、地层倾角较大，但地层能量不足，初期压力衰竭开采产量较低。由于渗透率低及水敏严重，后期水驱也未收到成效，目前注水困难，注不进采不出”的矛盾突出。因此，该区块正在考虑实施注气提高采收率技术。

注气已经成为一种有效的提高采收率方法，其原理主要在于增加或保持地层压力，提高驱油和波及效率，从而提高原油采收率。根据气源情况，有三种注气技术可以应用于Q131区块：**注空气、注 $CO_2$ 以及注 $N_2$**。本研究针对 Q131 工况，考虑了注气高效重力稳定驱替方式在 Q131 应用的优势，在不同注气技术在目标区块提高采收率机理分析的基础上，对三种技术的技术和经济可行性进行了分析。

论文对目标区块的生产历史和及实时数据进行了总结分析，并评估了在本区块进行注气提高采收率的可行性。结合理论分析、注气提高采收率机理、现场经验、室内试验研究、PVT 分析和油田生产数据历史拟合，运用 CMG-STARS 数值模拟软件，建立三种注气技术应用的油藏数值模拟模型。然后根据注入不同气体对保持地层压力、提高采收率、经济性、安全性等的影响进行筛选。

对于注空气工艺，在实验基础上建立低温氧化动力学模型并应用于油藏模拟中。注空气低渗岩心驱替实验表明注空气可以得到比水驱更高的采收率，并且其采收率随着地层倾角的增加而增加。温度在 130-170° C 的轻质油低温氧化实验表明，油层内的产生的自发低温氧化反应能完全消耗 $O_2$ 并且 $CO_2$ 转换率高达 58%。

油藏数值模拟结果表明，受注入井位置和数量限制，气体注入速率及注气量是影响原油产量的重要因素。累积产油量随着气体注入速度和注入量增加而增加，并有注入量的最优值。注空气过程中，在模拟的注入量下生产井未没有出现 $O_2$ 突破的现象。以单井 30000$m^3$/day 的速度向地层中注入空气、$CO_2$ 和 $N_2$ （4 口注入井）30 年，原油采收率分别可达到 35%, 36.5%, 35.5%，其中注入 $CO_2$ 的开采效果最好。气体早期突破及油井产出气油比太高是注气工艺的重要问题，关闭的高气油比井是降低气体产出的有效手段。敏感性分析表明，在维持相同注入量下，但采用关闭高气油比油井的方法降低气体产出量，其 20 年的注入空气、$CO_2$ 和 $N_2$ 的原油采收率可分别达到 33.5%, 36%, and 34%，使得注气项目具有更高的经济性。

初期的经济性和安全性分析也证明三种注气技术都具有可行性和经济性。其中，由于操作成本低，注空气成为三种方法中最具前景的方法。此外，详细讨论了不同注气技术安全性和防腐问题，也对低渗油藏更有效开发提出了建议。

**关键词：**注气；提高采收率；数值模拟；经济安全性评价。

**Screening of Gas Injection Techniques for IOR in Low Permeability Reservoirs: Case Study of Q131 block in Liaohe Oilfield**

Ezekiel, Justin Chima (Oil and Gas Field Development Engineering)

Directed by Prof. Ren Shaoran

# Abstract

The targeted oil reservoir (Q131 block) is in Liaohe oilfield, Northeast of China, which is featured with light oil, very low permeability and sensitive to formation water, but with thick oil layers and large dip angle. The original reservoir pressure is of 33.4 MPa, reservoir temperature of 98-112 °C, and the OOIP is $2.53 \times 10^6$ $m^3$. The viscosity of crude at reservoir condition is of 0.5mPa.s. Low primary production and failed water flooding experience have shown that the sweep efficiency and hence oil recovery factor in the block is very low due to lack of reservoir energy and poor water injectivity as a result of the low permeability and high heterogeneity of the reservoir block. Gravity Stabilized gas injection method has been optioned as an alternative tertiary improved oil recovery (IOR) technique to increase and/or maintain reservoir pressure, increase sweeping and displacement efficiencies to improve oil recovery. For this purpose, three different gas injection techniques, namely **Air injection, Carbon dioxide ($CO_2$) injection and Nitrogen ($N_2$) injection** are carefully selected in this study to be investigated and screened, as possible IOR methods for application in the low permeable Q131 light oil block.

Real-time field data from this oil block were reviewed and summarized to evaluate feasibility of gas injection IOR technologies. The feasibility study of using these 3 gas injection methods for IOR was combined with literature review, theoretical analysis, knowledge of mechanisms of gas injection techniques, field application experiences, laboratory experimental studies, PVT analysis, history matching of the field's production data, building a generic reservoir static model and reservoir numerical simulation of the 3 different gas injection techniques using the compositional CMG-STARS simulation software. Further work is carried out on screening the corresponding effects of the injected gases on increasing reservoir pressure, improving oil recovery, project economics, and their associated potential safety, corrosion and risk factors

For the air injection process, kinetic models of low temperature oxidation (LTO) reactions for the air injection process were designed through laboratory experiments and used in the reservoir simulation study. The displacement experiments of air flooding indicate that air injection can achieve

relatively higher oil recovery than water injection in the block and the oil recovery increased proportionally with increasing dip of the reservoir. The LTO experimental results over a temperature range of 130-170°C of a typical light oil indicate that LTO reaction is effective to completely consume $O_2$ and have a high $CO_2$ conversion rate of about 58%.

The results of the reservoir numerical simulation study show that the cumulative produced oil increases as the gas injection rate increases, up to an optimum level and no oxygen breakthrough was observed at the production wells. For a 30 years period of injection using a base case 30000m$^3$/day of gas injection rate (4 injectors), an incremental oil recovery factors of 35%, 36.5%, 35.5% of OOIP were achieved in air, $CO_2$ and $N_2$ injection simulations respectively, with $CO_2$ having the best production performance. Early gas break-through and high GOR in producers are important factors to influence the gas injection performance. Sensitivity study indicates that shut-in of wells with high GOR can effectively reduce gas production, and a better reservoir performance of incremental oil recovery factors of about 33.5%, 36%, and 34% OOIP can be achieved for the respective gas injections in just an average period of 20 years. This is very favorable to the project economics.

Preliminary economic and safety screening analyses, also confirmed that the 3 injection techniques are feasible and they all are profitable, i.e. positive net profit value, with air injection proving to be the most attractive of the three methods in terms of net profit due to its low cost of operation. Safety operations and corrosion controls of the different gas injection techniques are discussed in details and some recommendations are also provided for better IOR process in low permeability oil reservoirs.

**Keywords:** Gas injection, IOR, numerical simulation, economic and safety assessments.

# CONTENT

# CHAPTER 1: INTRODUCTION

## 1.1 General Introduction

Enhanced Oil Recovery (abbreviated EOR) is a generic term for techniques for increasing the amount of crude oil that can be extracted from an oil field. Enhanced oil recovery is also called **improved oil recovery (IOR)** or tertiary recovery. Using EOR, 30 to 60 percent or more of the reservoir's original oil can be extracted, compared with 20 to 40 percent using primary and secondary recovery. Gas flooding is a general term for injection processes that introduce miscible, near miscible or immiscible gases into the reservoir, and it is presently the most-commonly used approach in enhanced oil recovery (Thomas, 2008). A miscible displacement process maintains reservoir pressure and improves oil displacement because the interfacial tension between oil and water is reduced which allows for total displacement efficiency and invariably increases ultimate recovery factor of any field. Gases used include $CO_2$, natural gas, and nitrogen. The fluid most commonly used for miscible displacement is carbon dioxide because it reduces the oil viscosity and is less expensive than liquefied petroleum gas. Immiscible displacements (in the cases nitrogen flooding in low-pressure reservoirs and recently flue gas generated during air injection) are not as efficient as miscible displacements but may still recover oil by swelling, viscosity reduction, permeability increase, or pressure build up; all of which also lead to improved oil recovery.

Three (3) different techniques of gas injection, namely **Air injection, Carbon dioxide $CO_2$ injection and Nitrogen $N_2$ injection** is currently being investigated as possible improved oil recovery (IOR) methods in a target low permeable Q131 oil block in Liaohe oilfield located in the Liaoning Province, Northeast of China. Large oil reserves have been discovered in the thick argillaceous sandstone Q131 block reservoir with very low permeability (about 10mD), dipping at an angle of 21° NE, featured with light oil (about 35°API) at depth of >3000m, relatively high reservoir pressure and temperature (~35MPa and 98˚C) and low oil viscosity (<0.5mPa.s). Primary production and limited water flooding experience have shown that the recovery factor in these reservoirs is very low due to lack of reservoir energy and poor water injectivity. Gravity Stabilized gas injection method has been optioned as an alternative tertiary technique to maintain reservoir pressure and increase sweeping and displacement efficiency to improve the recovery factor. In this study, the feasibility of gas injection via air injection low and high temperature oxidation (LTO & HTO), $CO_2$ and $N_2$ injection processes are to be studied and verified.

Q131 reservoir rock properties and typical sandstone reservoir properties are used to build a generic reservoir static model. Numerical reservoir simulation studies are carried out using the

compositional CMG-STARS modeling software, in order to predict the reservoir performances under these 3 gas injection schemes and to optimize their operational parameters. Physical effects during the gas flooding such as reservoir heterogeneity, viscous fingering, gravity segregation, diffusive forces, capillary forces, compositional effects, fractures, etc. are considered in the simulation work to give a comprehensive study of the reservoir. The oxygen consumption rates at the current reservoir temperature, miscible, near-miscible, and immiscible displacement and IOR potentials at different optimization scenarios are assessed for the Q131 reservoir block. The project economic evaluations of these proposed gas injection IOR for the target block are analyzed; which is aimed at developing numerous scenarios to reduce capital and operational costs, and ultimately maximize net profit. Issues related to safety, risks and corrosion control during gas injection are also discussed in details.

This project focuses more on the numerical simulation studies of gas flooding of the Q131 block, and most results/information used in the numerical simulations are gotten from the various experimental analyses carried out on the Q131 reservoir rock and contained fluids.

## 1.2 Background of the Study

During oil and gas production, it has been observed that there is still a large quantity of hydrocarbon remained in the un-swept zone of the reservoir after the primary recovery stage, during which the reservoir natural energy, i.e. from pressure drawdown, gas expansion or gravity drainage, is sufficient to support the oil production from the reservoir (Dake, 2004). When the reservoir pressure can no longer sustain an economical production, an external compactible fluid is injected into the reservoir in order to provide extra pressure support and to assist with the displacement of the oil towards the producer. The recovery factor of primary recovery stage is about 10%; while the secondary recovery, it increases by 15% to 40%. After secondary recovery process, different methods can be employed to modify the reservoir or fluid's characteristics to enhance the oil recovery after the reservoir's energy becomes insufficient to support the production.

A considerable portion of current world oil production comes from mature fields and the rate of replacement of the produced reserves by new discoveries has been declining steadily over the last few decades. To meet the growing need for economical energy throughout the world, the recoverable oil resources in known reservoirs that can be produced economically by applying advanced IOR technologies will play a key role in meeting the energy demand in years to come.

This research presents a comprehensive application of gas injection IOR techniques (namely air injection, $CO_2$ and $N_2$ gas injection) using the reservoir simulation approach and an economically

screening analysis of the different methods including increased cumulative oil produced, cost of unit oil produced, prospect revenue generated and the risks involved. The emphasis of this research is on the Q131 block of Liaohe oil field. Real-time field data from this field is reviewed and summarized to evaluate feasibility of gas injection IOR technologies where water injection has failed to push the oil to the producing wells efficiently because of the low permeability of the reservoir rock containing the oil. Gas injection option is widely accepted in this field because firstly, the oil is light and thus can easily be driven by the injected gases immiscibly and also by miscible displacement. Secondly, the reservoir block has a high dip of 21°NE which will be favorable for gas-assisted gravity segregation drive. Gas injection has proven to be an effective IOR technique in many oil fields with low permeability reservoirs (Manrique E. et al, 2010). IOR potential or incremental oil recovery depends on achieving improved gas sweep and favorable oil/gas relative permeability during gas injection process. Laboratory and field projects have showed that gas injection into oil fields with or without water flooding could yield a high recovery. $CO_2$ has been considered as an effective injectant for IOR due to its high miscibility with oil, and $CO_2$ from natural sources has been used all over the world. Likewise, there have been also many successful field projects of $N_2$ and air injections in recent years (Kumar V.K. et al 2007; 2008; Gutierrez D. et al 2008b). For many mature fields, the application of gas injection is limited by gas availability and cost. In the last few years, the increase in the price of crude oil and gas coupled with a stable demand and declining production, has made IOR a favorable option. It is also proposed that $CO_2$ can be injected into oil reservoirs as an option to reduce the greenhouse gas emissions, along with the motive to improve oil recovery.

In this proposed research, the potential of various gas injection techniques are investigated for application in a low permeability oil reservoir in Liaohe oilfield, Eastern China. A real reservoir model of Q131 block of Liaohe oilfield is adopted for reservoir simulations using an advanced compositional and thermal simulator. An improved Corey Correlation of relative permeability is introduced in the simulation to deal with the miscibility effect between oil and injected gases. The anticipated increase in oil production in applying these various gas injection scenarios are simulated and compared economically. Also the safety and risk assessments are analyzed and discussed in details.

## 1.3 Statement of Problem

Liaohe oilfield is located in the Northeast of China, in which oil reserves have been discovered in large economical quantities. Q131 reservoir block is one of the economically viable blocks of the

Liaohe oilfield with high oil reserve of 210 x $10^4$tons, with an effective reservoir thickness of 41.9m and disadvantaged with very low permeability (10mD). Low primary production and failed water flooding experience have shown that the sweep efficiency and hence recovery factor in this block is very low due to lack of reservoir energy and poor water injectivity as a result of the low permeability. Gas injection has been optioned as an IOR technique to maintain reservoir pressure, increase sweeping and displacement efficiencies and improve the recovery of oil. Laboratory and numerical reservoir simulation studies are to be conducted in order to predict the reservoir performance under the near miscible $CO_2$ flooding and immiscible air and $N_2$ flooding schemes with the goal of optimizing oil production from the block. The oxygen consumption rates at prevailing reservoir temperature for the low temperature oxidation (LTO) process of air injection and IOR potentials using the 3 different injection techniques are to be assessed for the target block. In this study, the feasibility of different gas injection schemes are studied, effectively design best optimization schemes and compare their results based on increased oil recovery, economics and safety criteria.

## 1.4 Objectives of the Study

This gas injection-IOR case study objectively shows the technical viability of the three selected gas injection techniques as efficient methods of improved oil recovery particularly in a deep, high pressure, low permeability Q131 oil reservoir where water injectivity is limited and other recovery processes become unsuccessful and uneconomic. It focuses on effective gas injection strategies to optimize the oil recovery.

In summary, the technical objectives of this study are to:

(1) Investigate and improve our understanding of the mechanisms and feasibility of miscible, near-miscible, immiscible displacement of the different gas injection techniques by conducting phase behavior model (compositional) construction and appropriate reservoir simulation using CMG software package.

(2) Design kinetic models of LTO reactions for the air injection process through laboratory experiments and use the results in the reservoir simulation study to predict oxygen consumption in the reservoir, examine the reaction schemes, IOR mechanisms, and the thermal effect of oxidation reactions occurring during the air injection process

(3) Determine for the target Q131 block, by means of reservoir numerical simulation studies, the best IOR optimization scheme(s) using various kinds of optimization parameters of gas flooding including the gas injection rate, injection pattern, injection pressure and oil production rate, etc. to achieve increase in oil production in the low permeability reservoir of Q131 block.

Also, run different sensitivity analyses to determine the effects of the different variables on the IOR ability of each of the proposed injection gases. The corresponding results are compared, screened and analyzed economically.

(4) Analyze the project economics and technical challenges of using the proposed gas injection techniques. It is eminent to note here that the screening, selection and design of a gas IOR process depend on the IOR potentiality, gas availability and project economics.

(5) Business-wise, the study aims to improve oil recovery at the most minimal cost to maximize profit by selecting the best gas injection scheme.

(6) Address and reduce the effects of various issues related to safety, risks and corrosion control during gas injection processes.

## 1.5 Significance of the Study

With the availability and accessibility to the gas sources (air, $CO_2$ and $N_2$), it will be shown that a significant increase in the sweep and displacement efficiencies and ultimately the recovery factor of the low permeable Q131 reservoir block will be achieved using the most favorable recovery optimization scheme to be studied and developed in this research work from the use of experimental results and numerical reservoir simulation tools. Thus, providing more profit to the operating company that own the Q131 block, provide more detailed technical knowledge in the field of gas injection IOR techniques, discuss major safety strategies in gas injection method of IOR, and in a larger scale develop new study methodologies and ideas in the area of oil and gas field development. Also the economic and technical challenges of gas injection using different gas sources are analyzed and compared for future application in similar fields with low permeability to save cost and maximize profit.

## 1.6 Research Content and Technical Route

Combining with literature review, theoretical analysis, mechanisms of gas injection techniques, field application experiences, laboratory experimental studies, PVT analysis, history matching of the field's production data, and reservoir simulation of 3 different gas injection techniques (namely CO2, air and N2) in low permeability light oil reservoir. Further work is carried out on screening the corresponding effects of the injected gases on improving oil recovery, project economics, and the associated potential safety and risk factors. Fig. 1.1 shows the technical route employed in this study.

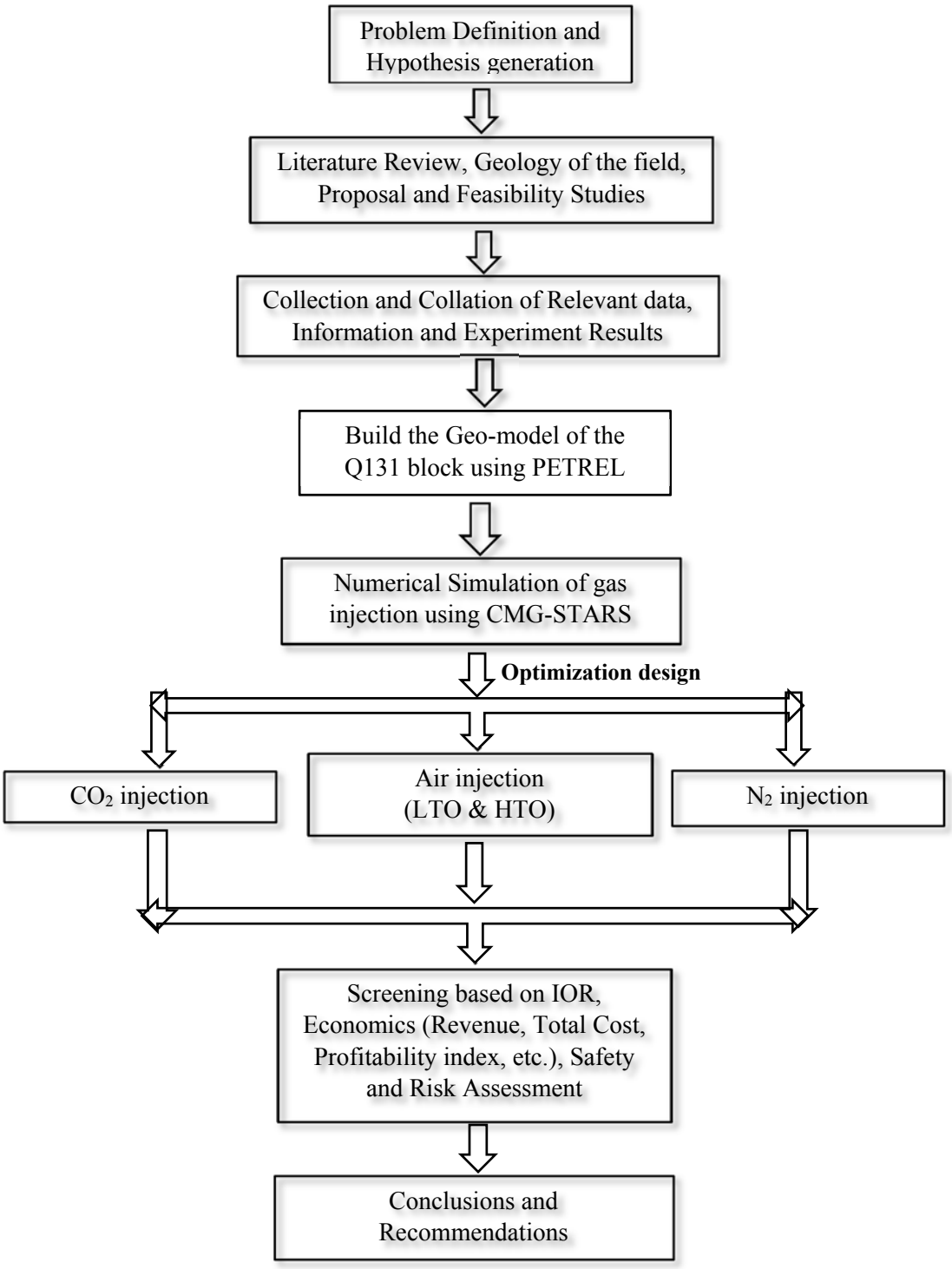


**Figure 1.1: Technical Route of the Study.**

## 1.7 The Geology of Liaohe Sub-Basin in the Bohai-Bay Basin

The study area (in Liaohe sub-basin) is located in the Bohai-bay (or locally called Bohaiwan) basin, which is shown embedded in a map of China in Figure 1.2. Liaohe oilfield is located in the plain of Liaohe middle-lower reaches, which is an important part of Bohai Gulf oil province (Figure 1.3).

### 1.7.1 Geographic Setting

The Bohaiwan basin is situated in Hebei, Henan, Liaoning, and Shandong Provinces of Eastern China (Fig. 1.2). Approximately 25 percent of the basin is located beneath Bohai Bay, a shallow marine embayment of the north end of the Yellow Sea. North Korea is within 200 kilometers (km) of the northeast end of the basin and Mongolia is within 550 km of the northwest end. A low-relief (<100 meters (m) above mean sea level) alluvial and coastal plain bordering Bohai Bay characterizes the present-day topography.

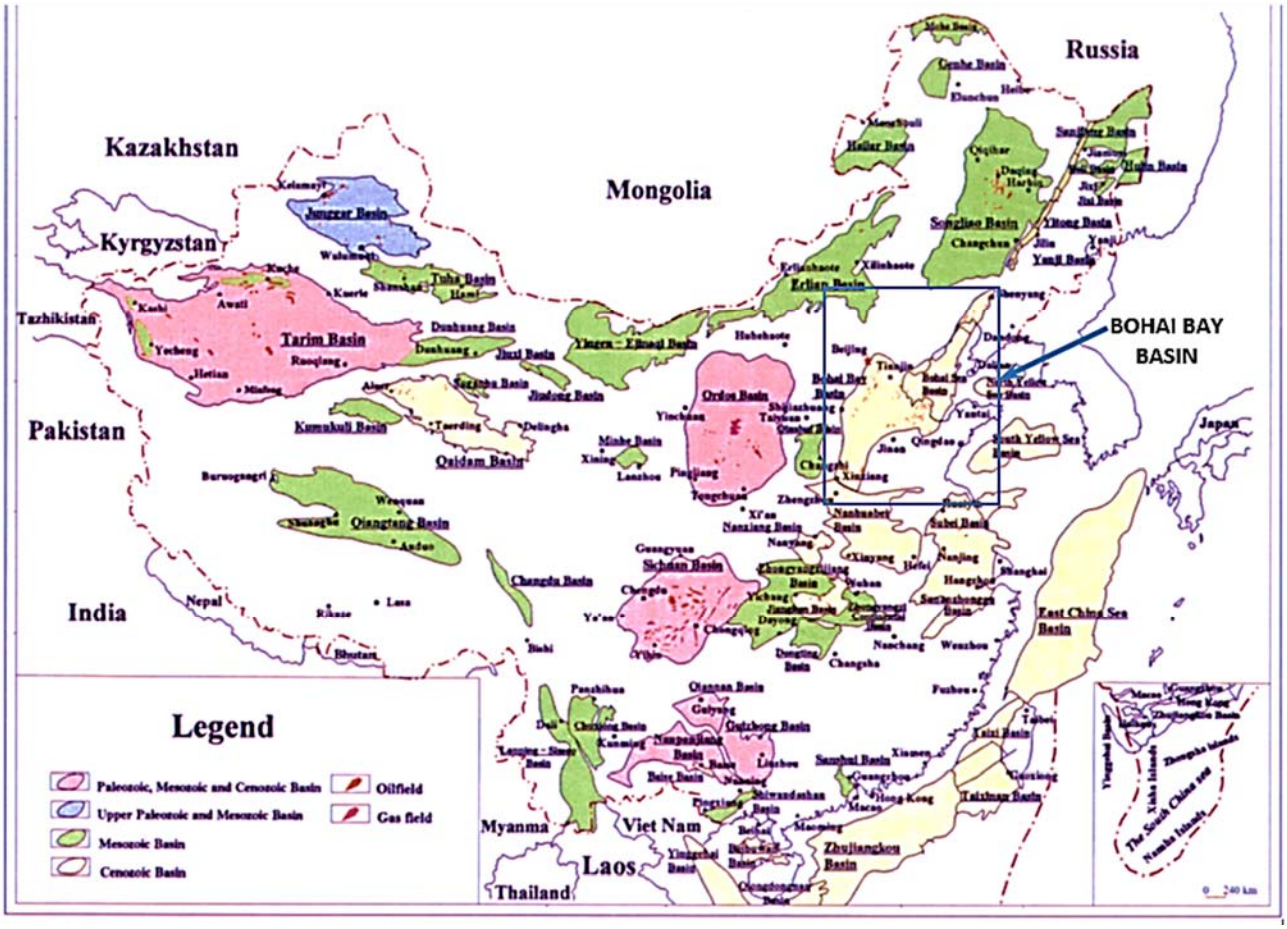


**Fig. 1.2: Distribution of hydrocarbon source rock in Chinese oil-gas bearing basins showing the location of Bohai Bay Basin.**

The Huang He (Yellow River) flows northeastward across the basin and empties its contents into the south end of Bohai bay, where it has built a delta. Several other large rivers flow across the basin, including the Liao He that empties into the north end of Bohai Bay. Surface air temperatures are hot (>20°C) in the summer and cold (<0°C) in the winter.

**Description of the Baohaiwan basin:** The assessment unit is characterized by oil and gas fields trapped in anticlines, fault blocks, and a variety of stratigraphic traps. Reservoirs consist of Tertiary lacustrine and fluvial sandstone. The fields are confined to six major sub-basins of extensional origin (Bozhong, Huanghua, Liaohe, Linqing/Dongpu, Jiyang, Jizhong), each having one or more pod(s) of active Eocene source rocks (Fig. 1.4). The Bozhong sub-basin is located in offshore Bohai Bay whereas the Jizhong, Linqing/Dongpu, and most of the Jiyang sub-basins are located onshore. The Huanghua and Liaohe sub-basins have large offshore parts. The giant Shengli field complex is located in the Jiyang sub-basin (Ryder, 2012)

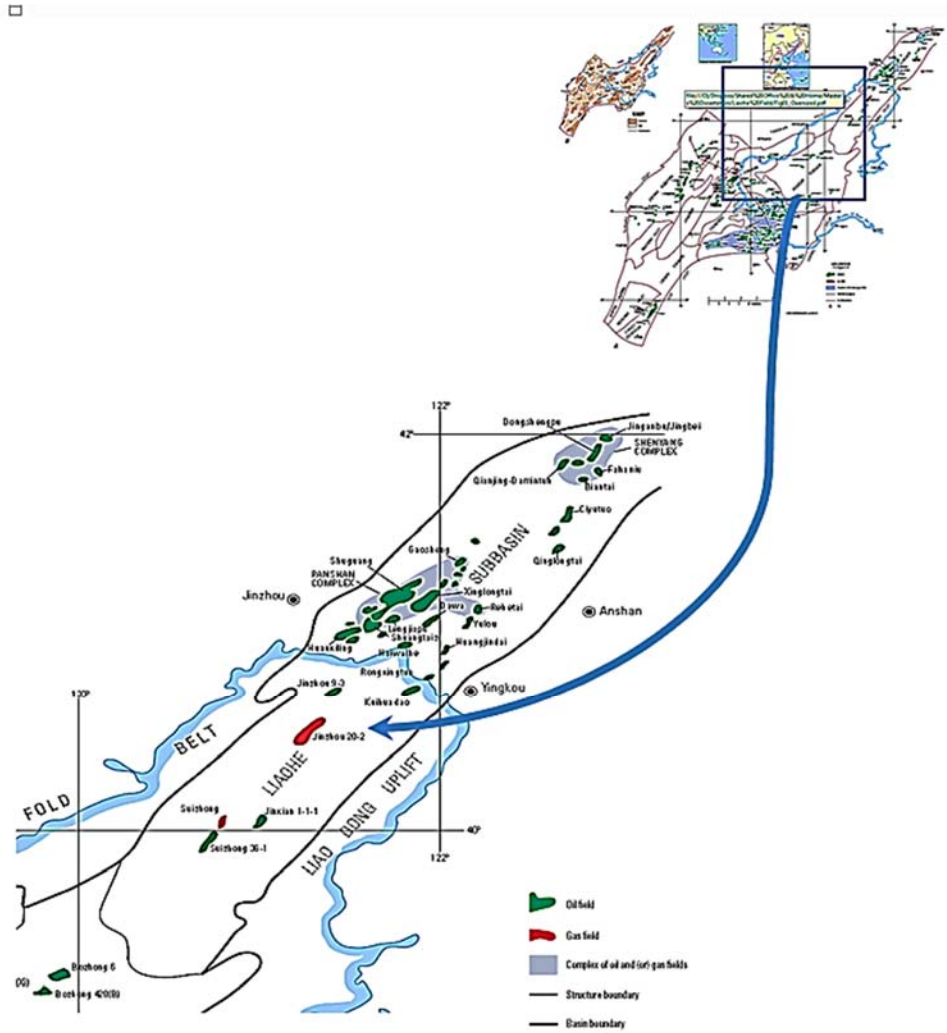


**Fig. 1.3: Maps of the Bohaiwan basin showing selected oil and gas fields and enlarged Liaohe sub-basin. Modified by Allen et al. (1997)**

### 1.7.2 Geologic Setting

**Source Rocks:** Source rocks are deep-water lacustrine shale and mudstone of Eocene and Oligocene age. The dominant source rock is the upper Eocene part of the Shahejie Formation (Member 3) as seen in Fig. 1.3. Additional source rocks are the lower Eocene part of the Shahejie Formation (Member 4), Oligocene part of Shahejie Formation (Member 1), and Eocene Kongdian Formation (Member 2). The thickness of Member 3 of the Shahejie Formation in each sub-basin is approximately 1,000 m and its total organic carbon (TOC) values range from about 1 to 4.5.

**Reservoir Rocks:** Reservoir rocks are deep-water lacustrine turbidite, lacustrine deltaic, and fluvial sandstone units of Tertiary age. These sandstone reservoirs occupy the Eocene part of the Shahejie Formation (Members 2, 3), Oligocene Dongying Formation, Miocene Guantao Formation, and Miocene/Pliocene Minghuazhen Formation. Typically, the reservoir sandstones are feldspathic arenites.

**Traps and Seals:** The major traps are rollover and compaction anticlines and fault blocks of extensional origin. Stratigraphic traps (lithologic, onlap, and unconformity varieties) account for about 25 percent of the traps. Regional seals consist of the upper parts of the Dongying and the Bohaiwan basin (3127; USGS World Energy Assessment Project numeric code) in northeastern China is the largest petroleum-producing region in China (Klett et al, 1997). The basin consists of six rift-controlled subbasins (Liaohe, Bozhong, Huanghua, Jiyang, Jizhong, and Linqing/ Dongpu1), all of which produce oil and gas. The general structural styles of the subbasins and adjoining uplifts in the Bohaiwan basin are shown on the geologic cross sections in Figure 1.4. In addition, more than 50 smaller structural depressions (sags), commonly flanked by tilted fault-block uplifts (buried hills), are recognized throughout the basin (Allen et.al., 1997).

A Paleogene lacustrine black shale and mudstone unit (Fig. 1.4) represent one of several stages of maximum expansion of the sub-basin-centered lakes, is the major source rock. Paleogene and Neogene non-marine sandstones constitute the major reservoir rocks, especially where they are interbedded with lacustrine black shale and mudstone source rocks. Also, Paleozoic and Middle to Late Proterozoic marine limestone and dolomite and highly weathered Archean crystalline basement rocks are important reservoirs. (Fig. 1.4).

Technically, each of the 6 sub-basins constitutes a separate total petroleum system because the sub-basins are separated from one another by structurally high fault blocks (horst blocks) that are largely impervious to the migration of oil and gas.

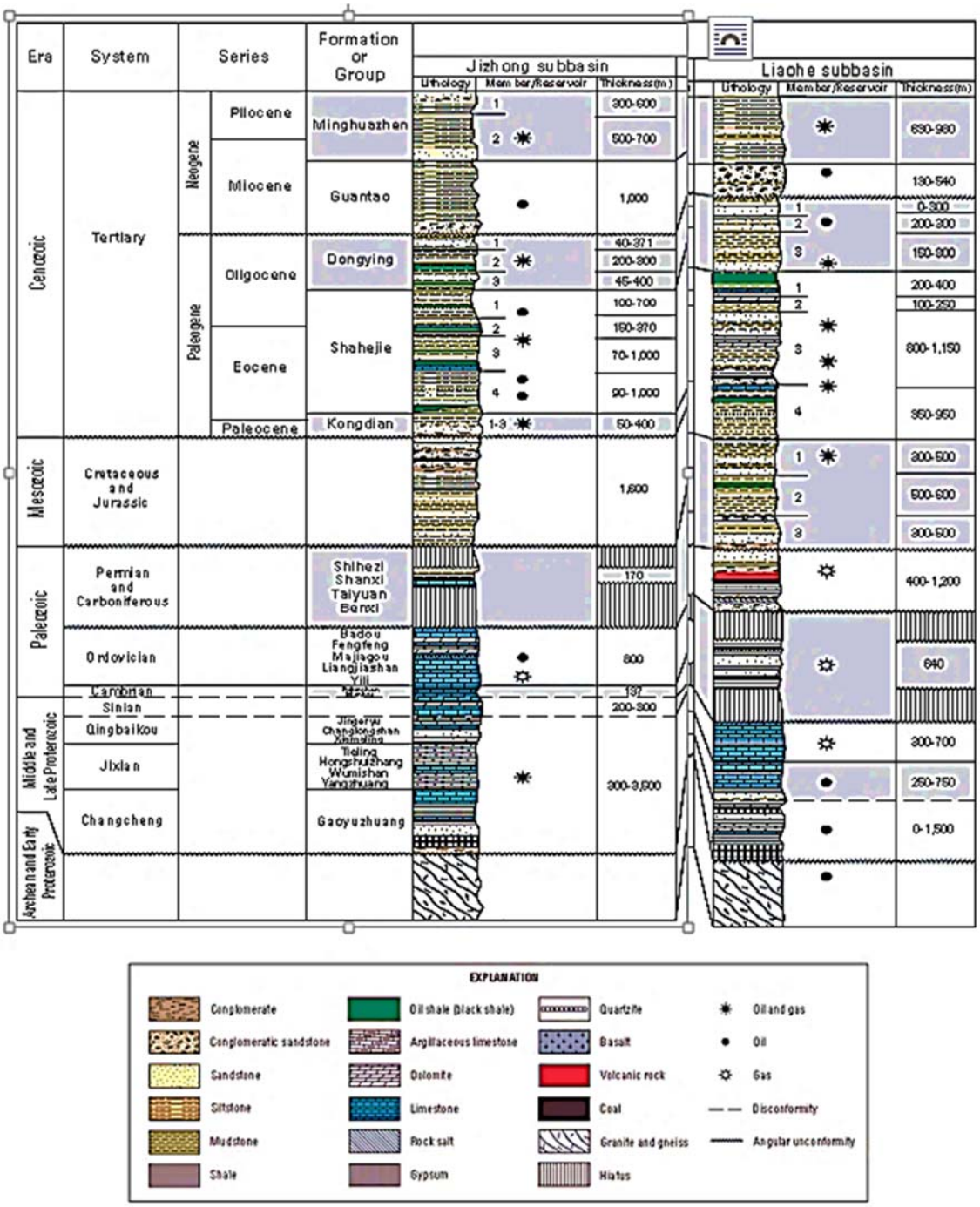


**Figure 1.4: Stratigraphy of the Liaohe sub-basin in the Bohaiwan Basin (Chang, 1991).**

### 1.7.3 Tectonic Setting

The Bohaiwan basin is a large (~200,000 km$^2$) intracratonic rift basin composed of Precambrian, Paleozoic, Mesozoic, and Tertiary sedimentary rocks underlain by Precambrian crystalline basement rocks and overlain by unconsolidated Quaternary sediments. The basin is largely surrounded by mountain ranges and uplifts composed of a variety of Precambrian, Paleozoic, and

Mesozoic rocks. Complex block faulting in the subsurface has little, if any, surface expression. The length of the basin between its narrow southwest and northeast extensions is approximately 1,100 km and the width of the basin at its rhomboid-shaped central area is approximately 400 km (Figs. 1.2 and 1.3). The basin is underlain by Archean and Early Proterozoic metamorphic rocks that constitute the North China (Sino-Korean) block or craton (Tian et. al., 1992).

A complex basin evolution involved the following events:

(1) Several stages of Proterozoic and early Paleozoic shelf sedimentation (~1,700 to 458 Ma);

(2) Early to middle Paleozoic regional sub-aerial exposure and erosion (~458 to 320 Ma);

(3) Late Paleozoic foreland basin sedimentation and contractional deformation (~320 to 250 Ma);

(4) Mesozoic contractional deformation, extensional deformation, and volcanism (~240 to 230 Ma and ~160 to 70 Ma);

(5) Early Tertiary (Paleogene) extension and rifting (~55 to 24 Ma); and

(6) Late Tertiary (Neogene) to recent post-rift subsidence (~22 Ma to present) (Allen et al., 1997).

Previous work (Compiling Group of Petroleum Geology of Liaohe Oilfield, 1993) has investigated the tectonic development and depositional filling in a number of sags of the Bohai Basin (Fig. 1.5). The characteristics of the fault basins are summarized as follows:

1) The tectonic styles are relatively simple and mainly include graben, half graben, or complex graben. Of these, half graben, or complex graben. Of these, half graben is the most common style. The control faults and boundary faults are mainly normal faults or syndepositional faults.

2) The multi-eposidic tectonic evolution involved an early rifting (faulting) stage related to extension and mantle uplift and a late post-rifting depression stage related to thermal decay and subsidence.

3) The faults were most active at the edge and within the basin. Episodic faulting controlled the depositional evolution as well as regular changes in the sediment filling of the basin.

4) A slope break belt, which was formed by the long-term activity of syndepositional faults, restricted the changes in the accommodation space for sediment filling and controlled the development of depositional systems as well as the distribution of sand bodies.

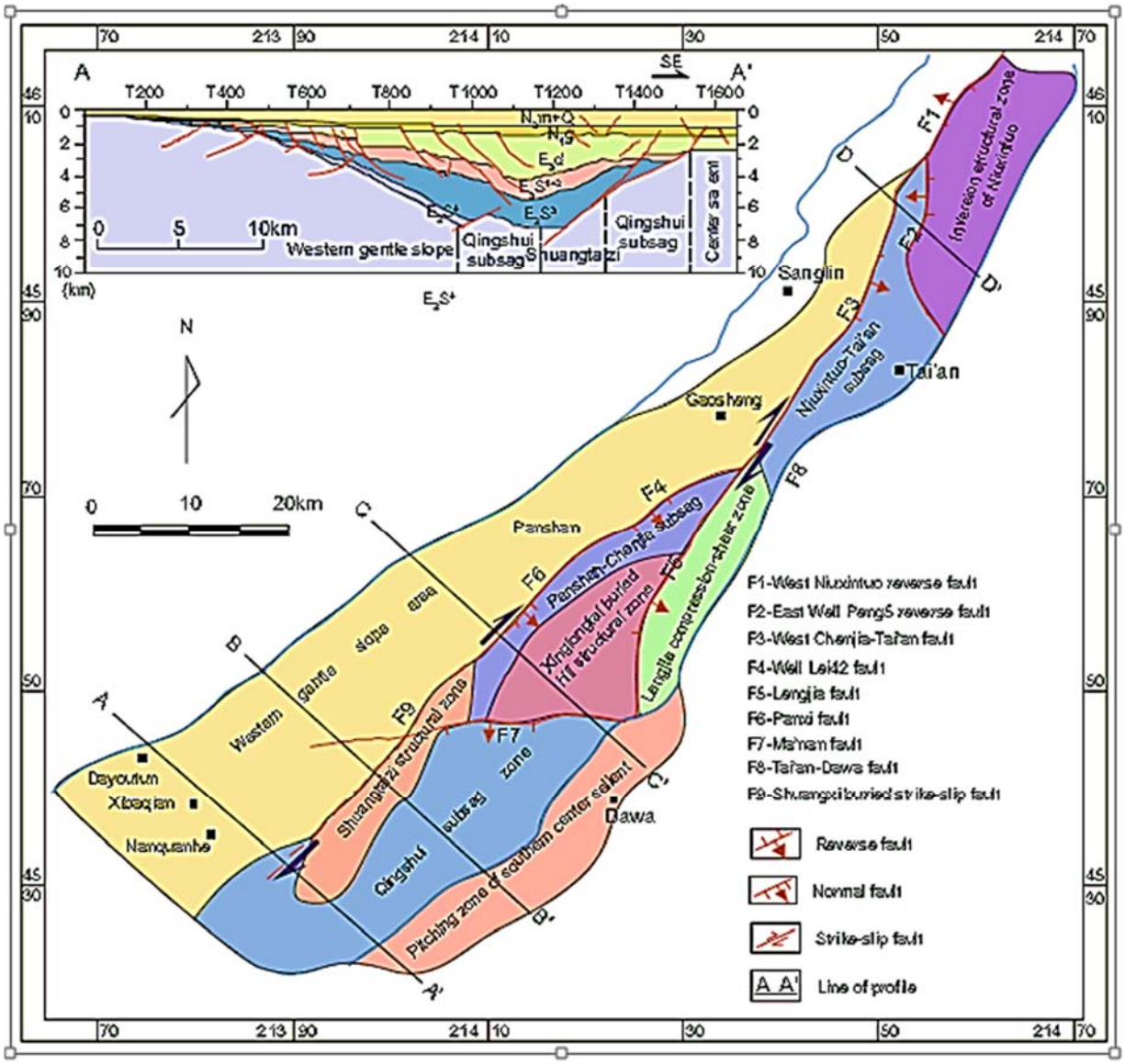


**Fig. 1.5: Tectonic Units and Division of the Fault Systems of the Western Liaohe Depression. (Yin and Nie, 1996; Allen et. al. 1997)**

### 1.7.4 History of Liaohe oilfield - Study Area

Oil was first discovered in the Jiyang subbasin in 1961 at the giant Dongxin field. In the early 1980s, exploration began in earnest in the Bohai Bay part of the Bohaiwan basin and resulted in oil and gas discoveries in the Bozhong (1951) and Liaohe (1954) sub-basins. Liaohe oilfield exploration and development cover an area of 112,800m$^2$. In Liaohe oilfield, oil reservoirs are distributed primarily in the plain of Liaohe middle-lower reaches and the eastern part of Inner Mongolia and the shoal of Liaodong bay.

In Liaohe oilfield, oil and gas exploration begun in 1955. The oil flow from well Xin 1 in Liaohe basin revealed the oilfield on 9th September, 1969. As a result of exploration over more than 30 years, 36 oilfields in various sizes have been found totally with $19\times10^8$ tons (t) proven OOIP and $670\times10^8$ $m^3$ OGIP. There have been 26 oilfields built up and developed and 9 production bases established, including Xinglongtai, Suguang, Huanxiling, Jinzhou, Gaosheng, Shenyang, Ciyutuo, Lengjia and Kerbqin. Now, Liaohe oilfield has established an annual oil production capacity of $1500\times10^4$ t. Since 1994, the production in Liaohe oilfield has been stabilized consecutively for the following years. It is ranked No.3 among all the oilfields in China and No.2 among the oilfields in China National Petroleum Company (CNPC). Liaohe oilfield is a super-giant oilfield dominated by heavy oil production with its proven heavy oil OOIP accounting for 50% of its total oil reserves, but the block of interest i.e. Q131 has light oil.

# CHAPTER 2: LITERATURE REVIEW

## 2.1 Literature Review of Air Injection

The first field pilot of air injection began in 1963 on Sloss Field in Nebraska (Parrish et al., 1974) and this process was first commercially introduced as a secondary recovery technique in the North and South Dakota portions of the Williston basin, (USA). It was started in 1979 and continues to be a technical and economic success (Fassihi et al., 1996; Kumar et al., 2006). Air injection in the Buffalo field reported to have recovered a total of 17.2 million barrels of incremental oil an equivalent of 9.4 percent of the OOIP (Gutierrez et al., 2008).

♣ **Literature Review on Air Injection Practices in China.**

There are also a few field pilots of air injection in China recently, mostly applying air and air foam techniques for IOR in reservoirs with relatively low and high permeability including Xinjiang, Shengli oilfields, etc. (Ren, S.R. et al, 2011).

Hongmin Yu et al (2008) in his air injection and air foam injection for IOR studies concluded that the crude oil of the Hu-12 Block in Zhongyuan oilfield has good LTO reaction characteristics, which can consume oxygen effectively in a short time at reservoir conditions. The presence of air foams may reduce the reaction rate at static conditions, while the air foam has little effect on oxidation at dynamic (flowing) conditions. Oxidation kinetics models were also derived for the oil and formation rock systems, which can be used in reservoir simulations.

Jiang Y et al. (2010) investigated the displacement mechanism of air injection in low-permeability reservoirs (permeability ranges from 0.2 to 1.0md, average permeability is 0.6md) through the method of combining physical simulation and numerical simulation. The results of research have proved air injection technique, which plays an active part in the exploitation of low-permeability reservoirs, can be used as an effective method to improve development effects and enhance oil recovery.

♣ **Literature Review on LTO Air Injection.**

In the 90s, the IOR team of the university of Bath (Greaves et al., 1999a; Ren et al., 2002) was the first to put forward the air injection low-temperature oxidation rate of oxygen consumption concept, using the designed high voltage, constant temperature static reactor (SBR), Crude oil static oxidation experiment was carried out to study the effects of factors such as temperature, pressure on the oxygen consumption, reaction rate and gas composition. They proved that low temperature oxidation reaction of crude oil is in line with the Arrhenius kinetics theory, and that pressure,

temperature, water content, and oil saturation can influence the reaction rate. If the oxidation reaction rate is too low, it will not be detected at the experimental temperature range.

**Ren, et al. 2002** carried out several sensitivity studies on LTO process of air injection and reported that:

a. Injection Rate Sensitivity: They presented that a high air flux not only increases the temperature in the reaction zone, but it also increases the velocity of both the thermal and gas displacement fronts, and the latter reduces the effect that the thermal front has on oil recovery.
b. Dip Angle Sensitivity: For a gravity drainage process, air can be injected at the crest of the reservoir, into the gas cap, or up-dip. The gas front stabilized by gravity pushes the oil column into the down-dip producer, achieving both high volumetric sweep and gas displacement efficiency. As the dip angle is decreased, oil breakthrough time is shortened.
c. Permeability and Oil Phase Viscosity: They showed that when gas breakthrough, oil production decreases. Oil production increases with the increasing permeability and lower oil viscosity. There is a significant reduction in oil production at a low kh/kv and high oil viscosity. This is because of lower oil mobility, lower effective sweep, and reduced displacement efficiency.
d. Initial Reservoir Temperature and Heat Loss: They stated that a low initial reservoir temperature delays the time at which a thermal zone is formed, particularly during the earlier stages of air injection. However, this has very little effect on the consumption of oxygen. As time increases, the temperature in the reaction zone rises to a higher level. The maximum temperature developed when there is no heat loss is greater than that when there was heat loss. The length of the heated zone (temperature higher than the original reservoir temperature) is shortened when compared to the case without heat loss.
e. Grid sizes in 3D Field Scale Simulation: The grid sizes used had little influence on the oil production profile. This indicates that the gas displacement process is not sensitive to the grid size, providing that no extreme transmissibility, or pore volume gradients, are created when there is reservoir heterogeneity.

Furthermore, they stated that the main problem concerning air injection is the oxygen in the air, which could lead to oil contamination (oxidation and emulsification), bacteria growth, corrosion and safety (explosion) problems both in injector and producer in case of oxygen breakthrough. Laboratory research and reservoir simulation has shown that, for a properly selected oil reservoir, oxygen can be completely removed by the LTO process, and there is a substantial separation between the reaction front and the gas displacement front (Ren S.R. et al., 2002). Therefore, air injection in light oil reservoirs can be viewed as conventional gas injection processes (such as $N_2$

or flue gas) as long as the oxygen is removed by spontaneous LTO reactions in the reservoir. They also conducted a simulation study in three stages: the reaction models were formulated based on results obtained from the SBR experiments and matching of oxidation tube experiments. Then, using a 2D cross-section base model to assess sensitivity. Finally, a 3D small-section field simulation was carried out. The thermal reservoir simulator, STARS (CMG, Calgary) and PVT software, WinProp (CMG, Calgary), were used in their study and several conclusions made. .

In the study of LTO process of air injection for light oil reservoirs of Greaves et al. (1998), showed that measurement of the rate of pressure reduction under static conditions can be used to monitor the oxygen consumption rate during reaction. A drop in pressure was normally observed during their test, due to oxygen being consumed by LTO reactions, and some gas dissolving in the oil. They also stated that the low temperature oxidation (LTO) process removes oxygen in the injected air, to produce displacement flue gas (mainly nitrogen and then $CO_2$) in the reservoir in order to achieve incremental IOR. All of the oxidation reactions are exothermic, producing heat, which increases the reservoir temperature at least locally in the formation, depending on the balance of heat generated and the rate of heat loss by conduction and gas convection. Spontaneous ignition, typically around 100-120°C for light oils at reservoir conditions may be triggered, resulting in high temperature oxidation (HTO or combustion), but only if a high air injection rate can be supplied. Otherwise, the LTO reaction mode will prevail. This flue gas displacement front formed in the reservoir is believed to drive the light oil faster than the high temperature front. More studies are being carried on this phenomena.

♣ **Literature Review on the Effects of Reservoir Minerals on Air Injection Kinetics.**

Reservoir minerals composition, clay minerals and metallic additives have an important influence on the oxidation thermo-kinetics of crude oil. It is known that actual reservoir cores have very complex composition, and contain various clay minerals such as illite, illite/smectite, smectite, kaolinite, and metallic additives. These ingredients have different catalytic effects on oil oxidation kinetics. Vossoughi et al. (1983) studied the effect of sand, silica and kaolinite on crude oil combustion, indicating that kaolinite had a catalytic and surface area effect on crude oil combustion/ cracking reactions, but sand had no effect. Castanier et al., (1992) indicated that water soluble metallic salts have catalytic effect on fuel deposition and iron/tin can increase the efficiency of the combustion, reducing the amount of oxygen. A study conducted by Jia et al., (2012) to determine the effects of different clay mineral types on oxidation kinetics of light crude oil and to understand the contribution of different kinds of clays on catalytic effect revealed that smectite is ranked first,

illite is ranked second followed by chlorite and kaolinite in the aspect of catalytic ability for crude oil oxidation.

♣ **Literature Review on Numerical Simulations of Air Injection.**

Sakthikumar et al (1995) simulated the process of HPAI as an isothermal immiscible nitrogen flood to assess the feasibility of air injection into a waterflooded light oil reservoir. The simulations were performed using SST's therm- a 3D compositional thermal simulator. Air injection process in the Maureen field was modeled as a miscible gas injection process by Fraim et al (1997). The simulator used in the study was a 3-D, 3 phase black oil simulator (any benefits from NGL stripping and production were ignored). Glandt et al (1999) designed their study to build a calibrated simulation model by matching Coral Creek's production history and to assess the recovery potential of HPAI in this field, they modeled the process as an isothermal flue gas flood with a 10 component, equation-of -state (EOS) model.

Based on a homogeneous single porosity reservoir model used in a light oil air-injection performance study by Adetunji et al., (2005), the following conclusions were arrived at:

a. The tighter the reservoir, the smaller the project life; recovery is accelerated in lower permeability reservoirs.
b. The tighter the reservoir, the lower the system temperature at the end of air injection.
c. The perforation profile has a great impact on the cumulative oil production. For optimum recovery, all hydrocarbon-containing layers should be perforated for production.
d. The cumulative oil production is independent of the cumulative amount of water injected before the start of air injection.

Ren et al (2002) conducted a simulation study in three stages: the reaction models were formulated based on results obtained from the SBR experiments and matching of oxidation tube experiments; then, using a 2D cross-section base model to assess sensitivity; finally, a 3D small-section field simulation was carried out. The thermal reservoir simulator, STARS (CMG, Calgary) and PVT software, WinProp (CMG, Calgary), were used in their study. The simulation results showed the increased cumulative oil recovered.

Kuhlman (2000) evaluated the predictions obtained from different simulation approaches for a viscous dominated (Horse Creek) and a gravity stable (West Hackberry) reservoir. The study used a thermal combustion model, a flue gas EOS model, and injection of reservoir gas in a black-oil model. Kuhlman concluded that a thermal model with at least six hydrocarbon components is preferred for modeling light-oil air injection and that EOS model can be used for hot, thick, very

light oil reservoirs but is not useful in cooler reservoirs and when low porosity is combined with low thickness or low API gravity, while, black oil models can predict the response to gas injection but should only be used as scouting tools. These conclusions were based on models that used the same grid block sizes for each approach, and that included up-scaled-kinetics for the thermal simulations. EOS simulations showed increased production when compared with the thermal simulations.

Pascual et al., (2005) constructed a simulation model using the RMS software in a layer cake structure of 50×50 cells areally of 56m×51m, and 13 vertical layers of approximately 5m thickness, resulting on a total of 21567 active cells. Properties population was performed with maps constructed in CPS-3 and the final geological model was export in ECLIPSE format to build a black simulation model. In the compositional simulation study, the experimental PVT data was imported into CMG's equation of state PVT software package WINPROP to regress a pseudo component compositional representation and generate a K-value compositional model and the experimental laboratory combustion tube profiles were imported into CMG visualization software for matching with simulation.

De Zwart et al., (2008) addressed the role that combustion plays on the incremental recovery of HPAI. In their study, the numerical simulations were conducted in a 3D model with real geological features and a reservoir simulator with dynamic gridding capabilities was used to capture more realistically the physics of the combustion front. Combustion and its associated temperature effects presented based on isothermal simulations and multi-component combustion runs result in a total desaturation of the air swept zones, and, furthermore, as the combustion front approaches the producer, medium molecular weight components (C7-C15) are transported and produced in the gas phase, thus significantly increasing peak production rates.

Van Batenburg et al (2011) presented a new robust semi-implicit method of nested dynamic local grid refinement, and which can be successfully implemented in a general purpose flow simulator, including simulation models with water-flooding, chemical-flooding, gas injection, and in-situ combustion. In this method, there is an additional condition on the completion of a time step, based on how well the grid fits the current solution, determining if the grid needs to be adapted and the Newton-Raphson process continued.

Reservoir simulation studies conducted by Akkutla and Yortsos (2002) suggest that variation in vertical permeability adversely affect the volumetric sweep. They have suggested that injecting water at the top of the oil column can improve oil production by reducing the effect of gas override.

Simultaneous water/gas injection or gas injection after in-situ combustion initiation was proposed in their studies.

Ren et al, (2002) investigated the effect of reservoir dip on the cumulative oil production through numerical simulation. They showed that, as the dip angle is decreased, oil breakthrough time is shortened, and this is also associated with earlier gas breakthrough. Oil production also decreases. There is little effect on the ultimate oil recovery when the dip angle is greater than 10°. Hence, large dip angle and low heterogeneity are all favorable factors for air injection. In the study, the results obtained from the SBR experiments using North Sea light oil samples show that the rate of LTO for the light oils investigated is independent of the total pressure and also oxygen partial pressure, i.e. when the amounts of oil is in excess, at low reservoir temperature.

♣ **Literature Review on Air Injection In-Situ Combustion.**

Field experiences and project designs by Germain, P. et al., (1997), indicate that spontaneous LTO reaction, leading to in-situ combustion, may occur in the field with relatively high reservoir temperatures (90- 120 °C) and pressures. However, this process is restricted to those oil candidates which exhibit a continuous adiabatic exotherm, i.e. will progress to combustion at a temperature greater than 300°C. On the other hand, if the adiabatic exotherm is discontinuous, this means that the oil will only undergo LTO at much lower temperatures. Also Germain, P. et al, in their subsequent publication on New Air Injection Technology for IOR Operations in Light and Heavy Oil Reservoirs, they introduced THAI – "Toe-to-Heel" Air Injection, is a new EOR process, which integrates advanced reservoir technology and horizontal well concepts, to achieve potentially very high recovery of heavy oil. It can also realize very substantial in situ upgrading by thermal cracking, producing upgraded oil to the surface. The process operates in a gravity stabilized manner by restricting drainage to a narrow mobile zone. This causes the flow of mobilized fluids to enter directly into the exposed section of a horizontal production well. The process can be operated as a co-process where the advantages of high thermal efficiency are required. This is achieved by concentrating the energy required for oil mobilization, recovery and thermal upgrading in the reservoir. Combined with clean technology design, THAI offers a pathway to future economic success for the heavy oil industry.

In the studies of Christopher C.A. (1995), he used an accelerating rate calorimeter (ARC) to screen light reservoir oils for continuous exothermicity. For light oils they found that about 20% were good candidates for propagating full in-situ combustion. This suggests that perhaps a majority of light oils will sustain only low temperature oxidation (LTO). Thus, when the primary objective is only

to generate nitrogen and carbon dioxide in situ, then a less intensive oxidation process, without combustion, is sufficient. The focus is therefore on a spontaneous LTO process, which can be applied in all light oil reservoirs with sufficiently high reactivity to react with (and consume) oxygen in the injected air. The end result is a gas drive recovery process, whereby the flue gas resulting from LTO reaction will effectively be used to provide the needed energy for production.

Ren, S.R. et al (2011), in their work stated that the air injection process for light oil reservoirs is quite different from that of traditional air injection processes for in-situ combustion (ISC), normally applied in heavy oil reservoirs. In the latter case, a vigorous high temperature oxidation (HTO) front, or combustion front, needs to be maintained by using a sufficiently high air flux. Also, artificial means of ignition have to be used in most cases to initiate the process. Oil recovery, in this case, relies on the heat generated by the combustion to reduce the viscosity of the heavy oil, combined with steam and flue gas drives. Air injection in a light oil reservoir can be viewed as a conventional gas injection process, so long as the oxygen in the infected air is removed efficiently in the oil formation. For this purpose, only spontaneous LTO reactions are needed in the oil formation at the prevailing reservoir conditions, to consume oxygen and produce a "flue gas". Transition to from LTO to high temperature oxidation (or combustion) may occur, but is not necessary.

Moore et al. (1998) showed that based on numerous laboratory tests conducted at the University of Calgary, air injection in light oils generally show air requirements in the range of 100 to 175 $sm^3$ of air per $m^3$ (100 to 175 $scf/ft^3$) of reservoir swept, compared to heavy oils and bitumen, for which air requirements of 200 to 400 $sm^3/m^3$ (200 to 400 $scf/ft^3$) are typical. Combustion in light oils also operates with significantly lower peak temperatures, in the range of 300°C (572 °F) compared with 500-600°C (932°F-1,112°F) for heavier reservoirs. They also commented that while the history of air injection-based EOR is littered with the perception of failed projects, many of the failures were associated with low oil prices. In other cases, failures were due to compressor problems, or incorrect concepts of how air injection processes operate. Ineffective ignitions, failure to inject enough air, and applications in reservoirs that had no hope of success, explained the trouble with many past projects.

♣ **Literature Review on Improved Oil Recovery and Economics of Air Injection.**

Moore R.G. et al (2012), in his paper reviewed some of the successful air injection projects in higher gravity oil reservoirs and discusses the elements that are critical for success. These include the ability to ignite and continuously burn a fraction of the oil at reservoir conditions, the suitability of

the reservoir for a gas-injection based recovery process, the availability and suitability of preexisting infrastructure, and a reasonable prediction of how much air should be injected and how much oil recovery could be expected. The paper also discussed possible options for taking advantage of the product gas stream.

Kumar et al (1996) in their studies, concluded that the Medicine Pole Hills Unit (MPHU) reservoir – a deep, high-temperature, light-oil reservoir, proved to be a suitable candidate for high-pressure air injection (HPAI) with a tremendous increase in oil recovery. After 6 years of operation, the air injection project achieved an attractive air-(oil-plus-Natural Gas Liquid) average ratio of 8MSCF/STB. They also pointed out the great success of the project had dependence on the optimized operation of the compressor facility, the monitoring of producing wells to ensure maximum productivity, and the efficient application of technology and innovations based on experience that allowed successful and safe operation of the high pressure air-injection project.

Also Kumar V.K. et al (in 2006) compared air injection project in West Buffalo Red River Unit and water flood project in West Buffalo "B" Red River Unit. They presented a summary of the incremental recovery performance per year which contains the projected primary production, the actual unit improved recovery production and the incremental recovery per year. Clearly, throughout the years the air injection project in has been technically more successful in terms of incremental oil recovery, quicker response and higher production compared to its twin West Buffalo "B" Red River Unit water flood project. They concluded that the choice of either method depends mainly on the reservoir studies, reservoir fluid properties and economics.

Gutierrez et al. (2008b) pointed out that although air injection process has been a proven low-cost EOR technique for light-oil reservoirs, compared with other gases, early investment is still enormous. Hence, a serious feasibility analysis is essential before implementing the project and a set of screening criteria needed to be built, whilst economic factors (oil price and investment) are needed to be considered. Generally, some conventional and unconventional methods are used. Analogy with successful injection projects somewhere is necessary when information available is not enough, combining numerical simulation and experience together.

♣ **Literature Review on Safety and Corrosion Issues in Air Injection.**

Ji Ya-juan et al (2008) described that there are concerns on safety and corrosion issues that could be the main reasons why air injection has not been well received in the industry. These must be addressed seriously in the design and implementation of air injection projects. It should be noted that, due to relative mobility effects, air injection is better given preference for gravity drainage rather than horizontally flooding or pushing oil up-structure, particularly in designing a tertiary air

injection project. These should be stressed in all air injection projects. Corrosion was found to be a serious problem during the air foam injection project of Zhongyuan Oilfield China, which mainly includes corrosion caused by oxygen in air injection wells at the early stage of the project while gas has not broken through to the producers. They stated that the main safety consideration for the injection well is to prevent oil and gas flow back into the injector wellbore to mix with air in the case of compressor system failures.

## 2.2 Literature Review of Carbon Dioxide ($CO_2$) Injection

$CO_2$ injection has been proved to be an effective IOR technique in numerous field projects. $CO_2$ flooding has been the most widely used EOR recovery method of medium and light oil production in sandstone reservoirs during recent decades, especially in the U.S., due to the availability of cheap (when compared with current oil prices) and readily available $CO_2$ from natural sources. $CO_2$-EOR has become one of the preferred EOR processes globally using $CO_2$ from natural and industrial sources (Bauer, 2006; Muro et al., 2007).

Taber et al., (1983) listed some aspects of oil reservoirs that should be considered for $CO_2$ EOR technique include reservoir depth, oil density, storage capacity, water and oil volumes in place, and formation thickness. Usually $CO_2$ injection projects in oil reservoirs have focused on oil with densities between 29 and 48°API (855 to 711 kg/m$^3$) and reservoir depths from 760 to 3700 m (2500 to 12,000 ft.) below ground surface.

♣ **Literature Review on $CO_2$ Injection Practices in China.**

There have been a few field pilots of $CO_2$ injection in China (Zhang *et al*. 1995; Lv *et al*. 1999, Luo *et al*. 2005; Guo *et al*. 2006), mostly using $CO_2$ from natural sources or from chemical plants via lorry tank transportations. Recently, with the prospective application of the CCS technique, problems associated with limited $CO_2$ source can be solved, more and more reservoirs, therefore, might become the targets for $CO_2$ IOR and storage. For many tight and light oil reservoirs studied in China (Xuan and He 2010), the MMP is typically higher than the reservoir pressure, which limits the operation of miscible displacement. Therefore, $CO_2$ near miscible displacement might be an attractive IOR technique, which is more flexible and can be easily realized with less restriction to injection pressure and $CO_2$ and crude oil compositions.

In a recent study of Ren, S.R. et al., (2011) on Screening of Gas Injection Methods for IOR in a Low Permeability Reservoir of Xinjiang Oil Field, they concluded that $CO_2$ injection produces the best performance in terms of oil production because of its miscibility effect, while air injection is also favorable over $N_2$ and flue gases due to the thermal effect generated during oxygen/oil reactions. Gas injection (as tertiary recovery) of 20 years period produced an incremental oil of 5.01-7.17% OOIP after 15 years of secondary water injection recovery in the low permeability reservoir they studied.

♣ **Literature Review on $CO_2$ Minimum Miscibility Pressure MMP**

Miscible recovery of reservoir oil can be achieved by $CO_2$ displacement at a pressure greater than a certain minimum. This minimum pressure is hereafter called as the $CO_2$ minimum miscibility

pressure (MMP). $CO_2$ MMP is an important parameter for screening and selecting reservoirs for $CO_2$ EOR. For the highest recovery, a candidate reservoir must be capable of withstanding an average reservoir pressure greater than the $CO_2$ MMP. MMP depends on crude oil composition and reservoir conditions, and is typically determined using slim tube tests. If gas is injected above the pressure that miscibility is achieved (the minimum miscibility pressure for multiple contact miscibility), then a higher fraction of residual oil can be displaced from the pores. Minimum miscibility pressure (MMP) is a direct function of oil and injected gas composition (Stalkup, 1983; Lake, 1989). Injected gas composition should be designed in a way that MMP can be achieved. Low MMP is perhaps the most important advantage of $CO_2$ as injectant over other gases. Highly efficient miscible displacement can be achieved at low pressures, increasing oil production and reducing injection cost.

Experimental results indicated that immiscible supercritical (SC) $CO_2$ is capable of mobilizing oil in the very low permeability environment (0.16 mD) with reasonable displacement efficiency. Also, higher displacement efficiencies could be obtained if the flooding process started earlier, i.e. at higher oil saturation, as there is a critical starting oil saturation required to optimize the displacement efficiency (Zekri, A.Y. et al 2006).

A simple or modified correlation can be used to determine the minimum dynamic miscible displacement pressure for a $CO_2$ flood. It usually requires knowledge of the reservoir temperature and the composition of the oil in place. The National Petroleum Council (NPC) in the United States (1976) developed an MMP correlation that predicts $CO_2$ MMP according to reservoir temperature and reservoir oil API gravity. Lee (1979) proposed a model to predict $CO_2$ MMP as a function of reservoir temperature by considering $CO_2$ vapor pressure. Yellig and Metcalfe (1980) experimentally investigated the effects of temperature and oil composition on the $CO_2$ MMP. They developed a rough correlation relating the reservoir temperature to $CO_2$ MMP. Mungan (1981) presented a graphical correlation to predict $CO_2$ MMP as a function of reservoir temperature and molecular weight of $C_{5+}$ fraction in crude oil. Johnson and Pollin (1981) published an accurate empirical correlation to predict the pure and impure $CO_2$ MMP from readily available field data for a wide variety of live oils and stock oils with both pure and diluted $CO_2$. This correlation relates the $CO_2$ MMP to oil gravity, molecular weight, reservoir temperature, and injection gas composition. Shokir (2007) presented a model for predicting the impure and pure $CO_2$/oil MMP that relates MMP to variety of oil compositions, reservoir temperature and $CO_2$ impurities components.

### ♣ Literature Review on Near-Miscible $CO_2$ Flooding.

In recent years, the concept of near-miscible $CO_2$ flooding has been received more and more attention. The research of near-miscibility effect can be tracked back to early 1980s', when Orr and colleagues (Orr *et al*. 1981) published their studies on phase behavior of $CO_2$/crude oil mixture, they indicated that the inflexion point in the slim-tube experimental curve may not necessarily signify the transition from immiscible to miscible displacement, instead it can represent a near miscible state because a full miscibility is not achieved, whereas this "near-miscible" phase behavior can be also good for effective oil displacement. Shyeh-Yung and J-G, J (1991) pointed out that a near-miscible $CO_2$ IOR process has potential to economically recover oil.

Hadlow (1992) stated that application of $CO_2$ flooding in reservoirs where a near miscible condition exists can be one of the most significant opportunities for utilization of $CO_2$. Case studies by Thomas *et al.* (1994) showed that many reservoirs historically designed as miscible flooding would be better described as near miscible. It was suggested that a compromise between mobility and interfacial tension (IFT) depending upon pore size distribution should be evaluated, while to pursue or emphasize a zero IFT during designing a gas injection process would be an overkill.

Laboratory investigations via core flooding experiments and numerical simulations in different modes of $CO_2$ injection revealed that good oil recovery can be achieved at a near miscible pressure region (Bardon *et al*. 1994; Dong *et al.* 2001; Sohrabi *et al.* 2005). Extraction/vaporization can be accounted for high oil recovery efficiency as demonstrated in the literatures of Hossein *et al.* 2005; 2008; and Tsau *et al.* 2010. Also, the sweep efficiency for near-miscible flooding at low pressures will be improved since $CO_2$ mobility is increased as pressure decreases (Shyeh-Yung and J-G, J 1991). However, Grigg *et al*. (1996) found that, from core flooding data and the analysis of the density behavior of $CO_2$, the extraction process of $CO_2$ flooding at a near-miscible operation was not efficient.

### ♣ Literature Review on Density and Viscosity of $CO_2$.

Common advantage of $CO_2$ and the various gas injection techniques include:

- At high pressures, $CO_2$ density has a density close to that of a liquid and is greater than that of either air, nitrogen ($N_2$) or methane ($CH_4$), which makes $CO_2$ less prone to gravity segregation compared with air, $N_2$ or $CH_4$.
- In addition, at high pressures, viscosity of $CO_2$ is also greater than that of air, $N_2$ or $CH_4$, resulting in better mobility control and better sweep efficiency compared with other gases.

Due to low viscosity, $CO_2$ has a high mobility, which is a major issue in the optimizing oil recovery and sequestration. High mobility causes lower reservoir sweep and early production of $CO_2$, which can lead to lower oil recovery and lower storage of $CO_2$. Several different techniques such as WAG, SAG and foam have been used for controlling the $CO_2$ mobility for the purpose of enhanced oil recovery. Prieditis and Paulett (1992) studied the use of a surfactant-foam to reduce the $CO_2$ mobility for San Andres cores.

♣ **Literature Review on the Effects of Dipping Reservoirs on $CO_2$ injection.**

Steeply dipping reservoirs are often suitable for downward $CO_2$ displacement to utilize gravity forces to stabilize the displacement and increase the sweep of the injected $CO_2$ (Perry, 1982; Nute, 1983). The critical superficial velocity, $U_c$ to achieve a gravity stable displacement can be calculated from:

$$U_c = \frac{k\lambda^{\circ}_{r1}\Delta\rho g \sin\alpha}{M^{\circ} - 1} \tag{2.1}$$

Where $k$ is the permeability, $\lambda^{\circ}r_1$ is the end point mobility of displacing fluid, $\Delta\rho$ is the density difference between displacing fluid and displaced fluid, $\alpha^{\circ}$ is the reservoir dip angle, and $M^{\circ}$ is the end point mobility ratio.

As it can be seen from the equation above, reservoirs with high permeability will have a higher critical rate and therefore may be candidates for gravity stable displacement, whereas those of lower permeability will have a critical rate too low for economically flooding in a gravity stable mode. Effect of reservoir dip angle and injected gas mobility is also significant. In this type of displacement process because of late $CO_2$ breakthrough and highest sweep possible both of maximum storage and oil recovery can be achieved if the feasibility of project is validated.

For reservoirs with no dip or low dip, as the gravity to viscous force ratio decreases, the tendency of solvent to override decreases and vertical sweep efficiency improves. Therefore the vertical permeability is a key factor in determining vertical sweep efficiency and oil recovery in $CO_2$ floods (Elsayed et al. 1993). In addition to above mentioned issues on gravity stable displacement, by adjusting the $CO_2$ density, $CO_2$ slug can be spread between the less dense gas cap and the more dense oil column causing more contact between $CO_2$ and reservoir oil (Johnston, 1988). $CO_2$ can be injected at the top of the reservoir depending on the gravity segregation effect of reservoir fluid and the vertical permeability of the reservoir rocks.

### ♣ Literature Review on the Effects of Well Types on $CO_2$ injection.

There are some other strategies that can help to optimize recovery and storage. Employing horizontal or combination of horizontal and vertical wells depending on the project conditions can be one of these techniques (Lim et al. 1994). The application of $CO_2$ flooding using horizontal wells significantly shortens project life, thus substantially improving project economics. For very tight reservoirs where $CO_2$ and brine injectivities strongly affect project economics, the use of horizontal injectors may be a more attractive alternate than vertical wells. The use of horizontal injectors in conjunction with vertical producers in tertiary $CO_2$-WAG flood generally resulted in oil recovery that was as good or better than using both horizontal injector and producer and always higher than using all vertical wells (Lim et al. 1992). The injectivity of $CO_2$ and brine using horizontal wells, and hence the oil recovery at reasonable project life, is very sensitive to the permeability in the vicinity of the wells.

Malik and Islam (2000) believed that in the Weyburn field, horizontal injection wells have proved to be efficient for $CO_2$ flooding process to improve recovery while increasing the storage of $CO_2$. Besides employing horizontal wells, applying different well control techniques including partial completion of both injection and production wells can improve the amount of injected and stored $CO_2$ as well as oil recovery (Jessen et al. 2005).

### ♣ Literature Review on the Effects of Injection Patterns on $CO_2$ injection.

Dicharry, M.R. et al (1973) work with reservoir models, showed that alternately injecting slugs of $CO_2$ and water during the $CO_2$ injection program would be more effective than continuously injecting a single $CO_2$ slug driven by water. The alternating slug program offered the additional advantage that the flank pattern injection could be developed earlier than would be possible under the continuous $CO_2$ injection program. Injecting water in the pattern areas before injecting $CO_2$ should not be detrimental to the $CO_2$ displacement process. It is desirable to inject water into pattern areas to increase reservoir pressures to the operating levels required by the $CO_2$ process before injecting $CO_2$. They achieved under this alternating $CO_2$ water injection program as planned, the predicted ultimate oil recovery of approximately 230 million bbl. which is more than is expected from the original water injection program in Chevron Oil SACROAC Unit i.e. they area of study of Dicharry et al (1973).

However, in a study by Campbell and Orr (1985), visual observations of pore-level displacement events indicate that $CO_2$ displaced oil much more efficiently in both first contact and multiple contact miscible displacements when water was absent. Water from a prior water flood restricted access of $CO_2$ to the oil. The low viscosity of $CO_2$ aggravated effects of high water saturations

because $CO_2$ did not displace water efficiently. Given enough time, $CO_2$ did however contact trapped oil by diffusing through water to reach, to swell and to reconnect isolated droplets.

### ♣ Literature Review on $CO_2$ Sequestration

In recent years, the amount of greenhouse gas in the atmosphere has increased, causing concerns about climate change (Herzog et al., 2000). One approach to reducing the carbon content in the atmosphere is based on capturing $CO_2$ from large emission sources and injecting it into deep geological formations. There are several ways to do this: by injecting $CO_2$ into deep saline aquifers, by injecting $CO_2$ into mature oil and gas reservoirs for the purpose of enhanced oil and gas recovery (EOR or EGR), by injecting $CO_2$ into depleted oil and gas reservoirs, or by injecting $CO_2$ into coal seams. These are structures that have stored crude oil, natural gas, brine and other types of gases over millions of years

$CO_2$ injection is getting most of the attraction as an EOR method and potentially as a sequestration strategy in recent years. However, $CO_2$-EOR projects in operation are mostly concentrated in the U.S. (especially in the Permian Basin) and associated to natural sources of $CO_2$. $CO_2$-EOR / sequestration projects are not expected to grow in the near future until industrial sources of $CO_2$ are produced at much lower costs and the proper regulatory framework is in place (Manrique, et al 2010).

It is well known that $CO_2$-EOR has become as an attractive $CO_2$ storage method within the options currently available. However, it is important to note that storage capability of $CO_2$ in oil and gas reservoirs is limited (Manrique and Araya, 2008). Additionally, actual capture, compression and transportation costs combined with the lack of proper regulatory framework among other issues (i.e., public perception), an important increase is not foreseen in the number of projects implementing $CO_2$-EOR from anthropogenic sources in the near future.

Ghomian Y. et al (2008), after their statistical analysis of the simulation results, the most to least influential factors for maximizing both profit and amount of stored $CO_2$ are the produced gas oil ratio constraint, production and injection well types, and well spacing. Also for a $CO_2$ flood, no significant reduction of profit occurred when only the storage of $CO_2$ was maximized. In terms of the economic parameters, it was demonstrated that the oil price dominates the $CO_2$ EOR and storage. His study showed that sandstone reservoirs have higher probability of need for $CO_2$ incentives. His study demonstrates that compositional reservoir simulation in conjunction with experimental design and the method of response surfaces can be used efficiently in optimization studies in coupled $CO_2$ sequestration and enhanced oil recoveries.

The effect of the employing horizontal wells in improving sweep efficiency and incremental oil recovery of a $CO_2$ flood has been studied by Lim et al., 1994, and Malik and Islam, 2000. It should be considered that due to the recent drilling technology improvements, drilling costs for horizontal wells is not much higher than vertical wells. Combination of horizontal and vertical wells also might help to delay the $CO_2$ breakthrough and increases its storage.

♣ **Literature Review on the effects of Tax Incentive in $CO_2$ Sequestration and EOR**

Ghomian et al. (2007) also studied the probabilities of need for tax incentives and quantified $CO_2$ credit which makes coupled $CO_2$ sequestration and EOR projects feasible. This is important because the cost of $CO_2$ capture and transportation dominates the economics of these type of projects.

$CO_2$ can be separated from flue gases in a power plant, and transported to oilfields for injection. But the induced extra cost needs to be compensated in some kind of mechanisms, such as incremental oil production and carbon tax (Celius, H.K. et al, 1996), to ensure a positive economic return on $CO_2$ injection and sequestration in oil and gas reservoirs.

## 2.3 Literature Review of Nitrogen ($N_2$) Injection

Interestingly, the very first reported use of nitrogen injection in reservoirs also coincided with the advent of EOR in the U.S. The origins of nitrogen injection and thus EOR in the U.S. can be traced back to the prolific Permian Basin in West Texas. In 1945 Atlantic Richfield discovered an unusual field, which they called Block 31. The success of Block 31 led to the emergence of a number of other enhanced oil recovery projects utilizing nitrogen in Texas, Louisiana, Wyoming, Utah, Oklahoma and California (Mungan N., 2000).

In a review of 1982, more than 30 fields had used $N_2$ for IOR (Clancy J.P. 1985). In 1997, there were more than twelve (12) $N_2$ injection projects on the list of NIJECT Services Co., a company supplying gas injection facilities in the USA (Tulsa, OK 74172-0123). As far as petroleum engineering is concerned, $N_2$ injection into oil reservoirs does not present any major problems. $N_2$ used for field injection is mainly from air separation. The cryogenic process had been mostly used in the past while cost effective membrane separation has been developed in recent years. In oil field applications, $N_2$ is a substitute for natural gas and $CO_2$ because it is more available and may be less costly than natural gas and $CO_2$.

The nitrogen injection project in the Cantarell Complex, offshore Mexico, implemented in May 2000, has been the most ambitious pressure maintenance project around the world regarding incremental oil, production rate, nitrogen injection rate, and investment (Sanchez, et al., 2005). Reservoir simulation studies indicated that implementing a pressure maintenance program in the fields would yield optimized oil recovery in the Cantarell complex. It was also reported in the nitrogen project of Cantarell field in New Mexico that the measured pressure response of the wells has been found to be consistent with that predicted by reservoir simulation. Detailed analysis of the pressure response to changes in the nitrogen injection rate showed very short transient flow periods, followed by pseudo-steady state flow regimes, which confirmed an extremely high transmissibility in the target reservoir**.**

The pressure maintenance project to improve oil recovery by nitrogen injection in Cantarell has proven to be very successful, both technically and economically. The Conclusions drawn from the effect on oil production rate of the two main components of the Cantarell optimization project: pressure maintenance and additional drilling-expansion of production facilities after four years of the project are:

1. In the first four years of the pressure maintenance project in Cantarell, a cumulative volume of 1,400 BSCF of nitrogen has been injected into the target reservoir. The volume of gas in the secondary gas cap before injection was 1,800 BSCF.

2. Pressure in the oil column has been kept at 1455 psi. Had not the pressure maintenance project been implemented, reservoir pressure would have dropped to 1220 psi by 2004, as updated estimations indicate.
3. Overall nitrogen concentration in the produced gas of Cantarell increases only when the gas-oil contact reaches the producing wells, or when nitrogen is used in gas lifting operations.
4. Data obtained from the monitoring program indicates that nitrogen is segregated in the gas cap and that its concentration in the oil column has not changed, indicating an immiscible displacement mechanism.

Nitrogen ($N_2$) flooding has been an effective recovery process for deep, high-pressure, and light oil reservoirs. Generally for some types of reservoirs especially carbonate rocks, nitrogen flooding can reach miscible conditions. However, immiscible $N_2$ injection also has been used for pressure maintenance, cycling of condensate reservoirs, and as a drive gas for miscible slugs. However, $N_2$ injection still represents an option that can be justified for high pressure and high temperature (HP/HT) light oil reservoirs if there is no access to other gas sources (Mungan, 2000).

It has been estimated that, in Exxon's Hawkins field nitrogen injection project (Langenberg et al 1995) about 80% of the incremental oil production came from sweep efficiency improvement due to the $N_2$ injection. Secondly, the displacement efficiency is improved by gas flooding, wherein a typical residual oil saturation after water flooding of 25% - 30% can be reduced to 10% - 20% by gas displacement. This is called double displacement process (DDP), as first presented by Fassihi and Gillham (1993). Laboratory studies and field experience of nitrogen and air injection has proved the effectiveness of DDP.

In the study performed by Sinanan B. and Budri, M. (2012) on nitrogen injection application for oil recovery in Trinidad, they found that the overall results suggest that nitrogen injection is a real alternative and much more practical and economic than previously envisioned by investors. The technology of modern day reservoir simulation has made analysis fast and efficient using structural, stratigraphic and reservoir properties that reflects the subsurface in Trinidad. The encouraging results of their study means nitrogen injection for enhancing oil recovery can now be seriously considered by mature acreage operators who wish to lengthen the economic life span of their fields. The results of the study indicate that the injection of nitrogen into the secondary gas cap is the optimum injection strategy to enhance oil recovery. They also observed three (3) major production mechanisms in the injection of nitrogen up dip into a secondary gas cap:

**A) Partial maintenance of reservoir pressure.**

The injection of nitrogen gas into the reservoir helps provides energy for maintaining the reservoir pressure to sustain oil production. By maintaining the reservoir pressure, the pressure difference between the reservoir and production states that the flow rate is directly proportional to pressure differential. In the simulation study, the low injection rates used was able to maintain the reservoir pressure at around 700 psi.

**B) Displacement of oil by nitrogen both horizontally and vertically.**

For crestal or gas cap injection of nitrogen, the force of gravity tries to stabilize the downward nitrogen/oil displacement process by keeping nitrogen on top of the oil and counteracting the unstable nitrogen/oil viscous displacement process. As nitrogen is injected it invades the originally oil-saturated sand as the GOC moves down-dip because of oil production farther down-dip. The oil drains vertically downward through the nitrogen invaded region and forms a thin layer with high oil saturation that drains along the base of the reservoir interval to the remaining down-dip oil column.

**C) Vaporization of the liquid hydrocarbon components from the oil column and possibly from the gas cap by nitrogen.**

Nitrogen injection is associated with mass transfer compositional effects. The injected nitrogen/oil composition interactions involve stripping effects i.e. various light components from the oil phase is transferred to the injected nitrogen.

Also from their study, several important concepts regarding immiscible nitrogen/oil displacements were learnt. These included:

- The immiscible nitrogen/oil displacement is generally an inefficient oil displacement process because nitrogen is a highly mobile fluid. Our study will ascertain the validity of this concept.
- The immiscible nitrogen/oil displacement process becomes efficient and desirable when gravity works to keep the low density nitrogen on top of the higher-density oil and when there is mass transfer of components from the oil to the nitrogen.
- The immiscible nitrogen/oil displacement process also becomes desirable when the depositional environment is indicative of an upward fining sequence, as this helps to reduce the upward migration of the less dense nitrogen gas to upper zones in lower dip environments.
- The most optimum strategy for nitrogen injection involves injecting nitrogen into the crestal secondary gas cap, with the oil wells producing from as far down-dip as possible, by maximizing the distance from the gas cap both vertically and laterally.

- Nitrogen also has compositional mass transfer effects on the reservoir fluids. One nitrogen/oil compositional mass transfer effect is oil swelling. However, the effect in nitrogen is very small in this case as nitrogen has a very low solubility in oil as compared to other gases such as carbon dioxide.
- The other nitrogen/oil compositional mass transfer effect is stripping or vaporization of light hydrocarbon components from the oil by the nitrogen. Nitrogen is able to strip or vaporize the C1-C5 components which cause the density and viscosity of the oil to increase. This effect is very small and occurs with all types of oils but is more significant for lighter or higher API gravity oils.
- Upon contact with water present in the underlying aquifer, nitrogen has no effect on the water viscosity. However, an increase in water density is observed which is due primarily to the very low solubility of nitrogen in the water phase.

Other points of interest by the authors include:

- Nitrogen can be more reliably supplied (on site production) than carbon dioxide (remote supply). This fact reduces many infrastructure security concerns and production hiccups.
- Nitrogen does not have the health and safety issues on humans and environment as carbon dioxide. Nitrogen breakthrough at surface sites due to faulting or degraded old well infrastructure does not have the detrimental effects as using carbon dioxide. Also, nitrogen will not make fresh water aquifers toxic.
- Nitrogen injection will attract any government incentives for EOR projects.
- Small scale nitrogen (immiscible) injection projects are very much economically viable.

# CHAPTER 3: MECHANISMS OF GAS INJECTION

## 3.1 General Concept of Gas Injection Techniques for IOR

In this study, gas injection involves injecting natural gas, air, nitrogen or carbon dioxide ($CO_2$) into the reservoir. The gases can either expand and push oil through the reservoir, or dissolve in the oil, decreasing its viscosity and facilitating oil flow to the production well(s) especially when assisted by gravity in the case of dipping reservoirs like the Q131 block. It is reported that other EOR methods decline over the years, gas injection projects increased from 18% in 1984 to about 48% in 2008, proving to be the most popular method in the U.S. (Gutierrez et al., 2008b) and presently gaining much grounds in exploitation of petroleum resources in China (Ji et al., 2008).

In comparison with water injection, the advantages of gas injection IOR in low permeability oil reservoirs mainly include high injectivity, less formation sensitivity and damage, and high sweeping efficiency. The mechanisms of gas injection techniques for IOR can be classified into the following categories (Ibukunoluwa et al., 2010):

1. **Pressure maintenance:** Gases are injected into an oil reservoir (mostly at the top of the reservoir) to maintain the reservoir pressure above the bubble point or dew point of the reservoir fluids, or to enlarge a gas cap and stabilize the oil-gas contact.
2. **Gravity drainage:** Gases, with lower density than oil at reservoir conditions, are injected into the crest or top of the reservoir to enhance a down dip displacement of oil. In some cases, gas can be injected into the base of the oil zone and allowed to migrate to the crest by gravity segregation. Reservoirs with a dipping or thick hydrocarbon zones can be considered as the most beneficial candidates for a gravity drainage process.
3. **Water alternating gas (WAG) injection:** Water and gas are injected into the reservoir in a cyclic basis with varying water/gas ratio and the pulse length of gas injection. Oil production can be increased by improving (gas) injectivity, pressure maintenance and better sweep of non-swept oil and capillary trapped oil after water flood.

The displacement of oil by gas can be said to be single contact miscible or multiple-contact miscible processes, near-miscible and immiscible depending on the existing pressure of the reservoir, properties of the gas injected and the reservoir fluids at reservoir conditions, though these three processes are usually not distinguished in a real field process. Generally, at miscible conditions, the injected gas and the hydrocarbons are completely miscible and form a single phase fluid, which promotes oil swelling, reduces fluid viscosity and increases its mobility. Near-miscible

displacement occurs at pressures around a minimum miscible pressure (MMP), in which the effect of dissolution and condensation is declined with descent pressure. At immiscible phase, there is less interchange of components or mixing zones between the gas injected and the reservoir fluid.

### 3.1.1 Key Drivers of Gas Injection Performance

The key factors that impact performance of gas injection projects are reservoir pressure, fluid composition, reservoir characteristics, and relative permeability.

#### 3.1.1.1 Reservoir Pressure

Pressure is a key parameter in determining whether or not the injected gas will be miscible with the in-situ oil that will be contacted in the reservoir. Oil recoveries for gas injection processes are usually greatest when the process is operated under conditions where the gas can become miscible with the in-place oil. The gas and oil can be first contact miscible or develop multi-contact miscibility by extracting light components from the oil (the "vaporizing" gas drive process), and/or by losing components to the oil (the "condensing" gas drive process). Miscibility can be achieved either by managing the reservoir pressure and/or by changing the composition of the injected gas by addition of either heavier hydrocarbons or acid gas components. Gas injection can also be used to immiscibly displace oil and for reservoir pressure maintenance. Also, because gas injection will require compression, the pressures of both the source gas and the receiving reservoir are important for facilities cost and design reasons.

#### 3.1.1.2 Fluid Composition

Lighter oils are generally more amenable to displacement by gas injection because they develop or approach miscibility with injected gas more readily than heavier oils. In addition, the mobility ratio is generally more favorable for lighter oils due to lower viscosity and there is less potential for precipitation of heavier ends and asphaltenes after contact of the oil with injected gas. Asphaltene behavior is also affected by the degree of under-saturation of the oil at the current reservoir pressure. "Swelling" and "slim-tube" tests are commonly conducted in addition to standard PVT tests to determine conditions under which a candidate gas injectant becomes miscible with the oil. The tests are also used to determine phase volumes, densities, and viscosities for solvent/crude oil mixtures as a function of pressure and solvent content. The results of these tests are used to develop a set of equation of state (EOS) parameters that characterize the solvent/crude system. The resulting EOS model is then used to create phase behavior and viscosity input for simulation.

#### 3.1.1.3 Reservoir Characteristics

The sweep efficiency of gas injection in high permeability reservoirs is usually poorer than that of water injection because gas has a greater tendency to finger through the more viscous in-place fluids, channel through high-permeability streaks, and break through prematurely to producing wells. In general, to accurately represent gas fingering and channeling behavior, the distribution and connectivity of permeability must be represented in the simulation model on a finer scale than in waterflood simulation. In field application, foams or gel can be used to block the channels and also reduce the mobility ratio of the injected gas. This is generally not a major problem in steep low permeability reservoir because of gravity segregation and no gas channeling to cause the injected gas to breakthrough quickly.

***Gravity override*** may occur in horizontal floods because the gas is usually less dense than the oil it is displacing. When vertical communication is high, gas "floats" to the top of the reservoir and sweeps only the top part of that zone. In situations where gravity override may be expected, it is important that the simulation model include a sufficient number of layers to accurately represent the vertical segregation process. For some steeply dipping reservoirs or reservoirs with high vertical communication, it is advantageous to inject less-dense gas at the top of the reservoir in a gravity stable process. Gas sweep efficiency and oil recovery for a gravity-stable process, or "vertical" flood, and can be quite high, provided there is sufficient vertical continuity (Douglas and Weiss, 1991).

Reservoir characteristics that can favor gas injection include:

- High dip angles (gravity stable displacement)
- Lower degree of permeability heterogeneity
- The presence of vertical permeability barriers or baffles to slow the rate of vertical segregation of injected gas.
- Fining upwards deposits (low permeability overlying higher permeability).

#### 3.1.1.4 Relative Permeability

The occurrence and severity of both viscous fingering and gravity override depend, at least in part, on the mobility of the displacing and in-place fluids, which in turn depend on the relative permeability. Saturation history can have a significant impact on relative permeabilities, especially in WAG processes. For example, in mixed-wet rock, significant hysteresis in water relative permeability occurs between imbibition and secondary drainage. When conducting experiments to measure relative permeability it is important to ensure that the saturation history mimics that

expected in the field. The simulation model should also accurately represent three-phase effects and hysteresis.

Given the complexity of most reservoirs, predicting the performance of gas floods requires use of detailed geologic models combined with appropriately gridded simulation models that accurately capture reservoir pressure behavior over time, the fluid properties of both the in-situ and injected fluids, and the reservoir characterization. Furthermore, the laboratory and simulation analyses must accurately reflect the physics of the gas-oil-water interaction. Specific examples of laboratory and simulation capabilities necessary for implementation of successful gas floods are discussed in the latter chapters of this thesis.

## 3.2 Mechanisms of Gas Injection for this Study

The gas injection mechanism applied during this research is targeted at **Gravity Stabilized Gas Injection.** Considering a gravity drainage process where gas is injected at the crest of the reservoir structure into the gas cap or up-dip, and due to the steep dip characteristics of the Q131 reservoir block , gravity segregation and miscible/near-miscible/ immiscible displacement occur and the gas front which is stabilized by gravity pushes the oil column into the down dip production wells achieving both high volumetric sweep and displacement efficiencies depending on the displacing gas, miscibility and the pressure of the reservoir. In air injection, there exist a thermal front created by the consumption of oxygen from the injected air and depending on the reservoir heating and injection rate leads to either low temperature oxidation (LTO) or high temperature oxidation (HTO) that also helps in the oil displacement. The latter may constitute of in-situ combustion and mostly common for heavy oil IOR. The mechanisms of the different gas injection techniques ($CO_2$, air and $N_2$) for the target block will be discussed further in other sections.

The methodology proposed for this research consists of three parts. In the first part, existing experimental/laboratory results obtained for the light oil are used to characterize the processes involved in each recovery mechanism associated to the air injection technique. The second part considers the parameters and findings from the individual experiments are integrated into a simulation model, which is fine-tuned to match the experimental results. Thirdly, different sensitivity cases are run to optimize the flooding. Vast amount of sensitivity analysis and reservoir simulation studies are necessary to inspect the impact of different optimization factors and their corresponding uncertainties affecting the whole process. Also having combination of aforementioned factors may give different results compared to the single variables sensitivity analysis. Therefore, performing large number of simulation runs is needed, to investigate the effect of different variables as well as combination of variables in the form of some scaling groups.

Screening of candidate reservoirs for application of the gas injection process concentrated on the reactivity of the oil, reservoir characteristics and conditions, miscibility capabilities, oil and gas saturation, oil viscosity, and reservoir permeability.

### 3.2.1 Screening Criteria of the Gas Injection Proposed for IOR in Q131 Case Study

For various IOR techniques being implemented all over the globe, screening criteria research is essential to guarantee candidate reservoirs being suitable for operation. This screening is dependent on improved oil recovery of each of the gas injection techniques, economic conditions (profitability), and safety conditions. Also a rough screening criteria is favorable to investigate the potential of different injected medium (gas in this case) used for improving oil recovery in a specific reservoir. Before any expensive reservoir description and economic evaluation, a screening criteria of reservoir is very useful (Taber et al., 1997a; Turta and Singhal, 2001; Moore et al., 2002).

The screening procedure for this study will generally include the following:

1) Reservoir characterization and geologic modeling of the target block
2) Remaining reserves volumetric estimation and evaluation;
3) The ability of injected gas to propagate in reservoirs;
4) In the case of air injection, using laboratory experiments to determine the ability of oil to ignite spontaneously and sustain continuous consuming oxygen and form combustion gases that is near miscible with the reservoir oil.;
5) The ability of the injected gas to be form a miscible or near-miscible phase with the oil.
6) Numerical simulation, results interpretation and comparison.
7) Economic assessment based on the benefit-cost ratio of the gas injection, which indicates the cost of producing one barrel of oil using the different gas injection techniques, and the profit derived after sales of the produced oil.
8) Safety issues associated with each of the selected gas injection techniques.
9) Risk assessment in the application of the gas injection techniques in the study area.
10) Recommendations for better reservoir performance, increased oil recovery, and safe applications of the different gas injection techniques.

## 3.3 Mechanisms and Methodology of Study – $CO_2$ injection

### 3.3.1 Mechanisms of $CO_2$ Injection IOR

The use of $CO_2$ as an oil recovery agent in petroleum reservoirs has been investigated for many years. Both laboratory and field studies (Holm 1959) have established that $CO_2$ can be an efficient oil-displacing agent. The various mechanisms by which it can displace oil from porous media have

been of particular interest to the petroleum industry. .The mechanisms include: (1) solution gas drive, (2) miscible $CO_2$ drive, (3) hydrocarbon-$CO_2$ miscible drive, (4) hydrocarbon vaporization, (5) direct miscible $CO_2$ drive, and (6) multiple-contact dynamic miscible drive.

The characteristics of carbon-dioxide that are effective in removing oil from porous rock are:

1. It promotes swelling.
2. It reduces oil viscosity.
3. It increases oil density.
4. It is highly soluble in water.
5. It exerts an acidic effect on rock.
6. It can vaporize and extract portions of crude oil.
7. It is transported chromatographically through porous rock.

The advantages of a $CO_2$-flood include the following (Ibukunoluwa et al. 2010):

- Miscibility can be achieved at relatively low pressures.
- Displacement efficiency is high in miscible cases.
- Recovery of oil is aided by using a solution gas drive.
- Useful over a wider range of crude oils than hydrocarbon injection methods.
- Miscibility can be regenerated if lost.

Advantage of $CO_2$ compared to the other gas injection techniques:

- At high pressures, $CO_2$ density has a density close to that of a liquid and is greater than that of either air, nitrogen ($N_2$) or methane ($CH_4$), which makes $CO_2$ less prone to gravity segregation compared with air, $N_2$ or $CH_4$.
- In addition, at high pressures, viscosity of $CO_2$ is also greater than that of air, $N_2$ or $CH_4$, resulting in better mobility control and better sweep efficiency compared with other gases.

The disadvantages of a $CO_2$ flood may include the following:

- $CO_2$ is expensive to transport and not always available.
- Poor sweep and gravity segregation can happen under certain conditions.
- The risk of corrosion is increased.
- Special handling and recycling of produced gas is necessary.

#### 3.3.1.1 Concept of $CO_2$ Miscibility in IOR

Injection of $CO_2$ into oil reservoirs may develop different displacement or flooding processes, namely miscible, immiscible and near-miscible, which mainly depend upon the operating pressure, temperature, $CO_2$ fluid composition, oil and reservoir characteristics**.**

**Miscible displacement** is the most preferable mechanism for oil recovery with respect to high displacement and sweeping efficiency (Jeschke *et al.* 2000). However, miscible displacement is only realizable at pressure greater than MMP; therefore miscibility can be difficult to develop in many cases, such as mature oilfields due to the depletion of reservoir energy, and in low permeability reservoirs where a large pressure drop or difference may develop from injector to producer. The miscibility of oil and $CO_2$ is also affected by compositions of crude oil and purity of $CO_2$, rock heterogeneity and gravity segregation (Johns *et al.* 2002). Compared with miscible flooding**, immiscible flooding** is less effective, particularly for reservoirs with serious heterogeneity, in which high permeability channels, inverse mobility ratio and viscous "fingering" can lead to early gas breakthrough (Arshad *et al*. 2009; Zhang *et al*. 2010). For those reservoirs with relatively low pressure and less favorable for miscibility, a **near-miscibl**e process might be developed to maximize the interactions of oil and $CO_2$ and achieve high oil recovery.

The most efficient use of $CO_2$ as an oil-recovery agent is obtained at flooding pressures at which miscible displacement is achieved. The extraction of $C_5$ to $C_{30}$ hydrocarbons by $CO_2$ at these pressures promotes a displacement efficiency approaching 100 percent. Miscible recovery of reservoir oil can be achieved by $CO_2$ displacement at a pressure greater than a certain minimum. This minimum pressure is hereafter called as the $CO_2$ minimum miscibility pressure (MMP). MMP is the lowest pressure at which the oil and gas phases resulting from a first contact or multi-contact process, vaporizing or condensing, between reservoir oil and an injection gas are miscible in all ratios. Effect of temperature and pressure on the solubility of $CO_2$ in water

$CO_2$ MMP is an important parameter for screening and selecting reservoirs for $CO_2$ EOR. For the highest recovery, a candidate reservoir must be capable of withstanding an average reservoir pressure greater than the $CO_2$ MMP. MMP depends on crude oil composition and reservoir conditions. MMP is typically determined by slim tube tests in the laboratory and can also be calculated from existing correlation models of experimental results investigated by various authors. Stalkup (1983) have summarized some of the experience gained up to 1983, and stated that MMP increases with increase in reservoir temperature, high molecular weight distribution and decreases with increase in the total amount of $C_5$ to $C_{30}$ present in the reservoir oil, and presence of aromatics.

MMP does not require the presence of $C_2$ to $C_4$ and the presence of methane in the reservoir does not change the MMP appreciably.

The pressure at which $CO_2$ begins to extract significant amounts of hydrocarbons from crude oil increases with increasing temperature and with increasing initial oil volume in the reservoir. The amount of extraction increases with increasing vapor-phase volume (decreasing initial oil volume) and decreases with increasing temperature.

#### 3.3.1.2 Effects of some Parameters on $CO_2$ Dynamic Miscible Displacement

##### 3.3.1.2.1 Effects of Pressure (MMP)

Theoretically, the miscible displacement of oil from a rock will occur at the pressure where extraction of hydrocarbons from the oil by $CO_2$ begins. This would indicate that the pressure where this extraction occurs, as shown by the relative volume curves, is the miscibility pressure. It is apparent, however, that not enough hydrocarbons are extracted at that pressure or even at a slightly higher pressure to maintain a miscible displacement front for any appreciable distance. Furthermore, it has been noted that $C_2$-$C_4$ components vaporized tend to be carried ahead of the displacement front by the injected. The evidence of miscible displacement is, of course, the achievement of high oil recoveries in a long, linear porous system. At this miscibility displacement pressure, a sufficient volume of the extracted hydrocarbons is present at the displacement front to maintain the residual oil saturation at a minimum value throughout the flooding path. The laboratory and empirical methods are usually used to ascertain the MMP in any reservoir.

###### 3.3.1.2.1.1 Estimation of $CO_2$ MMP for the Q131 Reservoir

The $CO_2$ MMP calculation using derived empirical correlations have been highlighted in the literature review section of this paper. The miscibility of a reservoir's oil with injected $CO_2$ is a function of pressure, temperature and the composition of the reservoir's oil. The study's approach to estimating whether the reservoir's oil will be miscible with the injected $CO_2$, given fixed temperature and oil composition, was to determine whether the reservoir would hold sufficient pressure to attain miscibility i.e. by using empirical correlation methods to calculate the $CO_2$ MMP. To determine the minimum miscibility pressure (MMP) for the Q131 reservoir block, this study used the Improved Bai lian correlation (Chen B. et al, 2013). This fitting has a correlation coefficient of 0.9866, high precision and the fitting formula can reflect the sample numerical patterns. This formula (equation 3.1) is used to determine MMP based on reservoir temperature and the molecular weight (MW) of the pentanes and heavier fractions of the reservoir oil, without considering the mole percent of methane. The correlation is as shown below:

$$p_{m,min} = 3.9673 \times 10^{-2} t^{0.8293} [M_r(C_7^+)]^{0.5382} [x(C_1 + N_2)]^{0.1018} [x(C_2 \sim C_6)]^{0.2316} \quad (3.1)$$

Where: $P_{m,min}$ is $CO_2$ - minimum miscible pressure of crude oil, MPa; T - the reservoir temperature, ℃; $Mr(C_{7+})$ - the relative molecular mass of $C_{7+}$, 1; $x(C_1+N_2)$ - the mole fraction of volatile components $C_1$ and $N_2$, %; $x(C_2 \sim C_6)$ - mole fraction of intermediate light component ($C_2 \sim C_6$), %.

The result of this correlation gave **22.73MPa** as the $CO_2$ MMP.

***Alternative Calculation of $CO_2$ Minimum Miscibility Pressure***

This study also used the Yelling and Metcafe correlation (Yellig and Metcalfe 1980) in equation 3.2 is based on reservoir only and doesn't account for oil composition to roughly and quickly determine the minimum miscibility pressure (MMP) for the Q131 reservoir in order to verify the accuracy of the first calculation using the Chen Bailian's correlation equation. This formula is used to determine MMP based on reservoir temperature, T. The correlation is as shown below:

$$MMP_{pure} = 1833.717 + 2.2518055T + 0.01800674 * T^2 - \frac{10349.93}{T} \quad (3.2)$$

From the above correlation equation, the $CO_2$ MMP was calculated to be **3051.41psi (21.04MPa).**

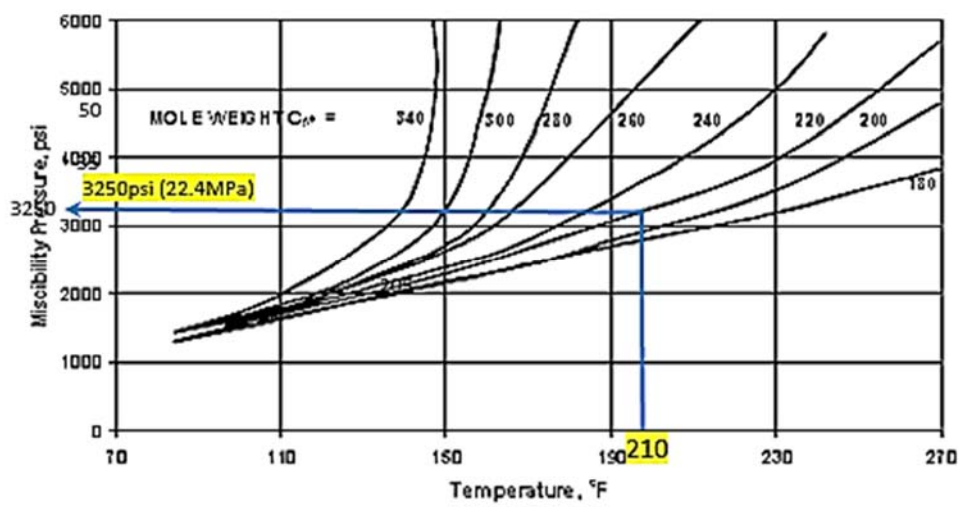


**Fig. 3.1 Correlation for $CO_2$ MMP as a function of temperature (Mungan, 1981).**

A third check was also done using a graphical correlation constructed by Mungan, 1881 as shown in Fig 3.1 was also applied the Q131 to roughly calculate the reservoir's MMP using the current Q131 reservoir temperature of 210°F and the MMP value of **32500psi (22.4MPa)** was obtained, which is close to the Chen Bailian's calculated $CO_2$ MMP of 22.7MPa.

Therefore we can conclude here that the $CO_2$ MMP of the Q131 reservoir block is about **22MPa** with an error of +/-1MPa.

#### 3.3.1.2.2 Effects of Flooding Temperature in $CO_2$ Dynamic Miscible Drive

Temperature makes a considerable **difference in the** pressure at which extraction of hydrocarbons can occur. The pronounced effect of temperature on the pressure at which extraction of hydrocarbons occurs is also illustrated by phase equilibrium data for $CO_2$ and individual hydrocarbons. For example, in Fig. 3.2 shows the critical locus for the binary systems – $CO_2$ and n-octane, n-undecane, n-tridecane, or n-hexadecane. These data are from Schneider et al (1967). For comparison, methane binary mixture data are also shown. At a temperature of 100°F, n-tridecane (boiling point 456°F) is completely miscible with $CO_2$ in all proportions at a pressure greater than 1,200 psia. At a temperature of 180°F, a pressure greater than 2,450 psia is required for complete miscibility. Tridecane and other gasoline and kerosene components should be readily extractable from a crude oil during the formation of multiple-contact miscibility, but higher pressures are required at higher reservoir temperatures.

#### 3.3.1.2.3 Effects of Crude-Oil Composition in $CO_2$ Dynamic Miscible Drive

These binary systems indicate that the composition of the crude oil also influences the pressure needed to obtain the miscible-type flood. The earlier and greater extraction at lower pressures caused the miscible-type displacement to occur at lower pressures with this stock-tank oil. Using $CO_2$, with a heavier crude oil (about an API of 32°) indicate that miscible-type displacement with high oil recovery can be obtained with any crude oil containing appreciable hydrocarbons in the range of $C_5$ to $C_{30}$.

#### 3.3.1.2.4 Effects of Hydrocarbon Gas on $CO_2$ Dynamic Miscible Displacement

In $CO_2$ displacement study by Johnson and Pollin (1981), it was found out that the presence of hydrocarbon gas, even as little as 10% methane, in the reservoir oil or in the injected $CO_2$ causes an appreciable increase in oil recovery efficiency. They also pointed out that a higher pressure is required for comparable oil recoveries using pure $CO_2$. This would be expected on the basis of the critical locus curves in Fig. 3.2. The presence of methane in the reservoir oil was seen to have an adverse effect on the $CO_2$ flood.

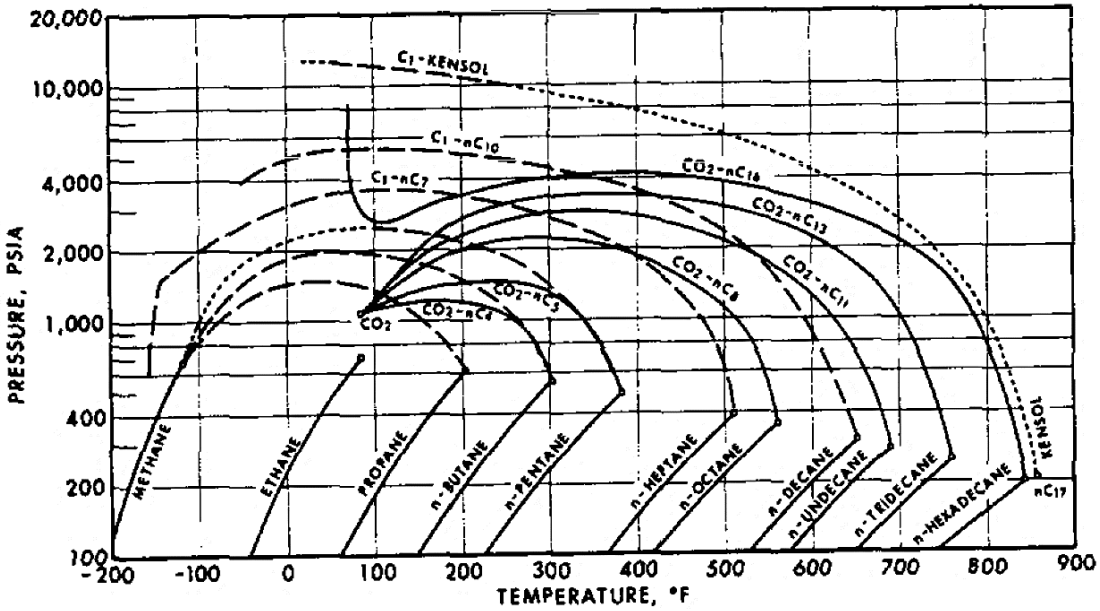


**Fig. 3.2: Critical Locus curve for binary mixtures of CO2-nalkanes and methane-alkanes.**

This presence of methane in the oil reduces the efficiency of extraction of hydrocarbons by $CO_2$ and extends the distance over which immiscible flooding takes place. This methane also creates a less favorable mobility ratio for a $CO_2$ flood. The methane expelled from the oil moves with displaced oil at a relative permeability lower than that of oil moving alone.

For a waterflooded sand system that was preferentially water-wet, the previous waterflood had no adverse effect on the displacement efficiency of $CO_2$. If the sand is made preferentially oil-wet by exposing it to asphaltenes, it would show early water breakthrough but about the same ultimate oil recovery at high WOR. A subsequent $CO_2$ flood of this watered-out sand showed both lower oil recovery at $CO_2$ breakthrough and lower ultimate recovery (Lee, 1979).

### 3.3.2 Methodology of Study – $CO_2$ Injection

Improved oil recovery (IOR) investigations using the $CO_2$ injections were done by performing reservoir simulation studies. Relative permeability function and PVT data for the models used in the simulators are two key factors that greatly affect the simulation results. Careful consideration are to be given to select the appropriate relative permeability model and generate accurate PVT data. More importantly, due to the importance of mass transfer and miscibility effects in these types of processes, compositional simulation is employed to provide better estimates of the combined fluid flow and compositional effects on oil recovery and the amount of available $CO_2$. It is also noted that the simulations of this process can have considerable compositional effects; therefore, applying compositional simulation will give more accurate results than using black oil simulations.

Through combination of $CO_2$ injection theory analysis and the referencing of already acquired results of some physical experiments of $CO_2$ expansion experiments, the near miscible flooding performance of $CO_2$ injection was evaluated and identified in the target block by using numerical simulation approach. Also the best production optimization scheme of $CO_2$ flooding is designed which includes injection rate, injection pressure, production rate, best injection pattern, oil production rate, best injection stop time, shut in of any production well with high gas-oil ratio (GOR), etc. Different flood design parameters such as the produced gas-oil ratio constraint, well spacing, production and injection well types, operational constraints for production and injection wells, shut/open strategy, recycling, along with some important reservoir characteristics such as Kv/Kh and average reservoir permeability is also studied to determine effective flood design strategies for gas injection EOR.

#### 3.3.2.1 Assumptions and Considerations in the $CO_2$ Injection Studies

$CO_2$ flow and transport in porous media are simulated using a conceptual model of multiphase fluid flow and multi-component transport within oil and water. The $CO_2$-EOR mathematical model is based the following assumptions:

1) Heterogeneity of the oil formation and compressibility are considered
2) Heat transfer in porous media is considered.
3) Flow and transport mechanisms include multiphase Darcy flow and multi-component diffusion, subject to adsorption and precipitation.
4) Mass components include $CO_2$, $H_2O$, and oil with some pseudo-oil components.
5) The flooding process is miscible
6) $CO_2$ adsorption on pore walls of the oil formation is considered.

A successful implementation of $CO_2$ flooding in any oil field requires a detailed engineering approach that addresses not only the technical issues, but also undertakes a thorough optimization study. A detailed and comprehensive understanding of real field is required for conducting winning $CO_2$ flooding projects. The following technical challenges are addressed in order to optimize the field operations:

• Improving performance of $CO_2$ flooding
• Early breakthrough of injected $CO_2$
• Viscous fingering and low volumetric sweep efficiency
• Injectivity loss
• Wettability and relative permeability alteration

• Potential corrosion issues
• Achieving and maintaining miscibility or partial miscibility
• Effect of temperature of injected $CO_2$ on reservoir

#### 3.3.2.2 $CO_2$ injection Laboratory Studies

Unlike the air injection experimental studies section, extensive laboratory studies were not conducted for $CO_2$ injection case for this study because of lack of the required equipment needed for the studies (very expensive to acquire in a short period of time) and also this thesis focuses more on the relative IOR efficiencies of the different gas selected for screening basically by the use of reservoir simulation. However, the mechanisms and procedures and methods of the laboratory studies of $CO_2$ are discussed in details in this section, so as to have a complete understanding of the processes involved with $CO_2$ reaction with oil at reservoir conditions.

In general, recovery mechanisms related to $CO_2$ flooding include swelling effect, viscosity reduction, interfacial tension reduction, solution gas drive, light-components extraction and blow down recovery.

**Experimental Procedure for $CO_2$ Flooding**

The schematic experimental setup of this experiment is shown in Fig. 3.3 (Chengyao et al., 2012). Prior to the each flooding experiment, the porosity of core samples is measured. The procedure for porosity measurements is briefly described as follows. Core samples are first completely evacuated by using a vacuum pump. Then the synthetic brine is injected into the rock samples. Consequently, porosity, absolute permeability of the core samples can be measured by implementing the following procedure. Synthetic brine is injected into the core samples at different flow rates ranging from 0.10 cc/min to 0.50 cc/mm. The resulted pressure drops are correspondingly measured, while the absolute permeability of the core samples can be calculated by applying the Darcy's law. Finally, the core samples are flooded with the collected light oil at a constant rate of 0.05 cc/min until irreducible water saturation is reached. The initial oil saturation is determined by knowing the amount of oil injected as well as the pore volume of the rock samples.

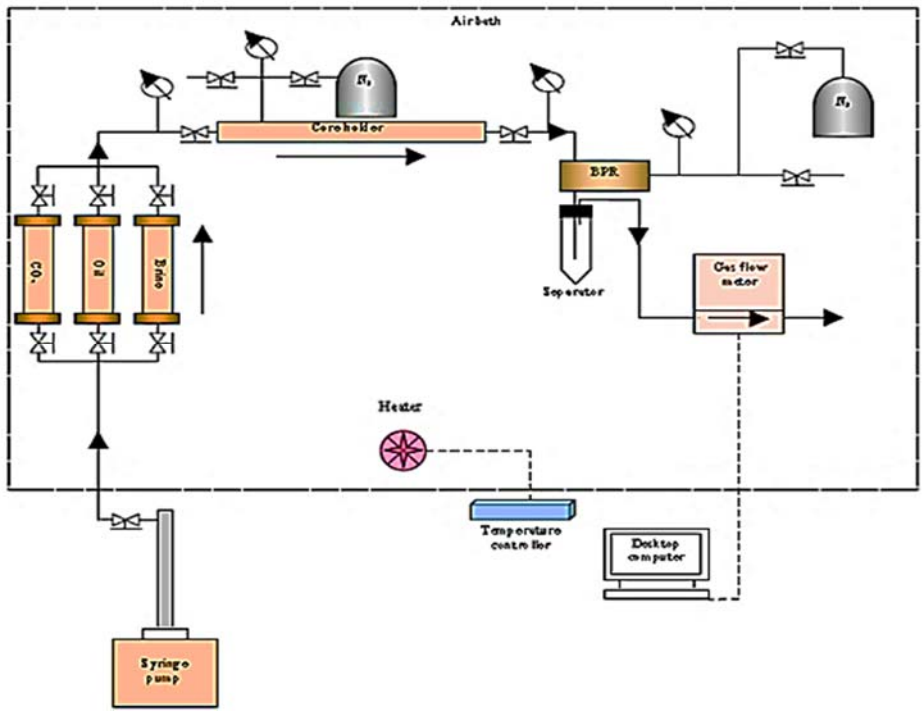


**Fig. 3.3: Schematic diagram of the $CO_2$ core flooding experimental setup**

As for different scenarios, either water or $CO_2$ can be injected at a constant rate of about 0.1 cc/min. During each displacement process, the cumulative oil production and pressure drop are measured. The production pressure in one scenario is set to be at the MMP (22 MPa). The production pressure in Scenario #2 is set to be at a pressure which is about 2 MPa lower than the estimated MMP, in order to satisfy the so-called near-miscible condition. As for Scenario #3, the production pressure can be set to be higher than the MMP (24 MPa), to ensure that the experiments are conducted under miscible conditions. It should be noted that, in Scenarios #2-3, once the $CO_2$ displacement is terminated, the back pressure regulator (BPR) pressure is decreased in a stepwise manner to initiate the blow down recovery. As for each pressure level, oil production is recorded, until the system pressure reaches the atmospheric pressure.

The results can be used to infer what happens in the reservoir under the different pressure regime. More oil production and recovery is noticed from Scenario #3, followed by Scenario #1 and then #2. This verifies that the miscible $CO_2$ drive gives more recovery than the near miscible and immiscible drive.

## 3.4 Mechanisms and Methodology of Study – $N_2$ injection

### 3.4.1 Mechanisms of $N_2$ Injection IOR

Nitrogen injection has been applied in many oil field situations. These applications can be simplified into four general categories; pressure maintenance, immiscible displacement, miscible displacement, or as a driving agent for a miscible slug. The presence of structure, thick formations or gas caps tend to aid in the use of $N_2$.

Nitrogen ($N_2$) flooding has been an effective recovery process for deep, high-pressure, and light oil reservoirs. The mechanism for $N_2$ injection is mostly the same for the LTO air injection whereby the gas pushes the oil down-dip to the production wells and re-pressurizes the reservoir with the added advantage of no oxygen produced in the reaction. The resulting displacement of reservoir oil by the injected gas may be either miscible or immiscible which depends on the pressure, temperature and oil composition. In the case of Q131 oil block, the prevailing reservoir temperature tends to suggest that immiscible displacement will be achieved in $N_2$ injection because nitrogen has a lower viscosity, poor solubility in oil and requires much higher pressure to generate or develop miscibility. The validity of this point will be ascertained in the next section on estimation of $N_2$ MMP by using existing correlations.

As far as petroleum engineering is concerned, $N_2$ injection into oil reservoirs does not present any major problems. Its source and use in the oilfield injection is mainly from air separation. The cryogenic process had been mostly used in the past while cost effective membrane separation has been developed in recent years. In oil field applications, $N_2$ is a substitute for natural gas and $CO_2$ because it is more available and may be less costly than natural gas and $CO_2$. Nitrogen can also be considered for use as a chase gas in hydrocarbon miscible or carbon dioxide floods. Nitrogen is inferior to hydrocarbon gases (and much inferior to carbon dioxide) from an oil recovery point of view for the miscible process.

Several important concepts regarding immiscible nitrogen/oil displacements known are:

- The immiscible nitrogen/oil displacement process becomes efficient and desirable when gravity works to keep the low density nitrogen on top of the higher-density oil and when there is mass transfer of components from the oil to the nitrogen.
- The most optimum strategy for nitrogen injection involves injecting nitrogen into the crestal secondary gas cap, with the oil wells producing from as far down dip as possible, by maximizing the distance from the gas cap both vertically and laterally.
- The other nitrogen/oil compositional mass transfer effect is stripping or vaporization of light hydrocarbon components from the oil by the nitrogen. Nitrogen is able to strip or vaporize the

$C_1$-$C_5$ components which cause the density and viscosity of the oil to increase. This effect is very small and occurs with all types of oils but is more significant for lighter or higher API gravity oils. The physical properties of nitrogen such as density and viscosity are very favorable. In the reservoir condition, nitrogen has a less density than the hydrocarbon phases and preferentially stays in the top of the reservoir because of gravitation segregation.

### 3.4.2 Estimation of $N_2$ MMP for the Q131 Reservoir

Correlations for predicting MMP have been proposed by a number of investigators and are important tools in the selection of potential reservoirs for gas miscible flooding. The available literature data on $N_2$ miscible displacement are very limited, and the $N_2$ MMP correlations published should be used with care Clancy, et al. (1985). The input parameters for these equations are the molecular weight of $C_{7+}$ in the stock tank oil, the reservoir temperature, and the mole percent methane and intermediates in the reservoir fluid. The effect of the input parameters on MMP with $N_2$ is related to the API gravity of the oil. In a typical field situation, the transition zone needed to obtain miscibility will be short compared with the total length of the flow path. There are severe other empirical correlations to determine the $N_2$ MMP shown in Table 3.1, but we will discuss these two (Glasco and Hudgin empirical correlation) because this is a preliminary evaluation of the MMP of nitrogen.

**Table 3.1: List of $N_2$ MMP correlations**

| | | |
|---|---|---|
| Hudgins et al. (1990)[25] | $P_{MMP} = 5568\, e^{R_1} + 3641\, e^{R_2}$ | $R_1 = 792.06\,[C_2\text{-}C_6] / M_{C7+}\,(T^{0.25})$<br>$R_2 = 2.158 \times 10^{8}\,[C_1^{5.632}] / M_{C7+}\,(T^{0.25})$<br>$[C_1]$ = mole fraction of methane in the reservoir oil<br>$[C_2\text{-}C_6]$ = mole fraction of ethane through pentanes (including $CO_2$ and $H_2S$). |
| Sebastian and Lawrence (1992)[21] | $P_{MMP} = 4603 - 3283 * (CL*T/MW) + 4.776 * (CL^2 * T^2/MW) - 4.008 * CI * T^2/MW) + 2.05 * MW + 7.541 * T$ | CL = Mol fraction of methane in oil<br>CI = Mol fraction of intermediates (C2-C6 & CO2) in oil<br>T = Res Temp in Rankin<br>MW = Mol weight of $C_{7+}$ fraction in oil |
| Firoozabadi and Aziz (1986)[20] | $P_{MMP} = 9433 - 188 \times 10^3 * (C_{C2}\text{-}C_{C6}/(T^{0.25} M_{C7+}) + 1430 \times 10^3 * (C_{C2}\text{-}C_{C6}/(T^{0.25} M_{C7+})^2$ | $C_{C2}\text{-}C_{C6}$=Concentration of Intermediates,mol<br>T = Res Temp in degree F<br>$M_{C7+}$= Mol weight of heptance plus |
| Glaso (1990)[19] | $P_{MMP\,API<40} = 80.14 + 35.25\,P^*_{MMP} + 0.76(P^*_{MMP})^2$<br>$P^*_{MMP} = M_{C7+}^{0.66} T^{0.11} / C_{2-6}^{0.04} C_1^{0.33}$<br>$P_{MMP\,API>40} = -648.5 + 2619.5\,P^*_{MMP} - 1347.6(P^*_{MMP})^2 \quad P^*_{MMP} = M_{C7+}^{0.46} T^{0.25} / C_{2-6}^{0.12} C_1^{0.42}$ | $M_{C7+}$= molecular weight of C7+ in stock tank oil<br>$P_{MMP}$ = MMP, bar<br>$P^*_{MMP}$ = correlating number for calculating MMP<br>T = reservoir temperature, ℃<br>$C_2\text{-}C_6$=Concentration of Intermediates, mol %<br>$C_1$ =Concentration of methane, mol % |
| Hanssen (1988)[24] | $P_{MMP} = 0.5216\,([C_2\text{-}C_6]/M_{C7+}\,T)^{0.5236}$ | $C_2\text{-}C_6$=Concentration of Intermediates,mol % <br>T = Res Temp in degree F<br>$M_{C7+}$= Mol weight of heptane plus |

**A)** Glasco (1985), proposed from graphical methods and regression analysis, the following relation was developed for oil with gravity less than 40° API. The nitrogen minimum miscibility pressure $P_{mm}$ (in bars) can be determined as:

$$(p_{mm})_{API<40} = k_1(M_{C_{7+}}^{0.88} T^{0.11} / C_{2-6}^{0.64} C_1^{0.33}). \tag{3.3}$$

Regression analysis on these data yielded the following equation:

$$(p_{mm})_{API<40} = 80.14 + 35.25 p^*_{mm} + 0.76 (p^*_{mm})^2;$$
$$\text{where } p^*_{mm} = M_{C_{7+}}^{0.88} T^{0.11} / C_{2-6}^{0.64} C_1^{0.33}. \tag{3.3b}$$

For oil with gravity greater than 40° API, the following relation was developed:

$$(p_{mm})_{API>40} = k_2(M_{C_{7+}}^{0.48} / T^{0.25} C_{2-6}^{0.12} C_1^{0.42}) \tag{3.4}$$

Regression analysis on these data yielded the following equation:

$$(p_{mm})_{API>40} = -648.5 + 2619.5 p^*_{mm} - 1347.6 (p^*_{mm})^2,$$
$$\text{where } p^*_{mm} = M_{C_{7+}}^{0.48} / T^{0.25} C_{2-6}^{0.12} C_1^{0.42} \tag{3.4b}$$

[$C_1$] = mole fraction of methane in the reservoir oil; [$C_2$-$C_6$] = mole fraction of ethane through hexane; T = Temperature (in °C); k= constant

For Q131, with oil gravity of 35°API (less than 40°), the $N_2$ MMP was calculated using the equation (3.7) and **42.6MPa** was gotten as the $N_2$ MMP using the Glasco (1985) graphical and regression methods.

**B)** In the work **of Hudgins et al**. (1990); they developed the following empirical correlation based on the literature data reported for pure N 2 displacement and the data obtained from this work: Here, nitrogen minimum miscibility pressure $P_{mm}$ (in psia) is calculated as:

$$(P_{mm}) = 5568e^{-R_1} + 3641e^{-R_2},$$

$$\text{Where } R_1 = 792.06[C_2\text{-}C_5]/M_{C7+}(T^{0.25})$$

$$\text{And } R_2 = 2.158 \times 10^6[C_1^{5.632}]/M_{C7+}(T^{0.25}) \tag{3.5}$$

Where [$C_2$-$C_5$] = mole fraction of ethane through pentanes (including $CO_2$ and $H_2S$) in the oil; T = Temperature (in °F).

They also compared the results of the calculated MMP vs the experimental MMP of 4 different oils studied. Calculated MMPs for different nitrogen injection fields were also included. In their MMP calculations comparison, the average absolute deviation for the MMP prediction was approximately 2% for the different 14 oils that was tested.

For Q131, at reservoir temperature of 210°F, $R_1$ and $R_2$ was calculated to be 4.72 and 2.85 respectively. $MC_{7+}$ was also estimated at 298.33, therefore the $N_2$ MMP was calculated to be **41.5MPa** using the Hudgins et al. (1985) empirical correlation equation (3.9)

This correlation showed that the data obtained from this work were consistent with other reported data (Glaso O, 1985) when the effect of methane in the oil was considered. Greater amounts of methane and intermediate components ($C_2$ through $C_5$) in the solution gas result in lower $N_2$ MMP's. Therefore, in most cases, the $N_2$ MMP decreases as the oil's solution GOR increases. The $N_2$ MMP also increases slightly with temperature.

In this case study of Q131 block, the reservoir pressure (20MPa) is much less than the required $N_2$ injection MMP, which is calculated above to be ~ 41.5MPa, for single phase miscible displacement to occur. Thus, $N_2$ injection considered in this study will have an immiscible displacement drive.

### 3.4.3 Methodology of Study - Nitrogen Injection

The methodology is same as the air injection LTO (which produces >80% $N_2$ after reaction with oil in the reservoir) because they both have the same mechanism of flooding where gas front immiscibly pushes the oil down dip to the production well(s). So the model for the optimization process for $N_2$ injection uses the same immiscible displacement mechanism used for air injection LTO process, excluding the reaction kinetics part of air injection mechanism because no reaction occurs between the injected $N_2$ and the crude oil..

***Nitrogen Miscibility in Crude Oil:*** The miscibility between a reservoir oil and injection gas is achieved when only one phase (at critical conditions) results from a mixture of two fluids. In the miscible process, increased recovery is caused by transfer of light components from the oil into the gas phase, where the resulting gas develops miscibility with the oil. This process is characterized by an absence of a discrete fluid interface between the injected gas and the reservoir fluid. The multiple-contact situation is described best by use of a ternary diagram (Fig. 3.4). With $N_2$, it is a vaporizing-gas process. The extractable components are the $C_1$ through $C_6$ fraction of the oil. Multiple contact of gas with oil will continue until a sufficient amount of $C_1$ through $C_6$ has been vaporized into the $N_2$ to teach the critical point on the phase envelope. Miscibility is attained if the composition of the reservoir fluid lies on or to the right of the limiting tie-line for a given reservoir pressure. Thus, if $N_2$ is the injection gas, the concentrations of methane and the intermediate components in the oil are important factors to obtain miscibility between the oil and gas. The phenomenon of miscibility between $N_2$ and a hydrocarbon multicomponent system is complex. The

pressure at which $N_2$ mixes (soluble) with the oil is very high, so miscible $N_2$ displacement can only be encountered in a very high pressured reservoir.

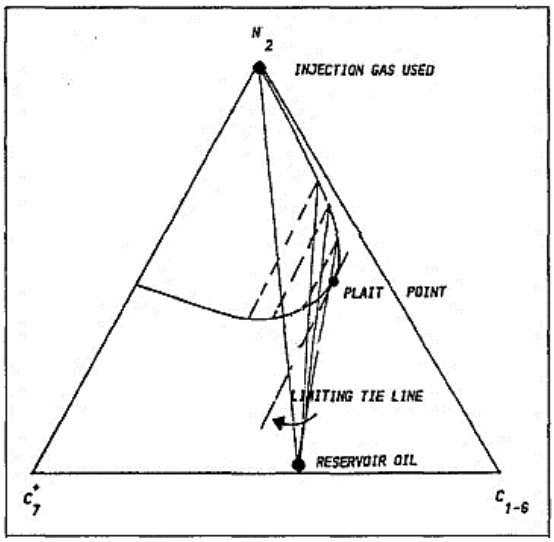


**Fig. 3.4: Pseudo-ternary diagram for nitrogen/reservoir- fluid systems.**

### 3.4.4 Experimental Studies of Nitrogen Miscible and Immiscible Displacement

Slim-tube displacement tests and core flooding tests can be performed with the oil to determine the displacement mechanisms of $N_2$.

#### 3.4.4.1 $N_2$ Slim-tube Displacement Tests

"Swelling" and "slim-tube" tests are commonly conducted in addition to standard PVT tests to determine conditions under which a candidate gas injectant becomes miscible with the oil. The tests are also used to determine phase volumes, densities, and viscosities for solvent/crude oil mixtures as a function of pressure and solvent content. The results of these tests are used to develop a set of equation of state (EOS) parameters that characterize the solvent/crude system. The resulting equation of state (EOS) model is then used to create phase behavior and viscosity input for simulation. This test is commonly used for determining MMP. No standard has been agreed on for the apparatus and testing procedure. The length and diameter of the slim tube and the packing material vary. Orr *et al. (*1982) reported a variety of characteristics of slim-tube experiments. Nouar and Flock (1984) reported that the length and injection rate will affect oil recovery. In previous tests, it was found, as they did, that increasing tube length increased oil recovery for miscible displacements but not for immiscible cases.

When $N_2$ gas is used as the displacing fluid, the concentration of methane and the $C_2$ through $C_5$ components in the reservoir fluid become very important factors in determining the miscibility pressure.

The slim-tube tests to determine oil recovery by displacing hydrocarbon fluids with $N_2$ is usually conducted in a coiled, one-dimensional stainless tube packed with sand. Fig. 3.5 is a schematic of the slim-tube apparatus (Hudgins et al., 1990). The column length of the tube can be variedThe porosity and permeability of the slim-tube column can be set according to the sand packs porosity and permeability properties. The PV's of the slim tubes is calibrated as a function of pressure and temperature. Both the reservoir fluid and the injection gas are transferred to the slim tube from bottles with a floating piston; the piston can be activated with refined mineral oil driven by an Altex high-pressure liquid chromatographic pump. A backpressure valve is placed close to the slim-tube outlet to reduce the dead volume, and a high pressure capillary sight glass is located between the packed column and the backpressure valve to allow visual observation of the effluent.

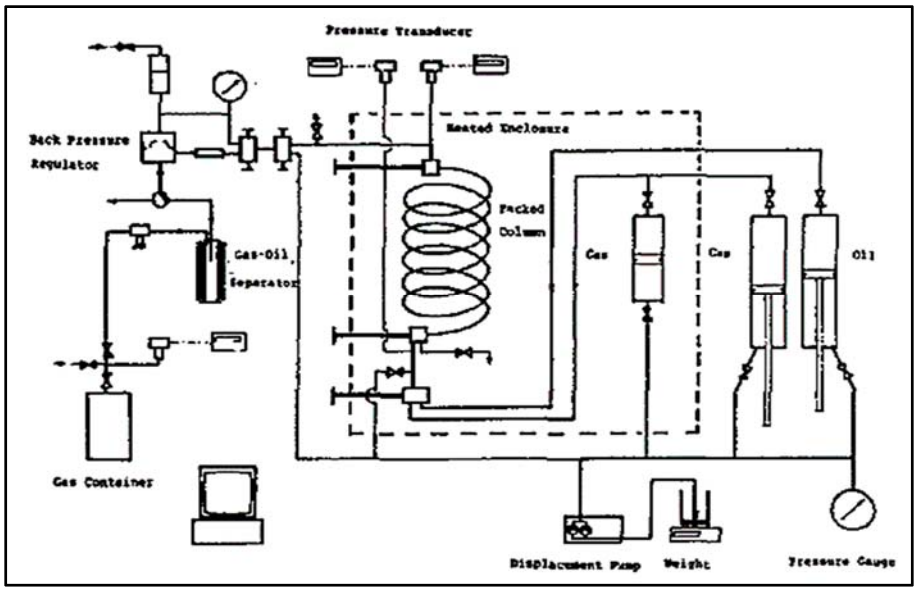


**Fig. 3.5: Schematic of slim-tube apparatus**

The effect of reservoir fluid composition, displacement velocity, column length, and temperature on slim-tube oil recovery with $N_2$ has been investigated by use of slim-tube experiments, phase behavior studies, and simulation tests (Glasco, 1990). The results show that the amount of methane and intermediates in the reservoir fluid has a significant effect on the MMP. The results also suggest that a reservoir fluid with low methane content needs a long path length and low displacement velocity to develop miscibility with $N_2$.

#### 3.4.4.2 Core Flooding Studies for $N_2$ Flooding

The use of a core to conduct flow studies offered the opportunity to perform laboratory tests under conditions as close as possible to actual reservoir conditions. One objective of this experimental study is to determine the displacement efficiency of the EOR process of $N_2$ miscible flooding in

laboratory cores. A second objective of the core flooding study was to investigate the relative recovery efficiency of different injection schemes for $N_2$ miscible flooding, such as tertiary-vs.-secondary recovery.

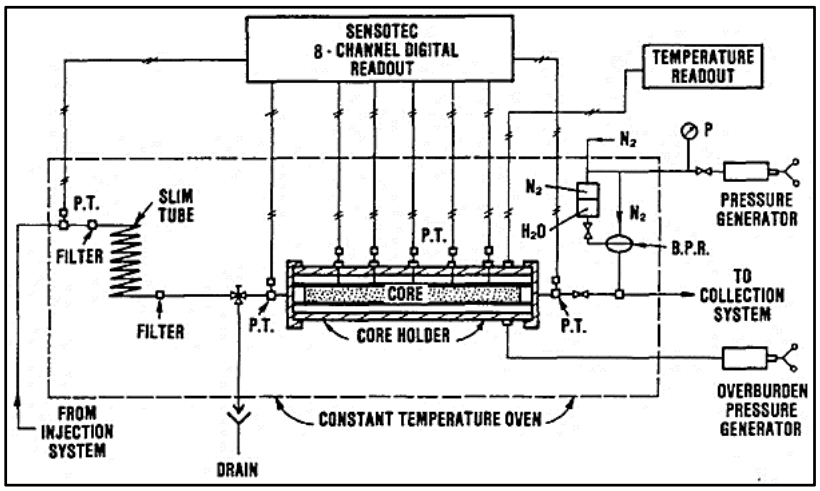


**Fig. 3.6: Gas miscible coreflooding test apparatus**

A typical example of the core flooding equipment is shown above in the Fig. 3.6. A biaxial coreholder is usually used. Biaxial meant that the core was stressed by the overburden pressure in all three dimensions, but the axial stress could not be varied independently from the other two dimensions. The coreholder's body could be made of high degree stainless steel, and the wetted parts are usually made of Hastelloy-C (an alloy composed of nickel, molybdenum, chromium and iron) for corrosion resistance. The apparatus showed below can be designed for a maximum pressure rating of 70MPa at 50°C. To eliminate leaks that can be caused by gas diffusion through the rubber, liquid (water) is usually used in the annulus between the sleeve and the coreholder body.

# CHAPTER 4: AIR INJECTION METHOD FOR IOR

## 4.1 Detailed Notes on Air injection for IOR

In this research, special interests are placed on understanding the mechanism of air injection for IOR because of its safety uncertainties in oilfield application. Therefore this study has to include detailed experimental studies to determine the oxygen consumption and IOR capabilities of the whole process of air injection into a light oil reservoir, with respect to Q131 block and its crude oil. Air injection can be a technically and economically attractive IOR technique in large prospects, particularly for deep and light oil reservoirs with low and ultra-low permeability, in which the application of conventional water injection technique is limited and other techniques are unavailable or uneconomic. Traditionally, air injection has been mainly used in heavy oil reservoir, where the heat generated by HTO or in-situ combustion is necessary for the recovery process. On the other side, air injection has also been successfully applied in many light oil reservoirs for more than 30 years and proven to be efficient in the recovery of light oils, and commonly referred to as high pressure air injection (HPAI) (Kumar et al., 1996, 2007, 2010; Fassihi et al., 1996; Hu et al., 2012). HPAI can be understood as the injection of compressed air into a deep light oil reservoir of high pressure and temperature. However, there has been an argument on which reaction process (HTO or LTO) is prevailed in light oil reservoirs, or whether heat generated during oil oxidation is essential to the recovery process as the case in heavy oil recovery (Ren et al., 2002; Greaves et al., 2000b). This study also focuses on addressing this eminent issue.

When air is injected into a light oil reservoir, reaction front or in-situ combustion can be initiated with oxygen in the injected air reacting with part of the reservoir oil at an elevated temperature. The reaction products include oxidized oil and a flue gas composed of primarily nitrogen and carbon oxides. The resulting flue gas mixture provides the main mobilizing force to drive the oil downstream of the reaction zone to production wells. Therefore, the IOR mechanism of air injection is complicated, including flue gas drive, oil-gas miscibility interaction, and high-temperature front sweeping. Chemical reactions, heat generation and transfer, and three-phase (water-rich, oil and gas) flow in porous media are the physical and chemical processes involved in HPAI. Based on the experience gained in field projects and laboratory studies, the following statements can be made in favor of the air injection process for light oil reservoirs in terms of cost of injection, gas sources, field operations and IOR:

- The advantages of air over other injectants, like hydrocarbon gas, carbon dioxide, nitrogen or flue gas are its unlimited availability and it does not pose any supply constraints. Thus, it has

significant cost benefits as an alternative to other gases. For oilfield applications, it does not need special purification, transportation or storage requirement, and its compression cost is similar to other types of gas injection. Air injection can be applied as a secondary or tertiary recovery technique on existing infrastructure in different oilfields (Fassihi et al., 1997).

- Air injection has been proven to have superior injectivity over water injection for low and ultra-low permeability reservoirs (Kumar et al., 2006). Air injection can also be used for pressure maintenance, gas flooding, as an alternative to water injection in areas with scarcity of water, and also for fields with large injector-producer distances (Hughes and Sarma, 2006). There is less requirement for post breakthrough water handling and disposal in an air injection project as compared to water-flooding projects. Like other gas injection, air injection can provide faster re-pressurization than water due to its high compressibility. Preference for gravity drainage to push the oil down-structure due to relative permeability effects (Gillham et al., 1997). It can also be applied in super-wet fields [14].
- Field experience has indicated technical and economic success in virtually all projects to date (Kumar et al., 2010; Fassihi et al., 1996, 1997; Gutierrez et al., 2008b).

The basis of the air injection process is to remove oxygen from the injected air through a reaction mechanism (LTO or HTO) for safety concerns, and to enhance oil production via one or a combination of the following IOR mechanisms, including reservoir pressurization or pressure maintenance, reduce residual oil saturation through flue gas stripping and oil swelling, high displacement efficiency and mobilization of oil from the reaction zone, gas driving, gravity drainage effect and water alternative air injection.

Air injection has some inevitable limitations, such as corrosion and safety problems due to the existence of oxygen. Explosion of natural gas mixture with oxygen in injection or production sites is the main safety risk if oxygen is not consumed or removed in the reservoir. Oxygen and $CO_2$ corrosion can cause severe damages of tubes and casing in wellbores. It also poses difficulties in handling produced gases, and the need to use fabricated compressors that may make air injection a costly operation. But in regards to all of these, various technological advancements have been achieved to reduce these effects and ensure a successful and safe application (Gillham et al., 1997). There are several effective corrosion and safety precautions reported on on-going air injection projects (Gutierrez et al., 2008a), such as injection of high temperature synthetic lubricants into injection lines to prevent corrosion, isolation of the annulus with a permanent packer and corrosion inhibitors, and using special anti-corrosion alloys for tubing and casing. For safety control in terms

of oxygen explosion, the main issues are to prevent natural gas back flow into injection wells and to consume oxygen in the reservoir through an effective reaction scheme.

It should emphasized that not all the reservoirs are suitable for air injection, therefore, it is essential to select appropriate candidate oil reservoirs by performing various laboratory tests and reservoir evaluation in terms of reaction and IOR mechanisms (Greaves et al., 2000a). The technical aspects include generation of numerical models to simulate the acquired laboratory test results and obtain enhanced oil recovery predictions (Kumar et al., 1987; Kuhlman et al., 2000). Typical laboratory research and reservoir simulation have shown that oxygen can be completely consumed in the reservoir by a LTO reaction process, and there is a significant separation between the reaction front and the flue gas displacement front (Ren et al., 2002; Moore et al., 2002). The economics and safety factors are also very important in the candidate reservoir selection for the process. However, there is always concerns on new field application over the reaction mechanism prevailed in the reservoir, its effect on oxygen removal and the thermal effect on oil recovery. It is advisable to conduct a detailed laboratory study and run a field pilot test to know if the application of the air injection for IOR is feasible in the candidate reservoir.

In this study, the mechanisms of reaction and IOR involved in the process of air injection in low permeability light oil reservoirs are analyzed based on field projects review, laboratory and reservoir simulation results of the Q131 light oil block. The study also highlighted the importance of gravity stabilized gas injection process in the Q131 block that has a high dip, which is considered to be one of the most efficient for gas injection IOR processes to achieve IOR in mature light oil reservoirs.

## 4.2 Air injection LTO Process

### 4.2.1 Description

When air is injected into a reservoir, the oxygen contained in the air (composed of approximately 78 % $N_2$ and 21% $O_2$) reacts with the hydrocarbon in place by oxidation reactions. Heat is generated in these reactions. When the thermal losses through the rock and formation fluids are limited compared with the heat generated by the reactions, the temperature in the reservoir increases. The oxygen in the injected air is reacted or consumed by the oil in a confined zone called reaction front or combustion front (in the case of in-situ combustion process). The length of this front depends on the air injection rate, the characteristics of the oil and the reservoir formation. In light oil reservoirs (API gravity higher than 35°), typical reaction front temperatures of 200°C to 350°C) are speculated. The produced combustion gases consist of $CO_2$ and CO, with the ratio $CO/CO_2$ depending on the temperature conditions and the nature of the oil (Bin et al., 2010; Niu et al., 2011).

In the reservoir, four main zones are distinguished as represented in Figure 4.1 (Ren et al., 2002; Moore et al., 2002):

1. The zone swept by the reaction front, where the residual oil saturation is very low and the temperature higher than the initial reservoir temperature. The temperature profile in this area depends on the reaction mode, the initial reservoir temperature and the heat transfer parameters of the formation.
2. The reaction front zone, is a thin zone where oxygen is used up. The temperature of this zone is typically between 200°C to 350°C). About 5% to 10% of the original oil in place (OOIP) is reacted, and the reaction produces a flue gas containing a lot of $CO_2$ and CO (typically 85% of $N_2$, 13% of $CO_2$, 2% of CO) and sweeps the reservoir oil downstream.
3. A zone downstream of the reaction front where thermal effects occur and participate in the formation of an oil bank. This oil bank is driven by the flue gas and the steam generated in the reaction, which can provide extra benefits for oil recovery.
4. A wide zone more downstream of the reaction front, where no thermal effect occurs. Here, the reservoir temperature is at its initial value. This zone contains original oil, not affected by the thermal effects. Gas related effects, e.g. gas swelling is dominant in this zone. Most of the produced oil comes from the drainage of this zone by the flue gas. Therefore, air injection into a light oil reservoir via LTO process is comparable to a classical gas injection with flue gas. However, differences exist between these two, because in-situ oxygen consumption for safety purposes must be ensured in air injection and also an additional recovery is expected from the thermal effects at the end of the project especially when the reaction front and oil bank is close to the producing wells.

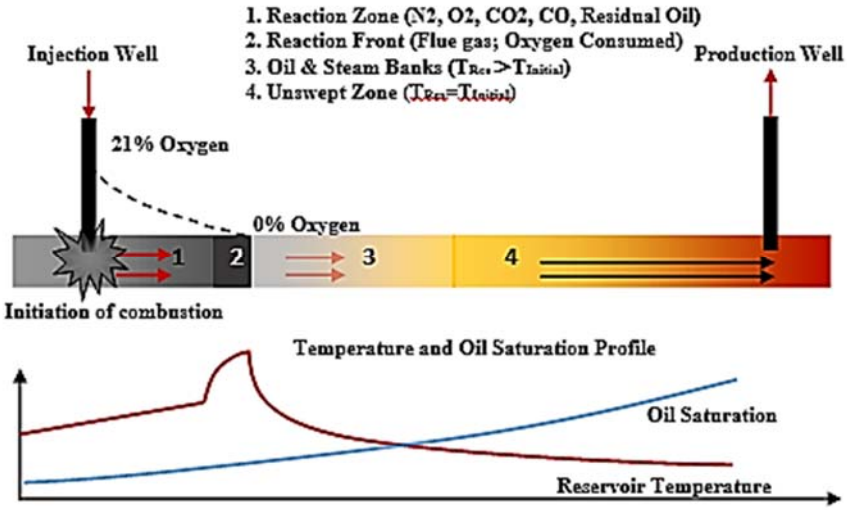


**Fig. 4.1: Conceptual representation of air injection thermal & flue gas drive process.**

### 4.2.2 Air Injection LTO Reaction Model

A reaction model, i.e. a rate equation and also stoichiometry, is needed in numerical simulations to predict oxygen consumption and any thermal effect occurring during the air injection process. The oxidation of hydrocarbon is a very complex process, involving hundreds of intermediate compounds. However, for the purpose of reservoir simulation, a simplified model was used. This model should represent the main features of the reactions occurring at reservoir conditions, i.e. the oxygen consumption rate and the final main products. Small batch reactor (SBR) experimental results obtained are usually used to quantify the reaction rate from the reduction in the oxygen partial pressure. The reaction products were determined by analyzing the produced gas (Greaves M. et al, 1999b).

Chemical analysis results have shown that carbonyl compounds are produced in the oil after the LTO reaction (Fassihi et al., 1990). The possible reaction products and paths of the LTO process of hydrocarbons can be summarized as shown in Figure 3.3 (Greaves, et al. 2000). The decarboxylation reaction may be responsible for the further reaction of oil oxides, leading to $CO_2$ and CO production

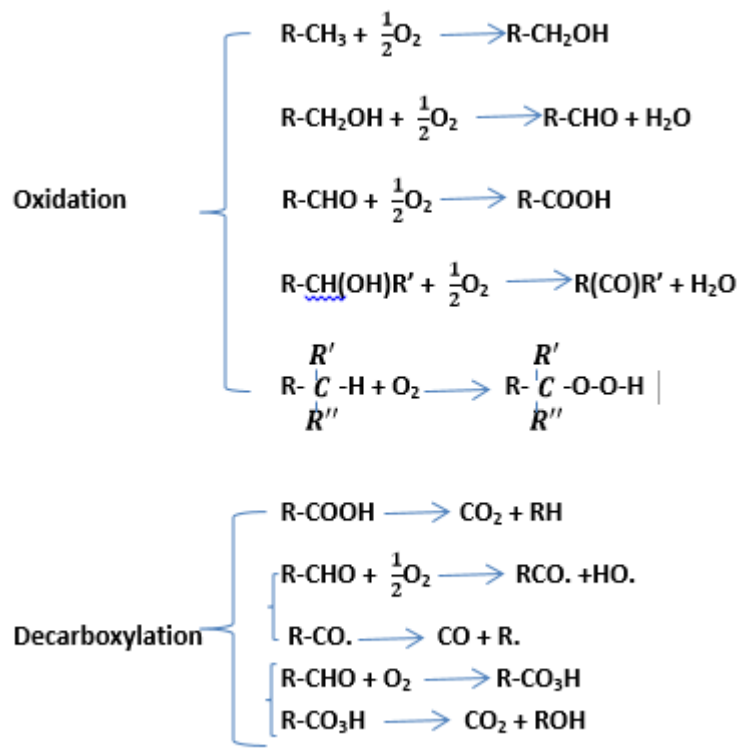


**Fig 4.2: Reaction schemes of LTO of hydrocarbons.**

A simplified description of the mechanism of the possible paths leading to the generation of carbon oxides in the LTO process is shown in Fig. 3.4. Several free radical reactions are involved in this mechanism, and $CO_2$ is the final gas product.

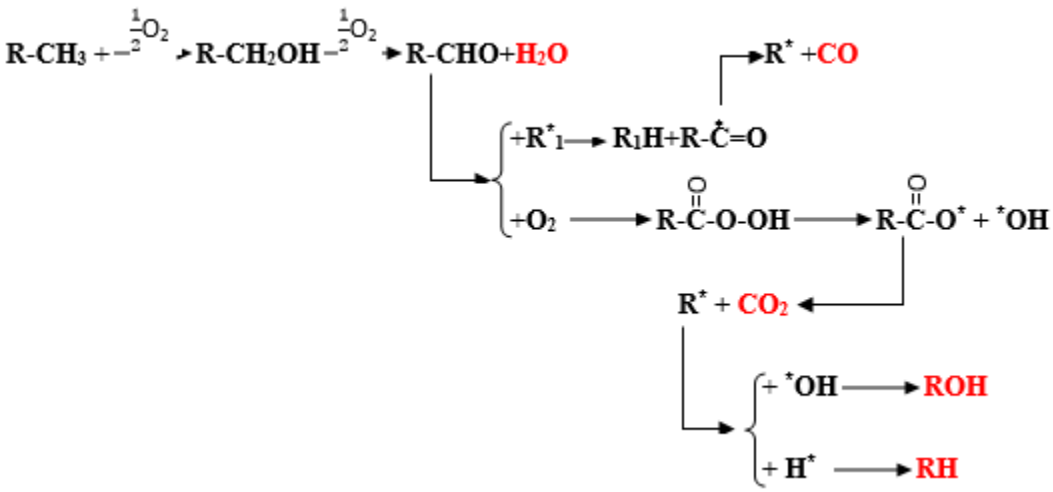


**Fig. 4.3: Mechanism of the LTO reaction paths during air injection**

The LTO reaction mechanisms can be described in details as follows:

(1) The molecules of hydrocarbon compounds are primarily oxidized into intermediate products, such as carboxylic acid, aldehyde, ketone, alcohol, ether, etc.

(2) Either the intermediate products may be directly subjected to the decarboxylation reaction and generate $CO_2$, CO, and water, or they can be first oxidized into hyperoxides and then undergo a decarboxylation process to produce $CO_2$, CO, and water.

(3) During the decarboxylation reaction, large oil components may transform into lighter components, which causes a higher activation energy requirement for further oxidation, and finally, this may terminate the reaction at certain temperatures.

The complete reaction scheme is very complex, and may involve hundreds of intermediate products and reactions. However, in an overall sense it can be described by two reactions: oxidation, which consumes oxygen and generates oxygenated compounds; and decomposition, which produces carbon oxides. The reaction rates for these two reactions are generally not the same. A general reaction scheme (two-step model) for the oxidation and decarboxylation processes can be summarized by the following two-step reaction model (Bin et al., 2010; Niu et al., 2011; Ren et al., 2002)

***Oxidation Process:***

$$C_xH_y + \frac{3}{2}O_2 \rightarrow C_xH_{y-2}O_2 + H_2O \qquad \text{(exothermic reaction)} \qquad (4.1)$$

***Decarboxylation Process:***

$$C_xH_{y-2}O_2 \rightarrow C_{x-1}H_{y-2} + CO_2 \quad \text{(endothermic reaction)} \qquad (4.2)$$

The reaction kinetics parameters are usually obtained from the displacement flooding and oxidation tube tests.

### 4.2.3 Kinetics Model of LTO Reaction

An Arrhenius kinetics model can be used to describe the LTO reaction rate (in terms of oxygen partial pressure reaction rate) as a function of temperature, oxygen partial pressure and oil concentration. The LTO reaction rate expressed by an Arrhenius-type equation, in which the kinetics parameters are determined from the SBR experimental data obtained at different temperatures. The overall rate of pressure reduction is related to the rate of reduction of oxygen partial pressure, due to the consumption of oxygen by LTO reactions.

$$\frac{dP_x}{dt} = k_0 e^{-E/RT} \left[P_x\right]^m \left[oil\right]^n \qquad (4.3)$$

Where *E, Ko*, m and n are the so-called reaction kinetics parameters, which are relevant to oil and reservoir rock properties, and can be derived from experimental results. Usually, when there is no mass transfer limitation, oil oxidation can be assumed as a first order reaction (m=1 and n=1) with respect to oil concentration and oxygen partial pressure. This is also required for modeling the oxidation reaction in reservoir simulation in order to maintain material balance in case where oil and oxygen were completely consumed in some area. However, in order to derive the activation energy *E* from the small batch reactor (SBR) experiments, the above model needs to be simplified (Greaves M. et al, 1999). Because the reaction rate is very low at low temperatures, and it is essentially independent of oxygen partial pressure, m can be assumed to be zero. Since the volume of oil loaded in the reactor is greatly in excess compared with limited amount of oxygen, n is also zero. The model is simplified as:

$$\frac{dP_x}{dt} = k_0 e^{-E/RT} \qquad (4.4)$$

The reaction rate can be calculated from the measured rate of the decrease in the total pressure in the reactor, and is a function of the absolute temperature only. For reservoir simulation studies, the reaction constant $k_0$ can be adjusted based on the results of the oxidation tube experiments and field data. Due to the complicity of the LTO reactions, only material balance is considered in the

stoichiometry, while the molecular change of the oil component is not considered. The activation energy and pre-exponential constant of the reactions was figured out by matching of experimental results. The results are shown later in the Numerical simulation sections 5.5.1 and 5.5.2.

### 4.2.4 Thermal Effect of the Reaction Zone

The influence of the thermal zone is secondary in IOR during the early life of an injector. The subsequent impact of the oil displaced directly by the reaction zone will depend on the effectiveness of the generated flue gas on oil displacement from outside of the reaction region.

A simulation study done by Chen et al. (2013) to determine the thermal effects of LTO reaction using a conception model, and showed that the thermal effect of LTO can contribute 2-3% OOIP on IOR in comparison to $N_2$ injection (no thermal effect). This incremental value is not high, but can be relatively significant for tertiary process. The thermal effect of the air injection process can vaporize some light oil compounds into the gas phase to generate a flue gas flooding (consisting of $N_2$, $CO_2$, and light hydrocarbons). High temperature can further reduce oil viscosity and make the oil swell, cause light oil components to evaporate, leading to the increase of movable oil and the decrease of residual oil, which can offer an additional effect on IOR. Also, the thermal effects can promote a further decarboxylation reaction, which generates more $CO_2$, enhancing the oil displacement effect of flue gas. Therefore, thermal effects in light oil reservoir LTO air injection process only indirectly aid in improving oil recovery.

Important parameters that help to evaluate the thermal effects in light oil reservoirs include air requirement, AOR, oxygen utilization function, H/C ratio, etc. The air requirement is one of the primary factors influencing the production cost for an HPAI project. The quantity of air required to recover $1m^3$ of oil, or air to oil ratio (AOR), is the basic parameter needed to evaluate the economic performance of the projects. The hydrogen to carbon ratio (H/C), or the percentage of oxygen converted to $CO_2$ (oxygen 'utilization) provides an indication of the reaction types (LTO or HTO). These parameters are practically obtained from the reaction tube test and are very relevant in the planning of air injection projects.

## 4.3 Review and Analysis of Prominent Air Injection Field Projects

The pioneer field pilot of air injection in light oil reservoirs began in 1963 on Sloss Field in Nebraska (Parrish et al., 1974) and then followed by the pressure-maintenance project in West Heidelberg of Mississippi, which commenced in 1971 (Gillham et al., 1998a; 1998b). Both projects were operated by Amoco. HPAI process was first commercially introduced as a secondary recovery technique in the North and South Dakota parts of the Williston basin, (USA). It was started in 1979

and continues to be a technical and economic success (Fassihi et al., 1996; Kumar ey al., 2007, 2010). Air injection in the Buffalo field of South Dakota reported to have recovered a total of 17.2 million barrels of incremental oil or 9.4 percent of the OOIP. The cumulative air/oil ratio (AOR) after 29 years of air injection is approximately 14 Mscf of air/bbl of incremental oil (Gutierrez et al., 2008b; Kumar et al., 2010). Another significant milestone in the advance of HPAI was the Medicine Pole Hills Unit HPAI projects in the North Dakota part of the Williston basin, which started in 1987 (Kumar et al., 1996). These reservoirs in the Williston basin are typically deep, high pressure, thin dolomites with low permeability in the range of 10-20mD and water flooding these reservoirs was very challenging due to poor injectivity and large well spacing.

Other reported successful air injection projects include Chevron-owned W. Heidelberg Gulf; Total owned Handil oilfields in Indonesia (Gillham et al., 1997; Pascual et al., 2005; Duiveman et al., 2005). In China, there are Baise oilfield (1996), Hu Central Plains 12-Block Zhongyuan (2007), Tuha (2003), Xinjiang oilfield (Hou, et al., 2010) and recently Q131 block in Liaohe oilfield (Ren et al., 2011; Hongman et al., 2008). The ground breaking successes of air injection in these fields (especially in the Williston basin), and the availability of their laboratory, simulation, field pilot, and long term field performance results have immensely contributed to the global implementation of the air injection for IOR.

**Table 4.1: Detailed reservoir characteristics and IOR potentials of four (4) air injection projects.**

| | Buffalo Red River Unit * | Medicine Pole Hills Unit * | Horse Creek ** | Coral Creek *** |
|---|---|---|---|---|
| **Place (Operator)** | S. Dakota (Koch) | N. Dakota (Continental) | Montana (Shell) | N. Dakota (Total Minatome) |
| **Project Initiation Date** | Feb. 1979 | Oct. 1987 | May 1996 | June 1997 |
| **Depth to Reservoir, ft.** | 8450 | 9500 | 9125 | 8850 (Ave.) |
| **Average Porosity** | 20% | B-19%, C-15% | 16% | 15.5% |
| **Average Permeability, md** | 10 | B & C 5 | 10-20 | 2-8 |
| **Average Net Pay, ft.** | 10 | 18 | 20 | 45 |
| **Average Water Saturation** | 45% | B-37%, C-48% | 35% | 40% |
| **Reservoir Temperature °F** | 215 | 230 | 220 | 206 |
| **Initial Reservoir Pressure, psi** | 3600 | 4120 | 4000 | 5000 |
| **Oil Gravity, API** | 30 | 39 | 32 | 33 |
| **Solution GOR, scf/stb** | 120 | 525 | 205 | 250 |
| **Original OOIP, MMSTB** | 37 | 40 | 45.74 | 104 |
| **Secondary Recovery** | None | None | None | Water Injection |
| **Estimated Primary Production, MMBBLS** | 2.2 | 6 | 4.536 | 2.83(22.71MM from water-flooding) |
| **Estimated Incremental Production, due to Air injection MMBBLS** | 5.8 (Dec, 2007) | 5.7 | 7.6 | 7.3 |
| **Total Recoverable Reserves, MMBBLS** | 8 | 11.7 | 12.14 | 32.3 |
| **Primary Recovery Factor (RF), %** | 5.95 | 15 | 9.92 | 24.0 (including water-flooding) |
| **Incremental RF,%** | 15.67 | 14.25 | 16.62 | 7 (Ave.) |
| **Total RF, %** | 21.62 | 29.25 | 26.53 | 31.0 |

***Data from Kumar et al., 2010; 1996; Fassihi et al., 1997; Gutierrez et al., 2008b; except Air requirement data (from Gladnt et al., 1999)**
****Data from Watts et al., 1997; Clara et al., 1998**
*****Date from Glandt et al., 1999**.

In a comprehensive review of previous major high pressure air injection projects, Tables 4.1 and 4.2 present detailed summaries and comparative assessment of field implementation and experimental testing results of four HPAI projects which includes Buffalo Red River Unit (BRRU); Medicine Pole Hills Unit (MPHU), and the two younger HPAI projects in the nearby Horse Creek and Coral Creek fields operated by Total Minatome Corporation and Shell respectively (Gladnt et al., 1999; Watts et al., 1997; Clara et al., 1998). Previous and current successful air injection projects can provide a good reference to understand its mechanisms and for the design of new projects being considered for high pressure air injection (HPAI) application.

**Table 4.2: Field & experimental results of four (4) air injection projects.**

| | Buffalo Red River Unit * | Medicine Pole Hills Unit * | Horse Creek ** | Coral Creek *** |
|---|---|---|---|---|
| **Cum. Air injected, Bscf** | 262 (Dec.2009) | 12 (Dec.1993) | 4.55 (May '96-Dec.1997) | N/A |
| **Air Oil Ratio (theoretical), Mscf/stb** | 20.3(33) | 8(16) | N/A(18) | N/A (19.6) |
| **Air Requirement, scf/sci-fi rock** | 176 (Ave.) | 370 | 175 | 235 |
| **Air Utility, Mscf/incr. bbl** | 14.5 (Ave.) | 12-20 | N/A | N/A |
| **Apparent H/C Ratio,** | 2.0 | 1.24 | 1.65 | 1.73 |
| **Oxygen Utilization,%** | 95 (Ave.) | 99(at higher T&P) | 90 | 96 |
| **Produced gases, % $O_2$; $N_2$; $CO_2$; $C_{1-5}$, $C_{6+}$** | 1.08; 81.16; 13.68; 3.75; 0.33 | <1; 72; 13.1; 13.1 plus trace gases | N/A | 4; 90% CO2+N2; others are HC gas; 12.8; 3.2 |

**Table 4.3: Comparative assessment of the average reaction zone volume and RF of 3 air injection projects.**

| | BRRU | WBRRU | MPHU |
|---|---|---|---|
| **OIIP, MM bbl** | 37 | 28.99 | 40 |
| **No. of years of injection*** | 30 | 22 | 6 |
| **Ave. Daily Injection Rate MMscf/D** | 12 | 3 | 9 |
| **Reaction Zone Vol. %** | 12 | 7 | ~2.4 |
| **~% Ave. Reaction Zone Vol. per year** | 0.4 | 0.32 | 0.4 |
| **~% Ave. incr. RF per year** | 0.61 | 0.36 | 0.29** |

*** Based on the years with available information for the different fields.**

**** Lower average recovery per year because of the number of years sampled is relatively small; the RF incremental rate will definitely increase in the later period of air injection.**

In addition, Table 4.3 below shows a relationship between percentages of average burned or "reacted" volume per year and the corresponding average incremental RF per year in the three air injection fields including the Buffalo (1978), West Buffalo (1987) (Kumar et al., 2010) and Medicine Pole Hills (1987) Units. The Buffalo and MPHU fields share the same geologic formations as they are both of the Williston basin in the South and North Dakota respectively of the USA. From the table below, it is observed that at the specified injection rate, the reaction front moves progressively in these low permeability fields, and accompanied by a proportional increase in recovery factor as the reaction front progresses. But it is also observed that the incremental RF

per year is inversely proportional to the median volume of the reaction zone per year indicating that the operation is in the LTO mode, and it can generate a flue that primarily drives the oil to the production wells, but the reaction and the size of the reaction zone or thermal effect did not significantly affect the recovery factor.

In summary from the above comprehensive review and analysis of the field projects of air injection conducted in terms of IOR and reaction mechanisms, it is observed that the IOR mechanisms of air injection vary from field to field, but it is notable that its operation in light oil reservoirs with low permeability is mainly in the LTO mode. Also it can generate flue gases composing of $N_2$, $CO_2$ and light hydrocarbons that primarily drive oil to production wells, while the reaction and the size of the reaction zone or thermal effect did not significantly contribute to the oil recovery.

## 4.4 Important Parameters for Air injection Application

Some of the key parameters that need to be considered for any high pressure air injection (HPAI) project include (Turta and Singhal, 1998; Moore et al., 2002):

- Remaining recoverable OOIP at the start of air injection: This helps decide the economic viability and operation time span of the project.
- Ability to inject air into the reservoir: The selection of the appropriate equipment for air compression and injection, plays an important role in the overall process. Less amount of injected air from the compressor(s) could lead to insufficient ignition, which will adversely affect the oxidation process and reaction front propagation.
- The ability of the oil to spontaneously ignite and sustain stable oxygen uptake reactions over the life of injectors: Laboratory testing of oil provides useful information concerning oil reactivity, oxidation characteristics, kinetic data, pressure effects, air and fuel requirements, product gas composition, air/oil ratios and other production related data (Fassihi et al., 1990, Pusch et al., 1991).
- Numerical Modeling: It is seen as a valuable and a cost effective step in the screening processes and optimizing HPAI implementation. It becomes very useful if immiscible or miscible gas flooding is considered to be the dominant recovery mechanism. Compositional simulators can accurately model immiscible/miscible gas flooding processes. However, modeling of the reaction zone(s) becomes much more difficult as the thermal fronts are usually very narrow, with respect to grid block size. Recent advances in front tracking techniques (Davies, 1989), which help minimize numerical dispersion and maintain proper temperature profiles ahead of the combustion front, may improve results.

- Regular monitoring of the product gas vent rates and composition: This is very important as the gas phase composition data provides information about mean temperatures, oxygen and carbon dioxide concentrations, which is useful in determining the efficiency of the overall process.
- Operating Strategies: In the event that the air injection process is not performing according to the expectations, assuming sufficient air is being injected, the best approach is to shut in the injector believed to be serving the producer. This affects the oxygen partial pressure and may change the oxidation mode from one of low temperature to high temperature. This change in the oxidation mode is often reflected in elevated amounts of carbon dioxide in the product gases. If no change in the carbon dioxide/nitrogen occurs following the shut-in, it is safe to assume that the temperatures in the reaction zone are lower than that required for effective operation, which may be due to that the injector in question does not possess good communication with the reservoir.

## 4.5 Air injection Experimental Studies and Results

The oxidation characteristics of a specific crude oil needs to be evaluated by testing the specific reservoir fluid sample under existing reservoir conditions. The experimental study is designed to determine if and how the crude oil will react in the reservoir, and the behavior of the system as any further reactions occur. It is also important to evaluate the main IOR mechanisms of air injection in the reservoir. The experimental results will provide the key data for field design such as injection rate, air flooding efficiency, and reaction kinetic parameters used in reservoir simulation. Importantly, it is useful in evaluating the potential economics of the project (Hughes et al. 2006).

Different types of tests are available and these operate at different pressures, temperatures, and hence can simulate different conditions and provide different information. The most common and widely applied tests for screening and design of an air injection project are Accelerating Rate Calorimeters (ARC) tests in adiabatic conditions, Combustion Tube experiments at quasi-adiabatic conditions and Oxidation Tube runs at isothermal conditions. Laboratory testing of potential air injetion candidates, under conditions of reservoir pressures and temperatures, serves several important functions as follows (Moore et al. 2002):

1) It provides an indication of whether the oil will react in the desired oxidation mode at reservoir conditions. Also, it aims to characterize the reaction mode (LTO or HTO) and the movement of the reaction front and its displacement behavior.
2) It determines the displacement and recovery efficiency by air injection.

3) To assess the oxygen consumption by the oil at reservoir conditions.
4) It can provide parameters, such as air and fuel requirements (how much air is needed to sweep a unit volume of reservoir, and how much fuel will be consumed in that process), and air/oil ratios that can be used in conducting preliminary economic assessments of field projects.
5) It determine the kinetic parameters of the chemical reactions (between oil and oxygen) for reaction and thermal simulations,
6) It can supply kinetic data that can be used for numerical simulations of the HPAI process.
7) It can provide produced gas compositions, water compositions and other production related data that have been shown to correlate well with the field, and can be used to monitor field performance.

The experiments conducted for this study includes the air flooding displacement to determine the IOR potentials of the air injection into the sand packs of similar reservoir characteristics as that Q13, and LTO reaction experiment to determine the oxygen consumption and $CO_2$ conversion rate of the air injection process. The following sections shows a detailed presentation of these experiments.

### 4.5.1 Air Flooding Experiments at Isothermal Conditions.

**Experimental Set-up and Results**

The displacement experiment of air injection using oil samples from the Q131 block was conducted at 98°C of the reservoir temperature and at 20MPa to study the displacement efficiency under air injection at various conditions. A core flooding set-up (Fig. 4.4) was used, in which a sand-pack tube of 25mm inner diameter, and 600 mm length was used to hold the oil sands. The experiments were performed in sand-packs with relatively low permeability ranged from 29md to 62md, and at different slanted angle to simulate the reservoir features (dip) of the Q131 block, and the experimental data and results are shown in Table 4.4 and Fig. 4.5. The presented results show that the oil recovery of air flooding process (without primary water flooding) is relatively high, in comparison with conventional water flooding which normally have the displacement efficiency of about 30% of OOIP. Oil recovery is mainly affected by the characteristics of the core materials, such as porosity, permeability and wettability, as well as the oil properties, namely composition, viscosity and density (Greaves, et al. 1998). It is also affected by the residual oil saturation and air injection rate. The oil recovery from the tests was generally high, and more than 40% OOIP was recovered. However, when air injection is used as a tertiary recovery method or the reservoir oil saturation is near the residual after water flooding, it may become much less effective.

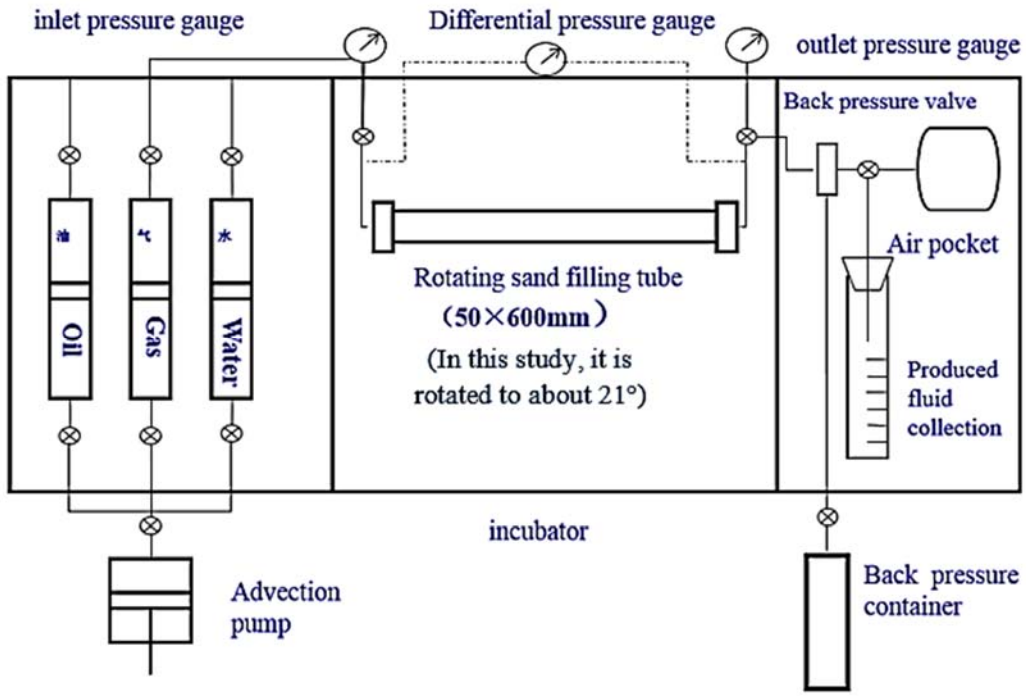


**Fig. 4.4: Schematics of the Core Flooding Experimental Set-Up Used for Air Injection**

**Table 4.4: Displacement Experiment Results of Three Sand-Pack Samples from Q131 Block**

| Test | Pore,% | Permeability, md | So, % | Dip, ° | Injection rate, ml/min | PV at Gas Break-through | Oil recovery, % |
|---|---|---|---|---|---|---|---|
| **A (No gas)** | 35.7 | 53 | 82.3 | 0, horizontal | 0.1 | 0.21 | 33.9 |
| **B (No gas)** | 36.0 | 69 | 70.7 | 45 | 0.1 | 0.29 | 37.2 |
| **C (No gas)** | 31.3 | 29 | 71.7 | 80 | 0.05 | 0.37 | 40.5 |
| **Live oil-1** | 22.8 | 3.71 | 40.3 | 80 | 0.05 | 0.42 | 45.93 |
| **Live oil-1** | 29.6 | 8.84 | 42.5 | 80 | 0.03 | 0.48 | 48.65 |

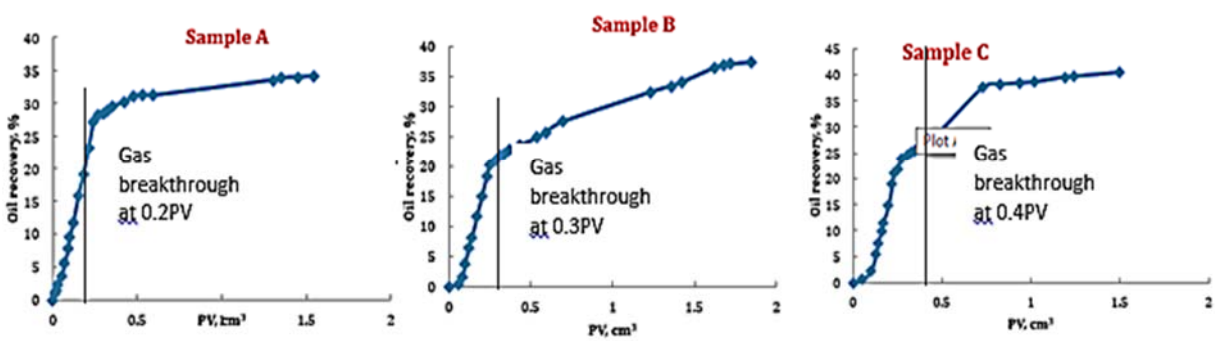


**Fig. 4.5: Experimental results of oil recovery for air flooding of the sand-pack tube slanted at different angles**.

The experimental results also show that the oil recovery increase proportionally with dip angle, which indicates that the effect of gravity stabilization is important for gas injection. Test C has the largest dip of 80° and lower oil saturation than A, but it achieved the highest oil recovery of 40%

OOIP. The examination of the sand-pack after the air flooding showed that residual oil in the middle part of the sand-pack was much lower than that in the two end parts of the tube due to end effects, which means the actual displacement efficiency via air flooding can be higher than the values of oil recovery listed in Table 4.4.

It was also observed that after air breakthrough, oil production rate was reduced, which indicates that early gas (air) breakthrough has a great effect on the oil recovery, and lower air injection rate and large dip angle can delay gas breakthrough and increase the final oil recovery.

The displacement experiments indicate that air injection, as a primary or secondary oil recovery method in light oil reservoirs under LTO mode (even without thermal effects) can achieve relatively high oil recovery better than water injection, and the thermal effect is not necessary or can be only as an extra bonus of the process as long as oxygen in the air can be consumed via a LTO or HTO reaction. However, when air injection (horizontally) is used as a tertiary recovery method or oil saturation is near the residual after water flooding, it may become much less effective. So that air injection can be more effective as an alternative to replace water flooding for low permeability reservoirs, while its application in a reservoir already having a high recovery factor by waterflood should be well investigated before field implementation. Oil recovery can also be further improved and early gas breakthrough avoided via applying low injection rate and maximizing the gravity stabilization effect.

**Effects of Viscosity on Oil Displacement**

Fig. 4.5 shows that the displacement result of live oil sample (low viscosity) has gas breakthrough time lag (0.42 PV) when compared with the results of the dead oil (0.37PV), and oil recovery increased by 5.5%. The crude oil viscosity is low in the live oil samples and thus a reduction in the mobility ratio of gas and oil can effectively slow down viscous fingering.

**Effects of Different Injection Rates on Oil Displacement**

Fig. 4.5 also shows that the injection rate at 0.05 ml/min can result in an oil recovery of about 44.44%, which increased by 7.24% more than the 0.1 ml/min, and gas breakthrough time increased from 0.25 to 0.37 PV. This result therefore shows that low injection rate is adequate for gravity stable displacement and delay the gas breakthrough time and increase recovery. It was also observed that when the live oil sample, injection rate dropped from 0.05 to 0.03 ml/min, the gas breakthrough time increased from 0.42 PV to 0.48 PV and ultimate recovery increased by 2.7%. These results confirms that under the condition of the gravity stable displacement, the lower the air injection rate,

the more conducive the oil displacement, thus reducing viscosity and increasing gas breakthrough time, as well as improve the ultimate oil recovery.

### 4.5.2 LTO Reaction Experiments

**Experimental Set-up and Results**

A schematic diagram of the experimental facility used is shown in Fig. 4.6, which is a static and isothermal reactor, so-called small batch reactor SBR (Ren et al., 2002) has a sample cell volume of only 100 ml, compared with 10 liters of the oxidation tube, was designed and used in this study to acquire data on the oxidation rates for a number of oils, at reservoir temperature and pressure. The small reactor was used to investigate the rate of oxygen consumption and gaseous reaction products, after the crude oil, or oil combined with crushed reservoir cores was contacted with air at high pressure and at reservoir temperature (isothermally), in a static system. The body of the reactor was made of a standard high pressure tube (D=2.54 cm, L=25 cm, SS3 16). The maximum operating pressure of the tube is set at 25MPa. The reactor is located horizontally in a cylindrical heater, in which the temperature is controlled to 100°C. In the experiments, known quantities of oil or oil + core were loaded into the reactor cell. A free volume was left to be filled with reactant gas (air) at the required pressure. The reactor was then heated to the required operating temperature.

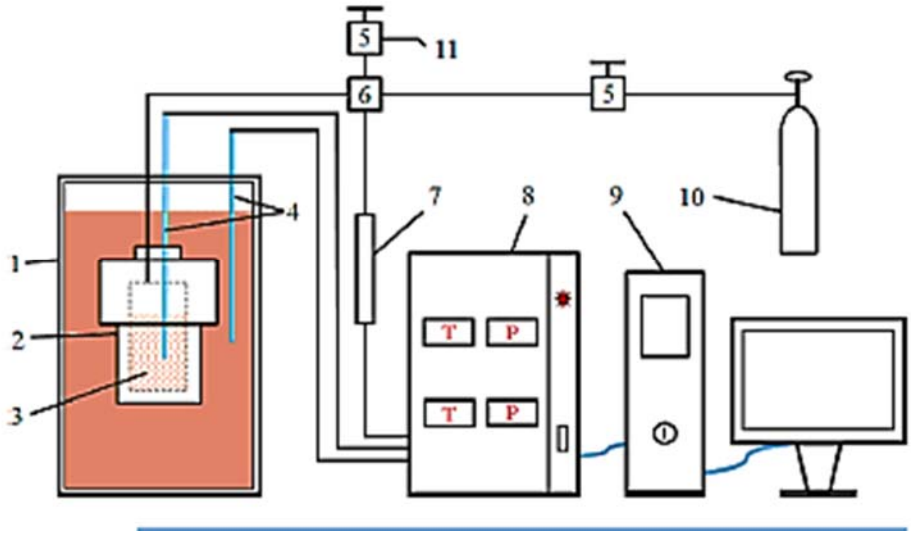


**Fig. 4.6: Schematic Diagram of experimental setup of LTO at isothermal conditions**

1. Isothermal oil bath; 2. High pressure reactor; 3. Oil sands; 4. Temperature sensor; 5. Valve; 6. Four-way valve; 7. Pressure sensor; 8&9. Acquisition system and computer (PC); 10. High pressure air tank; and 11. Gas sample connection.

The LTO reaction experiment was carried out with two oil sands (light oil samples of Q131 of 35°API and C-09 of 32°API) at different temperatures (130 -170°C) and pressures (21.2-23.4MPa)

accordingly with the reservoir temperatures of each oil sample, to assess the oxidation properties of the oil samples with air. The above mentioned oil sands were loaded in the reactor vessel (100 ml) filled with air (21% $O_2$ and 78% $N_2$) at high pressure. The reactor was then immersed in an oil bath set to run at a given temperature. A reduction in pressure was normally observed, due to oxygen being consumed by LTO reactions, and also because some gas dissolved in the oil. The latter effect was fast and constant at the pressure and temperature of the experiment. No shaking or stirring occurred during the run. To terminate the experiment, the reactor was taken out of the heater, and left at room temperature to cool down. The exhaust gas in the reactor was discharged to gas analyzers via a pressure regulator. A material balance was performed to determine the oxygen consumption, resulting from the reduction in pressure. Pressure-temperature equilibrium was assumed throughout, in order to determine the rate of oxygen consumption. It was assumed that the gas dissolution and its release from the oil are much quicker than time for LTO reactions to occur. After the experiments, the gas in the reactor was discharged through gas analyzers for the measurement of the gas composition ($O_2$ and $CO_2$). The reaction rate, or the oxygen consumption rate observed as a pressure reduction in the reactor, is calculated based on PVT and material balance analysis. The reduction in pressure in the SBR may also be affected by dissolution and release of gas from the liquids. In order to eliminate this effect, data was only taken from the region over which a steady decline in pressure was occurring, usually after several hours had the reaction elapsed. . The oxygen consumption rate and final exhaust gas composition were determined from these tests. To determine the kinetic parameters for a specific system, the oxygen consumption rate needs to be measured at several different temperatures and this will form part of a future program.

**Table 4.5: Results of LTO experiments using an isothermal reactor at static conditions**

| Oil Sample | T, °C | P, MPa | $O_2$% in produced gas | $CO_2$% in produced gas | Oxidation rate×$10^{-5}$ $mO_2$/h.ml oil | $CO_2$ conversion rate, % |
|---|---|---|---|---|---|---|
| Q131 | 98 | 20 | 11 | 3.8 | 0.304 | 53.67 (852 hours response) |
| | 130 | 21.2 | 6.5 | 3.4 | 2.01 | 31.59 |
| | 150 | 20.4 | 1.4 | 7.1 | 3.14 | 49.11 |
| C-09 | 140 | 21.7 | 1.0 | 6.8 | 2.10 | 40.21 |
| | 150 | 23.3 | 0.9 | 7.5 | 8.43 | 44.90 |
| | 160 | 23.4 | 0.7 | 8.2 | 18.60 | 50.12 |
| | 170 | 23.4 | 0.2 | 10.3 | 38.60 | 57.87 |

The experimental data and results are listed in Table 4.5, which shows a high oil reactivity in terms of oxygen consumption and $CO_2$ production especially at the higher reservoir temperatures. $CO_2$ was produced with a high conversion rate, which indicated that $CO_2$ is one of the main products of the LTO reactions.

The decreasing mole percent of the oxygen in the produced gas indicates that the air saturation in the sandpack (due to gas breakthrough) was gradually displaced by the produced reaction gases, exhibiting an increasing amount of $CO_2$ generated. The experimental results from the LTO reactions in the temperature range of 130°C up to 170°C, showed that LTO reaction is effective to consume $O_2$, and produce $CO_2$. The $O_2$ consumed was largely converted to $CO_2$ as seen from the increase in the $CO_2$ percentage in the produced gas. Nearly all the oxygen in the air can be consumed at the end of the experiments over 10 days. The final oxygen content was less than 2%.after the 10 days. More than 10% of $CO_2$ in the produced gas was also measured at the end of the run.

It is also observed that Q131 (35°API) has a lower oxidation rate than C-09 (32°API), which is in line with the rule that reaction (oxidation) rate varies inversely with the API value of oil. The $CO_2$ conversion rate can be as high as ~58%. In typical in-situ combustion process of crude oils, the $CO_2$ conversion rate can be around 85%.

Summarily, the preliminary experimental results from the small isothermal reactor suggests that, at reservoir temperature and high pressure, the reactivity of the light oils is sufficiently high to achieve a complete consumption of the oxygen at air injection rates which are comparable to those that might be used on a field scale. This means it should be possible to achieve virtually complete oxygen removal at the displacement front, or at least to reduce it down to a very low level. Furthermore, significant levels of $CO_2$ are produced (7-9%), which will achieve miscibility with the reservoir oil, further increasing incremental oil recovery.

# CHAPTER 5: NUMERICAL SIMULATION STUDIES

## 5.1 Reservoir Numerical Simulation Modeling

The main aim of this study is to carry out a numerical reservoir simulation of the different proposed gas injection techniques to evaluate the increased oil recovery of the target block, therefore the description of the concept of reservoir simulation and modelling is very important in this study.

Reservoir simulation is an effective method to help petroleum engineers estimate the oil and gas resources and nearly all major reservoir development decisions are made based on simulation results. Numerical modeling of potential IOR projects is recognized as a valuable and cost-effective method of screening processes and optimizing their implementation. Numerical modeling can also be an effective tool in situations where miscible or immiscible gas flood is considered to be the dominant recovery mechanism. In this situation, compositional simulators can provide adequate accuracy. In situations (the case of air injection) where accurate representation of the reaction zone is desired, the modeling is much more difficult. Generally, thermal fronts are very narrow, relative to typical grid sizes, and have proven difficult to represent accurately. Recent advances in front-tracking techniques may provide a solution to this problem. An additional limitation for numerical models is the inability to accurately represent the complex chemical reactions between the oxygen and the air (oxidation kinetics). Oxidation kinetics can presumes that bond scission and thermal cracking reactions are occurring, but these models fail to predict when a shift from bond scission to oxygen addition reactions may occur. Developing pseudo-kinetic models that will predict significant changes in the oxidation mechanisms, which in turn will impact the effectiveness of the oil displacement efficiency of the high pressure air injection process, remains as a significant technical challenge.

In practice, the numerical simulation requires many important steps before prediction and these include: the overall available reservoir data (rock and fluid properties), good understanding of the geology of the block (structural and stratigraphic) built into the geo-model (reservoir model building), PVT studies, thermal reaction kinetics models, relative permeability of the liquid and gas, history matching, initialization settings, block perforation, production optimization and forecasting. The Q131 block numerical simulation case study will be discussed in details in the following sections.

## 5.2 Reservoir Data

### 5.2.1 Overview of the Q131 Oil block

Q131 block is geographically located in the west slope of the western depression of Liaohe basin in Liaoning Province, North East of China as shown in Fig. 5.1. The prospective Q131 gas injection project is utilized as one of the cases to further expound on the mechanisms of gas injection for IOR in light oil reservoirs with low permeability. The reservoir lithology is mainly anisometric argillaceous conglomeratic sandstone with a low permeability of 0.1-85mD (~0.1 – 83.9 x $10^{-3}\mu m^2$) with an average permeability of 10.2mD (10 x $10^{-3}\mu m^{2)}$. The target reservoir unit in the Q-131 block is at a depth of 3025-3670 m, with an average thickness of 41.9 m. The reservoir has a large stratigraphic dip of about 20-21°NE. The bottom aquifer is not considered an active supporting energy source for the reservoir. Its primary drive mechanism is stabilized gas depletion and gravity drive. It has an oil-bearing area of about 1.0 $km^2$, light oil (35°API), geological reserves (OOIP) of 214.75 x $10^4$ tons (of 2.53 x $10^6$ $m^3$), Expected Recoverable Reserve (normal water flood) ER of 47.9 x $10^4$t (5.64 x $10^5$ $m^3$) i.e. 22.31% OOIP. The rock and fluid properties of Q131 reservoir block are summarized in Table 5.1.

**Table 5.1: Summary of the reservoir rock and fluid properties of Q131 oil block.**

| Q131 Rock Properties | |
|---|---|
| Area of oil block, $m^2$ | 1.0x$10^6$ |
| Dip, ° NE | 21 |
| Average effective thickness, m | 41.9 |
| Depth at top of formation, m | ~3025 |
| Permeability, $10^{-3}\mu m^2$ | 0.1-83.9 |
| Vertical to horizontal perm, ratio | 0.1 |
| Average porosity, % | 13 |
| Initial Pressure, MPa | 33.4 |
| Bubble Point Pressure, MPa | 15 |
| Current Reservoir Pressure (2012), MPa | 20.1 |
| Temperature, °C | 98.9 |
| **Q-131 Fluid Properties** | |
| Viscosity @ res. Condition, mPa.s | <0.5 |
| Density of crude oil @ surface. condition, g/$cm^3$ | 0.8489 |
| Gravity weight, °API | 35 |
| Viscosity, freezing point °C | 27 |
| Original gas-oil-ratio, GOR, $sm^3/sm^3$ | 112 |
| Paraffin content, % | 13.63 |
| Colloid + asphaltene, % | 8.54 |

### 5.2.2 Production History of the Q131 Block

The block started production in May, 1986 via a low rate depletion process and the first well drilled was named Q131, from thus came the name of the block. An appraisal well drilled was in March 2004 and subsequently other 7 wells including 2 horizontal wells were drilled in 2005-2006. In

2008, water injection started with 5 injectors converted from former production wells (Fig. 5.2). In 2011, water injection was stopped because of very poor injectivity and response due to its low permeability characteristics and high water sensitivity. Fig 5.2 shows a PETREL generated 3D view of the block and all the water injection wells and production wells. As at July 2012, there are total of 23 wells in the target block, which include 5 water injection wells (all are shut down now) and 18 production wells (16 vertical wells and 2 horizontal wells) as shown in Fig. 5.2. Out of the 18 wells, 11 wells are still producing, 5 are shut down, and 2 are abandoned. The cumulative oil produced till 2012/08/01 is 19x$10^4$t (2.25 x $10^5$ $m^3$) i.e. a total recovery factor (RF) of 7.67% OOIP including primary depletion and water flooding), which falls far below the expected recovery of 22.31%OOIP earlier mentioned. Thus, the application of an IOR technique is required in this block. The block meets all the criteria required for gas injection IOR and is expected to achieve better recovery via the mechanisms including a fast re-pressurization, gravity stabilized oil displacement by reduction of oil viscosity, gas sweeping, oil stripping, and swelling due to interaction with the injected gas. The large dip and thick oil layers of the block shown in Fig. 5.3, will facilitate gravity segregation as an important factor in IOR. The block developed with large well spacing has experienced poor water sweep, but it may be suitable for the injection of a much lighter fluid like compressed gas. This segregation effect makes it possible for the proposed gases to contact oil at the top layers that has not been contacted by previously injected water and increase the productivity of the block.

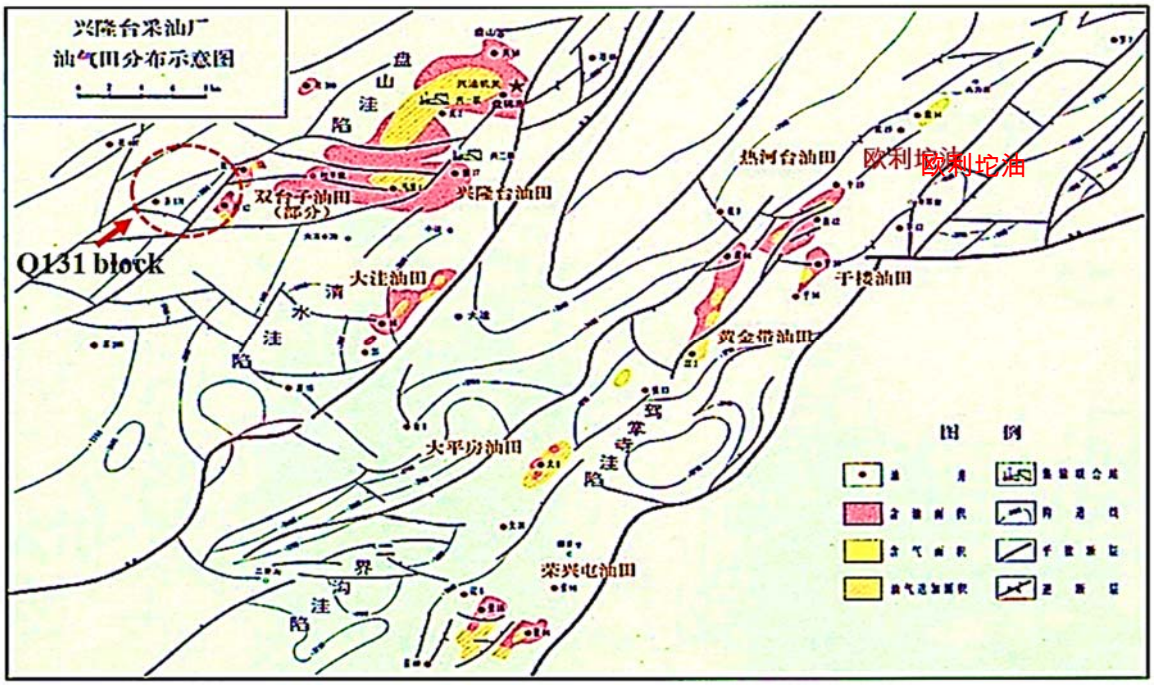


**Fig 5.1: Map Showing Q131 Block location in the Western Part of Liaohe Oil Field**

### 5.2.3 Reservoir Geo-Modeling of Q131 Block

A 3-D corner point reservoir model of Q131 (Fig. 5.4) was built using PETREL for the simulation case studies of the proposed different gas injection techniques and then stochastic permeability, porosity and other reservoir properties were assigned for the grid blocks using Builder function of Computer Modeling Group (CMG).

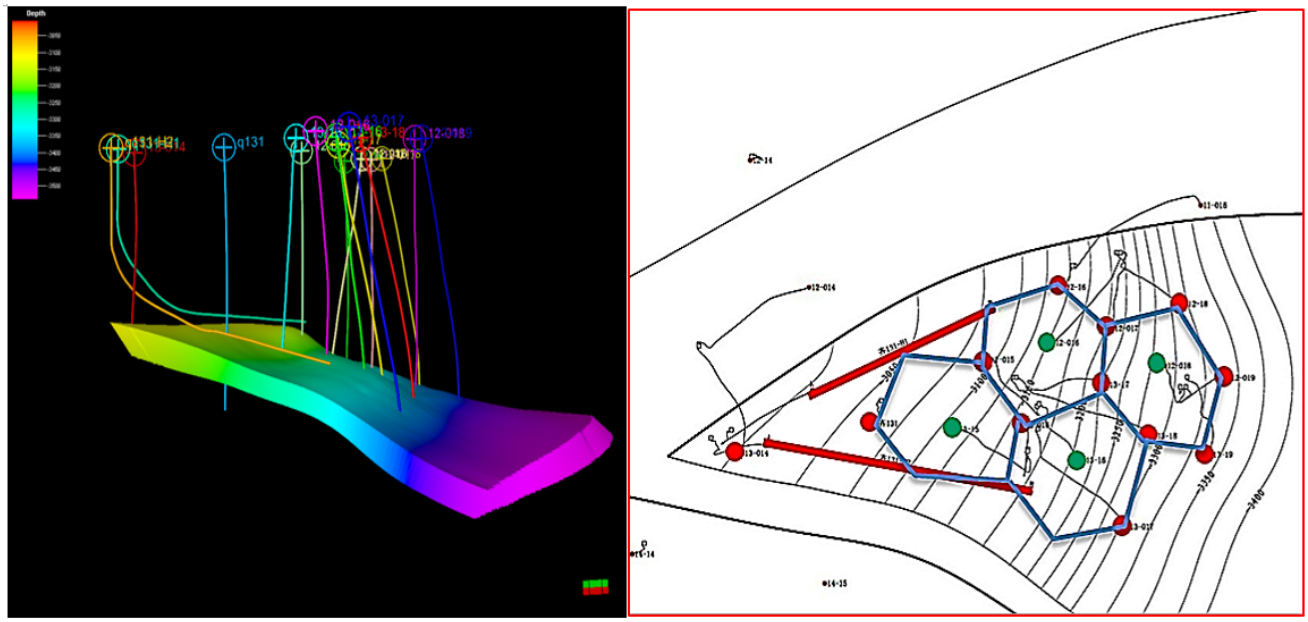

**Fig. 5.2: The 3D view of the Q131 block & wells (PETREL generated); and a 2D top depth map showing the initial 7 spot water injection well pattern design and the bounding faults of the block. Note this is from the 2008 production history.**

In the application of reservoir simulation to improve oil recovery processes using the different proposed gas injection schemes, an advanced compositional and thermal simulator (CMG-STARS) is used in the reservoir modeling and simulation studies. CMG-STARS (referenced) is used in the simulation to generate dynamic models for the $CO_2$, air, $N_2$ gas injection schemes in the target block using the geo-model built from PETREL as the static model, as shown in Fig. 5.4,and it can also be modified if needed.

The simulation grid used in the model has an area of $10^6 m^2$(~247acres), initial seven-spot pattern, with grid dimensions of 103x57 and 12 layers. A Local Grid Refinement (LGR) of 10:1 was applied for the grids around the injectors in order to monitor the reaction front. Predictive runs were performed with three (3) gas injection rates scenarios of 10000 and 20000 $m^3$/day (as low case scenarios), 30000 $m^3$/day (as base case scenario) and 60000 $m^3$/day (as high case scenario) over total period of 30 years (i.e. from 2012/08/01 – 2042/08/01).

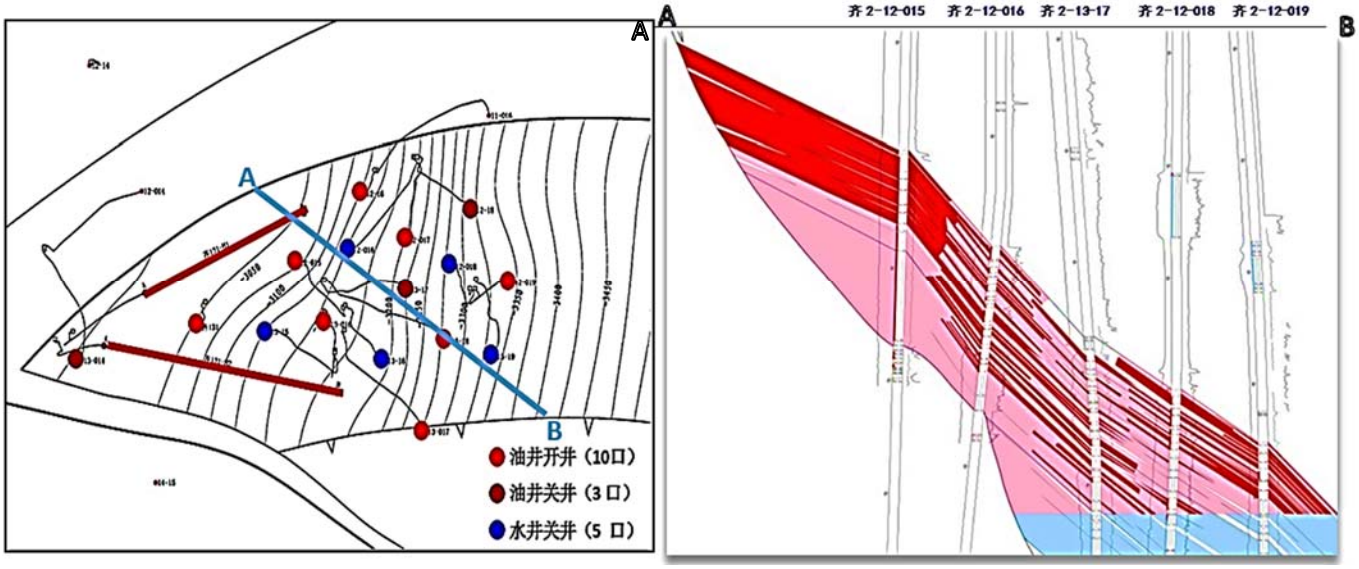


**Fig. 5.3: The depth structure map and the cross-sectional view of Q131 block showing the dipping layers.**

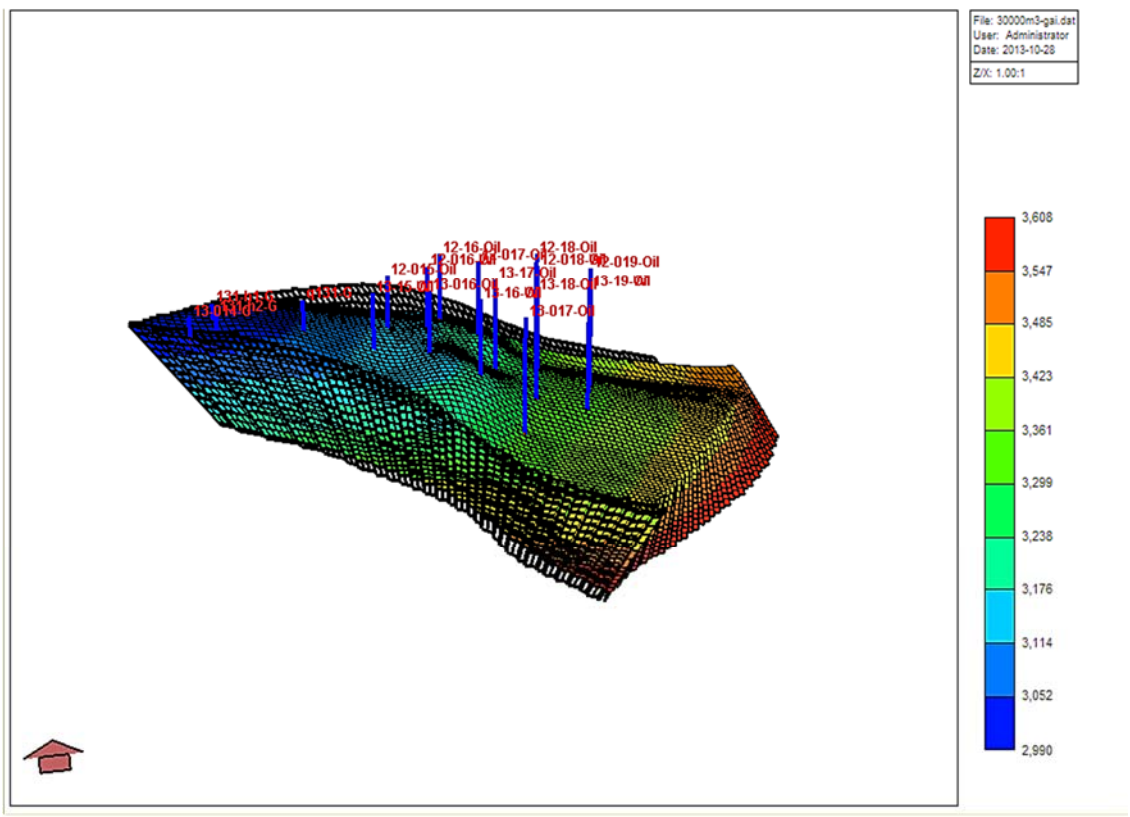


**Fig. 5.4: The 3-D corner point Grid top model of the Q131 oil block showing the present day wells.**

### 5.2.4 Selection of Injectors and Producers for Simulation Modeling

Intelligent selection of injectors are important in the simulation stage and usually made by the people who are familiar with the field under consideration. For economics purposes, it is advisable

to minimize the number of new wells that must be drilled; hence, it is important to select the injectors so as to make the best use of the existing infrastructure. If no new wells are to be installed, it is important to select an existing well that shows good communication with the reservoir. Four (4) injectors were installed at the start of the project as shown in Fig. 5.4, so to provide the opportunity to vary the rates at a given well without having to shut in the compressors or vent excess air. Injection wells in our study are located at the top structure of reservoir (up-dip part of the structure), which is best for gas injection project and optimization designs run to simulate the dynamic reservoir conditions when these injected gases are introduced into it and also bearing in mind the dipping characteristic of the Q131 reservoir block. The selection of future sites being dependent on the performance of the project.

The producers are located at the down-dip part of the block in an ordered pattern so as to efficiently drain the oil pushed down-dip by the injected gases. In this study, 14 existing producers (Fig. 5.4) are utilized in the production of oil. So there is no extra cost incurred in drilling new wells as existing wells are still functional and have reservoir connectivity to the injectors at the up-dip part of the block in the field.

## 5.3 PVT Studies

For the prediction of MMPs and PVT analysis, the WINPROP software was utilized. It is a compositional PVT equation of state based program in the CMG simulators. WINPROP is used to simulate experiments that have been conducted in the laboratory and to perform theoretical predictions to compare them with observed data. Any discrepancies between the measured and the calculated data are minimized by adjusting EOS parameters. The Peng–Robinson equation of state was used in this study. The parameters used for the regression were critical pressure, critical temperature, critical volume, Z-factor, acentric factor, and the volume correction factor of the heavy fraction sand the binary interaction coefficient. The upper limit for variation was relaxed within acceptable limits to avoid hitting the upper variation limit.

The fluids (dead and live oils) were lumped together as $C_1$, $C_2$-$C_4$, $C_8$-$C_{38}$, and also have $CO_2$ and $N_2$ components in the oil composition. Refer to Appendix Table A.1 for the detailed gas and oil compositions of the Q131 fluid and Appendix A (Table A.2) shows the detailed steps to calculate the reservoir fluid compositions shown in Table 5.2 which is used in the simulation runs of this project. In the PVT studies, the fluid composition given in Table 5.2 had some components lumped together to generate $C_1$ and three pseudo–components, which are $C_2$-$C_4$, $C_5$-$C_7$, and $C_8$-$C_{38}$ together with $CO_2$, $N_2$, $O_2$ and water, are used.

The STARS simulator uses K-values, which are a function of pressure and temperature. These were calculated using the "Win-Prop" PVT software. The K-values were generated by flashing five moles of secondary gas (88% $N_2$, 12% $CO_2$) with one mole of primary oil, at different pressure and temperature ranges. Fig. 5.5 shows the relative volume of oil against increasing pressure and the bubble point indicated at 14.98MPa.

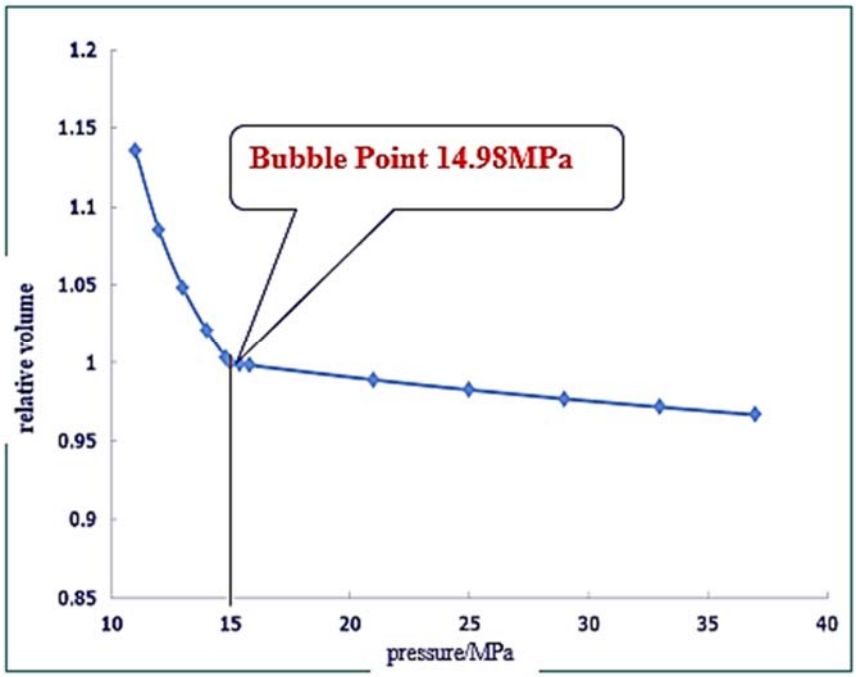


**Fig.5.5: Q131 crude oil block bubble point pressure determination**

**Table 5.2: Q131 reservoir fluid composition**

| Component | Mol, % | Component | Mol, % |
|---|---|---|---|
| $N_2$ | 0.30 | $C_7$ | 1.48 |
| $CO_2$ | 0.98 | $C_8$ | 2.18 |
| $C_1$ | 36.56 | $C_9$ | 1.68 |
| $C_2$ | 5.52 | $C_{10}$ | 1.67 |
| $C_3$ | 4.72 | $C_{11}$ | 1.83 |
| n &i $C_4$ | 2.61 | $C_{12}$ | 1.80 |
| n &i $C_5$ | 1.87 | $C_{13+}$ | 35.55 |
| $C_6$ | 1.25 | | |

Fig. 5.6 shows that as the pressure decreases, the gas evolves from the oil, density and viscosity of the Q131 reservoir fluid decrease, thus creating lighter components with the reduction in pressure. Table 5.3 shows that as $N_2$ is injected into the reservoir and its concentration increases, the

formation oil volume expansion occurred. Also it is seen as the $N_2$ mole fraction increases, the bubble point pressure increase, which indicates that less lighter components is evolved from the reservoir fluid with increase in the $N_2$ injection. Table 5.4 shows the solubility of Q131-crude oil in $N_2$ increases as the $N_2$ injection pressure increases. In the initial formation temperature and pressure (33.4MPa), the $N_2$ solubility in the crude oil is 14.21%mol., with the expansion coefficient of 1.02. The swelling ability of $N_2$ and air is limited and have little contribution to the oil recovery. This confirms that the $N_2$ injection will operate only in the immiscible phase because at the current reservoir of 20MPa, the $N_2$ solubility in the reservoir oil is only 4 mole%, which is very low.

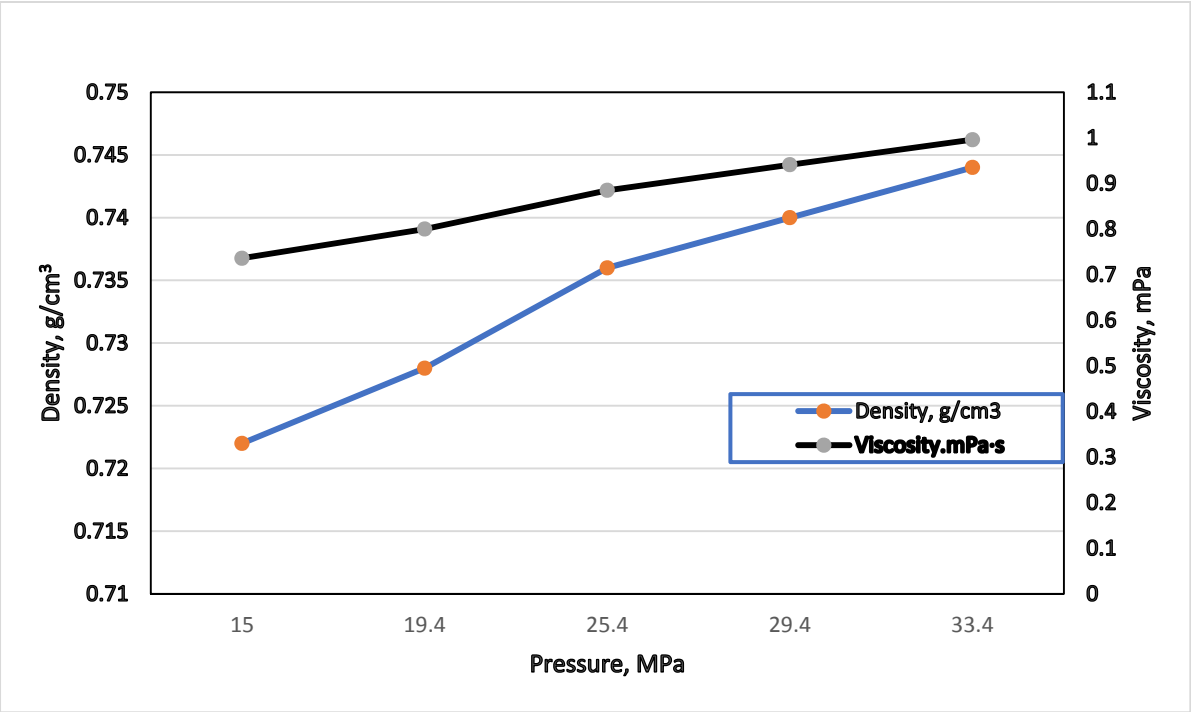


**Fig. 5.6: The formation of oil density and viscosity under different pressure**

**Table 5.3: Relationship between $N_2$ mole concentrations, bubble point and oil volume coefficient of expansion**

| $N_2$ injection Mol. fraction | Bubble Point Pressure/MPa | Volume Expansion Coefficient |
|---|---|---|
| 0.00 | 14.98 | 1.000 |
| 0.05 | 21.64 | 1.008 |
| 0.10 | 29.28 | 1.017 |
| 0.126 | 33.40 | 1.022 |
| 0.15 | 38.10 | 1.027 |

**Table 5.4: N2 solubility in crude oil under different Saturation Pressure**

| Saturation Pressure, MPa | $N_2$ solubility in oil, mole% |
|---|---|
| 20.24 | 4.16 |
| 23.09 | 5.38 |
| 26.10 | 8.69 |
| 29.28 | 11.11 |
| 34.41 | 14.94 |
| 38.10 | 17.65 |

## 5.4 Relative Permeability Model

Relative permeability is an important feature of rock and fluids interactions. It not only influences the early field performance, but also controls the ultimate oil recovery. It is particularly crucial for the evaluation of IOR potential of a mature reservoir.

For the crushed core experiments using a dead oil, the Corey exponents were tuned to match the oil and water production. For the simulation of a reservoir process using a live oil, the relative permeabilities are constructed on the basis that gas displacement will reduce the residual oil saturation behind the gas front to 10-15%, although lower $S_{org}$ values (<10%) have been found in many laboratory tests.

Relative permeability curves of multiphase flow are related with the characteristics of reservoirs, and also affected by the properties of oil and displacing agent. It is difficult to measure the oil-gas-water relative permeability in laboratory, but it can be calculated using semi-empirical models (such as the Corey or Stone correlations). The following are the typical forms of the Corey correlation, and Table 5.5 lists the relative permeability exponents of the Corey correlation for typical miscible and immiscible processes (Ren S.R. et al 2011).

For oil-water:

$$k_{rw} = \left[ \frac{(s_w - s_{wc})}{(1 - s_{wc})} \right]^{n_{rw}} \tag{5.1}$$

$$k_{row} = \left[ \frac{(s_o - s_{orw})}{(1 - s_{wc} - s_{orw})} \right]^{n_{row}} \tag{5.2}$$

And for gas-oil:

$$k_{rg} = \left[ \frac{\left(s_g - s_{gc}\right)}{\left(1 - s_{wc} - s_{gc}\right)} \right]^{n_{rg}} \tag{5.3}$$

$$k_{rog} = \left[ \frac{\left(s_o - s_{org}\right)}{\left(1 - s_{wc} - s_{org}\right)} \right]^{n_{rog}} \tag{5.4}$$

Where, $K_{rw}$ - water relative permeability at $S_w$; $K_{row}$ - oil relative permeability at $S_w$; $K_{rg}$ - gas relative permeability at $S_l$; $K_{rog}$ -oil relative permeability at $S_l$; $S_w$ - water saturation, %; $S_{wc}$ - irreducible water saturation; $S_g$ - gas saturation; $S_{gc}$ - residual gas saturation; $S_{orw}$ - residual oil saturation for water injection and $S_{org}$ - residual oil saturation for gas injection.

**Table 5.5 Corey Relative Permeability Parameters**

| Relative permeability | Endpoint saturation | Corey index | Miscible | Immiscible |
|---|---|---|---|---|
| $k_{rog}$ | $S_{org}$=0.10 - 0.15 | $n_{rog}$ | 1 | 3 |
| $k_{rg}$ | $S_{rg}$=0.05 - 0.1 | $n_{rg}$ | 4 | 4 |
| $k_{row}$ | $S_{row}$= 0.20 - 0.35 | $n_{row}$ | 2 | 2 |
| $k_{rw}$ | $S_{rw}$=0.3 - 0.4 | $n_{rw}$ | 4 | 4 |

It is important to choose proper relative permeability curves in gas injection process for different flooding mechanisms, which may have a significant effect on the result of simulation. For near-miscible process of $CO_2$ injection, an improved Corey model has been used (Ren Minyan et al, 2012) i.e. in equation (5.5) in which the correlation index ($n_{rog}$) is correlated with IFT or pressure to simulate the miscibility effect at various pressures of $CO_2$ injection.

$$n_{rog} = \begin{cases} 1 & P \geq P_{mmp} \\ \dfrac{2P + P_{nm} - 3P_{mmp}}{P_{nm} - P_{mmp}} & P_{nm} < P < P_{mmp} \\ 3 & P \leq P_{nm} \end{cases} \tag{5.5}$$

Where, $n_{rog}$ is the oil-gas relative permeability index, $P_{mmp}$ is the minimum miscibility pressure (MMP), $P_{nm}$ is the pressure for immiscible boundary.

In the simulation, a linear interpolation of the relative permeability based on the interfacial tension (IFT) of gas and oil phases will be adopted to model the miscibility effect between the miscible ($n_{rog}$=1) and immiscible ($n_{rog}$=3) cases. The IFT, as a function of pressure at the reservoir temperature, and is calculated using the PVT software part of CMG, the WINPROP. It has been suggested that a high IFT or low gas solubility in oil correspond to immiscible process, while a low IFT (or high gas solubility) can achieve a miscible or near-miscible displacement. Interfacial tension at high pressures can be measured in laboratory for specific oil/gas systems.

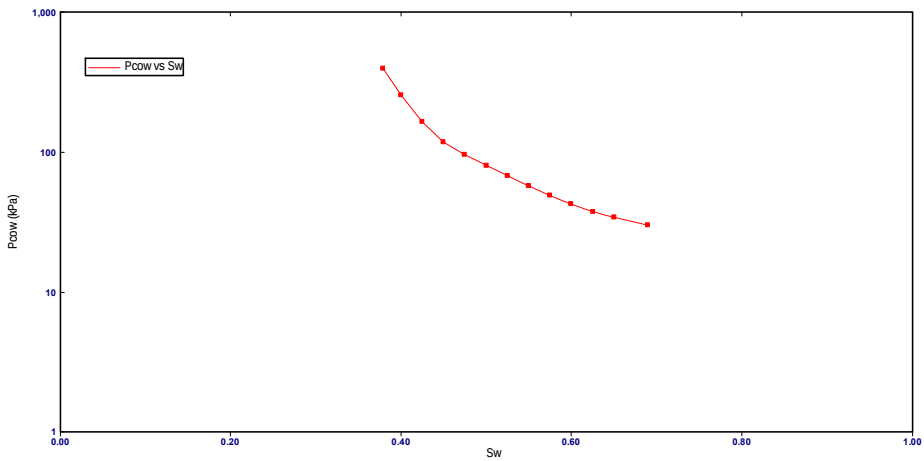


**Fig. 5.7: Plot of the capillary pressure vs. water saturation $S_w$**

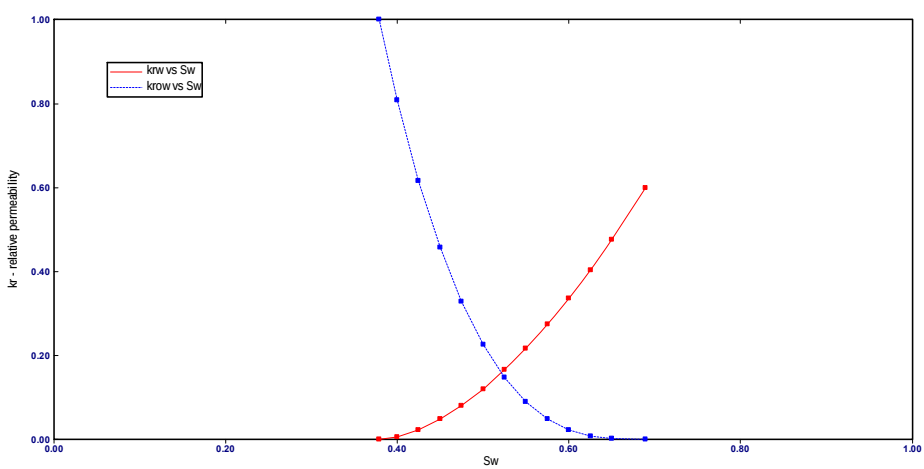


**Fig. 5.8: Plot of rel. permeabilities of oil and water vs. water saturation $S_W$**

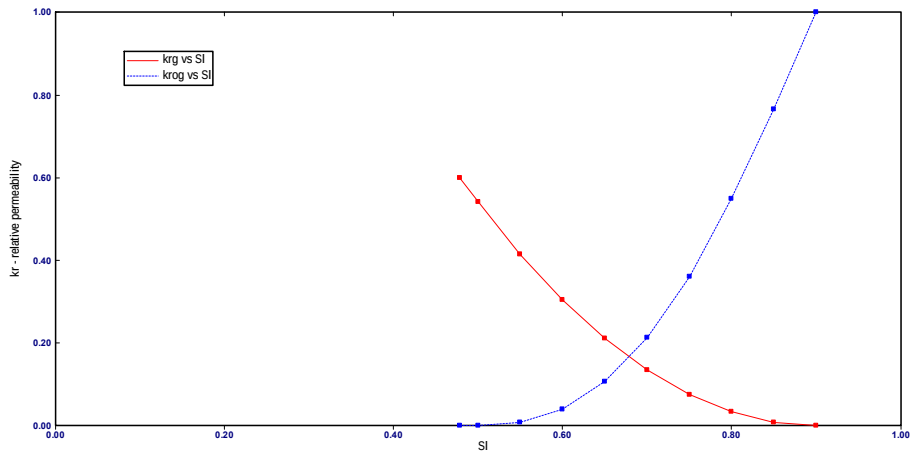


**Fig. 5.9: Plot of relative permeabilities of oil and gas vs. liquid saturation $S_L$**

The relative permeability data used in this numerical simulation study is shown in Fig. 5.7 to Fig. 5.9 which shows the capillary pressure curve variation with the water saturation $S_W$; the plot of relative permeabilities of oil and water vs. $S_w$ and the plot of relative permeabilities of oil and gas vs. liquid saturation. $S_L$ respectively.

## 5.5 Thermal and Reaction Kinetics Models (for Air Injection Only)

Reaction kinetics can be defined as the study of the rate and extent of chemical transformation of reactant to product. The oxidation reaction kinetics that takes place during heating of the samples can be obtained by thermal analysis method. A reaction model was used to simulate the LTO reaction in air injection. It is assumed here that only the heavy components ($C_{10+}$) involves in the oxidation reactions, which consume oxygen and produce $N_2$, $CO_2$ and heat. In simulating $CO_2$ and $N_2$ injections, isothermal conditions are applied to stabilize the simulation and reduce computation time.

### 5.5.1 Reaction Stoichiometry

In our study, the reactions can be run in two different reaction cases as shown in the equations below. This is set in the Component's sub-division part of CMG, called "Reactions" and used in the simulation modeling.

**Reaction 1:**

$$\mathbf{C_{8+} + 1.5O_2 \rightarrow H_2O + CO_2 + 0.94605\ C_{8+}} \tag{5.6}$$

**Reaction 2:**

$$\mathbf{C_{8+} + 27.35\ O_2 \rightarrow 19H_2O + 18CO_2} \tag{5.7}$$

Reaction 1 is LTO reaction and Reaction 2 is HTO reaction with the LTO reaction having just $1.5O_2$ and the HTO have higher molecules of $27.35O_2$. In the Reaction 1, when $CO_2$ is produced, one carbon atom will be broken out from the hydrocarbon chain and the oil molecules become less than one (about 0.94605). In the Reaction 2, having a higher activation energy shows that the hydrocarbon is totally consumed/burnt due to presence of high temperature and higher molecules of $CO_2$ and water are produced.

In this study, the technique of two simultaneous reactions were applied. This implies that the first reaction in the reservoir is expected to be dominantly LTO reactions, but at certain reservoir conditions (especially high temperature), LTO reactions can be automatically transferred to HTO reactions (Reaction 2) in the reservoir, usually at the immediate vicinity of the injectors.

Also the reactions are endothermic and thus the effects of heat loss must be acknowledged because it affects the resultant temperature of the reservoir. If the heat loss is high, the reactions tends to remain in the LTO mode, and vice versa for HTO reactions. This is therefore an important factor to be considered in the reaction mechanism of the air injection IOR technology.

### 5.5.2 Oxidation Reaction Kinetics Model

The Oxidation reaction kinetics model recommended and used in the modeling is:

$$v = k_0 e^{-\frac{Ea}{RT}} \cdot [\mathrm{O_2}]^m \cdot [\mathrm{oil}]^n \tag{5.8}$$

Where: k - Oxidation reaction rate constant; $[O_2]$.[oil] – the concentration of $O_2$ and the crude oil respectively; m, n – Reaction of $O_2$, crude oil series respectively in the experiment m = 0, n = 0; Ea, apparent activation energy, kJ/mol,; R - the universal gas constant, 8.314 J/(k. mol); T - thermodynamic temperature, K.

**LTO Mode Parameters:**

$$E_1 = 89.96\ \mathrm{KJ/mol},\quad k_0 = 1.27\times10^8\ \mathrm{L/(s\cdot kPa)} \tag{5.9}$$

**HTO Mode Parameters:**

$$E_2 = 99.0\ \mathrm{KJ/mol},\quad k_0 = 1.27\times10^9\ \mathrm{L/(s\cdot kPa)} \tag{5.10}$$

Therefore, their reaction rate equation can be expressed as:

$$\textit{Reaction 1:}\quad v_1 = 1.27\times10^8 e^{-89960/RT} \quad \text{(LTO)} \tag{5.11}$$

$$\textit{Reaction 2:}\quad v_2 = 1.27\times10^9 e^{-99000/RT} \quad \text{(HTO)} \tag{5.12}$$

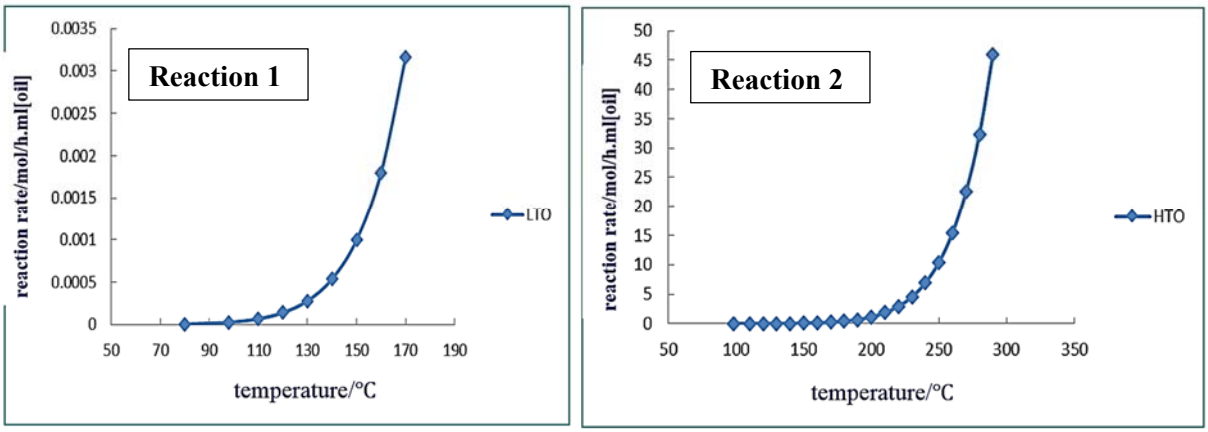


**Fig. 5.10: LTO and HTO reaction rates under different temperature**

Reaction A (Fig. 5.10) offer favorable exothermic behavior in the low temperature range with lower activation energies and low orders of reactions-the conditions typically favoring auto ignition. While Reaction B needs a much higher activation energy to ignite, and its order of reactions is very high and is likely to operate in the HTO reaction mode which consumes most of the residue oil close to the reaction zone and generate $CO_2$, water and heat.

The adopted parameters for the different reaction modes can reflect that at low temperature (<150°C), the oxidation reaction rate of LTO is higher than that of HTO (Fig. 5.10). The oxidation reaction of the HTO mode starts at a higher temperature (>250°C), which clearly defines the difference between the two modes. Also the activation energy required to start up reaction in the LTO is lower than that of the HTO.

## 5.6 History Matching Program Design

History matching is a required step before a reservoir model is accepted for making predictions of the future performance of the reservoir. History matching is the most time-consuming yet crucial part in reservoir study, with the objective to build a model that integrates all available data to reduce the uncertainties on production forecasts. One of the goals of this research is to develop and apply an efficient object-oriented framework to perform automatic history matching and reservoir development optimization. The history match for this field has already been done in a previous in-house study and the simulation in this work had its basis from it (Gas-IOR team report, 2012). Fig. 5.11 shows the field history production data which is a result of the history match carried out on the Q131 block.

## 5.7 Full-Field Black Oil and Compositional Modeling Schemes

A preliminary black oil model (Q131 block) was first developed to acquire a full field history match for the primary and water injection from 1986 to 2012 in order to tune the PVT parameters and oil-water relative permeability, and then the simulation of the gas injection processes was followed, using 4 gas injection wells located at the top of the crest of the structure and 14 production wells located at the down dip part of the structure as shown in Fig. 5.4. The LTO kinetics parameters applied only for the air injection, used were modified from the SBR experiments described above. Relative permeability of gas-liquid was adjusted using a Corey model based on the experimental results of air flooding and referenced experimental results of $CO_2$ and $N_2$ flooding. The residual oil saturation ($S_{rog}$) via air flooding was assumed as 20%. The use of the black oil model enabled us to obtain fast and fairly reliable results, regarding the incremental recovery and production scenarios required to make initial economic projections for the project.

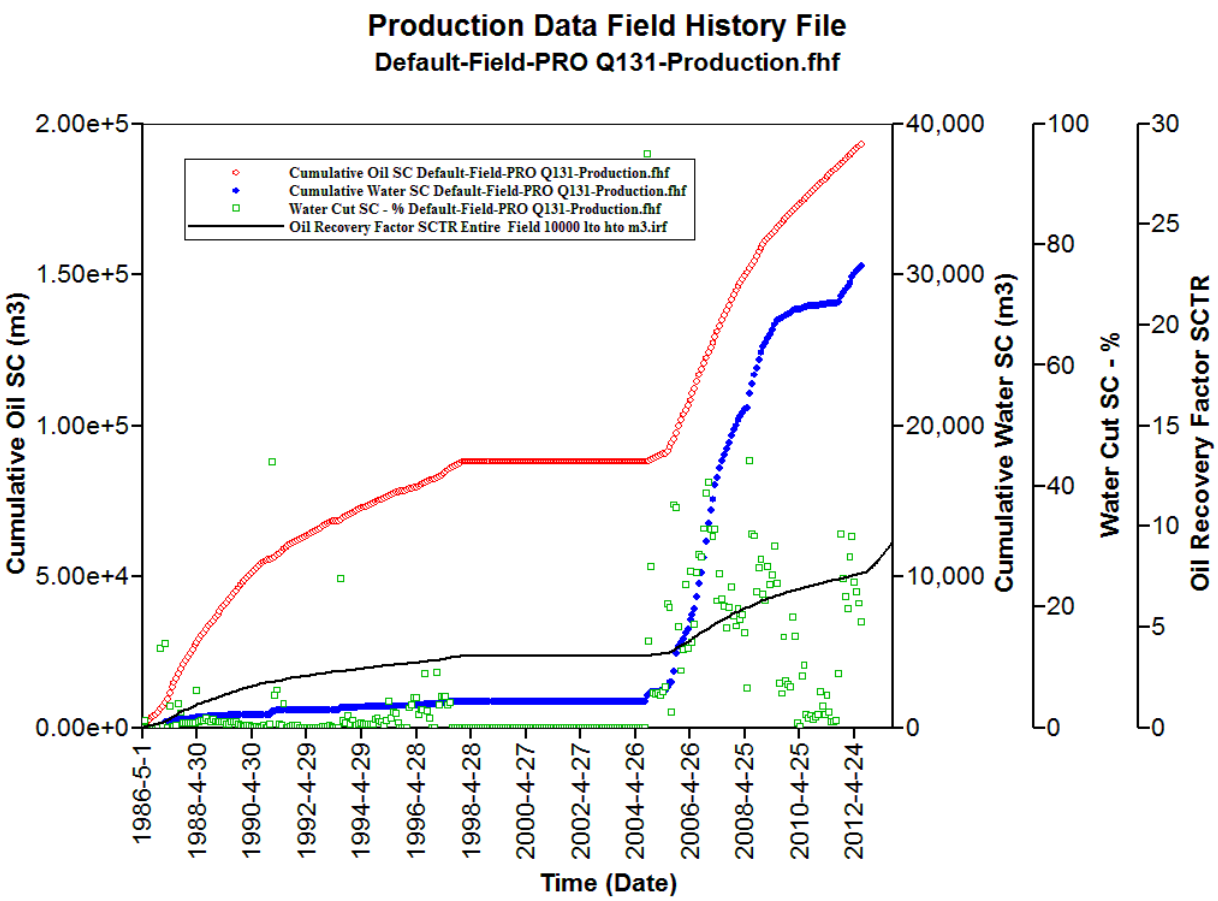


**Fig. 5.11: Plot of the Field Production History of Q131 block.**

A full field conceptual compositional reservoir simulation study of the 3 different gas injection schemes were carried out using CMG STARS thermal simulation package. The reservoir properties from the full field black oil model with a compositional description of the oil, and the introduction of chemical reactions enabling oil oxidation and $CO_2$ formation was also considered in the simulation study. The aim of this simulation study was to further evaluate and forecast the potentials (oil production, reservoir characteristics, and reservoir fluid dynamics, etc.) of the gas injection schemes for light oil candidates using already acquired experimental data set of the Q131 block. The corresponding results will be presented and discussed in Chapter 7.

# CHAPTER 6: NUMERICAL SIMULATION RESULTS AND DISCUSSIONS

Reservoir simulation has been performed using a thermal model to predict the reservoir response via gas injection in a group of wells for Q131 reservoir block (4 injectors and 14 producers). For the reservoir simulation of the different gas injection schemes, history matching was firstly done for the primary and water injection from May 1986 to 2012 in order to tune the PVT parameters and oil-water relative permeability, and then firstly air injection LTO/HTO numerical simulation process was conducted, then $CO_2$ and lastly $N_2$ injection.

## 6.1 Assumptions Considered

The injection rates and average reservoir pressures were assumed to be at constant values and applied in the reservoir numerical studies for the different gas injection schemes.

### 6.1.1 Gas Injection Rates

The influence of gas injection rate on the thermal effect in the reservoir is complex. Therefore to understand the effects of gas injection rate and determine the best injection rate to apply in the project. Three gas injection rate scenarios were considered in this study namely;

1) The low case scenario (10000 and 20000$m^3$/day)
2) The base case scenario (30000$m^3$/day)
3) The high case scenario (60000$m^3$/day)

### 6.1.2 Average Reservoir Pressure

In the simulation studies, the producers were set to operate under a constant bottom-hole pressure (BHP) of 25MPa. This is because, one of the objectives of the gas injection application in this oil block is targeted to maintain the original reservoir pressure at or above a minimum pressure of 20MPa and thus the reservoir BHP is expected to be of this minimum value. Fig. 6.1 showed that from the beginning of operations in the Q131 oil block, pressure decline has been steady, dropping from the initial average reservoir pressure of 36 MPa to about 20 MPa before the start of the injection at 2012. The gas injection simulation can be seen to have kept the average reservoir pressure constant at 21MPa for the 30 years period studied, because it is known that the immiscible and near miscible drives by the injected gases would also invariably maintain the existing reservoir pressure from dropping any further than 20MPa. So the average reservoir pressure will remain at or above 20 MPa during the gas injection years for all the gases injected.

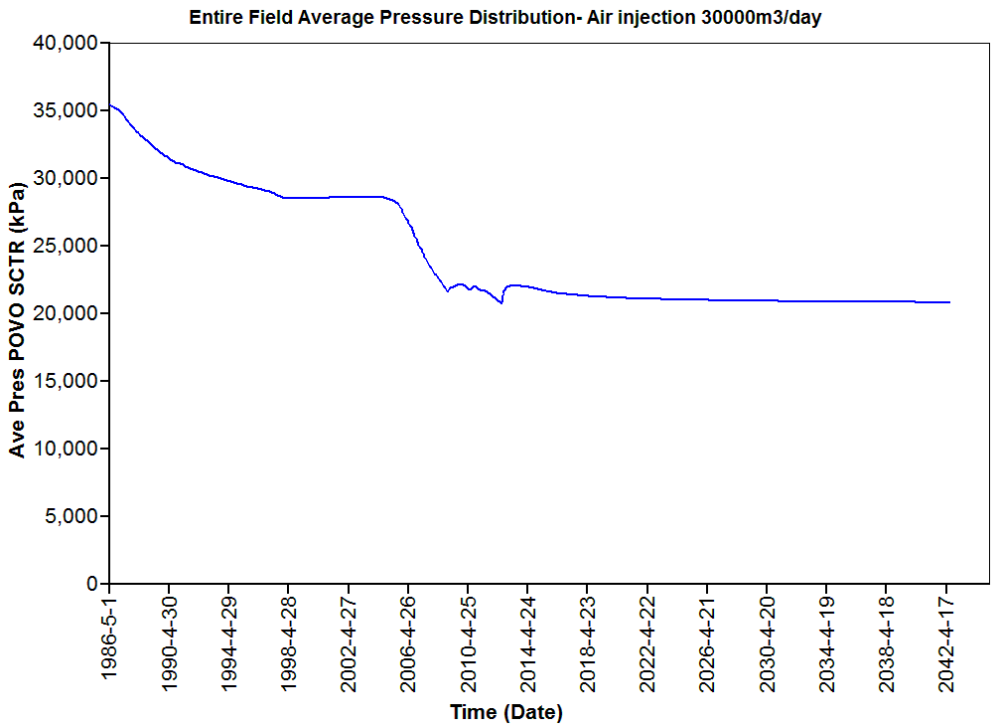


**Fig.6.1: Average Pressure field distribution for air injection, under 30,000m$^3$/day**

### 6.1.3 Injectors-Producers Separation

The injection-production wells separation in this simulation study is greater than 1200m. This long distance is set between these wells to ensure that the oxygen in the case of air injection is properly and completely consumed in the reservoir and does not breakthrough at the producers. Also for the case of $CO_2$ injection, it will ensure that the oil is adequately mixed with the injected $CO_2$ and have enough time and space to form a single phase flow that is more efficient in oil displacement.

## 6.2 Air, $CO_2$ and $N_2$ injection Simulation Results Presentation and Discussion

The following sections present and discusses in details, the results that are gotten from the numerical simulation of the different gas injection techniques which include: fluid saturation field, temperature field (for air injection), the gas composition migration regularity are analyzed, oil production rate, gas mole concentration in the reservoir, crude oil viscosity, and other results to reveal the advantages of the different gas injection mechanisms for improving oil recovery in Q131.

### 6.2.1 Air Injection Numerical Simulation Results and Discussion

In simulating the process of low-temperature oxidation air injection flooding is aimed at studying the flue gas and thermal effect on the effects of the air injection to improve oil recovery. The results are shown in Figs. 6A-D. Maximum temperature seen in the reservoir during the 30 years period is seen to be less than or approximately 240°C and confirmed that the process is in the LTO mode.

**The main results from the reservoir simulation study are:**

#### 6.2.1.1 Reservoir Temperature:

From the simulation results of the temperature field distribution displayed in Figures 6.2-A to 6.2-F (using the base case injection scenario, i.e. a constant injection rate of 30000m$^3$/day), it is observed that shortly after air injection began, there is an increase in temperature at the vicinity of the injectors. The figures show that with increase in the injection time, the elevated temperature zone moves from the injectors' vicinity towards the producers, indicating that a reaction front has been initiated and that it is propagating stably through the reservoir.

The reaction front did not reach the production wells over the 30 years period as seen from the temperature distribution in Figures 6.2-A to F for different time periods which also indicated that the reaction or oxidation front was far behind the gas flooding front, and that flue gas drive is the major displacement mechanism that resulted in efficient sweep of the reservoir. Fig. 6.3 shows that as the injection rate increases, the reservoir temperature gradually increased from 98°C to about 180°C in the injector wells location. This indicates that most of the reaction in this range of injection rates are dominantly in the LTO mode, because the maximum temperature observed is below 200°C. Thus we can deduce that more fuel gases were available to primarily drive the oil to the production wells. Also, the fuel gases is available to react in the reaction zone and gives the observed gradual increasing reservoir temperature, as more air is injected. Figure 6.3 also shows that the temperature field distribution varies with different injection rates. It is observed that the reservoir temperature stabilized back to the original reservoir temperature of about 98°C at about 800-1100m (according to the specific injection rate applied) away from the first injection well.

In Figure 6.4, the average reservoir temperature is observed to increase with time as injection rates are increased. These temperature increases in both cases (Figs. 6.3 and 6.4) are due to the advancing reaction fronts and oxygen consumption as fuel gases are produced, which elevates the overall temperature of the reservoir in the region that this reactions are taking place. The reservoir temperature remains the same (98-100°C) at the unaffected regions that are close to the producers, as shown in Figure 6.3. The increase in temperature of the reservoir primarily aids in the reaction and consumption of the oxygen, and oxygen does not breakthrough at the production wells as seen in the temperature field distribution in Figs.6.5-A and B, where the $O_2$ concentration is overlain on the temperature distribution between the injectors and producers (for 10000 and 30000m3/day rates). The figures showed that the oxygen concentration was about 20% from the injector positions and became 0% at 500m and 400m away from the producers for the 10000m$^3$/day and 30000m$^3$/day injection rates respectively.

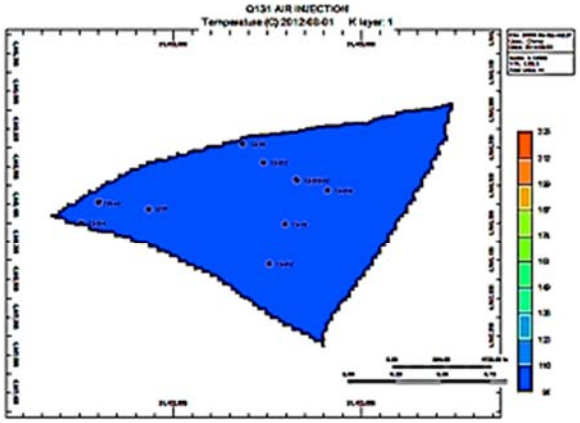


**Fig. 6.2-A: Temperature field distribution at 0 year of air injection.**

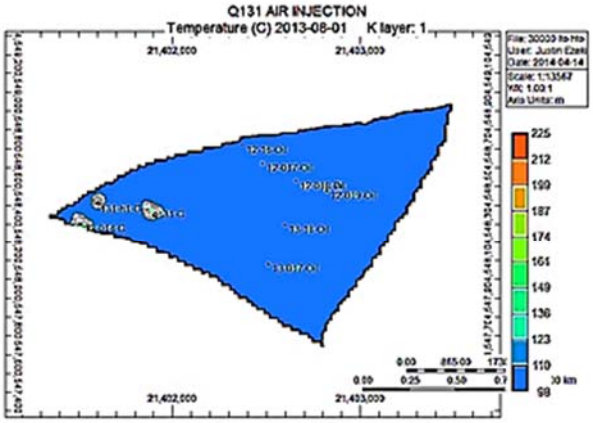


**Fig. 6.2-B: Temperature field distribution after 1 year of air injection.**

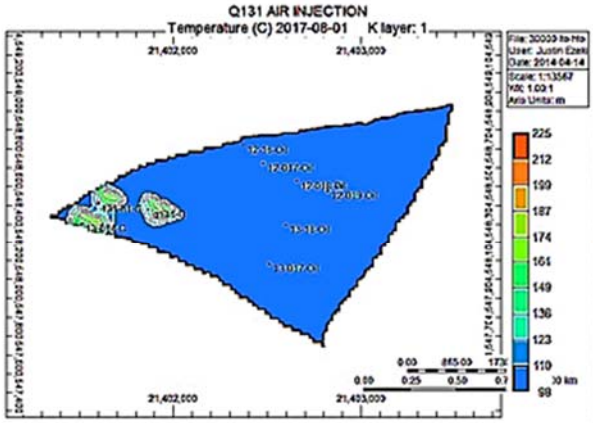


**©Fig. 6.2-C: Temperature field distribution after 5 years of air injection.**

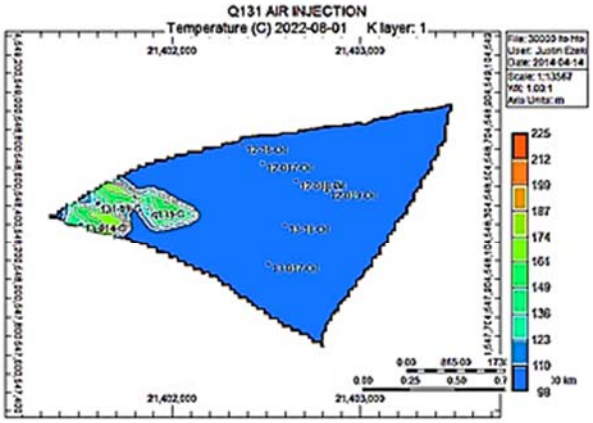


**Fig. 6.2-D: Temperature field distribution after 10 years of air injection.**

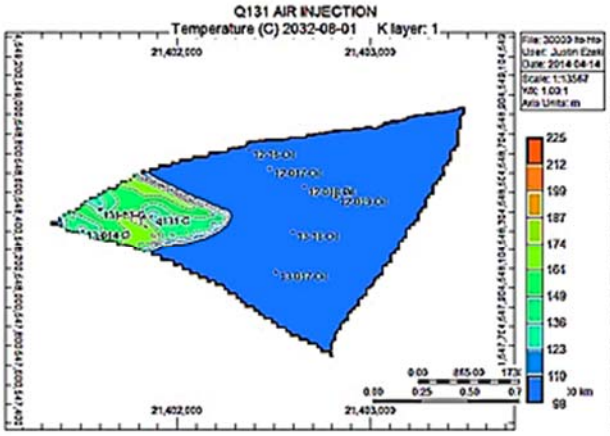


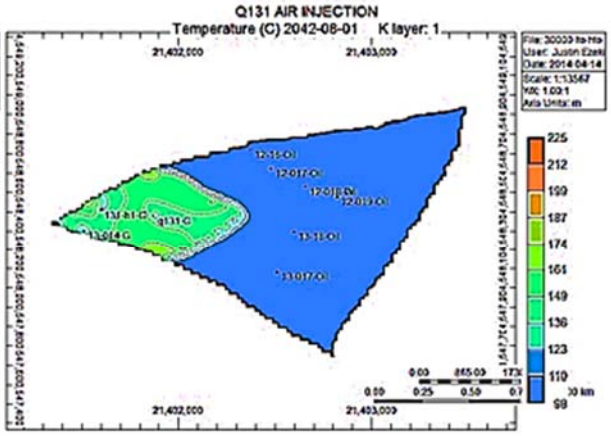


**Figs. 6.2-E and F: Temperature field distribution after 20 and 30 years of air injection respectively.**

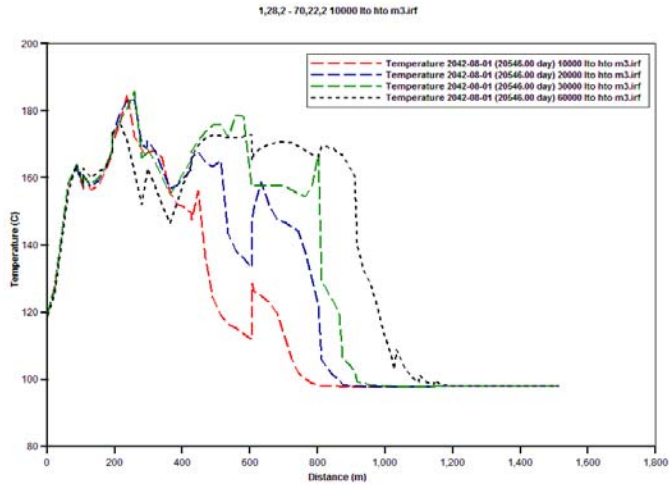


**Fig. 6.3: Temperature field distribution between injectors and producers at different air injection rates after 30 years.**

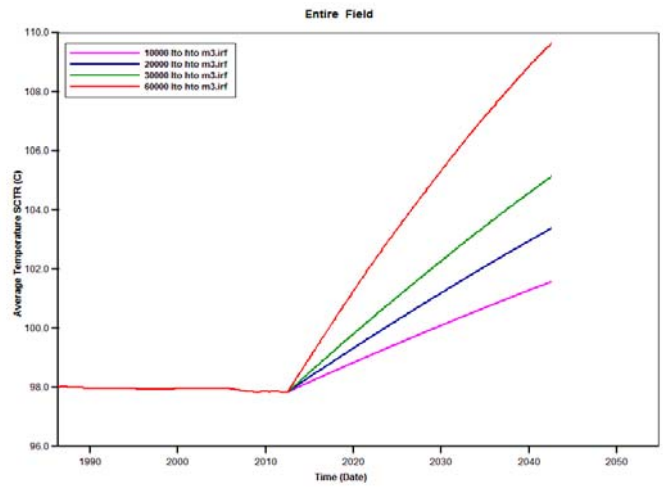


**Fig. 6.4: Average Temperature variation under different air injection rates.**

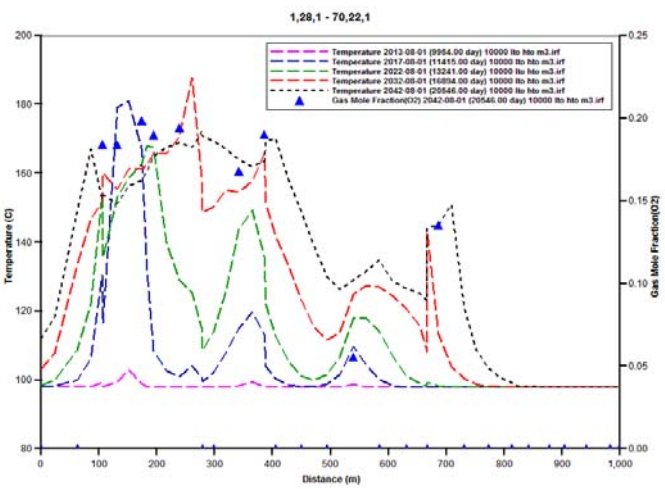


**Fig. 6.5-A: Temperature field distribution between injectors and producers at different times and comparison with $O_2$ concentration, under 10000m$^3$ air injection rate.**

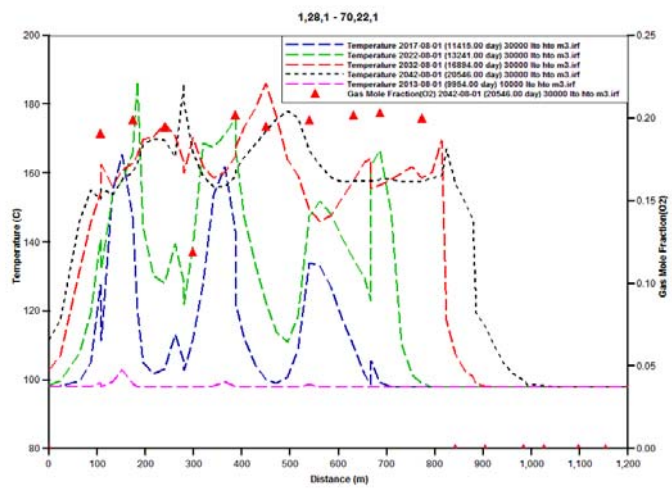


**Fig. 6.5-B: Temperature field distribution between injectors and producers at different times and comparison with $O_2$ concentration, under 30000m$^3$ air injection rate.**

#### 6.2.1.2 $O_2$, $CO_2$, and $N_2$ Concentration in the Reservoir

In any air injection process, wen air is injected $O_2$, $CO_2$ and $N_2$ are formed in the reservoir, with the latter two referred to as flue gases which primarily drives the oil to the production wells. The $O_2$ is expected to be consumed in the reservoir and not breakthrough at the producers, therefore it must be verified using this simulation study to know the concentrations of these gases at the reservoir and at the producer locations to ascertain if the oxygen is consumed in the reservoir. The following simulation results highlights the concentration of these gases in the reservoir between the injectors and the producers.

Oxygen concentration of about 20% was observed in the parts of the reservoir that are close to the injectors, as shown in Figs. 6.6-A to D, which showed the simulation results of the $O_2$ concentration field distribution between injectors and producers at different times, under the different studied injection rates. The 0% $O_2$ concentration zone distance away from the production wells can be easily calculated from the Table 6.1 for different injection rates scenarios and time (in years). The figures and table showed that as the injection rates increased, the oxygen front advances towards the production wells. The injection-production wells separation in this simulation study is about 1200m, so it can be observed that the oxygen concentrations at the production wells positions are zero, which indicates that the oxygen was completely consumed in the reservoir and it didn't breakthrough at any of the 14 production wells. This is one of the most important aspects of this study in which the oxygen non-breakthrough is a very important phenomenon in the success of air injection for IOR.

Figs. 6.7-A to D and Figs. 6.8-A to D showed the simulation results of the $CO_2$ and $N_2$ concentration field distributions between injectors and producers at different times, under the different injection rates. As earlier introduced, these two gases are called flue gases that are generated in the reservoir when air reacts with the hydrocarbon, and they have an important function to immiscibly drive the oil to the production wells. It can observed that significant concentration of these two gases are seen at the production wells locations, which indicated that the these gases breakthrough at the in the first line of the producers after 2-3years of injection, and their volumes increased as the injection rates increased from the low case to high case scenarios. The concentrations of the $CO_2$ ranges from 0.10 to 0.12 mole fraction, while the $N_2$ concentrations are seen to increase from 0.3 in the first few years to very high molar concentrations of about 0.8 to 0.9 at the latter years. The distances these gases cover from the injection wells to the production wells increases as the injection rates and injection times increased.

Fig. 6.9 showed the $O_2$, $CO_2$ and $N_2$ concentrations field distribution between injectors and producers after 30 years of air injection, under the base case scenario (30000m$^3$/day) injection rate and it is observed that the $O_2$, $CO_2$ and $N_2$ concentrations field distribution and observed that oxygen was

completely consumed at the reaction zone at 800m away from the injectors (more than 300m from the producers). Immediately after the oxygen concentration became zero, it is observed that $CO_2$ was seen to increase from zero to about 12%. This confirms that in the reservoir, as oxygen is consumed in the reaction zone $CO_2$ is instantaneously generated.

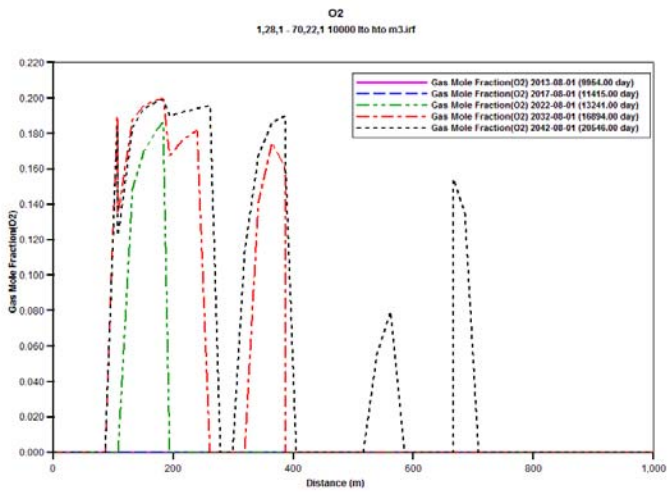


**Fig. 6.6-A: $O_2$ concentration field distribution between injectors and producers at different times, under 10000 $m^3$/day air injection rate.**

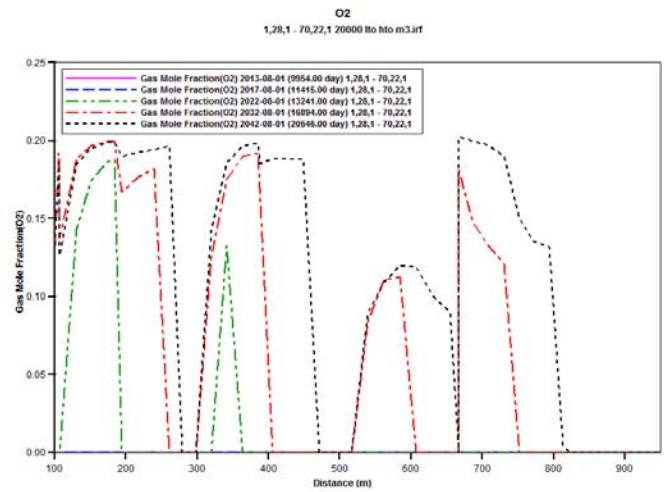


**Fig. 6.6-B: $O_2$ concentration field distribution between injectors and producers at different times, under 20000 $m^3$/day air injection rate.**

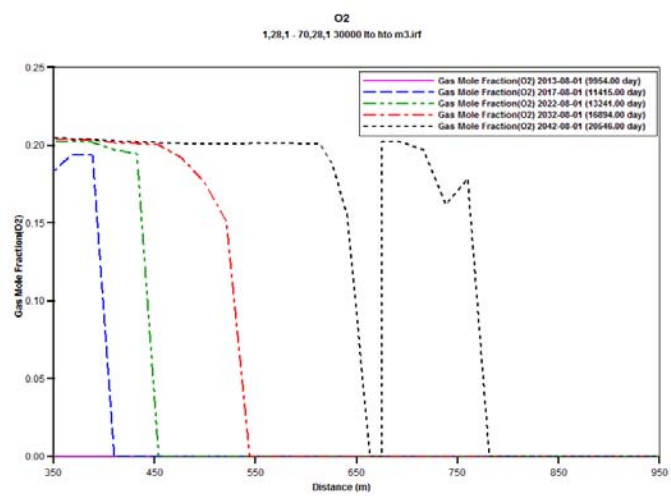


**Fig. 6.6-C: $O_2$ concentration field distribution between injectors and producers at different times, under 30000 $m^3$/day air injection rate.**

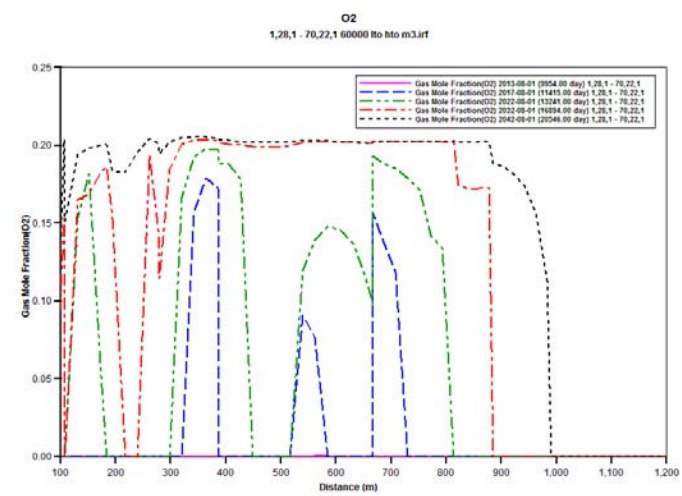


**Fig. 6.6-D: $O_2$ concentration field distribution between injectors and producers at different times, under 60000 $m^3$/day air injection rate.**

**Table 6.1: showing the distances between Injector-Producer that 0% oxygen concentration under air injection**

| Rates \ Time | 1year (2013.08) | 5years (2016.08) | 10years (2022.08) | 20years (2032.08) | 30years (2012.08) |
|---|---|---|---|---|---|
| **10000 $m^3$/day (Low-Case)** | -- | -- | 194.3 | 386.8 | 708.2 |
| **20000 $m^3$/day (Low-Case)** | -- | -- | 364.1 | 751.6 | 822.8 |
| **30000 $m^3$/day (Base-Case)** | -- | 410.3 | 454.2 | 544.4 | 781.2 |
| **60000 m3/day (High-Case)** | -- | 730.1 | 813.0 | 885.4 | 990.8 |

***Note: the Injector-Producer distance is about 1200m***

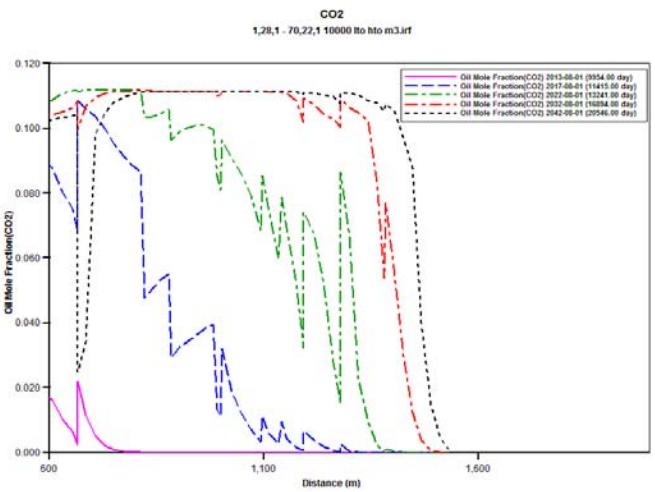


**Fig. 6.7-A: $CO_2$ concentration field distribution between injectors and producers at different times, under 10000 $m^3$/day air injection rate.**

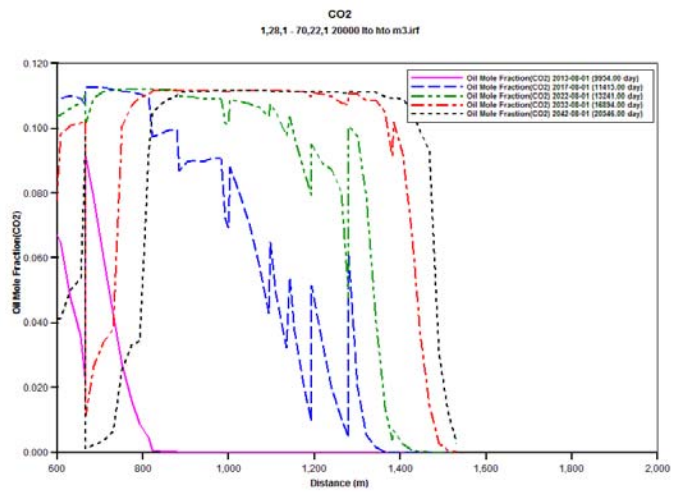


**Fig. 6.7-B: $CO_2$ concentration field distribution between injectors and producers at different times, under 20000 $m^3$/day air injection rate.**

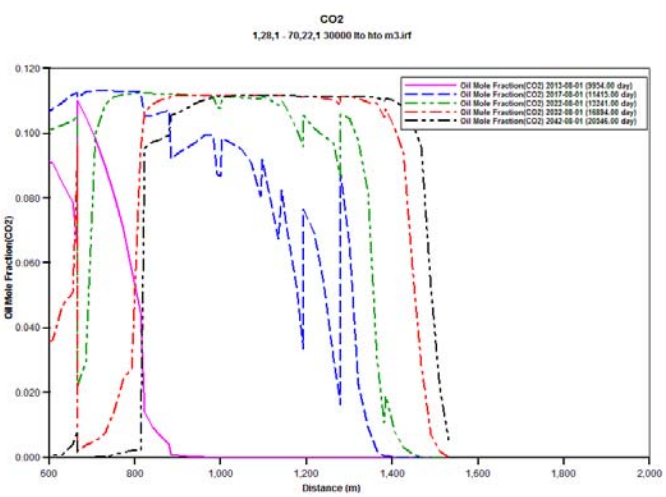


**Fig. 6.7-C: $CO_2$ concentration field distribution between injectors and producers at different times, under 30000 $m^3$/day air injection rate.**

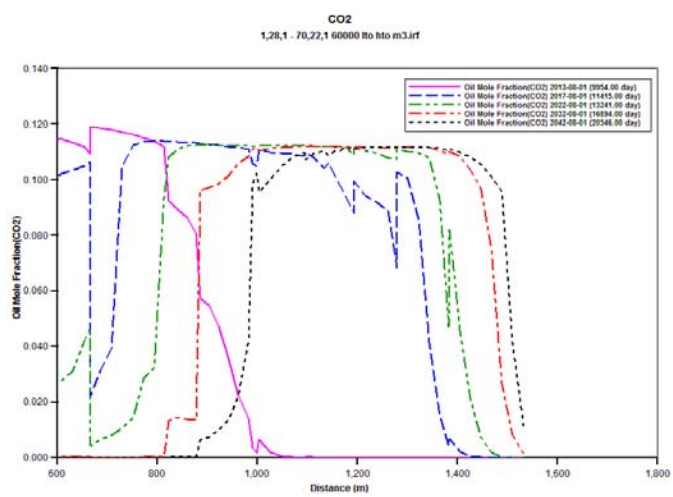


**Fig. 6.7-D: $CO_2$ concentration field distribution between injectors and producers at different times, under 60000 $m^3$/day air injection rate.**

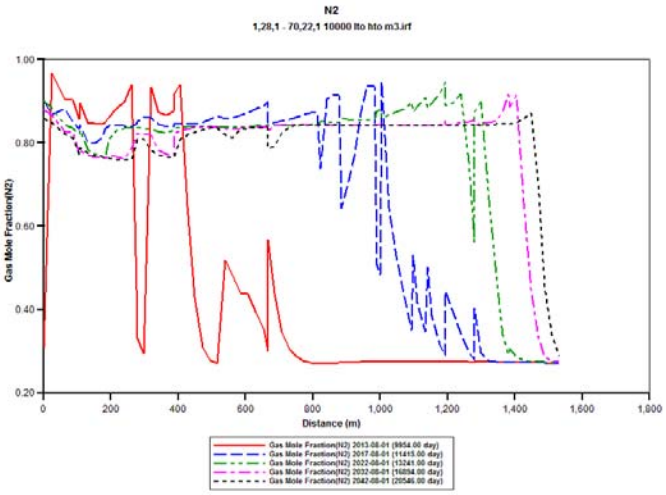


**Fig. 6.8-A: $N_2$ concentration field distribution between injectors and producers at different times, under 10000 $m^3$/day air injection rate.**

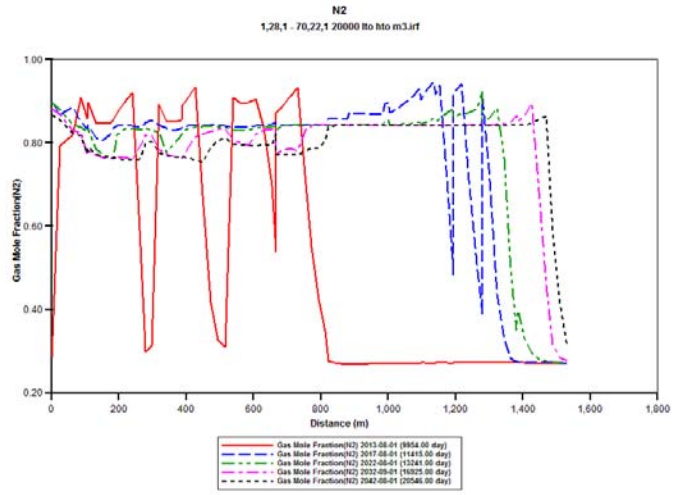


**Fig. 6.8-B: $N_2$ concentration field distribution between injectors and producers at different times, under 20000 $m^3$/day air injection rate.**

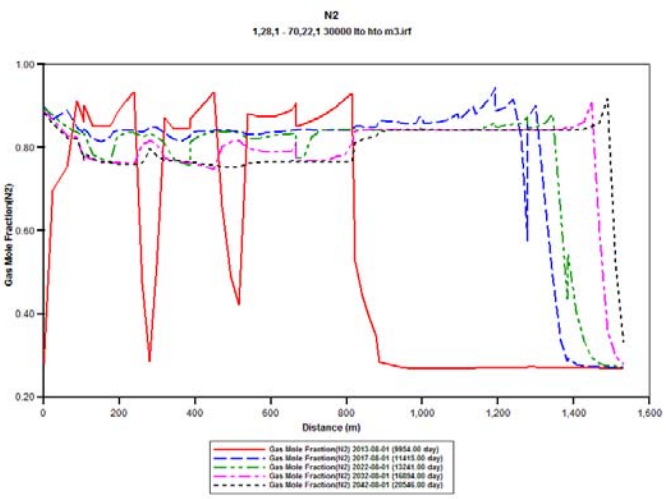


**Fig. 6.8-C: $N_2$ concentration field distribution between injectors and producers at different times, under 30000 $m^3$/day air injection rate.**

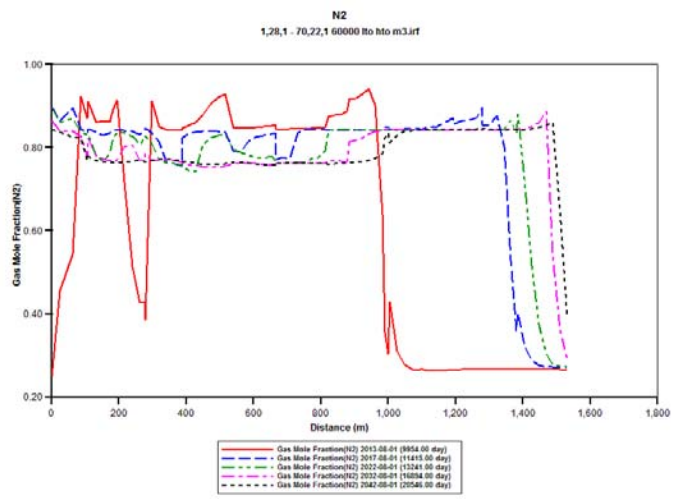


**Fig. 6.8-D: $N_2$ concentration field distribution between injectors and producers at different times, under 60000 $m^3$/day air injection rate.**

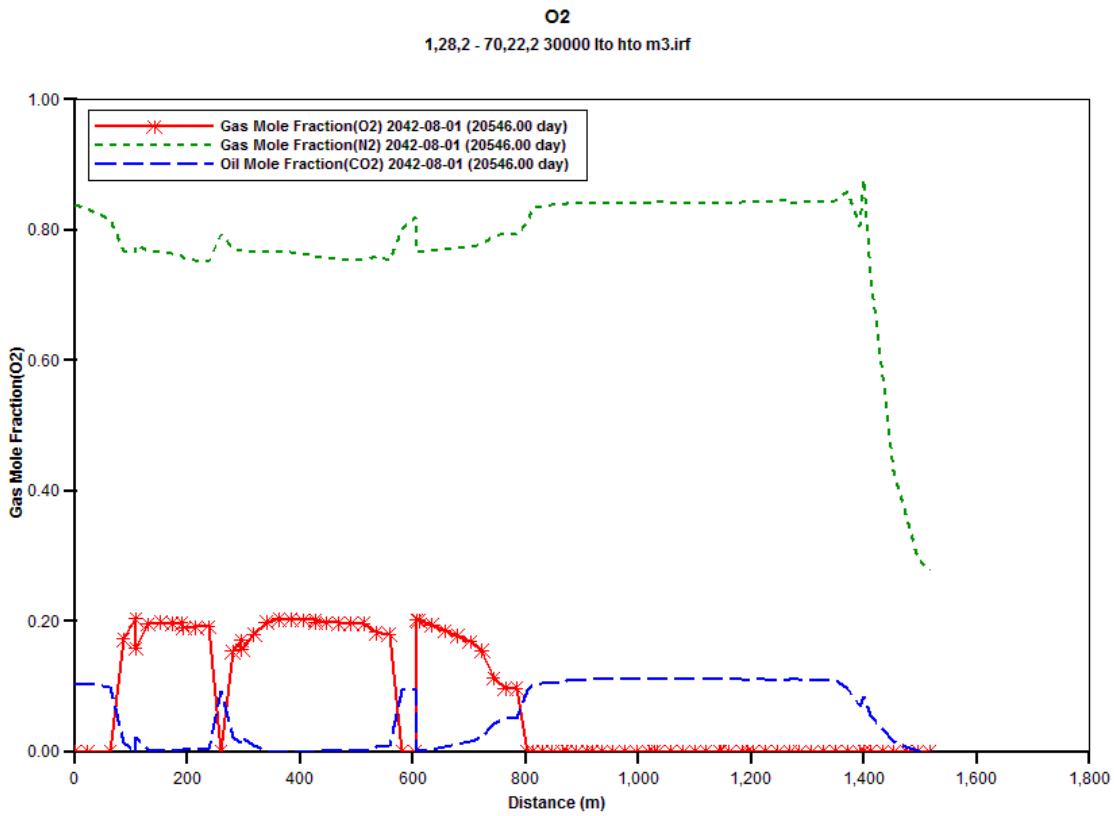


**Fig. 6.9: $O_2$, $CO_2$ and $N_2$ concentrations field distribution between injectors and producers after 30 years of air injection, under 30000 $m^3$/day injection rate.**

### 6.2.1.3 Fluid Saturation

#### 6.2.1.3.1 Gas Saturation Field Distribution

Fig. 6.10-A shows the gas saturation field distribution at the beginning, i.e. 1year after the injection started for the base case scenario of using 30000$m^3$/day air injection. A gradual progression of the injected gas is observed to move from the up dip structure of the oil block to the down structure, to cause an increase in the gas saturation distribution of the block. A 60% value is observed at the location of gas injection wells and about 33% in the regions close the injectors. The unaffected regions had a gas saturation of less than 5%. After % years of injection, the field's gas saturation increased to more than 65% at the injector locations and up to 45% at the others parts of the reservoir. This time, gas saturation distribution is more widely spread to most parts of the block. (Fig. 6.10-B). The gas saturation continued to increased and spread evenly at the top up dip structure to about 70% of the pore volume and lesser values of about 49% in the mid-region of the block as shown in Figs. 6.10-C to E), which is very close to the locations of the production wells. This shows that gas breakthrough in the production wells started before the 5years into the air injection process and the volume of gas that were produced increased over the years as more gas is injected and more gas saturated the reservoir.

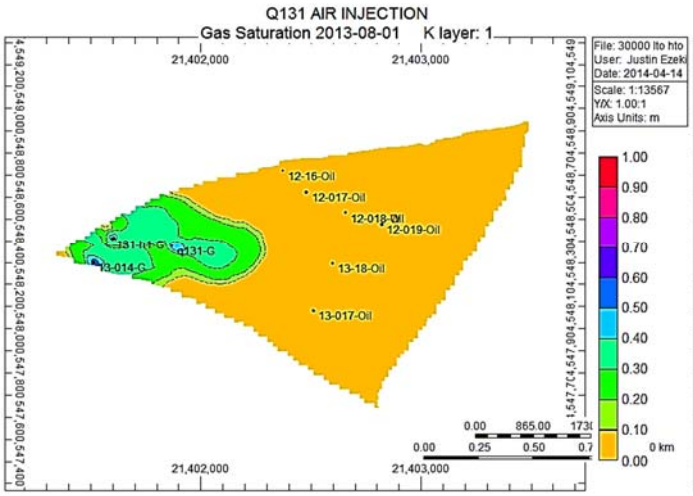


**Fig. 6.10-A: Gas saturation field distribution after 1 year of air injection.**

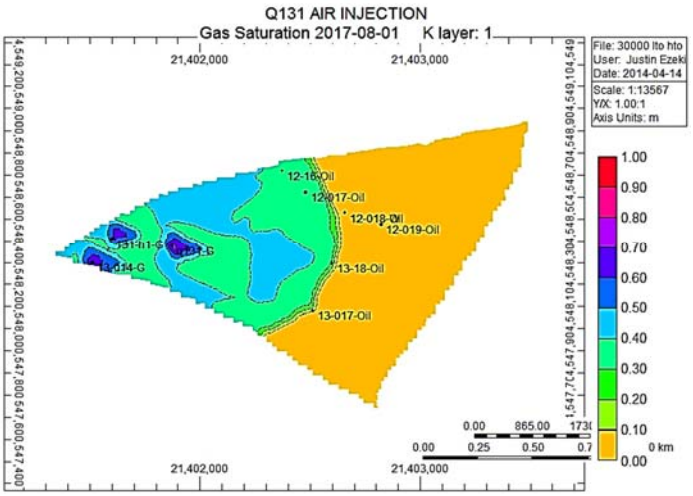


**Fig. 6.10-B: Gas saturation field distribution after 5 years of air injection.**

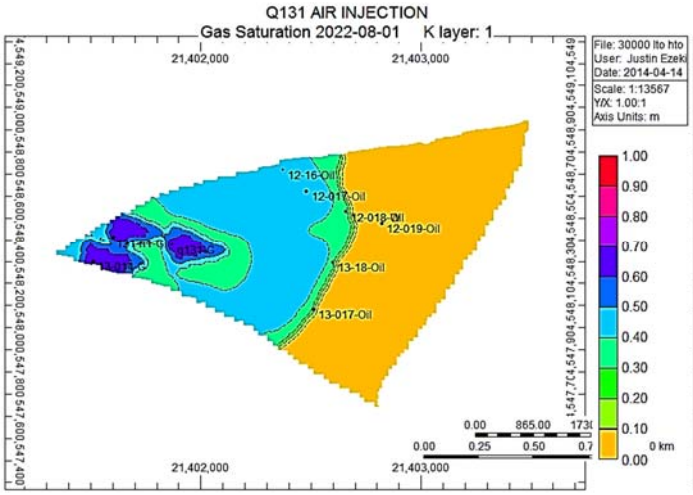


**Fig. 6.10-C: Gas saturation field distribution after 10 years of air injection.**

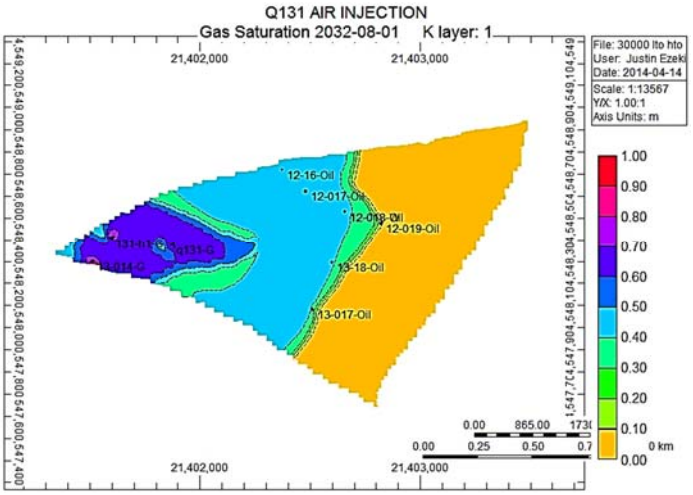


**Fig. 6.10-D: Gas saturation field distribution after 20 years of air injection.**

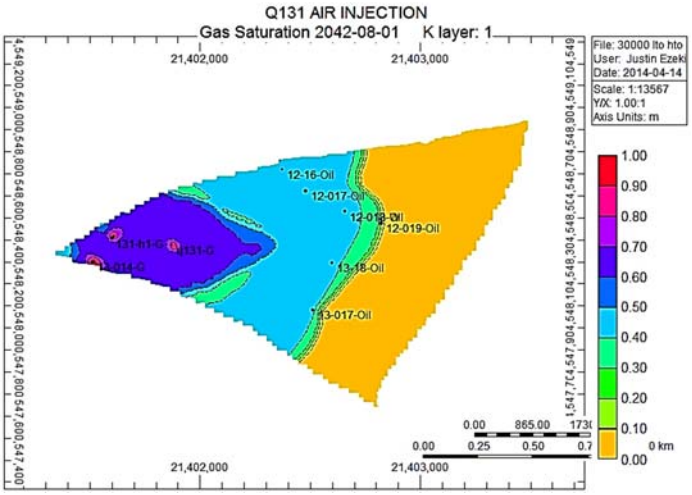


**Fig. 6.10-E: Gas saturation field distribution after 30 years of air injection.**

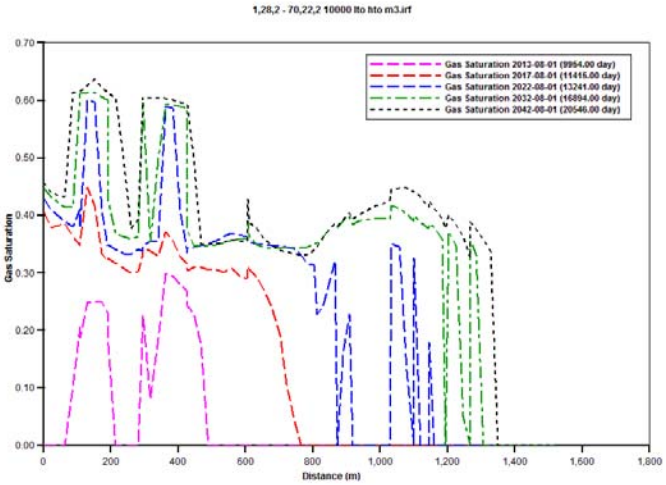


**Fig. 6.11-A: Gas saturation field distribution between injectors and producers at different times (years), under 10000 m$^3$/day air injection rate.**

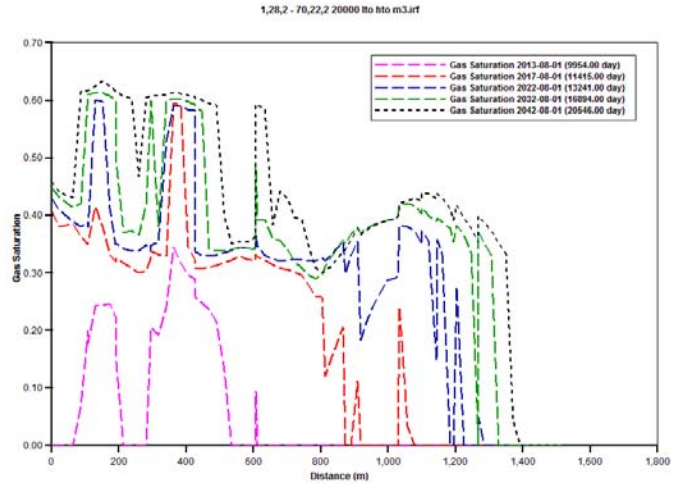


**Fig. 6.11-B: Gas saturation field distribution between injectors and producers at different times (years), under 20000 m$^3$/day air injection rate.**

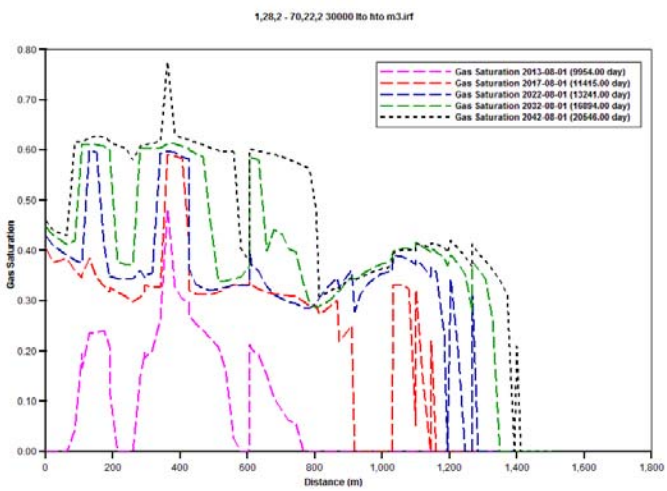


**Fig. 6.11-C: Gas saturation field distribution between injectors and producers at different times (years), under 30000 m$^3$/day air injection rate.**

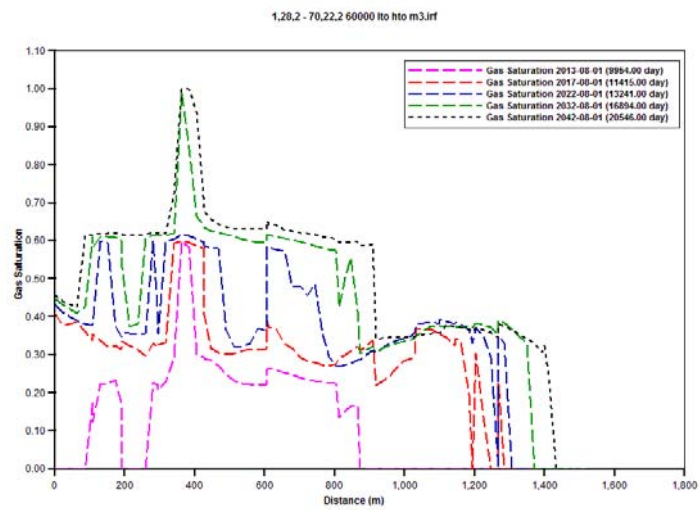


**Fig. 6.11-D: Gas saturation field distribution between injectors and producers at different times (years), under 60000 m$^3$/day air injection rate.**

Figs. 6.11-A to D show the increasing gas saturation distributions in the block as the injection time (years) increases and the injection rate increases from the low case injection rate scenario (10,000 and 20000m3/day) to the base case (30,000m3/day) and the high case scenario (60,000m3/day) with respect to this gas injection study. Table 6.2 gives a detailed presentation of the distances from the injectors that the gas saturation progress towards the producers with time (in years), using the different injection rate scenarios. The table also showed that the more the injection rate, the faster the movement of the injected gas in the reservoir, the further the distance the injected gas moves with respect to time of

consideration, the higher the gas saturation in the pore volume especially close the injection wells, and ultimately the earlier the gas breakthrough time.

**Table 6.2: Comparison between injection rates and time in terms of the maximum gas saturation and injector-producer distances traveled by gas front.**

| Injection Rate (m3/day) | Parameter | 1 year | | | 5 years | | | 10 years | | | 20 years | | | 30 years | | |
|---|---|---|---|---|---|---|---|---|---|---|---|---|---|---|---|---|
| | | Air | $CO_2$ | $N_2$ | Air | $CO_2$ | $N_2$ | Air | $CO_2$ | $N_2$ | Air | $CO_2$ | $N_2$ | Air | $CO_2$ | $N_2$ |
| 10000 (Low Case Scenario) | Max. Distance of Gas Front (m) | 490 | 446 | 513 | 764 | 812 | 812 | 1160 | 1119 | 1161 | 1307 | 1307 | 1307 | 1349 | 1349 | 1349 |
| | Max Gas Saturation (%) | 30 | 27 | 32 | 45 | 28 | 37 | 60 | 40 | 42 | 61 | 44 | 46 | 64 | 47 | 50 |
| 20000 (Low Case Scenario) | Max Distance of Gas Front (m) | 611 | 468 | 634 | 1079 | 918 | 1119 | 1225 | 1225 | 1225 | 1328 | 1328 | 1328 | 1400 | 1349 | 1371 |
| | Max Gas Saturation (%) | 35 | 32 | 35 | 59 | 35 | 39 | 60 | 40 | 44 | 61 | 45 | 50 | 64 | 47 | 55 |
| 30000 (Base Case Scenario) | Max Distance of Gas Front (m) | 764 | 634 | 802 | 1161 | 1101 | 1143 | 1285 | 1247 | 1285 | 1349 | 1329 | 1349 | 1411 | 1371 | 1411 |
| | Max Gas Saturation (%) | 48 | 34 | 37 | 59 | 37 | 41 | 60 | 41 | 45 | 62 | 46 | 52 | 78 | 48 | 60 |
| 60000 (High Case Scenario) | Max Distance of Gas Front (m) | 873 | 783 | 918 | 1285 | 1225 | 1247 | 1307 | 1307 | 1361 | 1371 | 1371 | 1371 | 1432 | 1432 | 1432 |
| | Max Gas Saturation (%) | 60 | 37 | 40 | 60 | 40 | 44 | 62 | 42 | 49 | 85 | 46 | 61 | 100 | 48 | 70 |

***Note the maximum gas saturation values are mostly observed and obtained at the injection wells location.***

We should note that as the gas saturation increases, it means that the corresponding field oil saturation decreases because as gas is injection into the pore volume and it saturates the reservoir, oil is being displaced by this injected gas and this the oil saturation decreases as more gas is injected into the reservoir.

A special case can be recognized in the Fig. 6.11-D, where after 30 years of constant 60000m3/day air injection, we have a 100% gas saturation field at the location of one of the injection wells (Q131-G). This indicates that the oil saturation at the point is zero, i.e. no oil left at this region. This shows that the reaction zone in the air injection zone consumes the oil in this zone and thus we have a 0% oil saturation at this point. This can be used to answer the questions of the combustion potentials of the low temperature oxidation air injection process. It is deduced from this study, that at a higher injection

rate, a burnt zone is observed at the immediate location of the injectors and an insignificant amount of oil is consumed by the reaction in this burnt zone.

#### 6.2.1.3.2 Oil Saturation Field Distribution

The oil saturation distribution using constant injection rate of 30000m$^3$/day for different years (Figs. 6.12-A to F) indicate that the oil was gradually and almost completely drained by the reaction in the reaction zone, which progressively moved from the regions close to the injectors towards the producers. In the region between the reaction zone and producers, the oil saturation reduced from 64% (1 year period) to 50% (5 years period) and then to approximately 15% (30 years period) indicating a good sweep of the reservoir by the flue gas assisted by gravity stabilization.

The vicinities of the injection wells appeared to be of very low oil saturation, of about 0-5% in the later years of injection. This can be an indication that the residual oil in these vicinities were continuously burnt as time progresses. This complements the theory that in air injection practice, high temperature is generated in the reaction between the hydrocarbon and the oxygen content of the injected air. Thus, the increased temperature is a function of the oxidation reaction where oxygen is consumed and in turn flue gases generated to drive the oil, while the remaining oil in the reaction zone is burnt as a result of the high temperature predominant in this region. An example of a special case can be observed in the immediate location of the injector Q131-G (Block 24, 25, 1) showed a 0% oil saturation (Fig. 6.12-C to F) and 100% gas saturation (Fig. 6.11D).

As we have earlier discussed in the previous section and observed that as gas saturation increases oil saturation tends to decrease. Figs. 6.13-A to D show that with increasing injection time the oil saturation reduces towards the producers, indicating that the process is primarily controlled by the increasing relative permeability of the injected gas in the reservoir and the corresponding decrease in the relative permeability of oil.

### 6.2.1.4 Oil Viscosity Field Distribution

The oil viscosity field distribution shown in Figs. 6.14-A to F, showed that oil viscosity drastically decreased as injection time increases, using the base case scenario i.e. 30000m3/day injection rate. This fast decline is more active in the regions close the injection wells. As time increased to about 5 years, almost zero-value oil viscosity were noticed in these regions and this is due to the increasing reservoir gas saturation and consumption of the residual oil in this reaction zone. Fig.6.15 shows that after 30years of air injection, the oil viscosity of the block decreased from the original 0.48mPa.s to about 0.40mPa.s in the mid-region between the injectors and the producers. An anomalous decrease to a value of 0.01mPa.s were seen in the vicinity of the injectors.

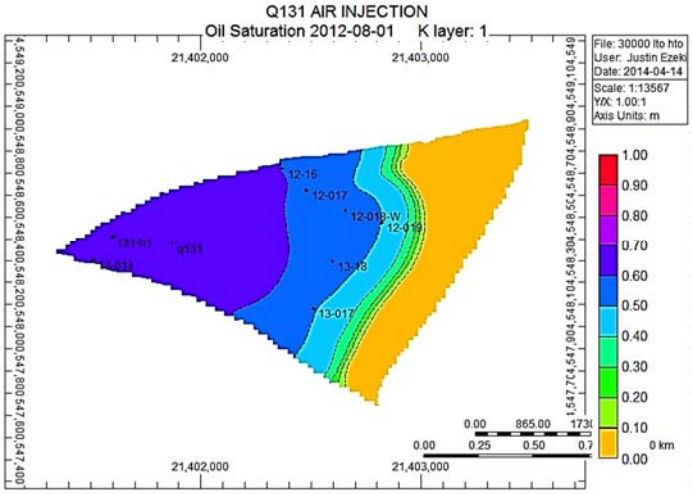


**Fig. 6.12-A: Oil saturation field distribution at 0 year of air injection.**

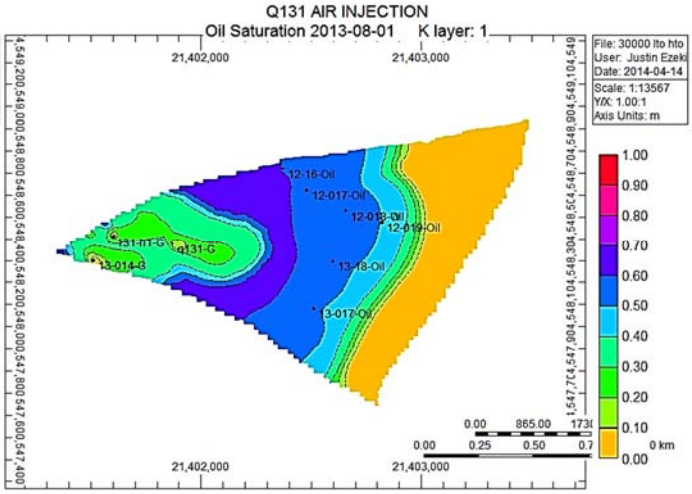


**Fig. 6.12-B: Oil saturation field distribution after 1 year of air injection.**

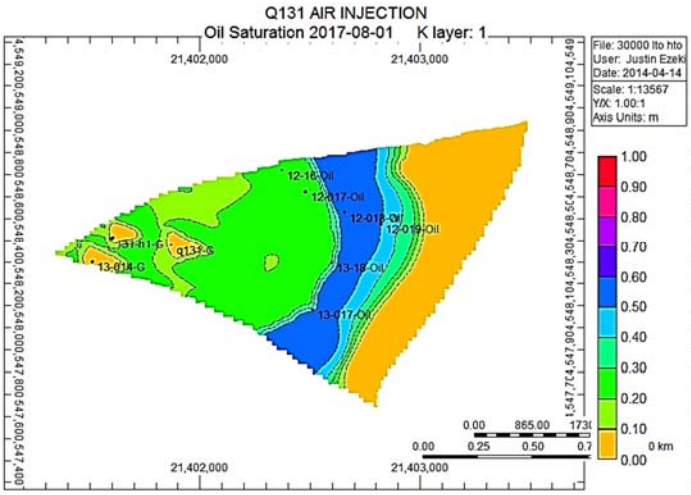


**Fig. 6.12-C: Oil saturation field distribution after 5 years of air injection.**

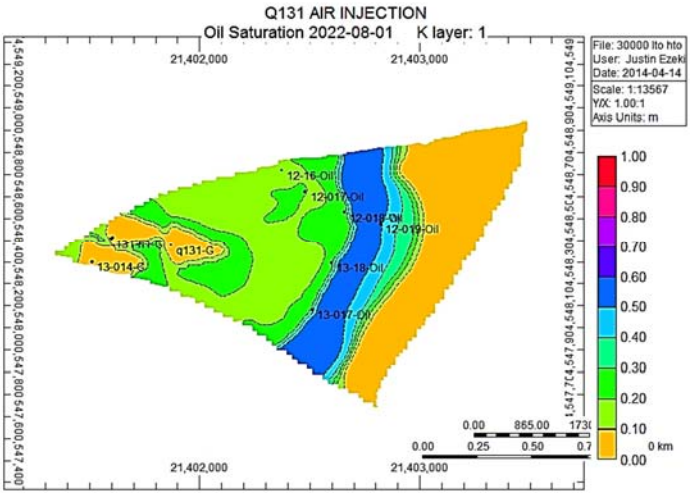


**Fig. 6.12-D: Oil saturation field distribution after 10 years of air injection.**

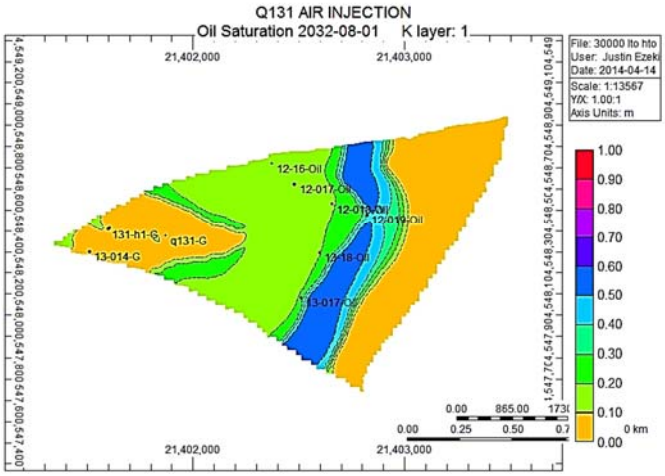


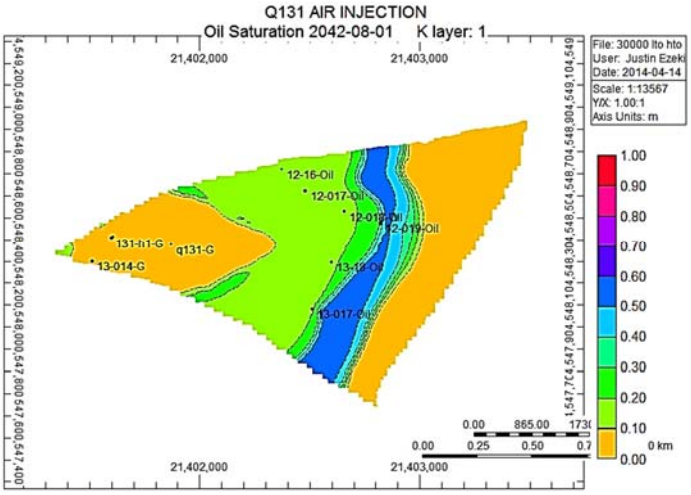


**Figs. 6.12-E and F: Oil saturation field distribution after 20 and 30 years of air injection respectively.**

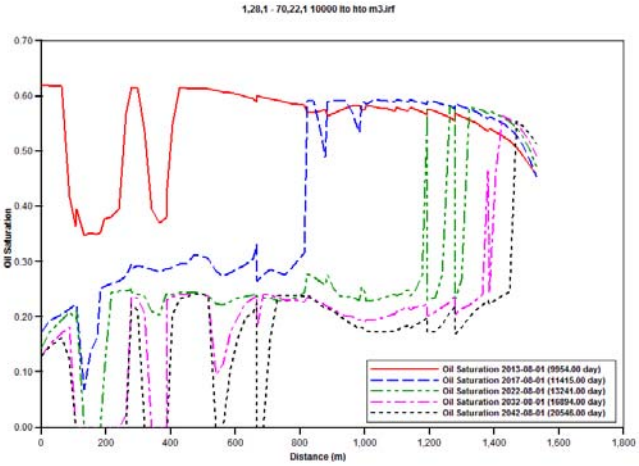


**Fig. 6.13-A: Oil saturation field distribution between injectors and producers at different times (years), under 10000 m$^3$/day air injection rate.**

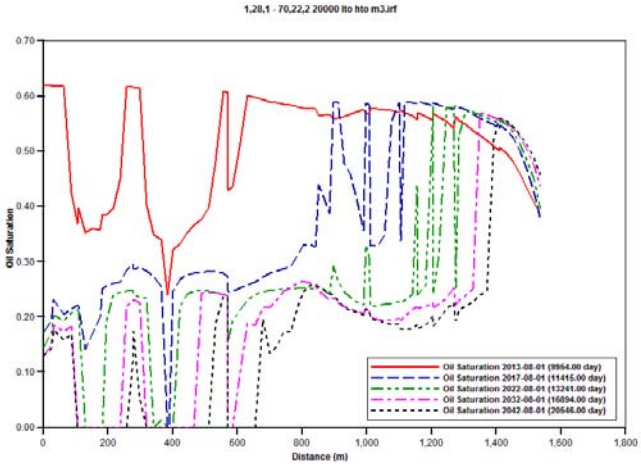


**Fig. 6.13-B: Oil saturation field distribution between injectors and producers at different times (years), under 20000 m$^3$/day air injection rate.**

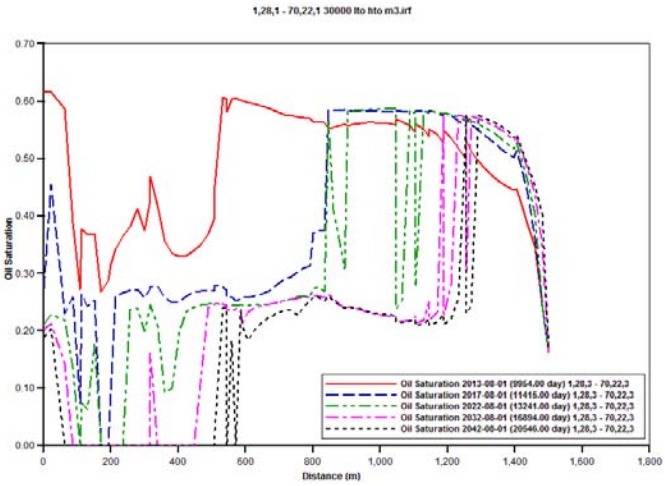


**Fig. 6.13-C: Oil saturation field distribution between injector and producers at different times (years), under 30000 m$^3$/day air injection rate.**

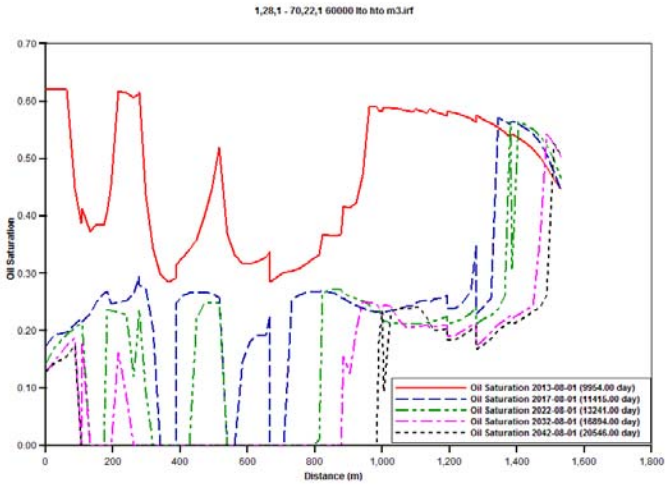


**Fig. 6.13-D: Oil saturation field distribution between injector and producers at different times (years), under 60000 m$^3$/day air injection rate.**

The vicinity of the injection wells with low oil viscosity also appeared to be of very low oil saturation, of about <5% in the later years of the injection (Fig. 6.14-D to F). This can be an indication that the residual oil in these vicinities are burnt/consumed increasingly as the injection rates increased. This goes a long way to complement the theory that in air injection, the high temperature created from burning the fuel gases generated in the reaction of the HC and the oxygen contained in the injected air. This process leads to the consumption of the oil in this area leading the observed very low oil saturation values in these areas close to the injection wells.

These areas close to the injection wells, also showed abnormal increase in temperature (Figs. 6.2-C to F and 6.3), which is different from the normal temperature of the other areas further away from the

injection well. Thus, part of the oil at or close to these areas were mobilized to move down the reservoir structure and the rest were burnt in the reaction zone as illustrated in Equation 5.7 in Section 5.5.1: Thermal and Reaction Kinetics Models.

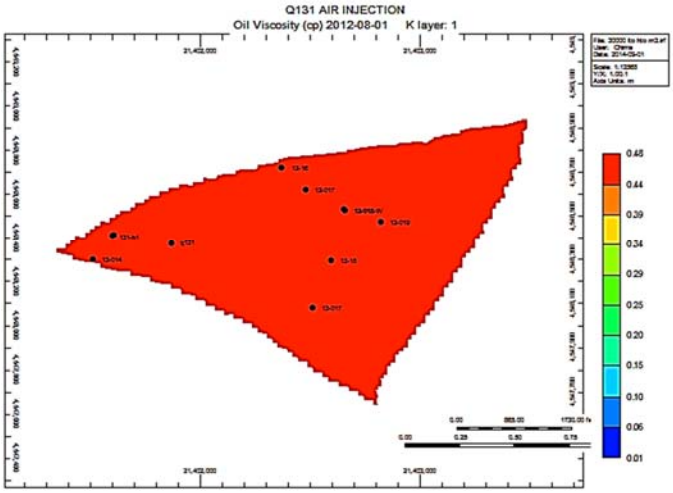


**Fig. 6.14-A: Oil viscosity field distribution at 0 year of air injection.**

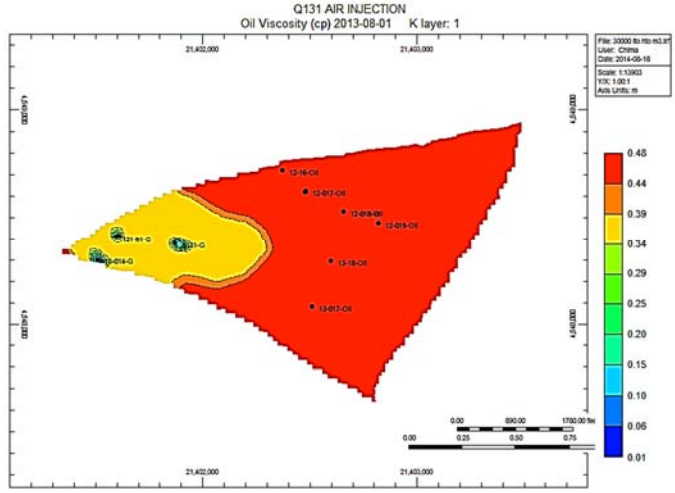


**Fig. 6.14-B: Oil viscosity field distribution after 1 year of air injection.**

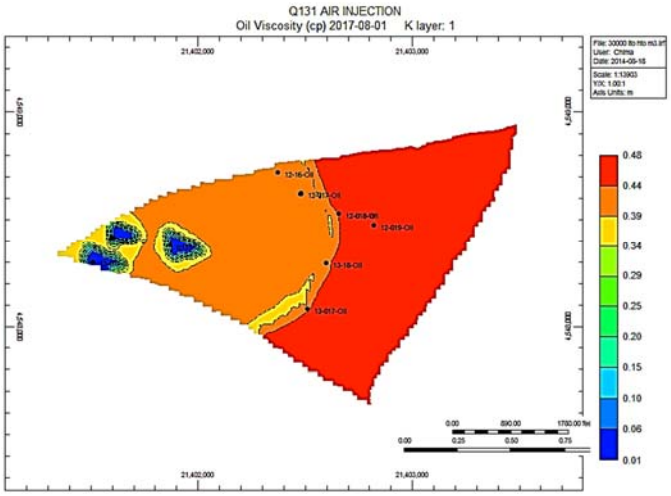


**Fig. 6.14-C: Oil viscosity field distribution after 5 years of air injection.**

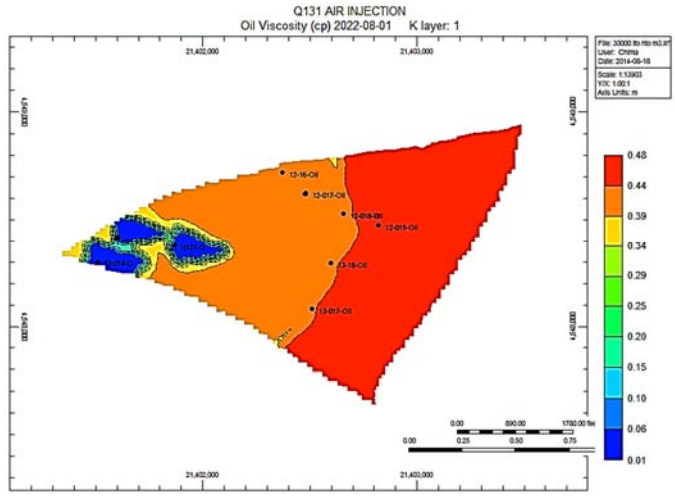


**Fig. 6.14-D: Oil viscosity field distribution after 10 years of air injection.**

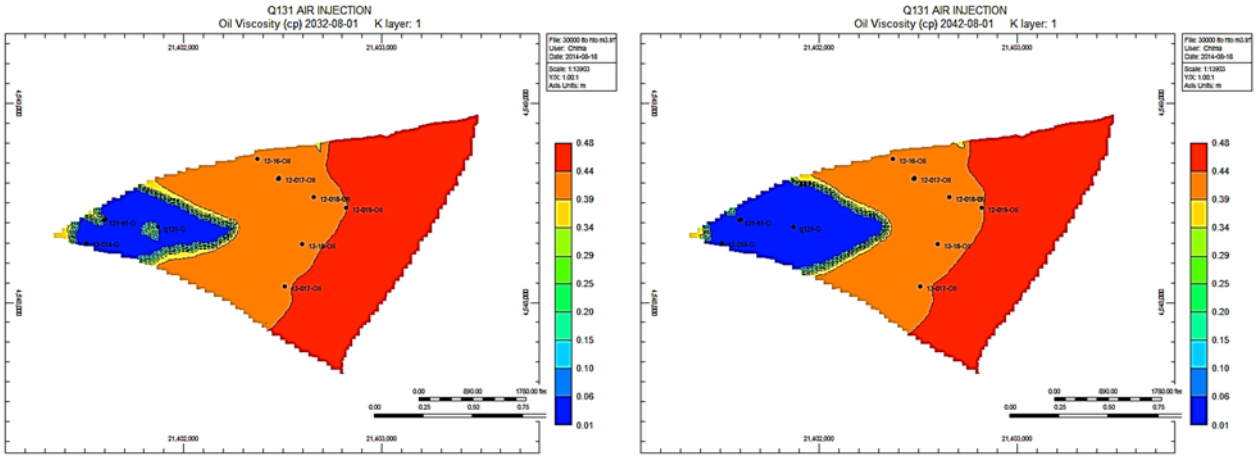


**Figs. 6.14-E and F: Oil viscosity field distribution after 20 and 30 years of air injection respectively.**

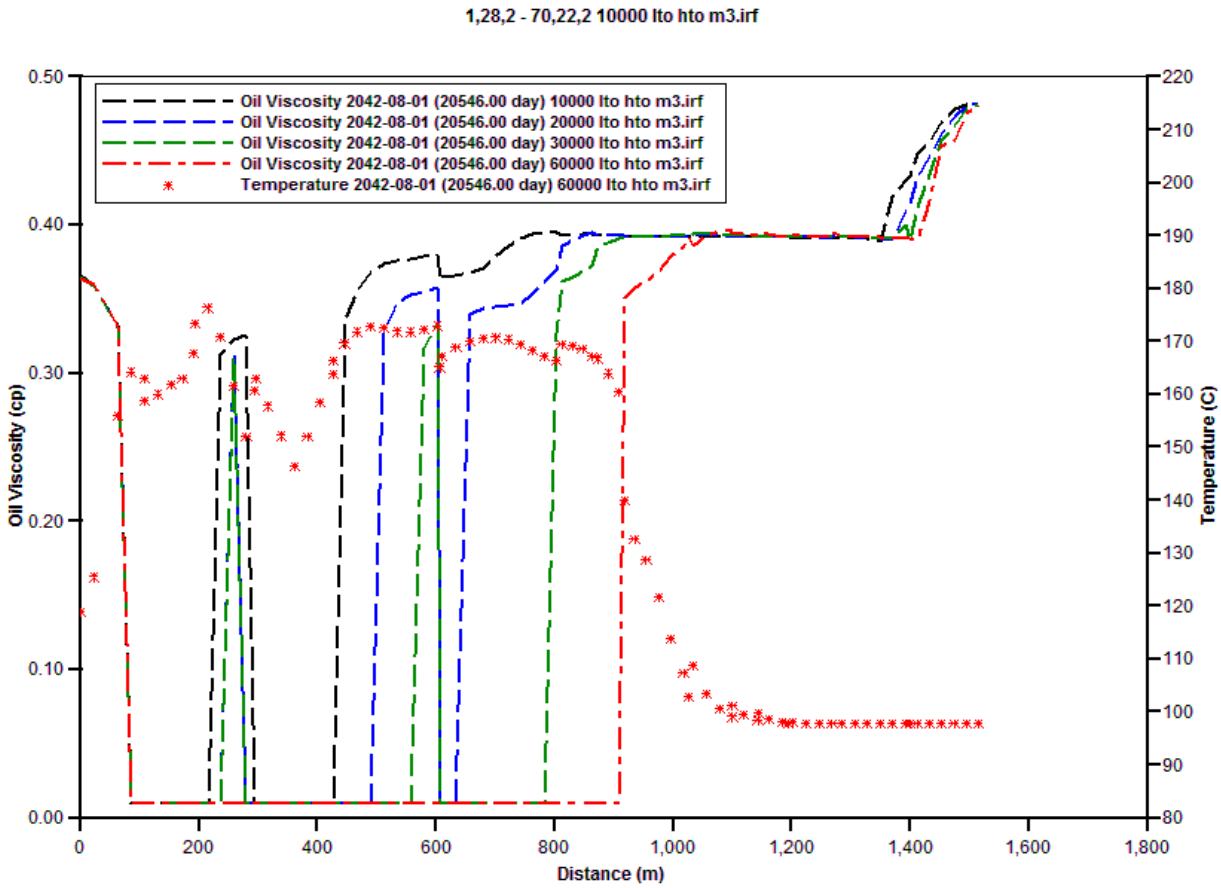


**Fig. 6.15: Effect of Temperature on Oil viscosity field distribution between injectors and producers at different air injection rates after 30 years.**

An overlay of the temperature field distribution to the viscosity field distribution (Fig. 6.15) at the 30th year, showed that the places with a low oil viscosity (<0.35mPa.s) at the vicinity of the injection wells and the midpoint regions have high temperature range from 150-180°C. Then the temperature started to decrease from 160 to 100 °C as the oil viscosity increased for 0.35 to 0.40mPa.s. The temperature is seen to stabilize back to the initial reservoir temperature (98°C) at the regions with >0.40mPa.s oil

viscosity and the initial normal oil viscosity of 0.48mPa.s. These interesting processes indicates that the systems of oil viscosity and temperature of the reservoir are inter-related. Oil viscosity is a dependent function of the temperature of the system. When a liquid (oil) heats up, its molecules become excited and begin to move. The energy of this movement is enough to overcome the forces that bind the molecules together, allowing the liquid to become more fluid and decreasing its viscosity. Generally, the viscosity of oil decreases as temperature increases

Also injection time, injection rates, and locations of the injection wells affect the oil viscosity field distribution, as seen in the Figs. 6.14-A to F and 6.15.

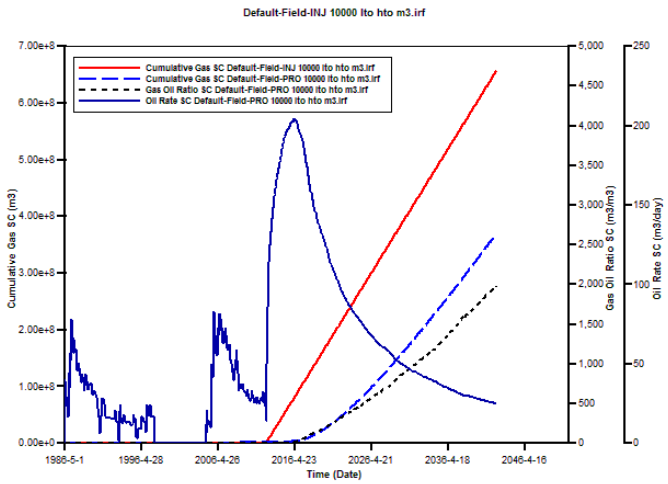


**Fig. 6.16-A: Cumulative gas injected and produced, Gas-oil ratio, Oil daily production rate under 10000m$^3$/day air injection rate.**

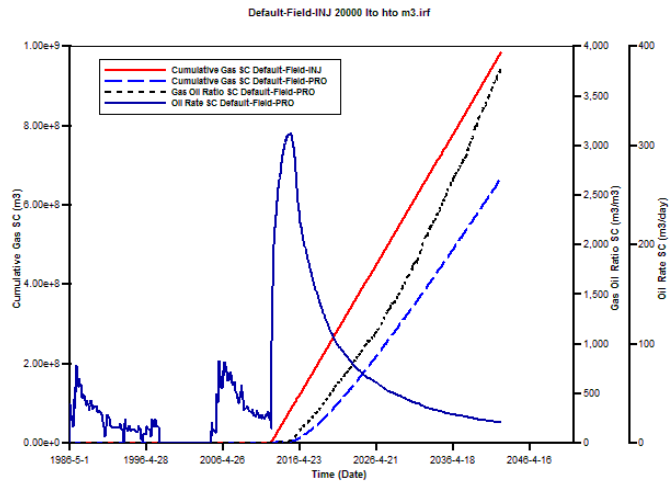


**Fig. 6.16-B: Cumulative gas injected and produced, Gas-oil ratio, Oil daily production rate under 20000m$^3$/day air injection rate.**

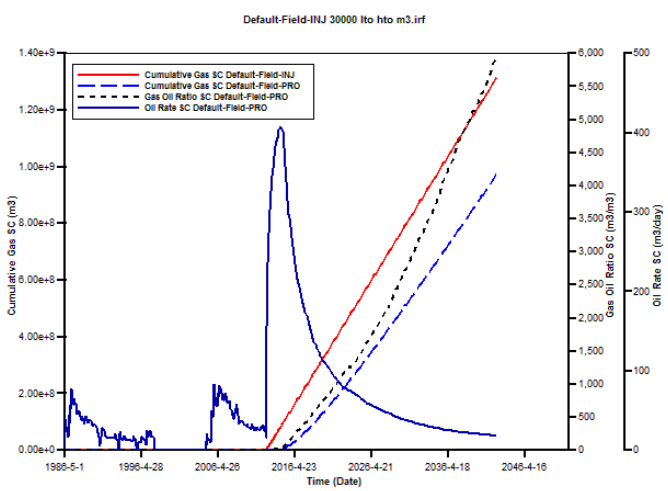


**Fig. 6.16-C: Cumulative gas injected and produced, Gas-oil ratio, Oil daily production rate under 30000m$^3$/day air injection rate.**

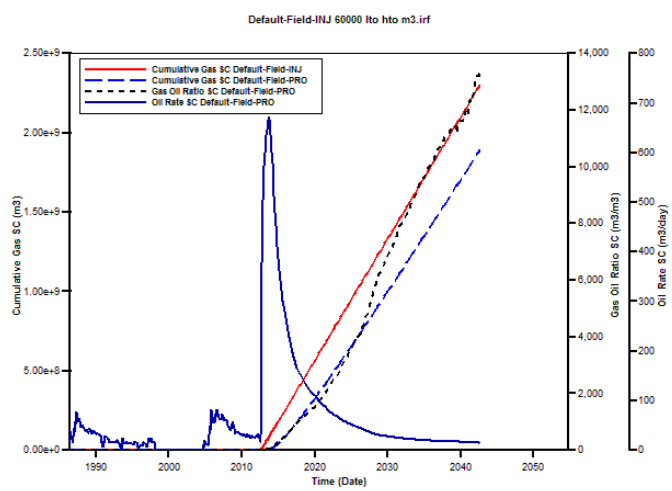


**Fig. 6.16-D: Cumulative gas injected and produced, Gas-oil ratio, Oil daily production rate under 60000m$^3$/day air injection rate.**

#### 6.2.1.5 Gas-Oil Ratio (GOR)

The **gas/oil ratio** is the ratio of the volume of gas that comes out of solution, to the volume of oil at standard conditions. It is known that oil will be produced along reaction-generated flue gas (N2 and CO2) as previously discussed on gas concentration (Section 6.2.1.2) and there was no oxygen breakthrough in the production wells which were set at considerable distance away from the injection to ensure proper and complete consumption of the produced oxygen in the reservoir. When these flue gas front reaches the production wells, GOR will increase rapidly as injection continues as shown in Figs. 6.16-A to D. There is a slow and continuous increase in GOR from the start of the simulated air injection, i.e. August 2012, which increases up to 13,500$m^3/m^3$ at the highest injection rate used (i.e. 60000m3/day ) in the 30 years period considered in this study. Table 6.3 summarizes the various GOR values in different years gotten in the air injection simulation while using different injection rates. **Fig. 6.17** shows that the GOR increased linearly as injection rate increases.

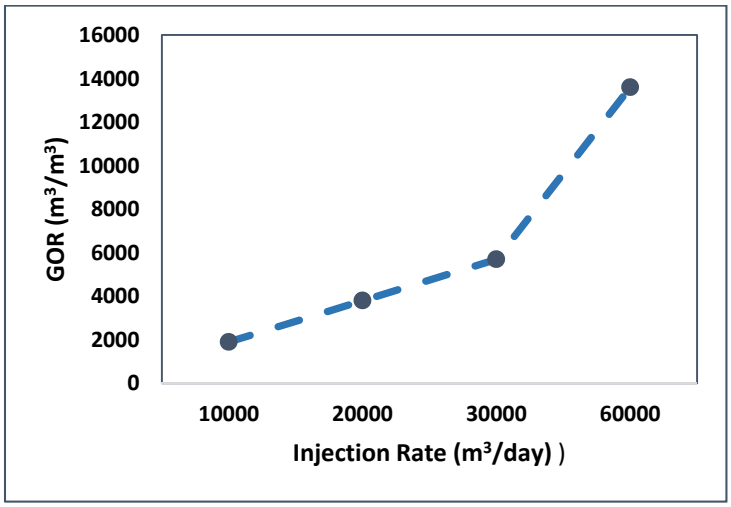


**Fig. 6.17: Plot of GOR vs. Injection rate after 30 years of air injection**

Higher injection rates are expected to cause higher GOR which makes it very difficult to handle the large produced gases or they ($N_2$ and $CO_2$) may be re-injected back into the reservoir through the gas injection wells located high on structure. So measures should be developed to avoid early gas breakthrough and reduce GOR. This is also one of the reasons why this study stopped the optimization injection rate at a maximum of 60000$m^3$/day, because we will have a very high GOR and cumulative produced gas if higher injection rates above this value are considered. An example is the case of applying 100,000$m^3$/day of air injection (Appendix C), we observed a very high GOR and cumulative gas produced of about 21200$m^3/m^3$ and 3.12E+09$m^3$ respectively. Although it has a very high cumulative oil produced and incremental recovery factor of about 1.39E+06$m^3$ and 39.8% OOIP respectively, but it is more economical to use the lower injection rates as applied in this study.

#### 6.2.1.6 Oil Production Rate

The oil production rate increases rapidly in the early years of air injection **(**Figs. 6.16-A to D**)** even up to a maximum value of about 700m$^3$/day before a sharp decrease in the oil rate began as both the gas breakthrough starts and GOR value increases. Since the drive is immiscible displacement, the GOR increases dramatically as the expanding gas cap reaches the highest wells on structure. The GOR continues to increase as the gas-oil contact moves farther down structure and also the injected gas production increases.

The oil production rate also increases with respect to increasing the injection rates (Figs 6.16-A to D, Fig. 6.18 and Table 6.3).The more the gas breakthrough, gas-oil ratio (GOR) increases and thus the lower the oil production rate (Fig. 6.18). This is not advantageous to our aim of improving oil recovery and also affects the market economics in terms of cost of produced gas handling and reduced oil production.

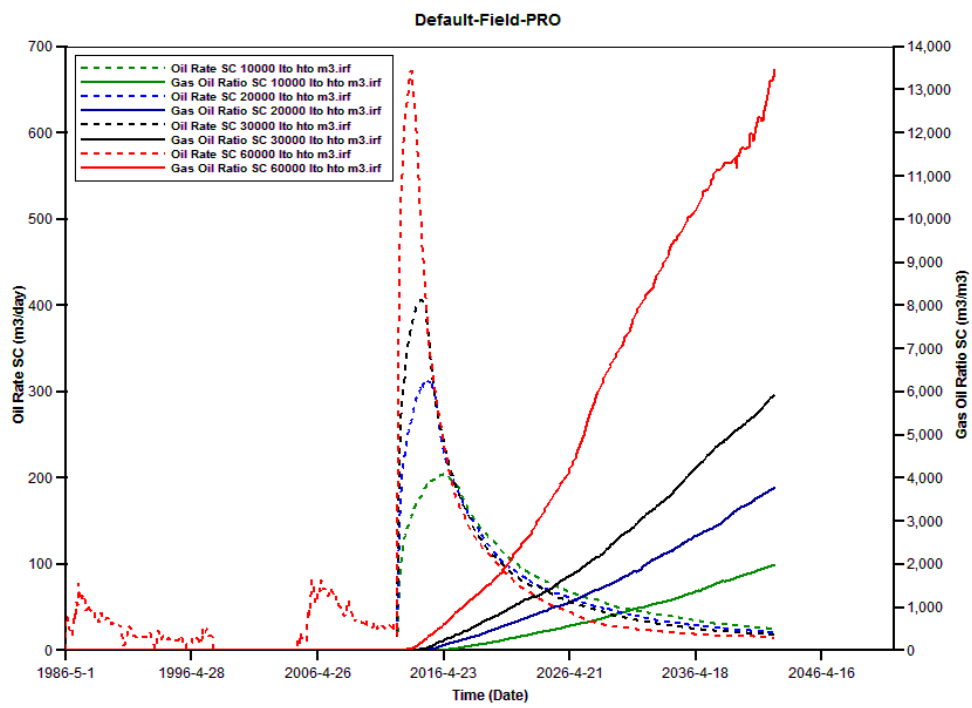


**Fig. 6.18: Comparison of Oil daily production rate and Gas-oil ratio of different air injection rates.**

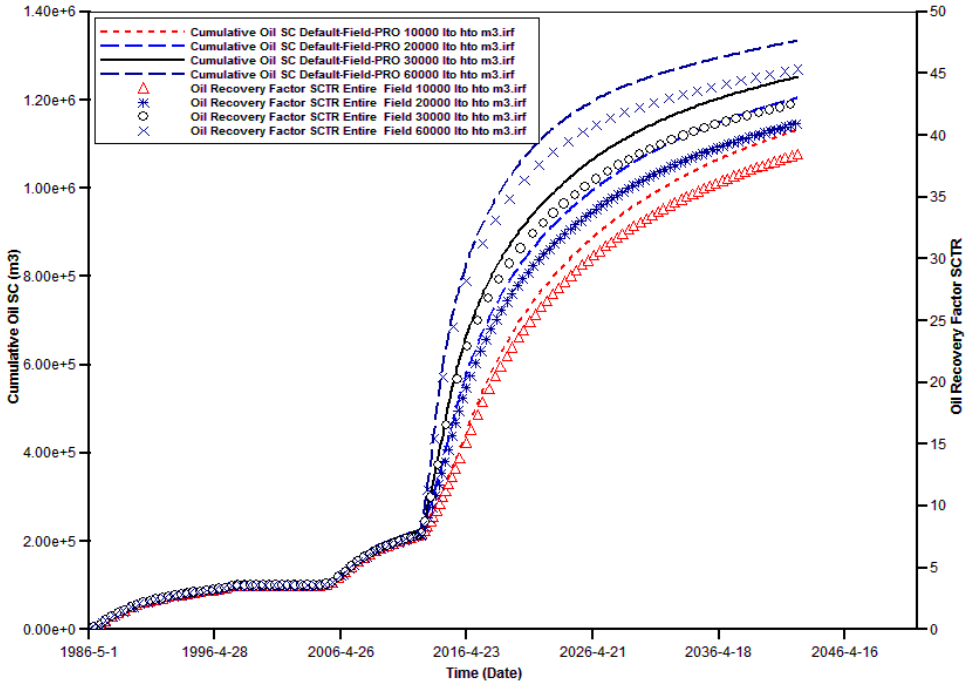


**Fig. 6.19: Cumulative oil produced and Oil recovery factor at different air injection rates.**

Gas breakthrough time can be gotten from the oil production rate plot (Fig. 6.18) as the time the curve starts to decline and it is known to be the time that the oil production starts to steeply decline. This fast gas breakthrough time observed in the results can be said to be caused by the relatively high permeability channels parts of the reservoir, which preferentially allows the quick movement of the injected gas to the production wells. It is recommended to apply selective chemical gels to block this parts of the reservoir to reduce the gas breakthrough and thus increase oil production rate and in turn increase overall oil recovery. It is also positively affect to the economics of produced gas handling. Typical production rates for the high production rate (plateau) period largely depends on the techno-economics of the field. Clearly for a field with a very large front loaded capital investment there is an incentive to have a high production rate during the plateau phase. The fast production decline phase can be delayed by methods to increase production. Such methods could include artificial lift, where the effort required to lift the fluids from the reservoir is carried out by a downhole pump or by using gas lift to reduce the density of the fluid system in the well.

**Table 6.3: Summary of the Various Simulated Parameters for the Air Injection IOR**

| 10,000m$^3$/day Injection Rate (Air injection) | 1year (2013.08) | 5years (2017.08) | 10years (2022.08) | 20years (2032.08) | 30years (2042.08) |
|---|---|---|---|---|---|
| **Ave. Reservoir Temperature, °C** | 97.99 | 98.53 | 99.17 | 100.41 | 101.58 |
| **Gas Oil Ratio m$^3$/m$^3$** | 649 | 57.016 | 329.58 | 1041.42 | 1967.79 |
| **Oil Production Rate m$^3$/day** | 149.058 | 184.973 | 93.669 | 43.448 | 25.289 |
| **Cumulative Oil Produced, 10$^6$ m$^3$** | 0.265 | 0.542 | 0.781 | 1.01 | 1.13 |
| **Incremental Cum. Oil Produced, 10$^6$ m$^3$** | 0.040 | 0.317 | 0.556 | 0.785 | 0.905 |
| **Recovery Factor, %** | 9.01 | 18.43 | 26.55 | 34.48 | 38.51 |
| **Incremental Recovery Factor, %** | 1.34 | 10.76 | 18.88 | 26.81 | 30.84 |
| **Cumulative Gas Injected = 6.57 x 10$^8$m$^3$; Cumulative Gas Produced = 3.7 x 10$^8$m$^3$** | | | | | |

| 20,000m$^3$/day Injection Rate (Air injection) | 1year (2013.08) | 5years (2017.08) | 10years (2022.08) | 20years (2032.08) | 30years (2042.08) |
|---|---|---|---|---|---|
| **Ave. Reservoir Temperature, °C** | 98.06 | 98.86 | 99.82 | 101.66 | 103.39 |
| **Gas Oil Ratio Cum m$^3$/m$^3$** | 806 | 228.709 | 722.207 | 2052.42 | 3786.38 |
| **Oil Production Rate m$^3$/day** | 258.160 | 177.980 | 85.127 | 36.307 | 25.289 |
| **Cumulative Oil Produced, 10$^6$ m$^3$** | 0.315 | 0.675 | 0.899 | 1.105 | 1.210 |
| **Incremental Cum. Oil Produced, 10$^6$ m$^3$** | 0.090 | 0.450 | 0.674 | 0.880 | 0.985 |
| **Recovery Factor, %** | 10.03 | 22.96 | 30.55 | 37.64 | 40.98 |
| **Incremental Recovery Factor, %** | 2.36 | 15.29 | 22.88 | 29.97 | 33.31 |
| **Cum. Gas Injected = 9.86 x 10$^8$m$^3$; Cum, Gas Produced = 6.69x 10$^8$m$^3$** | | | | | |

| 30,000m$^3$/day Injection Rate (Air injection) | 1year (2013.08) | 5years (2017.08) | 10years (2022.08) | 20years (2032.08) | 30years (2042.08) |
|---|---|---|---|---|---|
| **Ave. Reservoir Temperature, °C** | 98.14 | 99.20 | 100.47 | 102.90 | 105.15 |
| **Gas Oil Ratio m$^3$/m$^3$** | 10.173 | 400.54 | 1142.46 | 3207.09 | 5953.21 |
| **Oil Production Rate m$^3$/day** | 366.103 | 178.042 | 80.762 | 32.615 | 18.234 |
| **Cumulative Oil Produced, 10$^6$ m$^3$** | 0.326 | 0.761 | 0.974 | 1.165 | 1.252 |
| **Incremental Cum. Oil Produced, 10$^6$ m$^3$** | 0.101 | 0.536 | 0.749 | 0.940 | 1.027 |
| **Recovery Factor, %** | 11.08 | 25.87 | 33.12 | 39.61 | 42.59 |
| **Incremental Recovery Factor, %** | 3.41 | 18.2 | 25.45 | 31.94 | 34.92 |
| **Cum. Gas Injected = 1.32 x 10$^9$m$^3$; Cum, Gas Produced =9.72x 10$^8$m$^3$** | | | | | |

| 60,000m3/day Injection Rate (Air injection) | 1year (2013.08) | 5years (2017.08) | 10years (2022.08) | 20years (2032.08) | 30years (2042.08) |
|---|---|---|---|---|---|
| **Ave. Reservoir Temperature, °C** | 98.4 | 100.2 | 102.4 | 106.3 | 109.7 |
| **Gas Oil Ratio m$^3$/m$^3$** | 36.97 | 958.69 | 2506.15 | 8327.27 | 13480 |
| **Oil Production Rate m$^3$/day** | 661.11 | 166.6 | 72.07 | 23.11 | 14.56 |
| **Cumulative Oil Produced, 10$^6$ m$^3$** | 0.415 | 0.922 | 1.12 | 1.27 | 1.33 |
| **Incremental Cum. Oil Produced, 10$^6$ m$^3$** | 0.190 | 0.697 | 0.895 | 1.045 | 1.105 |
| **Recovery Factor, %** | 14.12 | 31.34 | 38.16 | 43.11 | 45.38 |
| **Incremental Recovery Factor, %** | 6.45 | 23.67 | 30.49 | 35.44 | 37.71 |
| **Cum. Gas Injected = 2.30x10$^9$m$^3$; Cum, Gas Produced =1.89x10$^9$m$^3$** | | | | | |

### 6.2.1.7 Cumulative Gas Injected and Produced

Figs 6.16-A to D showed the cumulative gas injected and cumulative gas produced increased as the injection rates increased from 10000 – 60000m$^3$/day for the 30 years considered. Table 6.3 shows the cumulative gas injected ranges from 6.57E+08m$^3$ to about 2.30E+09m$^3$, i.e. the values obtained from

the low case to the high case scenarios. The cumulative gas produced ranges from 3.78E+08m$^3$ to 1.89E+09m$^3$, which is lesser than the corresponding cumulative gas injected because:

1. Some of the injected gas reacted in the reservoir to produce the flue gases and $O_2$, but the $O_2$ was consumed in the reservoir and didn't reach the production wells, thus causing a reduction in the cumulative volume of gases to be produced.
2. From the gas saturation field distribution discussed earlier in Section 6.2.1.3.1, we can observe that after the 30 years of injection, that some of the injected gas were still left in the reservoir and did not reach the production wells and were they produced. This also contributes to the reduced cumulative volume of gas produced observed in the simulation results.

#### 6.2.1.8 Cumulative Oil Produced and Oil Recovery Factor

There is a remarkable increase in oil produced over the 30 years (2012-2042) of injection as shown in Fig. 6.19. Cumulative oil production is observed to increase proportionally as injection rate increases from 10000 to 60000m$^3$/day, which implies that more flue gases are released in the reaction to drive the oil down structure to the production wells, which lead to the increased oil recovery under the existing reservoir temperature and pressure.

It is observed from Table 6.3, that the cumulative produced oil increases as the air injection rate increases, ranging from about 1.13x10$^6$ m$^3$ (using 10000m$^3$/day) to 1.33x10$^6$ m$^3$ (using 60000m$^3$/day) for the period of 30 years investigated.

The actual oil recovery obtained depends on the amount of injected gas, the structural geometry and properties of the reservoir, and the way the field is managed, and this is the reason for this study to improve the oil recovery of this low permeability reservoir using the different gas injection techniques. Recovery increases with the increase in injection rate if gas production can be minimized. This can be easily done in the case of Q131 block because it is a steeply dipping reservoirs and also have thick oil columns which makes it possible for the wells to be perforated as far as possible below the gas-oil contact.

Fig. 6.19 and Table 6.3 showed that the total oil recovery factor of the block was observed to be about 38 – 45% of the OOIP and the incremental oil recovery factor from the start of the air injection was observed to be about 31 – 38% OOIP after the 30 years of air injection at the rates of 10000 – 60000m$^3$/day.

### 6.2.2 $CO_2$ injection Numerical Simulation Results and Discussion

As earlier mentioned, $CO_2$ can easily be miscible with the reservoir oil at right reservoir temperature, oil composition and pressure. The reservoir pressure must be at or above a pressure limit which is called the minimum miscible pressure (MMP) to have a miscible displacement IOR process by the $CO_2$ injection. Also we can obtain a near miscible displacement if the reservoir pressure is close to the MMP, and this will enables the formation of a single liquid phase to efficiently sweep the reservoir oil to the production wells which result to an improved oil recovery. In this study of the use of $CO_2$ injection for IOR for the low permeability light oil Q131 reservoir, we will be considering the $CO_2$ injection as a near miscible displacement drive because the reservoir's pressure (about 20 MPa) is close to the calculated reservoir MMP (about 22 MPa) which is was done using the already set correlations (Section 3.3.1.2.1.1). The mechanism here is that the $CO_2$ partially dissolves in the oil causing it to swell and reducing viscosity, although importantly it maintains reservoir pressure by creating an artificial gas cap which forces the oil down towards producing wells.

The miscibility effect of the $CO_2$ is taken into account in the simulation running for the case of the $CO_2$ injection. The simulation procedures applied for the air injection still remained the same for the case of $CO_2$ injection, with the reaction component of the simulation removed in the $CO_2$ injection case as there is no reaction of oil with the injected gas. **The simulation results for the $CO_2$ injection are displayed and discussed below:**

#### 6.2.2.1 Fluid Saturation

##### 6.2.2.1.1 Gas Saturation Field Distribution

Figs. 6.20-A to F show the gas saturation field distribution at different years for the base case scenario of using 30000m$^3$/day air injection and they showed that the gas saturation increased with the injection time. The gas saturation ranged from 27 to 48% throughout the 30 years $CO_2$ injection. A gradual progression of the injected gas front is observed to move from the up dip structure of the oil block to the down structure, to cause the increase in the gas saturation distribution of the block. Figs. 6.21-A to D presents the gas saturation results field distribution between injectors and producers at different times (years) under different injection rates, and it showed the increasing gas saturation distribution in the block as the injection time (years) increases and the injection rate increases from the 10,000 to 60,000m$^3$/day.

The gas saturation results can be seen in Table 6.2 (gotten from the Figs.6.21-A to D) and showed that maximum distance moved by the injected gas in the reservoir is lesser than those of air and N2 injection. The maximum distance the gas front travel is about 1440m, which definite shows that there was gas breakthrough. Also $CO_2$ injection showed lesser values for the maximum gas saturation seen in the

reservoir at different years and different injection rates. These can be said to complement the earlier statement that the $CO_2$ injected is partially miscible with the oil, which resulted in the reduced maximum $CO_2$ gas saturation and also the shorter distance moved by the gas front in the reservoir, because parts of the $CO_2$ injected are involved in the mixing with the oil, and thus reducing the relative permeability of the injected gas, thereby causing the gas saturation be lower than expected assuming it is an immiscible displacement as seen in air and $N_2$ injection.

#### 6.2.2.1.2 Oil Saturation Field Distribution

The oil saturation results are displayed in Figs. 6.22-A to F which shows the oil saturation field distribution after different years of $CO_2$ injection using constant injection rate of 30000m$^3$/day, and showed a decreasing oil saturation as injection time increases. In this near miscible displacement $CO_2$ injection process, it is expected that parts of the oil contacted by the injected $CO_2$ gas will become soluble with the gas and is seen to progressively flow from the regions close to the injectors towards the producers. In the region between the reaction zone and producers, the oil saturation reduced from 60% (1 year period) to 45% (5 years period) to 32% (10 years period) and then to approximately 12% (30 years period) indicating a better sweep of the oil in the reservoir (more than that observed in the air injection) by the partially miscible drive assisted by gravity stabilization. It is also noted that as the gas injection rate and time increases, gas saturation increases, and the oil saturation tends to decrease.

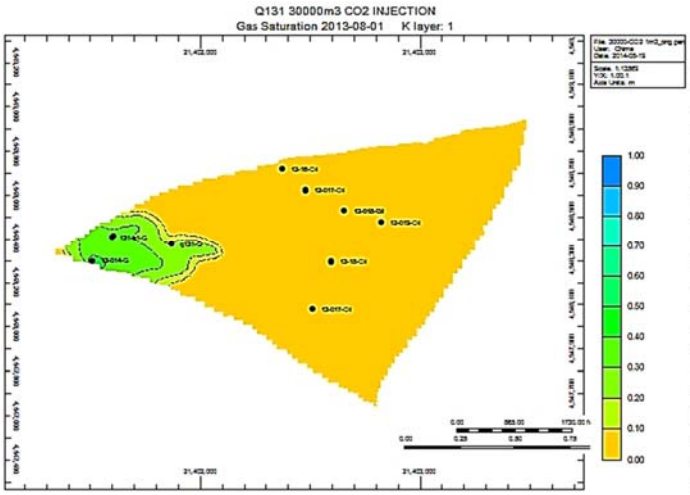


**Fig. 6.20-A: Gas saturation field distribution after 1 year of $CO_2$ injection.**

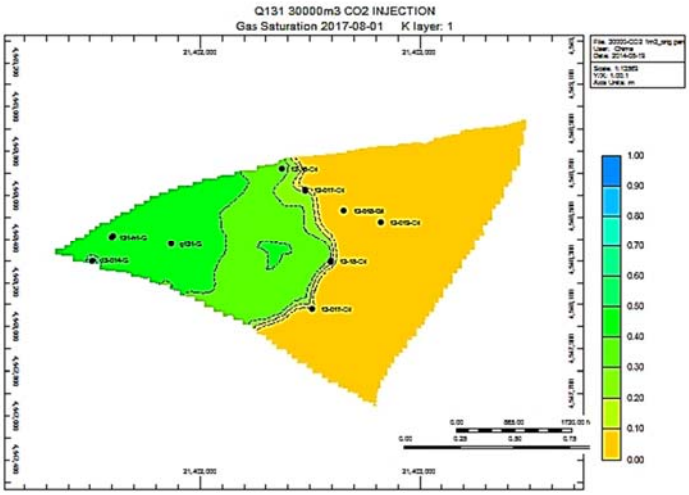


**Fig. 6.20-B: Gas saturation field distribution after 5 years of $CO_2$ injection.**

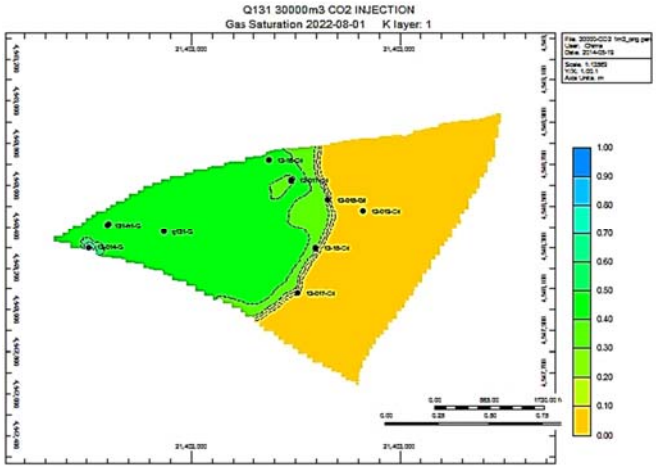


**Fig. 6.20-C: Gas saturation field distribution after 10 years of $CO_2$ injection.**

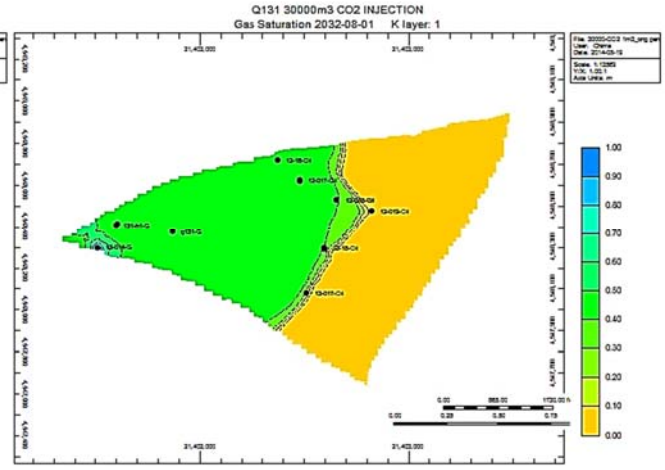


**Fig. 6.20-D: Gas saturation field distribution after 20 years of $CO_2$ injection.**

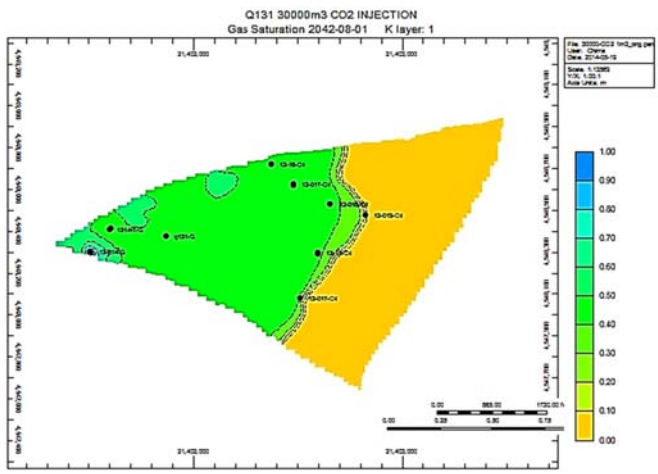


**Fig. 6.20-E: Gas saturation field distribution after 30 years of $CO_2$ injection.**

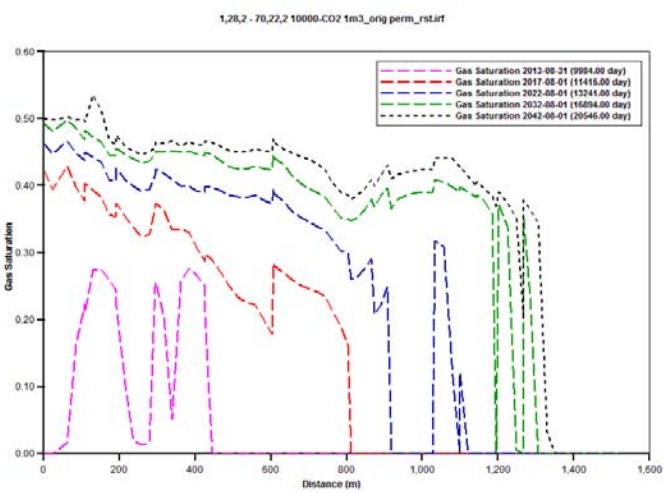


**Fig. 6.21-A: Gas saturation field distribution between injectors and producers at different times (years), under 10000 $m^3$/day $CO_2$ injection rate.**

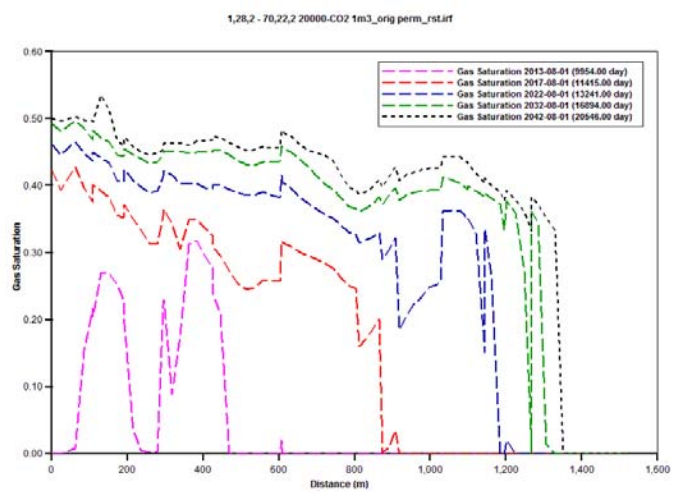


**Fig. 6.21-B: Gas saturation field distribution between injectors and producers at different times (years), under 20000 $m^{3/}$day $CO_2$ injection rate.**

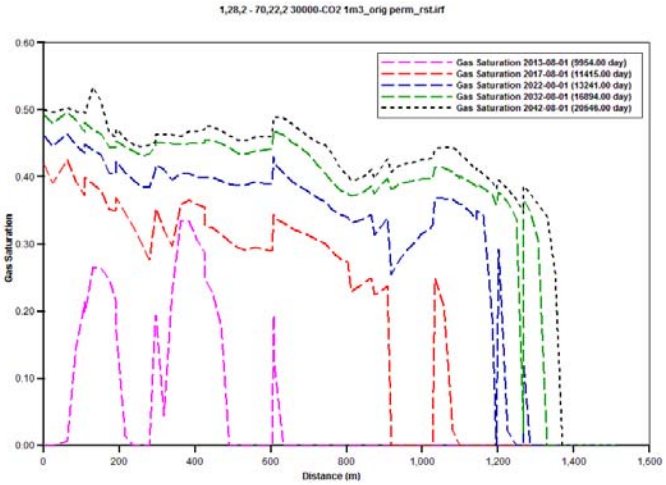


**Fig. 6.21-C: Gas saturation field distribution between injectors and producers at different times (years), under 30000 $m^3$/day $CO_2$ injection rate.**

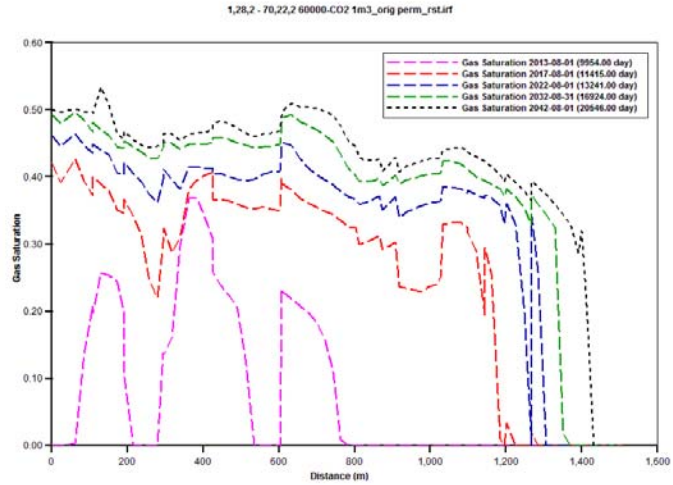


**Fig. 6.21-D: Gas saturation field distribution between injectors and producers at different times (years), under 60000 $m^3$/day $CO_2$ injection rate.**

Figs.6.23-A to D presents the oil saturation field distribution between injectors and producers at different times (years), under increasing $CO_2$ injection rates, and it showed that with increasing injection rate and time, the oil saturation decreases from the injectors towards the producers, indicating that the process is primarily controlled by the increasing relative permeability of the injected gas in the reservoir, the solubility of the gas in the oil to reduce the oil viscosity to flow easily, oil swelling, and the corresponding decrease in the relative permeability of oil leads to the increased production at the production wells.

It is interesting to point out that no part of the reservoir showed any abnormal high gas saturation (as in air injection), the injected gas uniformly spread throughout the crest and mid-region of the reservoir and gradually flowed down carrying oil to the production wells. Also on area of the reservoir showed any signs of high temperature or combustion as seen in air injection (discussed above) because no areas had close to zero oil saturation, which is associated with high temperature burning and reaction zones. These phenomena cannot be seen in the $CO_2$ injection operations and results.

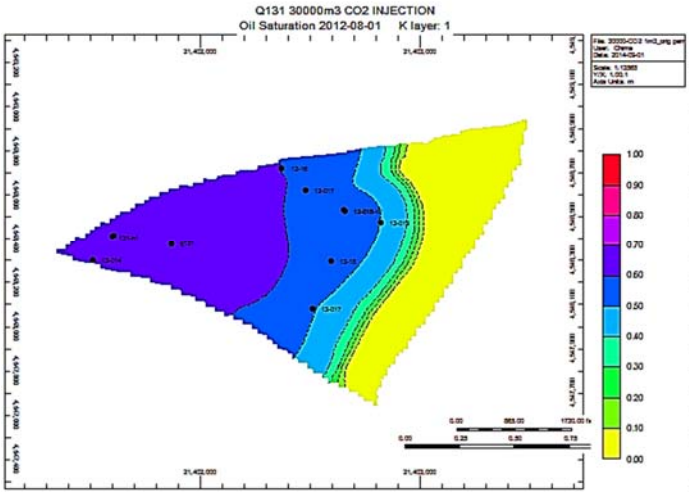


**Fig. 6.22-A: Oil saturation field distribution at 0 year of $CO_2$ injection.**

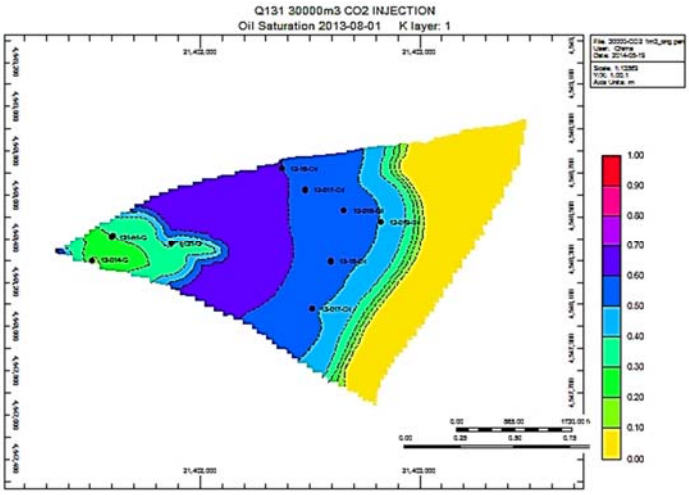


**Fig. 6.22-B: Oil saturation field distribution after 1 year of $CO_2$ injection.**

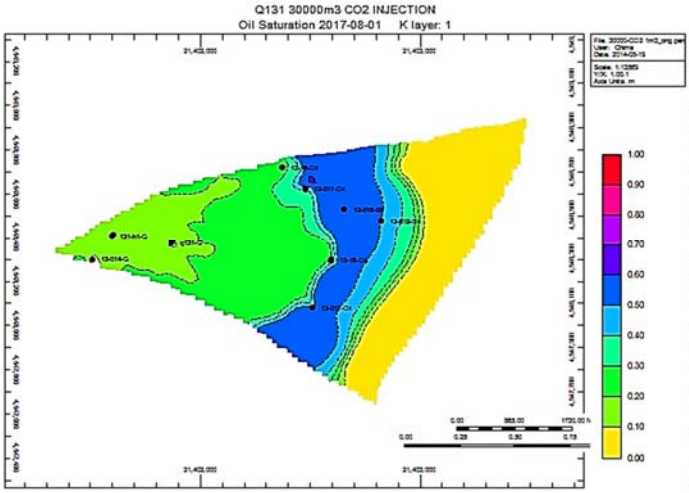


**Fig. 6.22-C: Oil saturation field distribution after 5 years of $CO_2$ injection.**

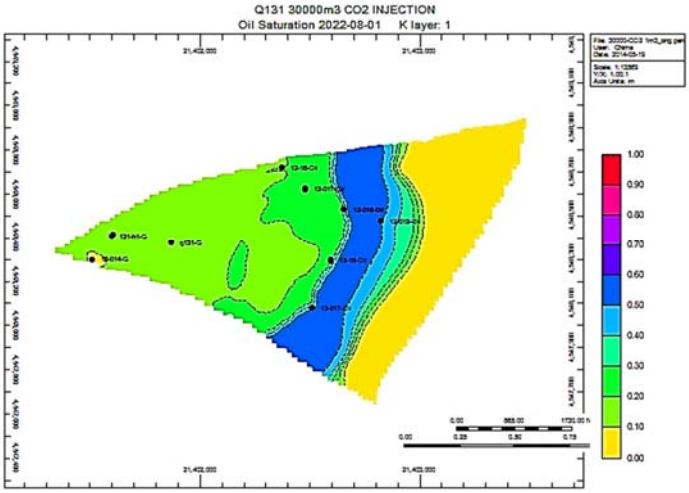


**Fig. 6.22-D: Oil saturation field distribution after 10 years of $CO_2$ injection.**

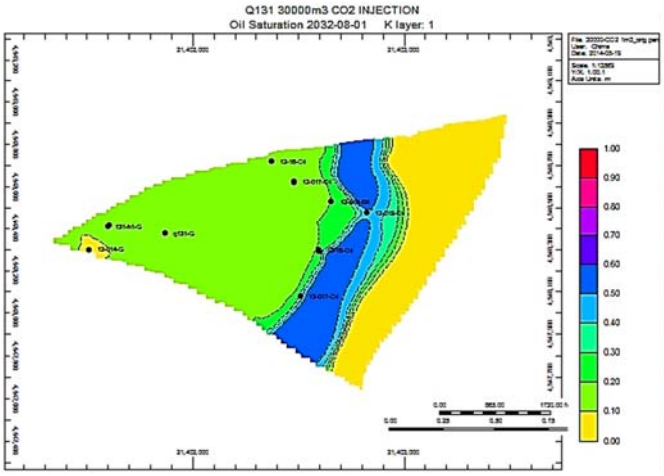


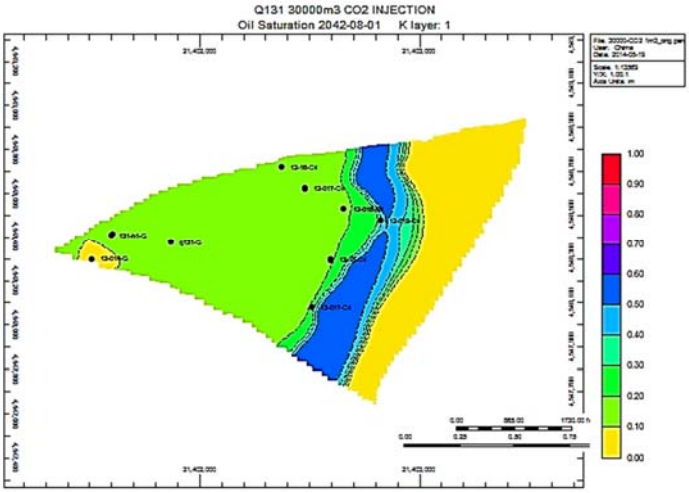


**Figs. 6.22-E and F: Oil saturation field distribution after 20 and 30 years of $CO_2$ injection respectively.**

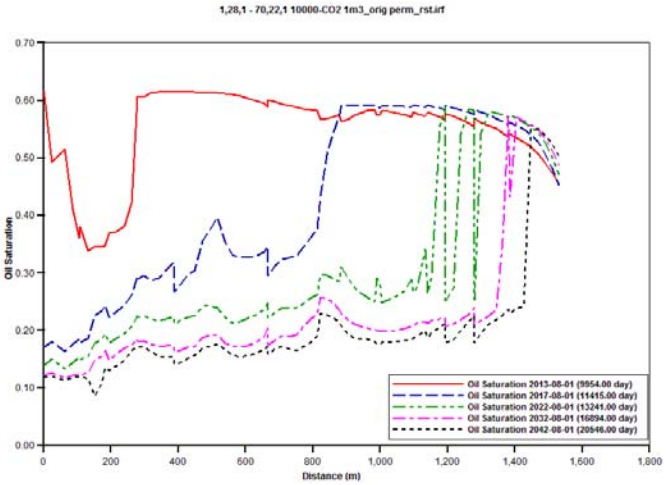


**Fig. 6.23-A: Oil saturation field distribution between injectors and producers at different times (years), under 10000 $m^3$/day $CO_2$ injection rate.**

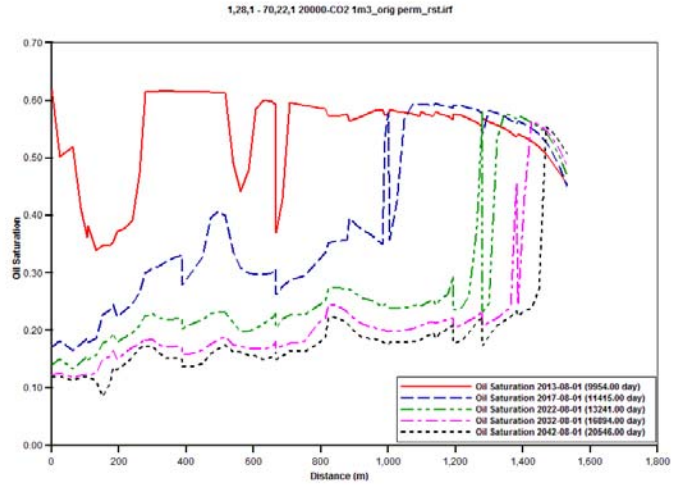


**Fig. 6.23-B: Oil saturation field distribution between injectors and producers at different times (years), under 20000 $m^3$/day $CO_2$ injection rate.**

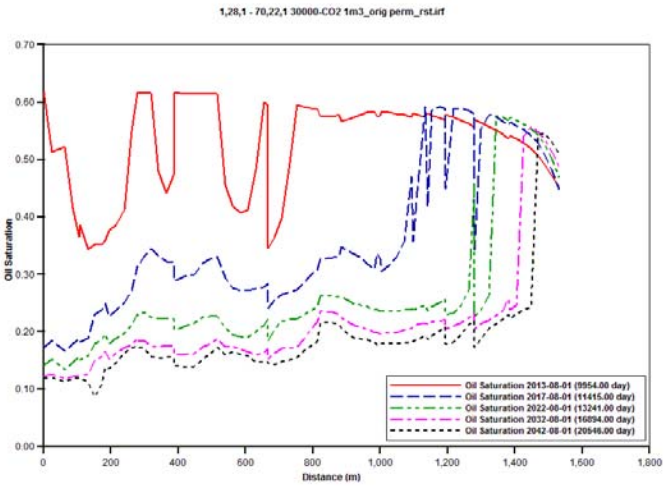


**Fig. 6.23-C: Oil saturation field distribution between injectors and producers at different times (years), under 30000 $m^3$/day $CO_2$ injection rate.**

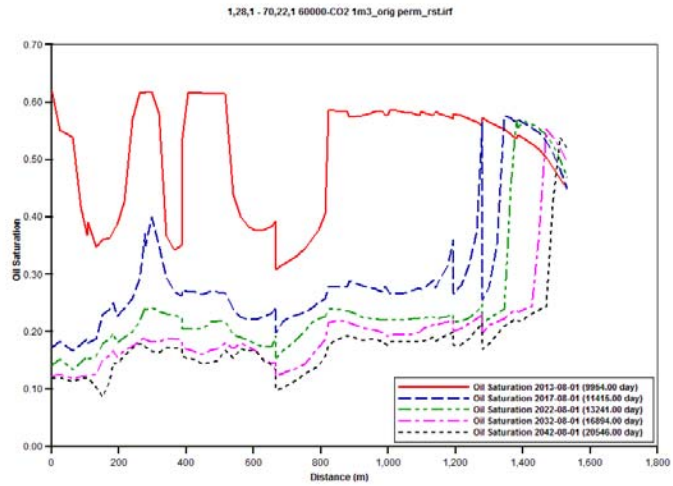


**Fig. 6.23-D: Oil saturation field distribution between injectors and producers at different times (years), under 60000 $m^3$/day $CO_2$ injection rate.**

#### 6.2.2.2 Oil Viscosity Field Distribution

$CO_2$ miscibility with oil is known to cause a reduction in the viscosity of the contacted oil. Figs. 6.24-A to F showed the oil viscosity field distribution after 0-30 years of $CO_2$ injection which showed clearly that oil viscosity was decreasing as time progressed from the 0 to 30 years. The oil viscosity reduction change is seen to be occurring proportionally to the gas saturation front, which implies that as the $CO_2$ gas encounters the oil and becomes partially miscible, there is an associated reduction in the oil viscosity at that zone. From the result presented in Figs. 6.24-A to F The oil viscosity gradually decreases from the injector locations (crest of the reservoir) downwards towards the producers. It seen

that after one year of injection (using the constant 30000m$^3$/day injection), the oil viscosity of the top structure decreased from 0.48mPa.s to an average of about 0.44mPa.s. After 5 years of injection, the area involved with decreasing oil viscosity widened and the average oil viscosity became 0.42mPa.s.

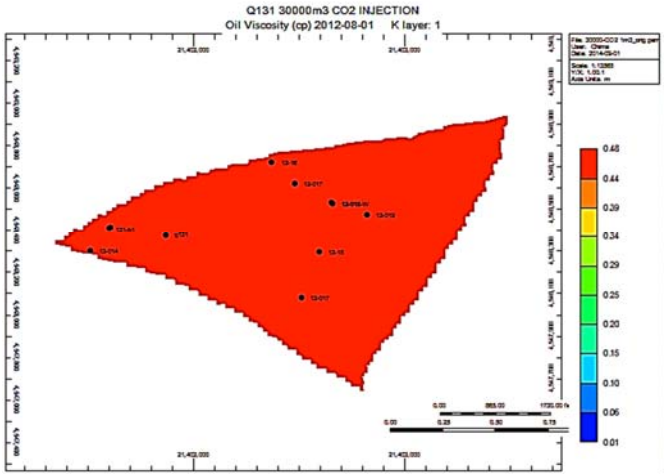


**Fig. 6.24-A: Oil viscosity field distribution at 0 year of $CO_2$ injection.**

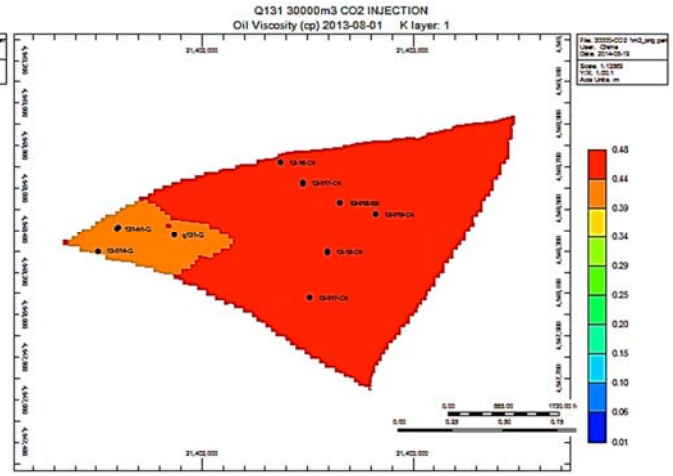


**Fig. 6.24-B: Oil viscosity field distribution after 1 year of $CO_2$ injection.**

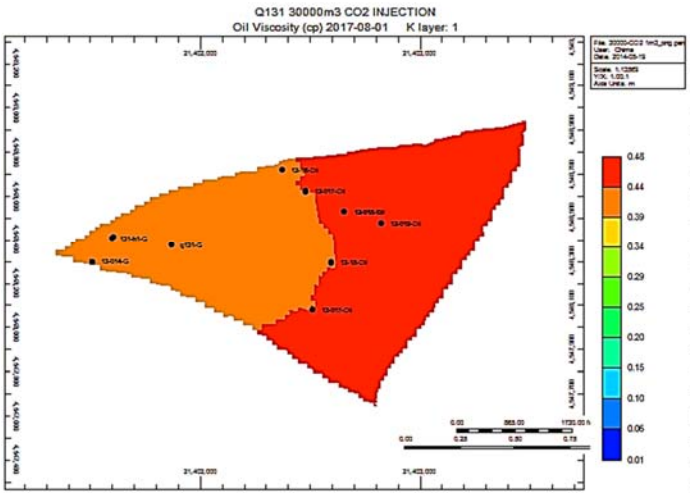


**Fig. 6.24-C: Oil viscosity field distribution after 5 years of $CO_2$ injection.**

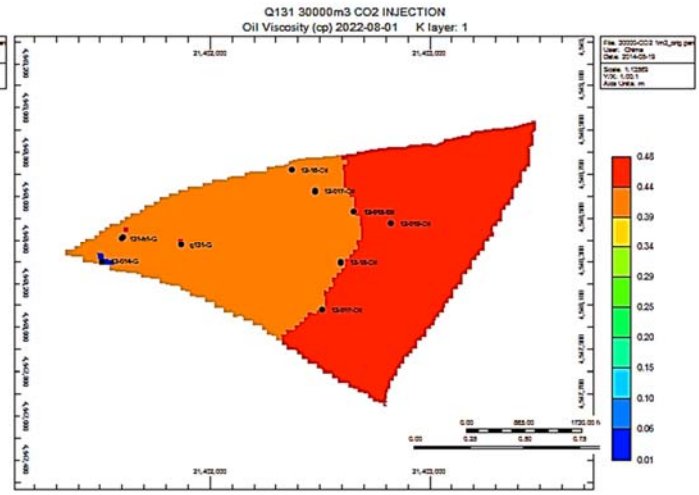


**Fig. 6.24-D: Oil viscosity field distribution after 10 years of $CO_2$ injection.**

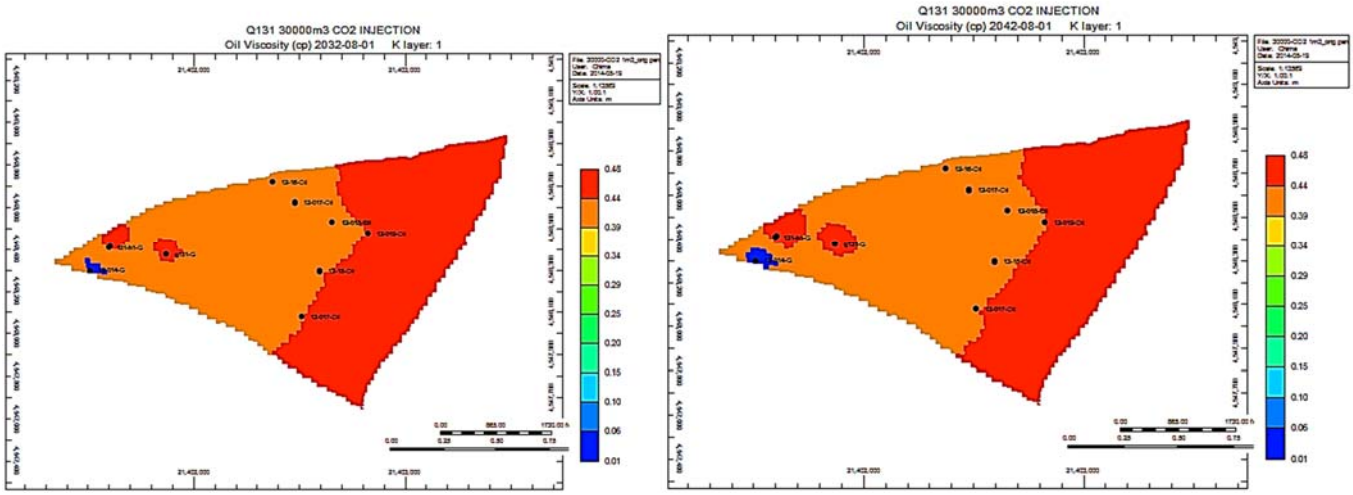


**Figs. 6.24-E and F: Oil viscosity field distribution after 20 and 30 years of $CO_2$ injection respectively.**

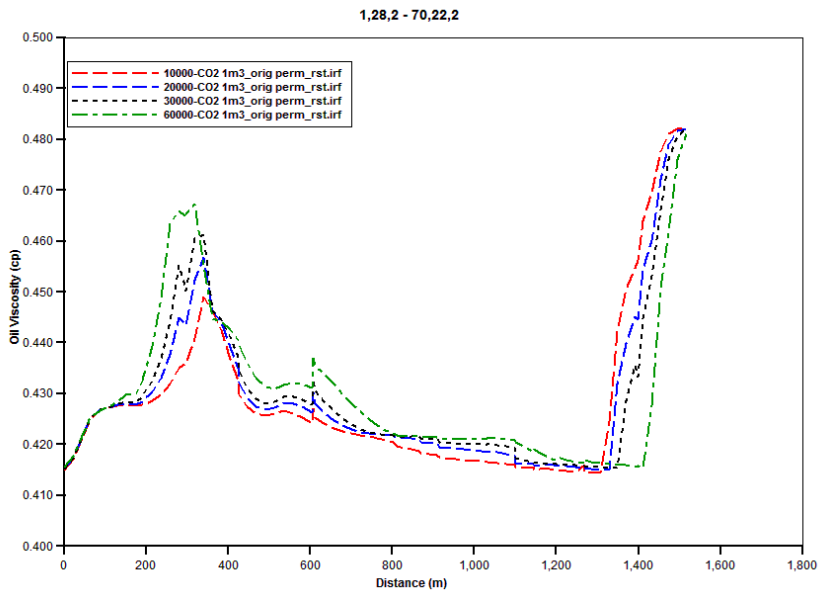


**Fig. 6.25: Oil viscosity field distribution between injectors and producers at different injection rates after 30 years.**

The average oil viscosity continuously slowly decreased to a value of about 0.41mPa.s. The reduction of the oil viscosity is of great benefit to the science of increasing oil recovery, because the oil can easily flow together in solution with the $CO_2$ to the producers, thus increasing the overall oil recovered. Figs. 6.24E and F showed a return to higher 0.48mPa.s oil viscosity values at the locations of two injectors after 20 years and above (also seen in Fig. 25. This can be explained to occur as most of the oil the oil at those locations have been displaced leaving behind formation and the recently injected $CO_2$, thus giving a higher oil viscosity value which can be said to apparent/pseudo oil viscosity.

It should be noted that the oil viscosity for the $CO_2$ injection has no significant change with increasing injection rate as shown in Fig. 6.25. The oil viscosity reduction change is seen to be occurring proportionally to the gas saturation front, which implies that as the $CO_2$ gas encounters the oil and becomes partially miscible in it, there is an associated reduction in the oil viscosity at that zone. Also, from the result presented in Fig. 6.25, the oil viscosity gradually decreases from the injector locations (crest of the reservoir) downwards towards the producers. It seen that after one year of injection (using the constant 30000m$^3$/day injection), the oil viscosity of the top structure deceased from 0.48mPa.s to an average of about 0.44mPa.s. After 5 years of injection, the area involved with decreasing oil viscosity widened and the average oil viscosity became 0.41mPa.s. The average oil viscosity continuously slowly decreased to a value of about 0.4mPa.s. The reduction of the oil viscosity is of great benefit to the science of increasing oil recovery, because the oil can easily flow together in solution with the $CO_2$ to the producers, thus increasing the overall oil recovered.

#### 6.2.2.3 Gas-Oil Ratio

After some years of injection $CO_2$ gas will eventually break through to the production wells, with some of the volume in solution with the produced oil. In the case of $CO_2$ injection, produced $CO_2$ gas is usually separated from the produced natural gas. When these flue gas front reaches the production wells, GOR will increase rapidly as injection continues (Figs. 6.26-A to D and 6.27). There is a slow and continuous increase in GOR which increases from about 1720m$^3$/m$^3$ (10000m$^3$/day injection rate) up to about 9500m$^3$/m$^3$ at the highest injection rate used (i.e. 60000m$^3$/day) in the 30 years period considered in this study as seen in Table 6.4. **Gas breakthrough and GOR in $CO_2$ injection is of a lesser volume than on air and $N_2$ injection (Table 6.4) because the tendency of** $CO_2$ solubility in the oil and formation water will delay the $CO_2$ breakthrough, and thus have less volume of gas produced (less GOR).

Proper field management of the produced gas gases should be set in place to collect, separate and dispose of the produced gases that are not needed. $CO_2$ sequestration or re-injection can be practiced to reduce the green house effects disadvantage of disposing $CO_2$ to the atmosphere.

#### 6.2.2.4 Oil Production Rate

Figs. 6.26-A to D presents the oil daily production rate under different $CO_2$ injection rates, and showed an increase in oil production rate as injection rates and time increases. Also, the oil production rate increases rapidly in the early years of $CO_2$ injection (Fig. 6.27) to a maximum of about 500m$^3$/day and it showed a broader plateau phase than the other gas injection techniques discussed. This implies that it would have more high oil production period than the other gas injection which showed a very sharp

decline and narrow plateau phase, but experiences a sharp decreases as both the gas breakthrough starts and GOR value increases.

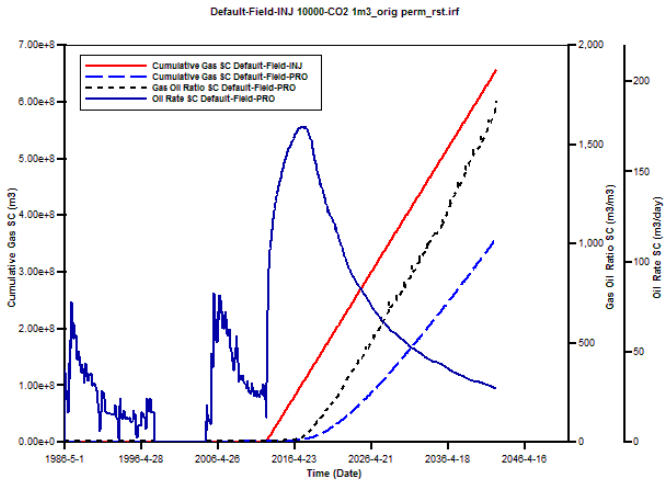


**Fig. 6.26-A: Cumulative gas injected and produced, Gas-oil ratio, Oil daily production rate under 10000m$^3$/day $CO_2$ injection rate.**

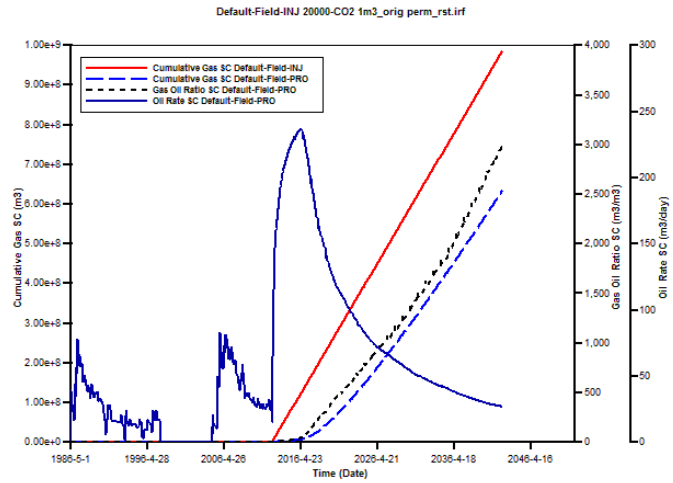


**Fig. 6.26-B: Cumulative gas injected and produced, Gas-oil ratio, Oil daily production rate under 20000m$^3$/day $CO_2$ injection rate.**

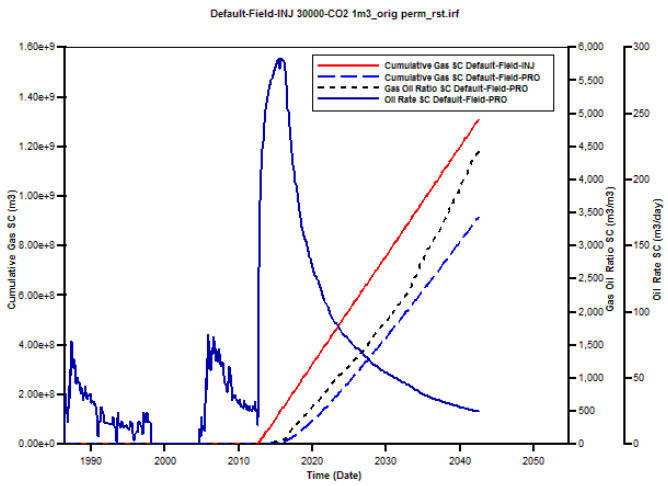


**Fig. 6.26-C: Cumulative gas injected and produced, Gas-oil ratio, Oil daily production rate under 30000m$^3$/day $CO_2$ injection rate.**

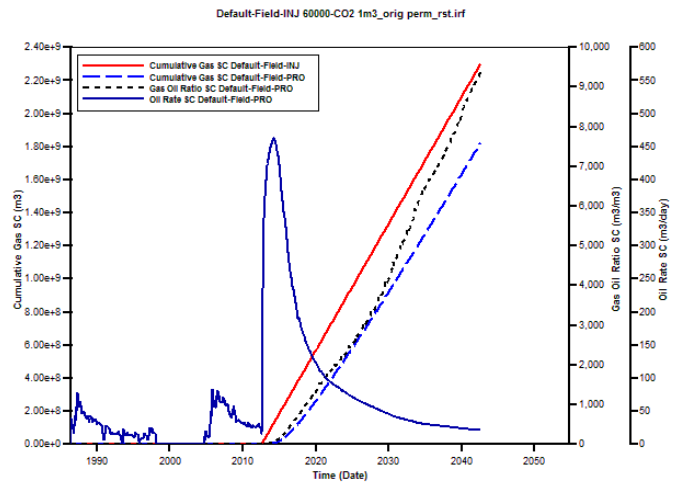


**Fig. 6.26-D: Cumulative gas injected and produced, Gas-oil ratio, Oil daily production rate under 60000m$^3$/day $CO_2$ injection rate.**

The more the gas breakthrough, gas-oil ratio (GOR) increases and thus the lower the oil production rate (Fig. 6.27), as also seen in the air and $N_2$ injection cases. This is not advantageous to our aim of improving oil recovery and also affects the market economics in terms of cost of produced gas handling and reduced oil production. It is important to note that due to the lower GOR seen in the $CO_2$ injection case, oil production rate is more significant than the other two gas (air and $N_2$) injection cases considered in this study, as seen from Table 6.4.

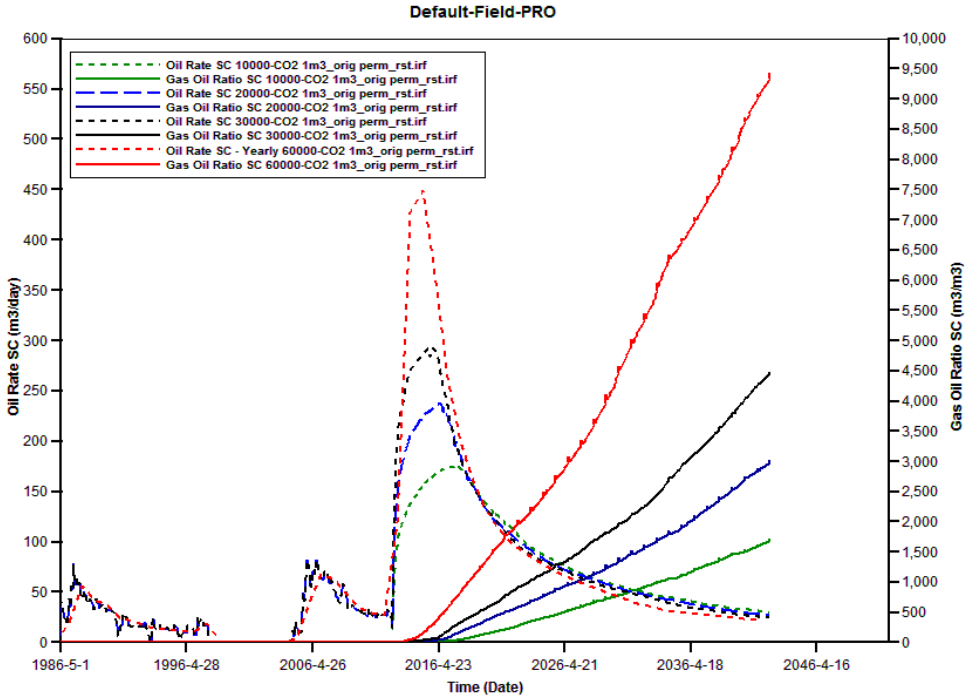


**Fig. 6.27: Comparison of Oil daily production rate and Gas-oil ratio of different $CO_2$ injection rates.**

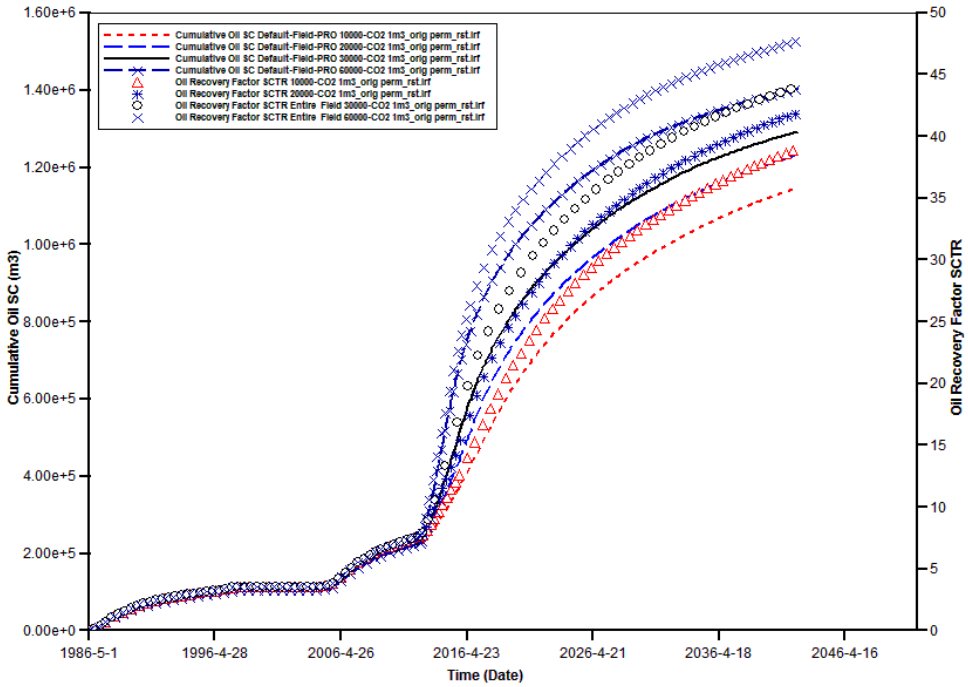


**Fig. 6.28: Cumulative oil produced and Oil recovery factor at different $CO_2$ injection rates.**

**Table 6.4: Summary of the Various Simulated Parameters for the $CO_2$ Injection IOR**

| 10,000m$^3$/day Injection Rate ($CO_2$ injection) | 1year (2013.08) | 5years (2017.08) | 10years (2022.08) | 20years (2032.08) | 30years (2042.08) |
|---|---|---|---|---|---|
| **Gas Oil Ratio m$^3$/m$^3$** | 7.65 | 33.20 | 277.56 | 945.12 | 1719.1 |
| **Oil Production Rate m$^3$/day** | 124.46 | 173.70 | 105.11 | 49.58 | 29.79 |
| **Cumulative Oil Produced, $10^6$ m$^3$** | 0.260 | 0.492 | 0.747 | 1.007 | 1.147 |
| **Incremental Cum. Oil Produced, $10^6$ m$^3$** | 0.035 | 0.267 | 0.522 | 0.782 | 0.922 |
| **Recovery Factor, %** | 8.82 | 20.37 | 25.41 | 34.25 | 39.02 |
| **Incremental Recovery Factor, %** | 1.15 | 12.7 | 17.74 | 26.58 | 31.35 |
| **Cum. Gas Injected = 6.57x$10^8$m$^3$; Cum, Gas Produced =3.60x$10^8$m$^3$** | | | | | |

| 20,000m$^3$/day Injection Rate ($CO_2$ injection) | 1year (2013.08) | 5years (2017.08) | 10years (2022.08) | 20years (2032.08) | 30years (2042.08) |
|---|---|---|---|---|---|
| **Gas Oil Ratio m$^3$/m$^3$** | 7.704 | 135.212 | 599.27 | 1559.91 | 3020.84 |
| **Oil Production Rate m$^3$/day** | 185.51 | 202.40 | 100.60 | 47.29 | 26.82 |
| **Cumulative Oil Produced, $10^6$ m$^3$** | 0.276 | 0.599 | 0.852 | 1.102 | 1.233 |
| **Incremental Cum. Oil Produced, $10^6$ m$^3$** | 0.051 | 0.374 | 0.627 | 0.877 | 1.008 |
| **Recovery Factor, %** | 9.41 | 20.37 | 28.96 | 37.50 | 41.92 |
| **Incremental Recovery Factor, %** | 1.74 | 12.7 | 21.29 | 29.83 | 34.25 |
| **Cum. Gas Injected = 9.86x$10^8$m$^3$; Cum, Gas Produced =6.35x$10^8$m$^3$** | | | | | |

| 30,000m$^3$/day Injection Rate ($CO_2$ injection) | 1year (2013.08) | 5years (2017.08) | 10years (2022.08) | 20years (2032.08) | 30years (2042.08) |
|---|---|---|---|---|---|
| **Gas Oil Ratio m$^3$/m$^3$** | 8.46 | 279.77 | 922.23 | 2254.85 | 4480.65 |
| **Oil Production Rate m$^3$/day** | 246.85 | 198.35 | 96.62 | 46.30 | 24.63 |
| **Cumulative Oil Produced, $10^6$ m$^3$** | 0.295 | 0.683 | 0.931 | 1.172 | 1.293 |
| **Incremental Cum. Oil Produced, $10^6$ m$^3$** | 0.070 | 0.458 | 0.706 | 0.947 | 1.068 |
| **Recovery Factor, %** | 9.92 | 23.22 | 31.67 | 39.87 | 43.96 |
| **Incremental Recovery Factor, %** | 2.25 | 15.55 | 24 | 32.2 | 36.29 |
| **Cum. Gas Injected = 1.32x $10^9$m$^3$; Cum, Gas Produced =9.21x $10^8$m$^3$** | | | | | |

| 60,000m$^3$/day Injection Rate ($CO_2$ injection) | 1year (2013.08) | 5years (2017.08) | 10years (2022.08) | 20years (2032.08) | 30years (2042.08) |
|---|---|---|---|---|---|
| **Gas Oil Ratio m$^3$/m$^3$** | 20.24 | 733.84 | 2024.39 | 5340.60 | 9432.40 |
| **Oil Production Rate m$^3$/day** | 437.70 | 188.56 | 87.72 | 36.10 | 21.14 |
| **Cumulative Oil Produced, $10^6$ m$^3$** | 0.352 | 0.858 | 1.090 | 1.306 | 1.404 |
| **Incremental Cum. Oil Produced, $10^6$ m$^3$** | 0.127 | 0.633 | 0.865 | 1.081 | 1.179 |
| **Recovery Factor, %** | 11.93 | 29.19 | 37.08 | 44.38 | 47.75 |
| **Incremental Recovery Factor, %** | 4.26 | 21.52 | 29.41 | 36.71 | 40.08 |
| **Cum. Gas Injected = 2.30x$10^9$m$^3$; Cum, Gas Produced =1.82x$10^9$m$^3$** | | | | | |

#### 6.2.2.5 Cumulative Gas Injected and Produced

**Fig. 6.26-A to D and Table 6.4 clearly** showed the cumulative gas injected and cumulative gas produced as the injection rates increased from 10000 – 60000m$^3$/day for the 30 years considered. The cumulative gas injected ranges from 6.57E+08 m$^3$ to about 2.30E+09 m$^3$, i.e. the values obtained from

the low case (10000 $m^3$/day) to the high case (60000$m^3$/day) scenarios. The cumulative gas produced ranges from 3.60E+08 to 1.82E+09$m^3$. This range is seen to be lower than that seen in the cases of air and $N_2$ injections because:

1. $CO_2$ is partially miscible with the oil and have less volume of injected gas production than would have been produced if it was an immiscible displacement as seen in the cases of air and $N_2$.
2. Lesser GOR observed in this $CO_2$ injection case
3. From the gas saturation field distribution discussed earlier, we can observe that even after the 30 years of injection, that some of the gas were still left in the reservoir and did not reach the production wells neither were they produced. This also contributes to the reduced cumulative volume of gas produced observed in the simulation results.

#### 6.2.2.6 Cumulative Oil Produced and Oil Recovery Factor

Cumulative oil production is observed to increase proportionally as injection rate increases from 10000 to 60000$m^3$/day, which implies that $CO_2$ enhanced by partial solubility in the oil drove the oil (less vicious) down structure to the production wells, which lead to the increased oil recovery under the existing reservoir temperature and pressure as shown in Fig. 6.28. It is observed from this plot and also from Table 6.5 that the cumulative produced oil increases as the air injection rate increases, ranging from about 1.15 x $10^6$ $m^3$ (using 10000$m^3$/day) to 1.404 x $10^6$ $m^3$ (using 60000$m^3$/day) for the period of 30 years investigated.

Fig. 6.28 and Table 6.5 also showed that the total oil recovery factor of the block was observed to be about 39 – 48% of the OOIP and the incremental oil recovery factor from the start of the $CO_2$ injection was observed to be about 31 – 40% OOIP after the 30 years of $CO_2$ injection at the rates of 10000 – 60000$m^3$/day. The near miscible displacement drive seen in the case of the $CO_2$ also had a better increased recovery than the air and $N_2$ injection cases by more than 3 and 2% respectively (calculated from Tables 6.3, 6.4 and 6.5).

### 6.2.3 $N_2$ Injection Numerical Simulation Results and Discussion

The $N_2$ injection considered in this study is immiscible displacement drive as the air injection. This is due to the reason that the $N_2$ gas cannot have a miscible or partial miscible front with the oil because the reservoir pressure is very low (20 MPa) when compared to the high MMP required to for oil to be soluble with the injected $N_2$ gas. Empirical correlations were used to calculate this $N_2$ MMP for the Q131 reservoir and the average value of 42.5MPa was obtained (Section 3.4.2).

The simulation procedures applied for the air injection still remained the same for the case of $CO_2$ injection, with the reaction component of the simulation removed in the this $N_2$ injection case as there is no reaction of oil with the injected $N_2$ gas. The $N_2$ injection process for IOR differs from the air injection as there is no increased reservoir temperature seen and no produced significant production or flue gases to preferentially drive the oil as seen in the air injection IOR. $N_2$ injection process for IOR also differs from the $CO_2$ injection for IOR because no miscibility or near miscibility effects are recorded in this $N_2$ injection case. The $N_2$ injection is most beneficial in pressure maintenance of the reservoir and also to immiscible drive the oil to the production wells. **The simulation results for the $N_2$ injection are displayed and discussed below:**

#### 6.2.3.1 Fluid Saturation

##### 6.2.3.1.1 Gas Saturation Field Distribution

Figs. 6.29-A to E show the gas saturation field distribution at different years for the base case scenario of using 30000m$^3$/day air injection and they showed that the gas saturation increased with the injection time. The gas saturation ranged from 32% to about 70% throughout the 30 years $N_2$ injection. Figs. 6.30-A to D present the gas saturation results field distribution between injectors and producers at different times (years) under different injection rates, and it showed the increasing gas saturation distribution in the block as the injection time (years) increases and the injection rate increases from the 10,000 to 60,000m$^3$/day. The gas saturation results can be seen in Table 6.2, (gotten from the Figs. 6.30-A to D) and showed that maximum distance moved by the injected gas in the reservoir is greater than those of air and $CO_2$. This can be explained as occurring due to its non-reactive and immiscibility nature of the injected gas with the reservoir oil, so the gas front moves the fastest (out of the three injection techniques) in the reservoir to the production wells.

##### 6.2.3.1.2 Oil Saturation Field Distribution

Figs. 6.31-A to F show the oil saturation field distribution results after different years of $N_2$ injection using constant injection rate of 30000m$^3$/day, and a decreasing oil saturation as injection time increases is observed. In the region between the injectors and producers, the oil saturation decreased from the

initial 60% (1 year period) to 48% (5 years period) to 36% (10 years period) and then to approximately 15% (30 years period) as shown in Figs. 6.32-A to D, which shows a good sweep of the reservoir by the immiscible displacement drive assisted by gravity stabilization. It is also noted that as the gas injection rate and time increases, gas saturation increases, then the oil saturation tends to decrease.

#### 6.2.3.2 Oil Viscosity Field Distribution

$N_2$ injection simulation results showed a fast-occurring small reduction in the oil viscosity (Figs. 6.33-A to F), from the original reservoir oil viscosity of 0.48mPa.s to about 0.45mPa.s. A further reduction to 0.40mPa.s is noticed close to the injection well locations. Even though this is of a little effect in the overall recovery process of the $N_2$ injection, but it is appreciable in microscopic details involved in improved recovery.

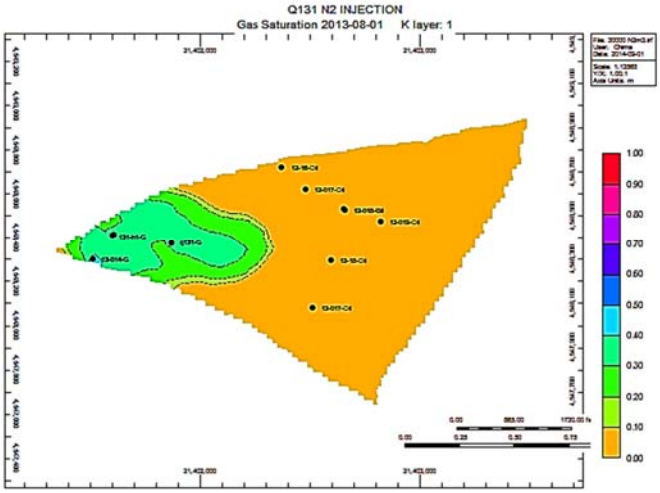


**Fig. 6.29-A: Gas saturation field distribution after 1 year of $N_2$ injection.**

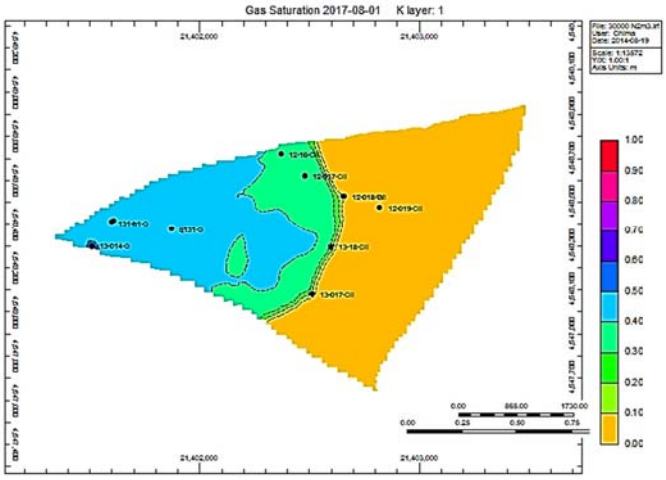


**Fig. 6.29-B: Gas saturation field distribution after 5 years of $N_2$ injection.**

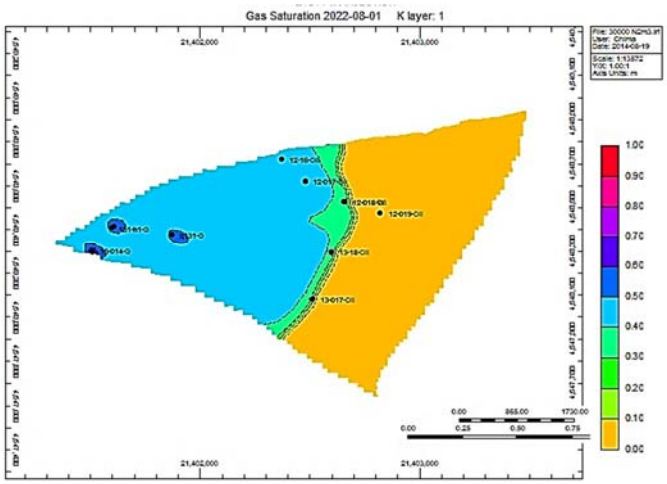


**Fig. 6.29-C: Gas saturation field distribution after 10 years of $N_2$ injection.**

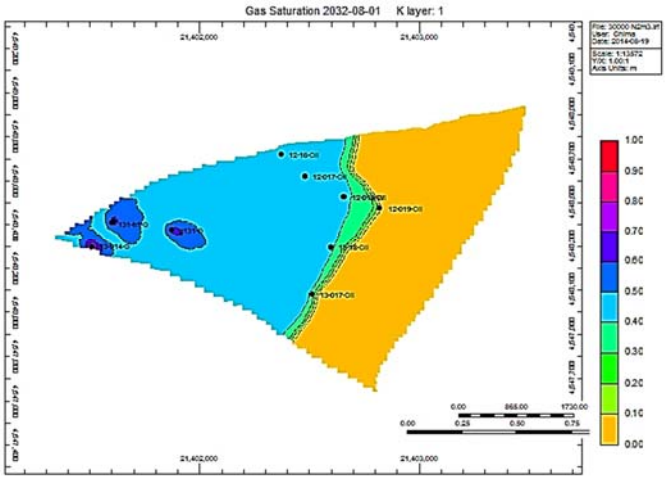


**Fig. 6.29-D: Gas saturation field distribution after 20 years of $N_2$ injection.**

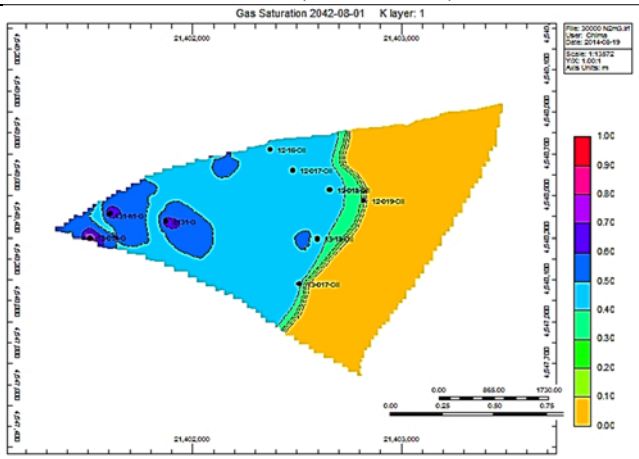


**Fig. 6.29-E: Gas saturation field distribution after 30 years of $N_2$ injection.**

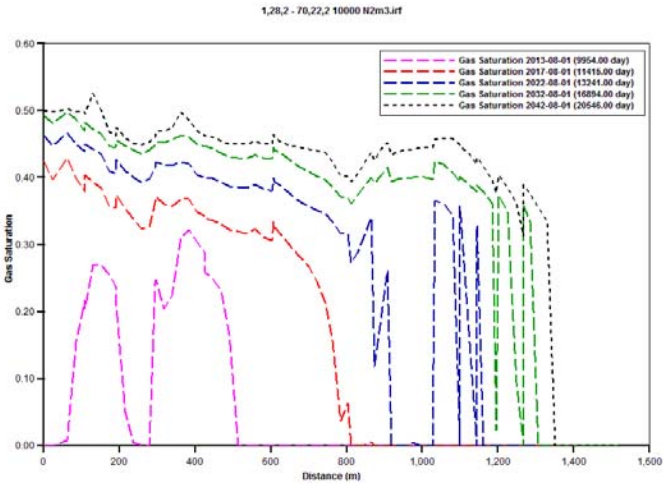


**Fig. 6.30-A: Gas saturation field distribution between injectors and producers at different times (years), under 10000 $m^3$/day $N_2$ injection rate.**

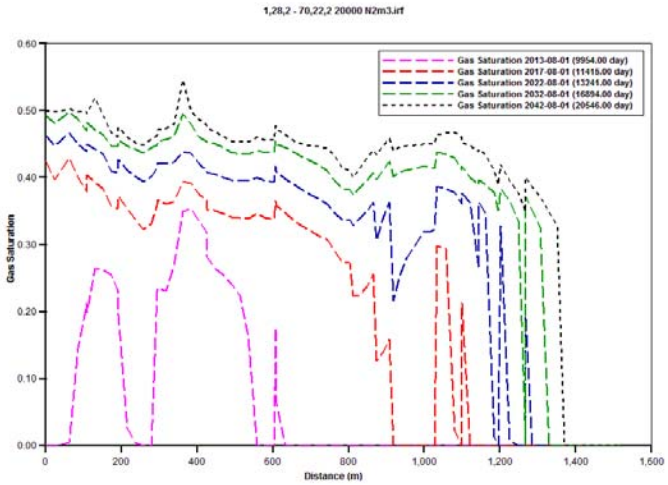


**Fig. 6.30-B: Gas saturation field distribution between injectors and producers at different times (years), under 20000 $m^3$/day $N_2$ injection rate.**

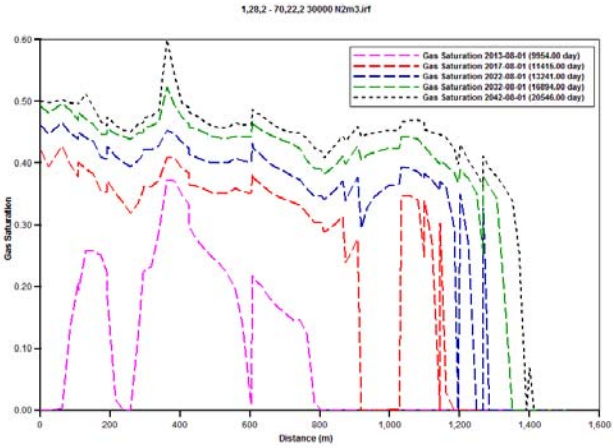


**Fig. 6.30-C: Gas saturation field distribution between injectors and producers at different times (years), under 30000 $m^3$/day $N_2$ injection rate.**

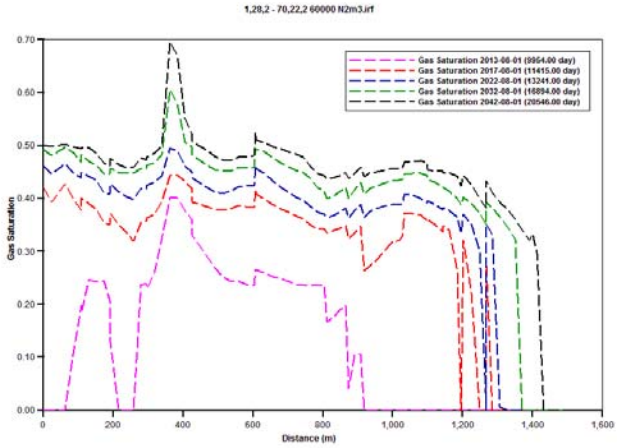


**Fig. 6.30-D: Gas saturation field distribution between injectors and producers at different times (years), under 60000 $m^3$/day $N_2$ injection rate.**

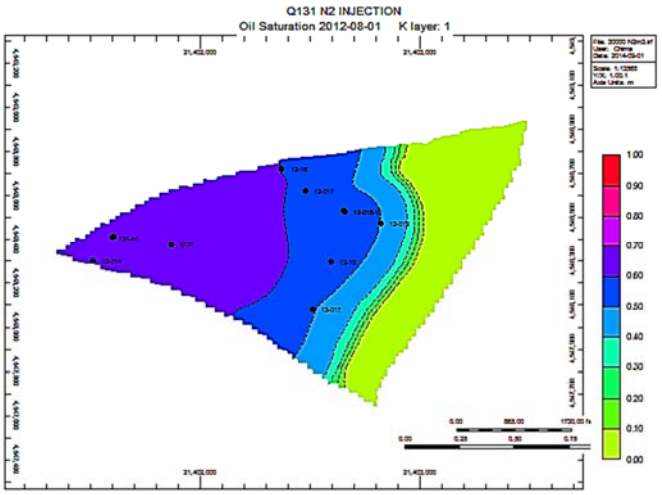


**Fig. 6.31-A: Oil saturation field distribution at 0 year of $N_2$ injection.**

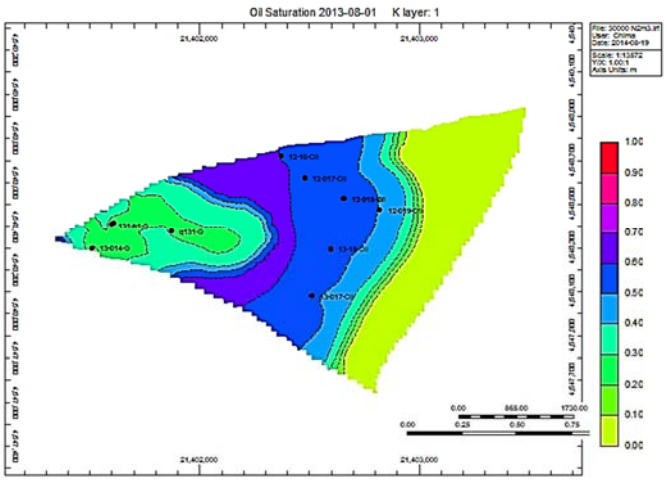


**Fig. 6.31-B: Oil saturation field distribution after 1 year of $N_2$ injection.**

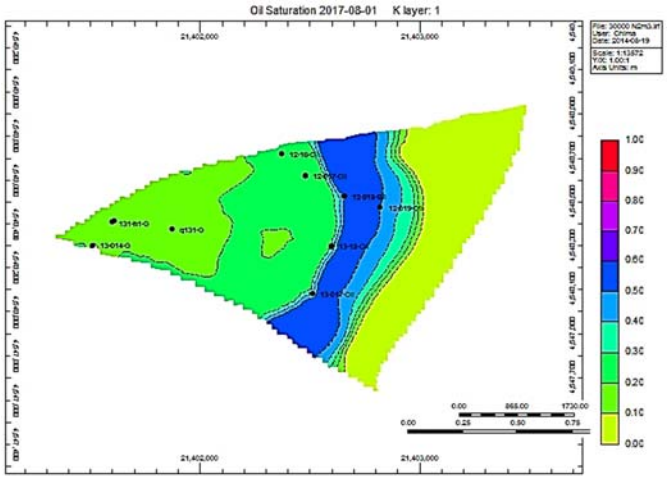


**Fig. 6.31-C: Oil saturation field distribution after 5 years of $N_2$ injection.**

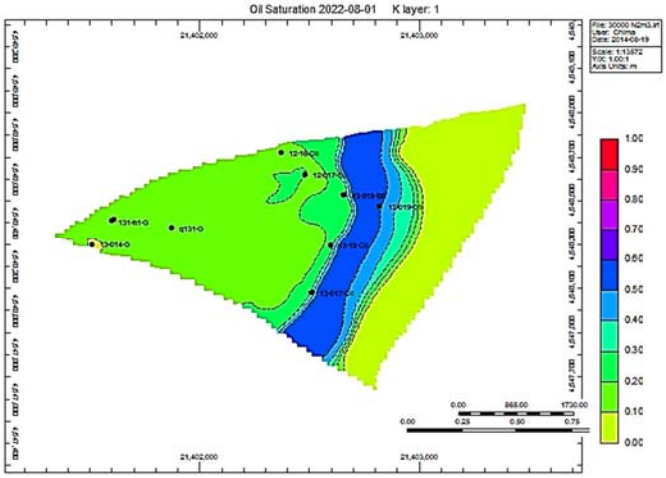


**Fig. 6.31-D: Oil saturation field distribution after 10 years of $N_2$ injection.**

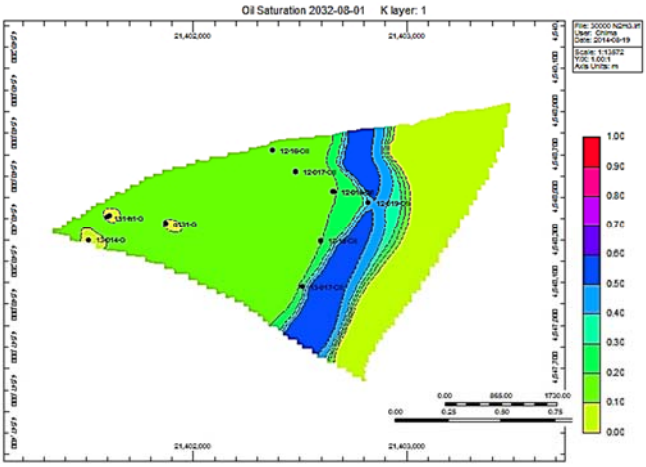


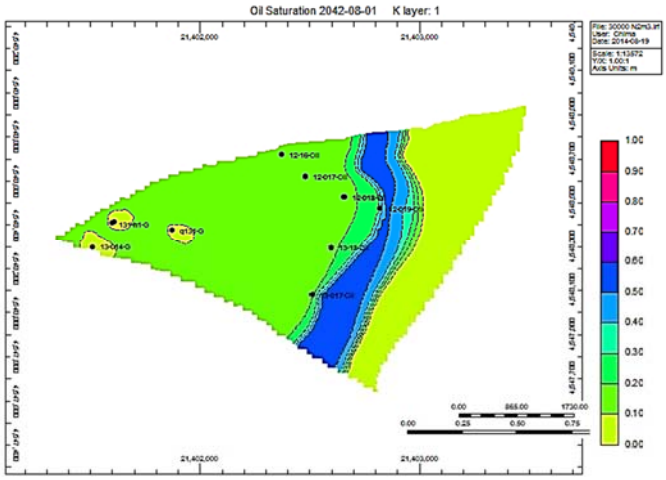


**Figs. 6.31-E and F: Oil saturation field distribution after 20 and 30 years of $N_2$ injection respectively.**

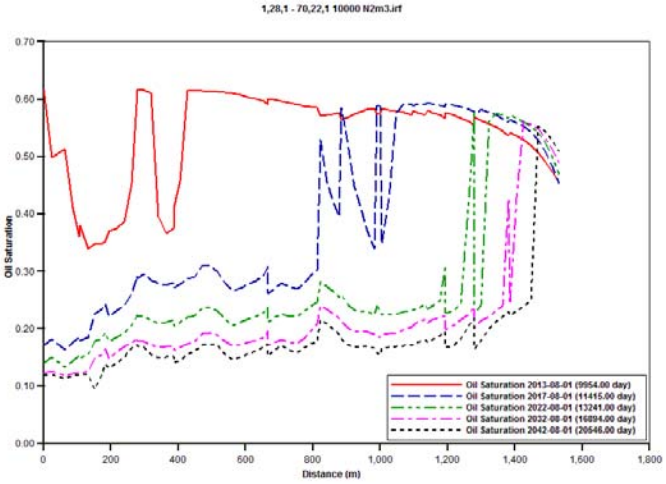


**Fig. 6.32-A: Oil saturation field distribution between injectors and producers at different times (years), under 10000 $m^3$/day $N_2$ injection rate.**

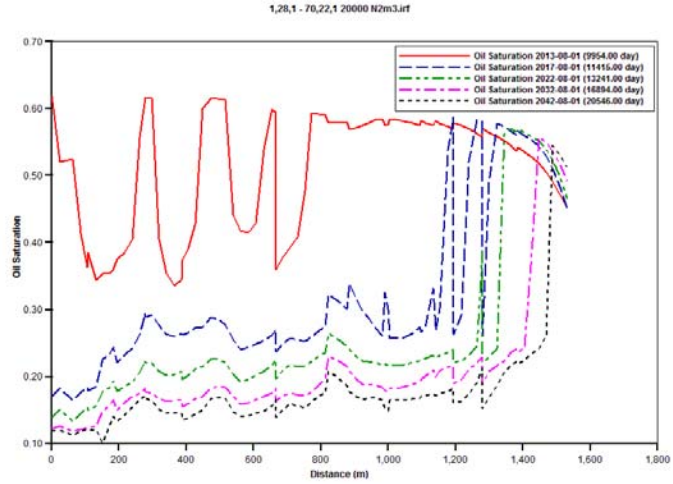


**Fig. 6.32-B: Oil saturation field distribution between injectors and producers at different times (years), under 20000 $m^3$/day $N_2$ injection rate.**

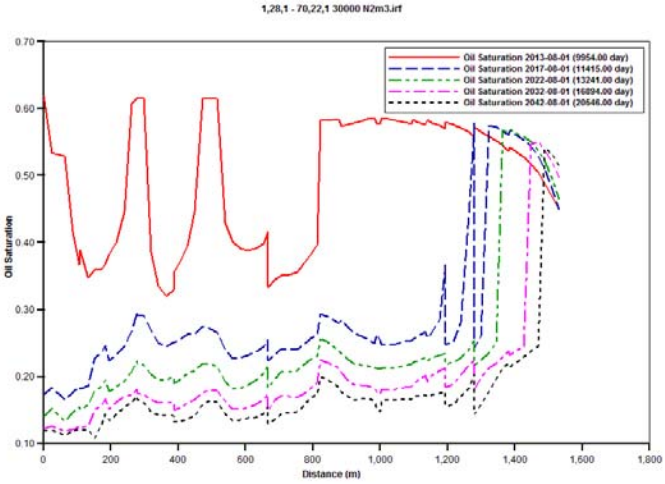


**Fig. 6.32-C: Oil saturation field distribution between injectors and producers at different times (years), under 30000 $m^3$/day $N_2$ injection rate.**

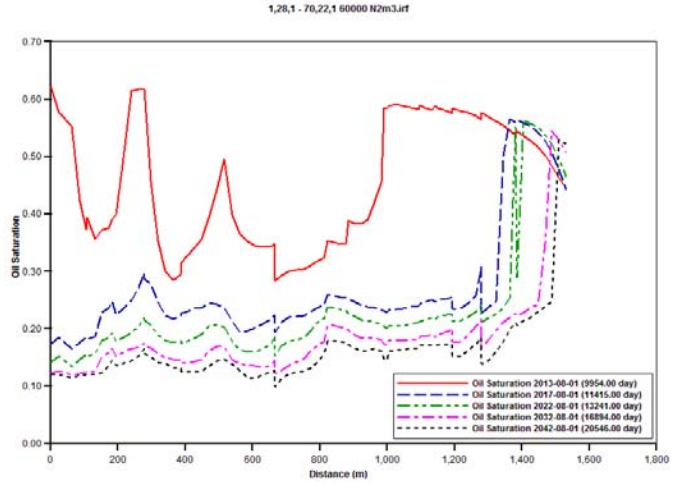


**Fig. 6.32-D: Oil saturation field distribution between injectors and producers at different times (years), under 60000$m^3$/day $N_2$ injection rate.**

#### 6.2.3.3 Gas-Oil Ratio

When the gas front reaches the production wells, GOR will increase rapidly as injection continues (Figs. 6.34-A to D and 6.35). There is a slow and continuous increase in GOR from the start of the simulated $N_2$ injection, which increases up to 11,600$m^3/m^3$ at the highest injection rate used (i.e. 60000$m^3$/day) after 30 years of $N_2$ injection. The gas breakthrough at the production wells at a faster rate than the cases of air and $CO_2$ injection (Table 6.5), but shows the lesser value of overall GOR than the air injection and more than that of $CO_2$ injection.

#### 6.2.3.4 Oil Production Rate

The oil production rate experiences the same features as that of the other two gas injection cases where the oil production rate increases rapidly in the early years of gas injection (Fig. 6.35) even up to a maximum value of 734m3/day before it experiences a sharp decline as both the gas breakthrough starts and GOR value increases. The immiscible displacement drive shows that as the injection rate and time increases, GOR increases. The GOR continues to increase as the gas-oil contact moves farther down structure. Higher injection rates are expected to cause higher GOR which makes it very difficult to handle the large produced gases and this is not economical in IOR practice. So measures should be developed to avoid early gas breakthrough and reduce GOR. The produced gas can be re-injected back into the reservoir through the gas injection wells located high on structure, which is economically favorable.

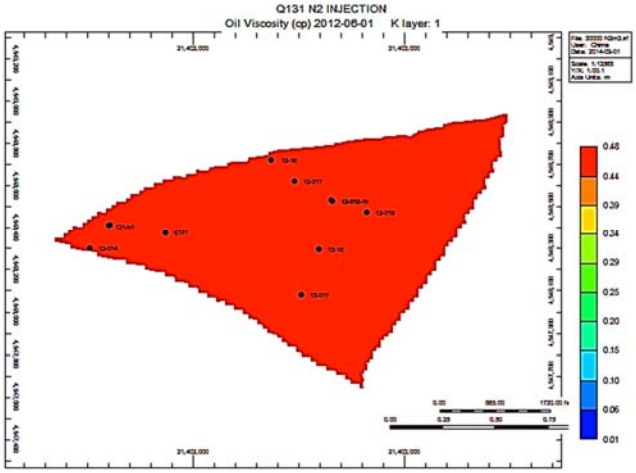


**Fig. 6.33-A: Oil viscosity field distribution at 0 year of $N_2$ injection.**

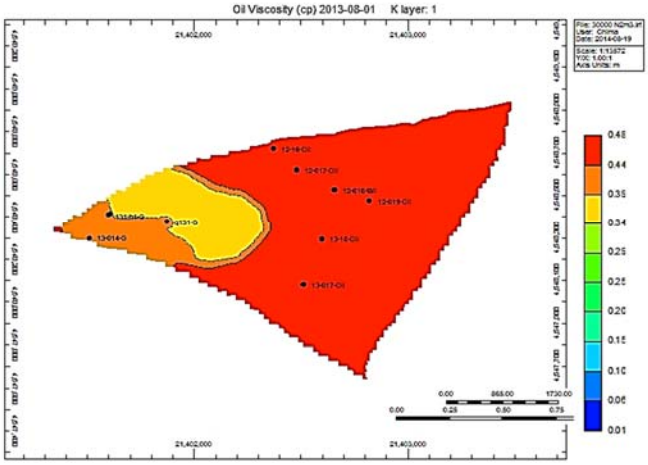


**Fig. 6.33-B: Oil viscosity field distribution after 1 year of $N_2$ injection.**

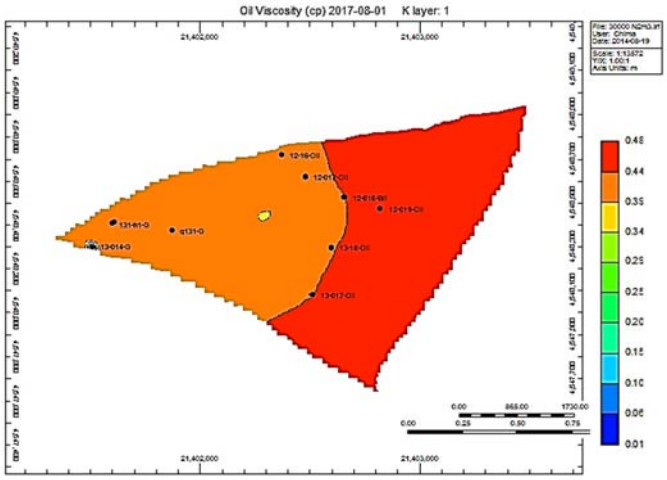


**Fig. 6.33-C: Oil viscosity field distribution after 5 years of $N_2$ injection.**

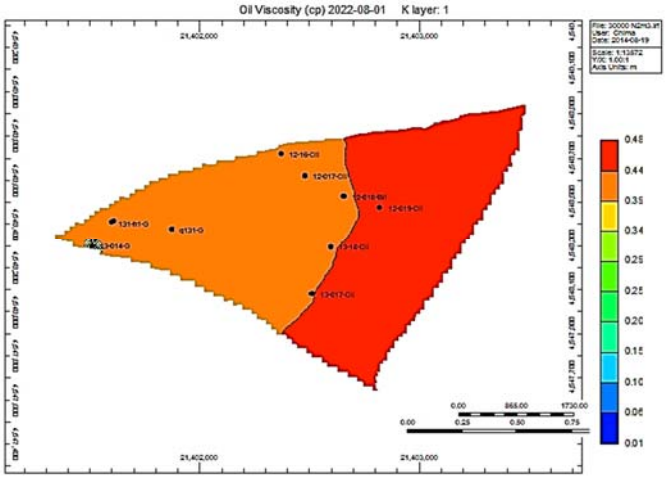


**Fig. 6.33-D: Oil viscosity field distribution after 10 years of $N_2$ injection.**

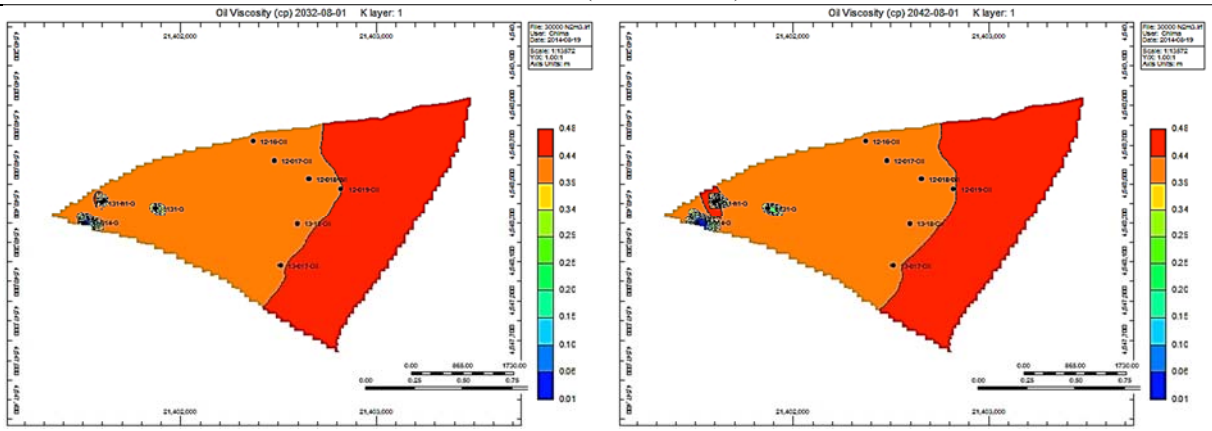


**Figs. 6.33-E and F: Oil viscosity field distribution after 20 and 30 years of $N_2$ injection respectively.**

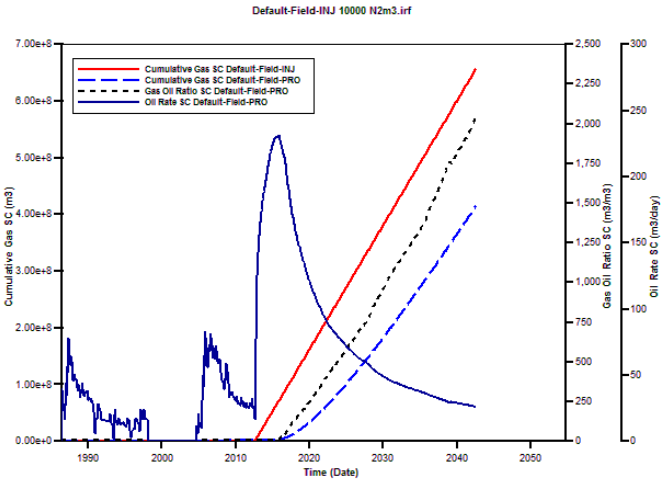


**Fig. 6.34-A: Cumulative gas injected and produced, Gas-oil ratio, Oil daily production rate under 10000m$^3$/day $N_2$ injection rate.**

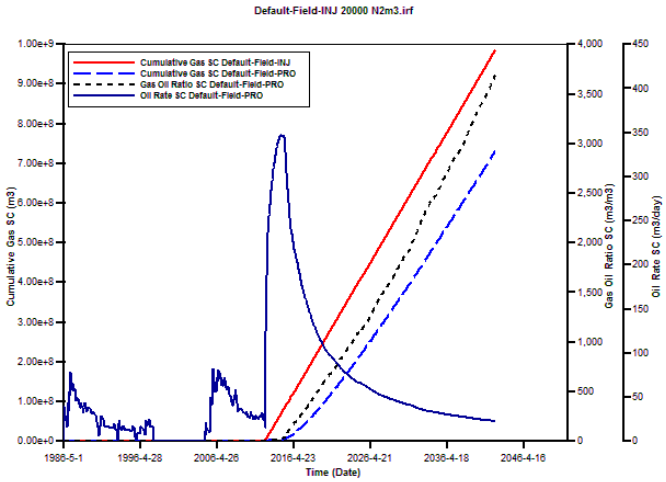


**Fig. 6.34-B: Cumulative gas injected and produced, Gas-oil ratio, Oil daily production rate under 20000m$^3$/day $N_2$ injection rate.**

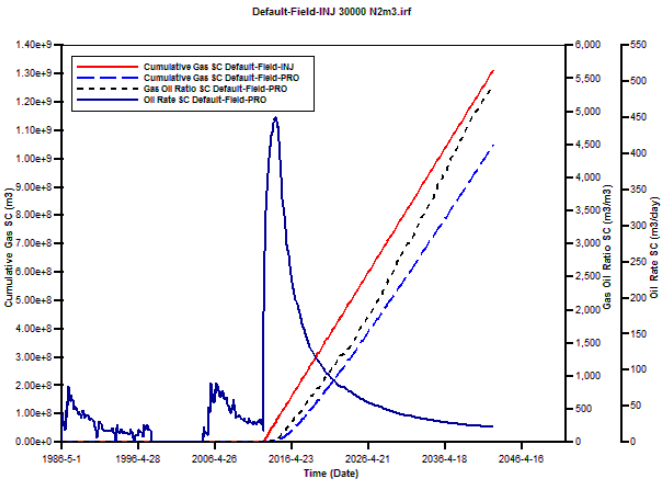


**Fig. 6.34-C: Cumulative gas injected and produced, Gas-oil ratio, Oil daily production rate under 30000m$^3$/day $N_2$ injection rate.**

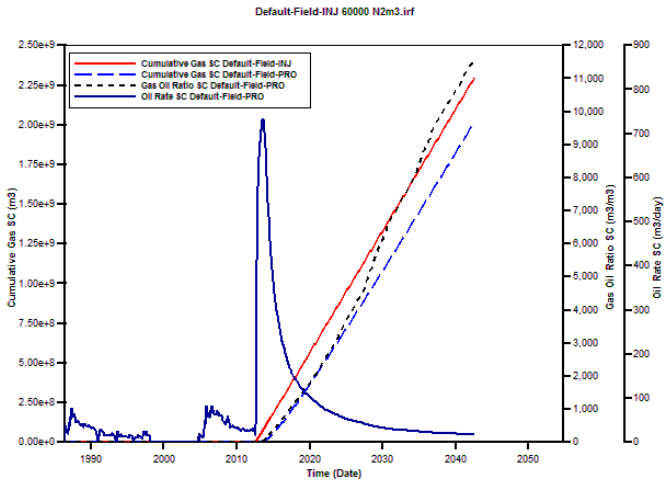


**Fig. 6.34-D: Cumulative gas injected and produced, Gas-oil ratio, Oil daily production rate under 60000m$^3$/day $N_2$ injection rate**

#### 6.2.3.5 Cumulative Gas Injected and Produced

Fig. 6.34-A to D showed the cumulative gas injected and cumulative gas produced increased as the injection rates increased from 10000 – 60000m$^3$/day for the 30 years considered. Table 6.5 showed that the cumulative gas injected ranges from 6.57E+08m$^3$ (for 10000m$^3$/day injection rate) to about 2.30E+09m$^3$ (for 60000m$^3$/day). The cumulative gas produced ranges from 4.15E+08m$^3$ to 2.02E+09m$^3$, which is lesser than the corresponding cumulative gas injected because some of the injected gas are still left in the reservoir and did not reach the production wells and are not produced within the 30 years considered in this simulation study.

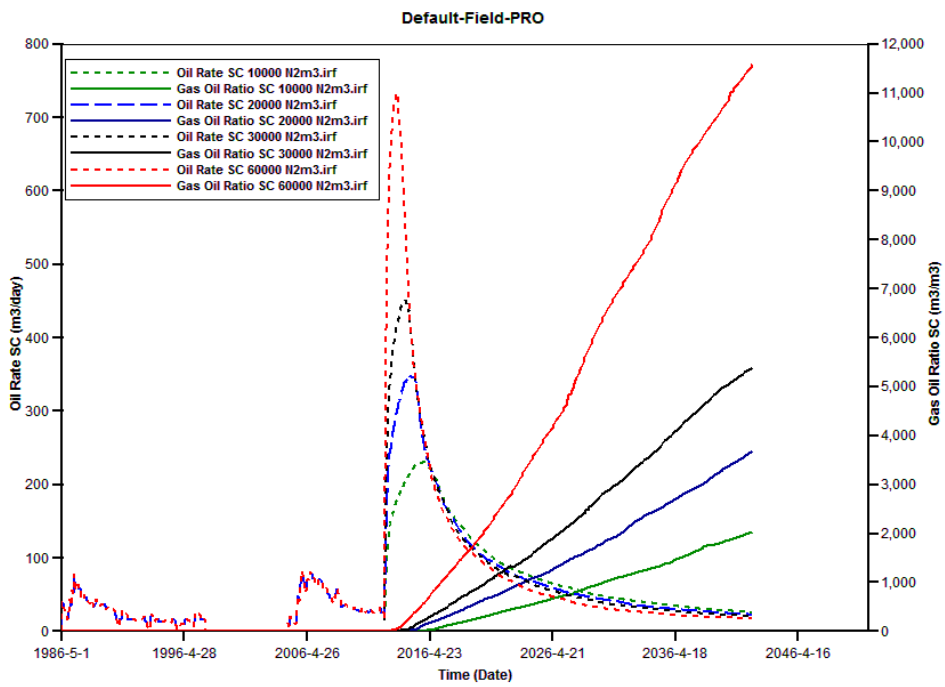


**Fig. 6.35: Comparison of Oil daily production rate and Gas-oil ratio of different $N_2$ injection rates.**

It can also be observed that the cumulative gas produced in the case of $N_2$ injection is the greatest out of the three gas injection techniques considered. This can be explained to have occurred because the $N_2$ doesn't react with the oil to form other gases nor does it need any consumption of the oxygen generated during the reaction (as in the case of air injection), also the injected gas does not go into solution with the contacted oil (as in the case of $CO_2$ injection). Therefore more gas is free to move to the production wells and thus have a higher cumulative gas produced more than the air and $CO_2$ injection cases.

#### 6.2.3.6 Cumulative Oil Produced and Oil Recovery Factor

The cumulative oil produced as the injection rate is increased is shown in Fig. 6.36. Cumulative oil production is observed to increase proportionally as injection rate increases from 10000 to 60000m$^3$/day, which implies that as the gas saturation increases in the reservoir, more oil are pushed down structure

towards the production wells and been produced. Table 6.5 also shows that the cumulative produced oil ranges from about 1.15 x $10^6$ $m^3$ (10000m3/day inj. rate) to 1.36x$10^6$ $m^3$ (60000$m^3$/day inj. rate) for the period of 30 years investigated.

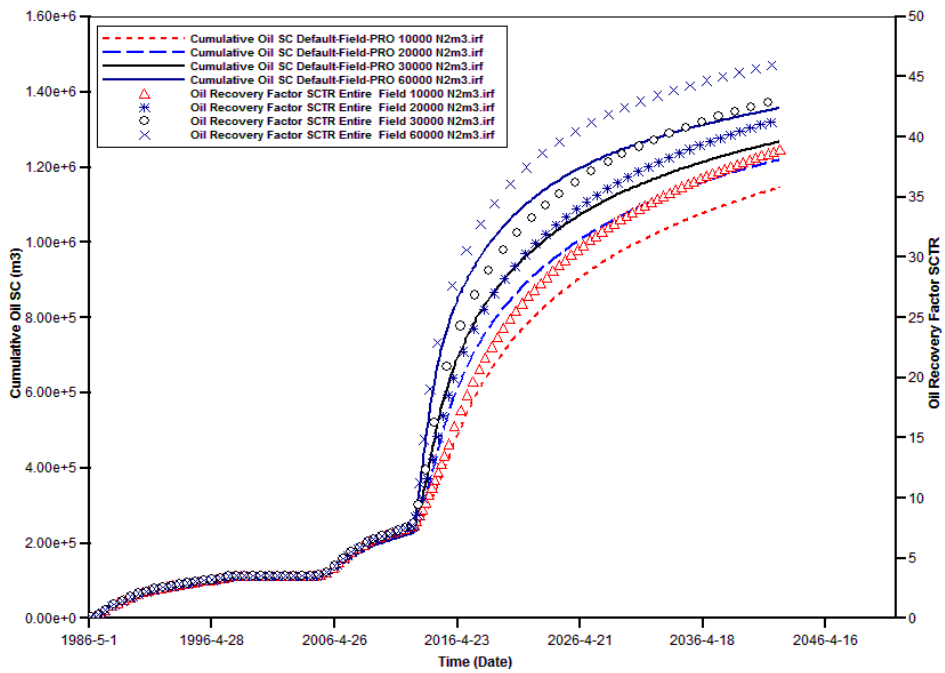


**Fig. 6.36: Cumulative oil produced and Oil recovery factor at different $N_2$ injection rates.**

Figure 6.36 and Table 6.5 showed that the total oil recovery factor of the block was observed to be about 39 – 46% of the OOIP and the incremental oil recovery factor is observed to be about 31 – 39% OOIP after the 30 years of $N_2$ injection at the rates of 10000 – 60000$m^3$/day.

From the simulation results, it is observed that the cumulative oil produced and oil recovery factor of $N_2$ injection is greater than that of air injection. This can be explained that because the oxygen part of the injected air volume are used up and consumed in the oxidation reaction going on in the reservoir, and only the produced flue gases, i.e. $N_2$ and $CO_2$ are involved in the oil displacement drive. This is definitely at a loss when compared to the 100% $N_2$ gas involved in the primary drive of the oil in the $N_2$ injection, and also the near miscible displacement drive seen in $CO_2$ injection Therefore, this leads to the lesser cumulative oil produced and ultimate oil recovery factor in the air injection case when compared with the other gas injection techniques studied.

**Table 6.5: Summary of the Various Simulated Parameters for the $N_2$ Injection IOR**

| 10,000m$^3$/day Injection Rate ($N_2$ injection) | 1year (2013.08) | 5years (2017.08) | 10years (2022.08) | 20years (2032.08) | 30years (2042.08) |
|---|---|---|---|---|---|
| **Gas Oil Ratio m$^3$/m$^3$** | 7.86 | 111.72 | 427.71 | 1161.77 | 2039.2 |
| **Oil Production Rate m$^3$/day** | 177.44 | 174.48 | 88.06 | 42.13 | 25.97 |
| **Cumulative Oil Produced, $10^6$ m$^3$** | 0.273 | 0.580 | 0.864 | 1.206 | 1.146 |
| **Incremental Cum. Oil Produced, $10^6$ m$^3$** | 0.048 | 0.355 | 0.639 | 0.981 | 0.921 |
| **Recovery Factor, %** | 9.29 | 19.72 | 27.35 | 34.88 | 38.97 |
| **Incremental Recovery Factor, %** | 1.62 | 12.05 | 19.68 | 27.21 | 31.30 |

**Cum. Gas Injected = 6.57x$10^8$m$^3$; Cum, Gas Produced = 4.15x$10^8$m$^3$**

| 20,000m$^3$/day Injection Rate ($N_2$ injection) | 1year (2013.08) | 5years (2017.08) | 10years (2022.08) | 20years (2032.08) | 30years (2042.08) |
|---|---|---|---|---|---|
| **Gas Oil Ratio m$^3$/m$^3$** | 8.01 | 299.19 | 847.04 | 2160.81 | 3696.69 |
| **Oil Production Rate m$^3$/day** | 297.94 | 170.75 | 81.99 | 37.10 | 22.68 |
| **Cumulative Oil Produced, $10^6$ m$^3$** | 0.307 | 0.703 | 0.914 | 1.115 | 1.220 |
| **Incremental Cum. Oil Produced, $10^6$ m$^3$** | 0.082 | 0.478 | 0.689 | 0.890 | 0.995 |
| **Recovery Factor, %** | 10.44 | 23.91 | 31.08 | 37.92 | 41.49 |
| **Incremental Recovery Factor, %** | 2.77 | 16.24 | 23.41 | 30.25 | 33.82 |

**Cum. Gas Injected = 9.86x $10^8$m$^3$; Cum, Gas Produced =7.31x $10^8$m$^3$**

| 30,000m$^3$/day Injection Rate ($N_2$ injection) | 1year (2013.08) | 5years (2017.08) | 10years (2022.08) | 20years (2032.08) | 30years (2042.08) |
|---|---|---|---|---|---|
| **Gas Oil Ratio m$^3$/m$^3$** | 13.59 | 483.39 | 286.3 | 3248.97 | 5398.24 |
| **Oil Production Rate m$^3$/day** | 415.12 | 169.77 | 78.19 | 34.13 | 21.17 |
| **Cumulative Oil Produced, $10^6$ m$^3$** | 0.340 | 0.782 | 0.984 | 1.173 | 1.268 |
| **Incremental Cum. Oil Produced, $10^6$ m$^3$** | 0.115 | 0.557 | 0.759 | 0.948 | 1.043 |
| **Recovery Factor, %** | 11.59 | 26.60 | 33.46 | 39.88 | 43.14 |
| **Incremental Recovery Factor, %** | 3.92 | 18.93 | 25.79 | 32.21 | 35.47 |

**Cum. Gas Injected = 1.32x$10^9$m$^3$; Cum, Gas Produced =1.05x$10^9$m$^3$**

| 60,000m$^3$/day Injection Rate ($N_2$ injection) | 1year (2013.08) | 5years (2017.08) | 10years (2022.08) | 20years (2032.08) | 30years (2042.08) |
|---|---|---|---|---|---|
| **Gas Oil Ratio m$^3$/m$^3$** | 46.28 | 1114.81 | 2711.90 | 7344.36 | 11585.70 |
| **Oil Production Rate m$^3$/day** | 734.06 | 157.25 | 70.96 | 27.54 | 17.70 |
| **Cumulative Oil Produced, $10^6$ m$^3$** | 0.438 | 0.932 | 1.121 | 1.279 | 1.357 |
| **Incremental Cum. Oil Produced, $10^6$ m$^3$** | 0.213 | 0.707 | 0.896 | 1.054 | 1.132 |
| **Recovery Factor, %** | 14.91 | 31.70 | 38.11 | 43.48 | 46.16 |
| **Incremental Recovery Factor, %** | 7.24 | 24.03 | 30.44 | 35.81 | 38.49 |

**Cum. Gas Injected = 2.30x$10^9$m$^3$; Cum, Gas Produced =2.02x$10^9$m$^3$**

### 6.2.4 Comparison of the Results from the Three Different Gas Injection Techniques

The initial $CO_2$ injection IOR scenario discussed above in Section 6.2.2, produced lesser ultimate GOR and cumulative gas produced than the corresponding initial air and $N_2$ injection scenarios (Figs. 6.36-A to D, Tables 6.3, 6.4 and 6.5) that was also discussed in Sections 6.2.1 and 6.2.3 respectively. This is can be explained as an evidence to prove that the $CO_2$ injection for IOR operated in a near miscible displacement process where part of the $CO_2$ injected into the reservoir went into solution with the oil under the prevailing reservoir pressure (20 MPa) which is close to the reservoir MMP, and thus the volume of injected, gas produced were lesser than that produced in the other cases, which resulted to more cumulative oil produced. The cumulative oil produced and oil recovery factor of $CO_2$ (Fig.6.28), was been observed to be greatest of the three gas injection techniques when compared with under the highest injection rate of 60000$m^3$/day in Fig. 6.38. It had a broader oil production rate curve than the other two gas injection schemes, and the curve steeped down slowest than the others, which shows that the oil production rate maintained a steadier less sharp decline than the air and $N_2$ injection. It is also observed that during the first 10 years of $CO_2$ injection, the oil production rate is lower than that of the other cases but becomes better in the latter 20 years to finally give the best ultimate recovery out of the 3 gases.

Under the different injection rates considered, $N_2$ injection case had more cumulative gas produced than air injection and $CO_2$ had the least as shown in Table 6.5 and Figs. 6.28-A to D.

From the simulation results, it is observed that the cumulative oil produced and oil recovery factor of $N_2$ injection is greater than that of air injection (Fig. 6.38, Tables 6.3 and 6.5). This can be explained that because the oxygen part of the injected air volume are used up and consumed in the oxidation reaction going on in the reservoir, and only the produced flue gases, i.e. $N_2$ and $CO_2$ are involved in the oil displacement drive. This is definitely at a loss when compared to the 100% $N_2$ gas involved in the primary drive of the oil in the $N_2$ injection, and also the near miscible displacement drive seen in $CO_2$ injection makes it have higher cumulative production than air. Therefore, these explain the observed lesser cumulative oil produced and ultimate oil recovery factor obtained in the air injection simulation case when compared with the other gas injection techniques studied.

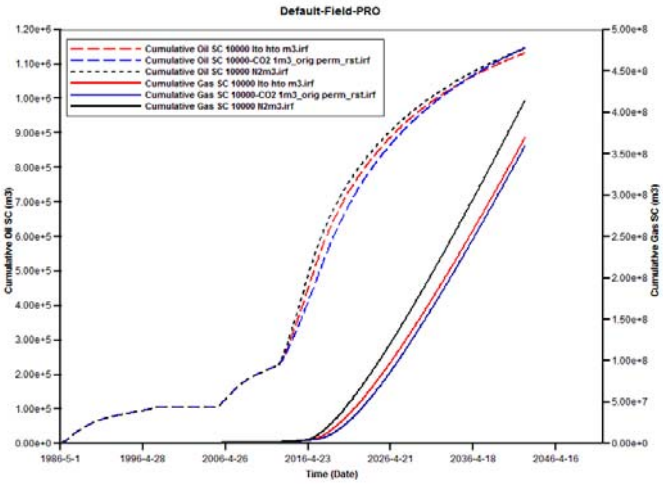


**Fig. 6.37-A: Comparison of the Cumulative gas produced and the corresponding Cumulative oil produced under 10000 m$^3$/day injection rate of different gases.**

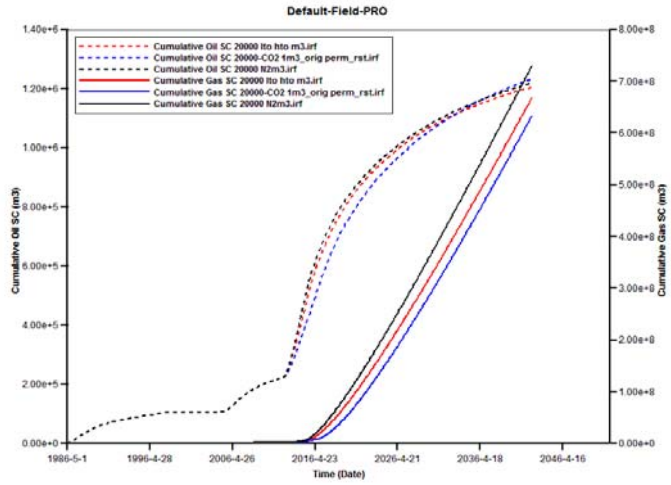


**Fig. 6.37-B: Comparison of the Cumulative gas produced and the corresponding Cumulative oil produced under 20000 m$^3$/day injection rate of different gases.**

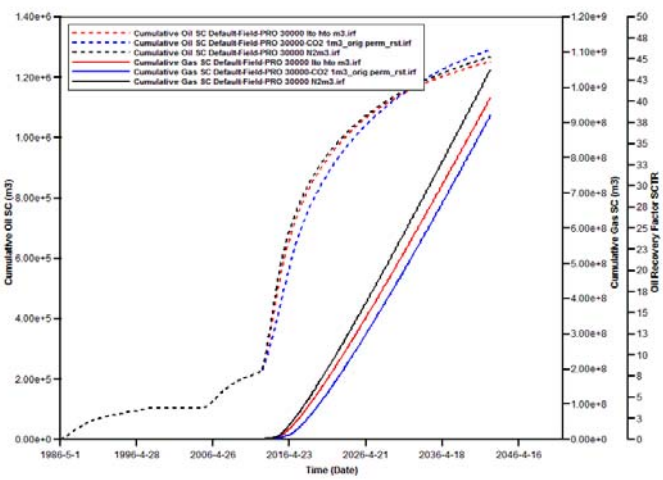


**Fig. 6.37-C: Comparison of the Cumulative gas produced and the corresponding Cumulative oil produced under 30000 m$^3$/day injection rate of different gases.**

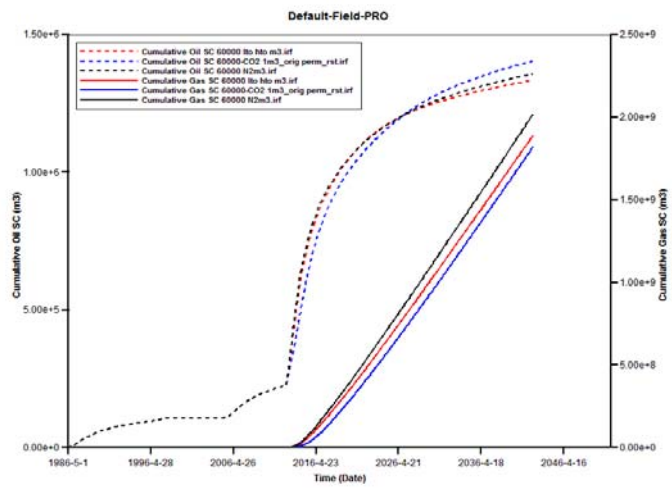


**Fig. 6.37-D: Comparison of the Cumulative gas produced and the corresponding Cumulative oil produced under 60000 m$^3$/day injection rate of different gases.**

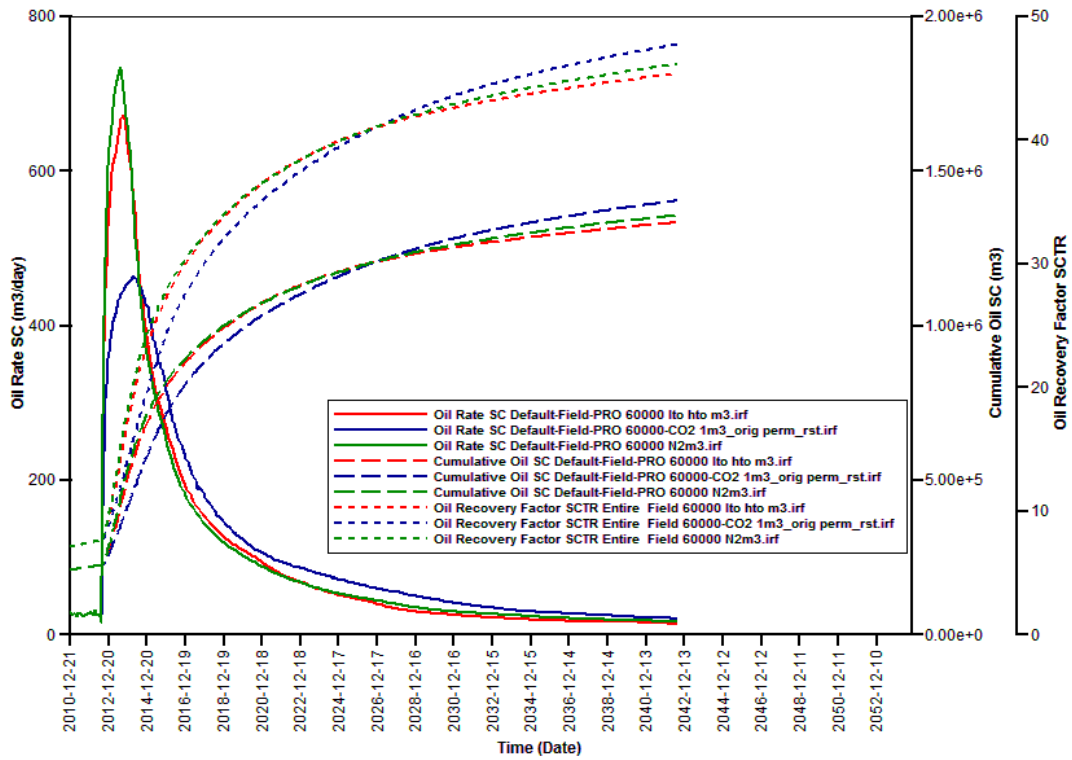


**Fig. 6.38: Comparison of the Oil recovery factor, Cumulative oil produced and the Oil daily production rate of the different gases studied, under 60000m$^3$/day injection rate.**

## 6.3 Numerical Simulation of Optimization Scenarios

### 6.3.1 High GOR Production well(s) Shut-in Case

One of the measures applied in this study to solve the problems of high gas breakthrough and the fast decline in the oil production rate is to initiate a well shut in operation of injector wells that produces more gas as indicated by their GOR values. Recovery can also be improved by shutting-in wells when they begin to produce large amounts of injected gas. This sensitivity study for the different gas injection techniques was run using a constant 30000m$^3$/day injection rate and set to shut in wells that reaches a GOR of 2000m$^3$/m$^3$. The results are discussed below.

The air injection simulation runs was set to shut-in wells that produced ≥2000m$^3$/m$^3$ of gas-oil ratio, and from the simulation results presented in Fig. 6.39-A, it was observed that the air injection IOR operation will reach the abandonment stage by 2029, i.e. 17 years from the start of air injection. The cumulative oil recovered is about 1.212E+06 m$^3$ (recovery factor of about 40.9% OOIP). Also, the observed cumulative gas injected is 7,45E+08 m$^3$ and the cumulative gas produced reduced to about

3.67E+08 $m^3$, which is much less than the initial value (about 4.68E+8$m^3$) observed in the initial air injection scenario (without high GOR production wells shut-in) presented in Figs. 6.16-C.

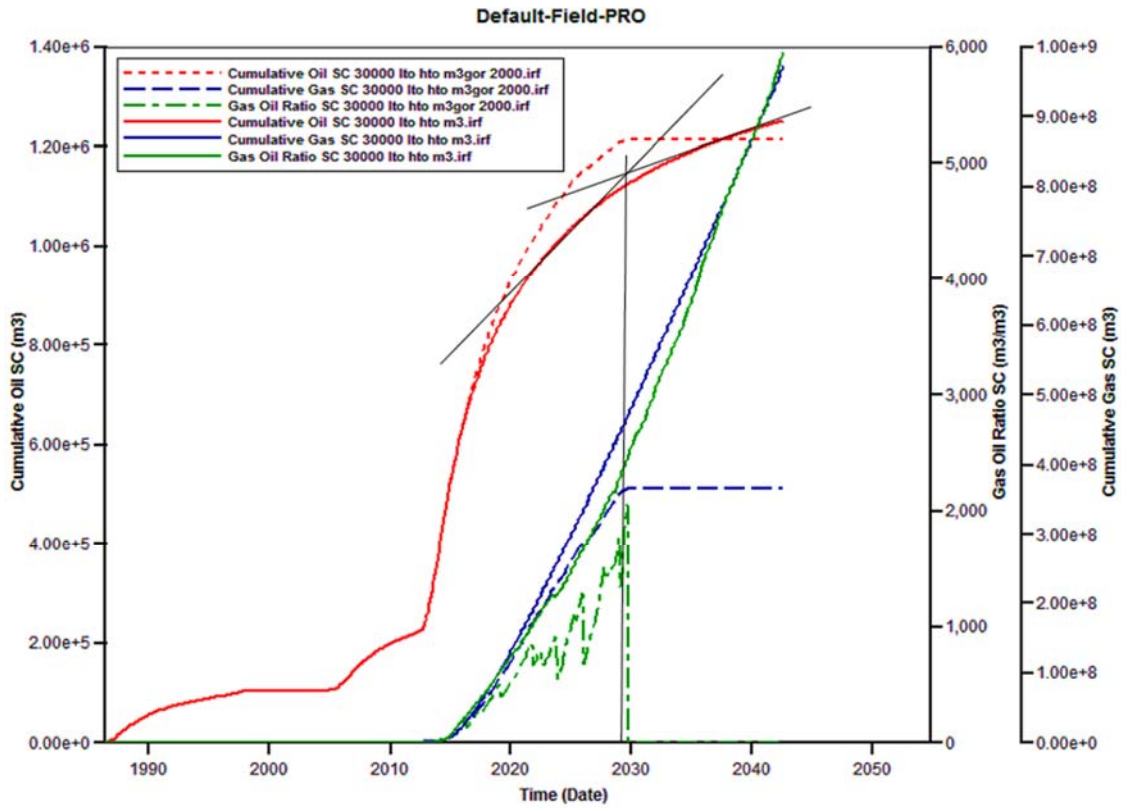


**Fig. 6.39-A: Simulation Results of the two (2) optimization scenarios for Air Injection**

Also for $CO_2$ injection, any production well that reaches a maximum GOR of ≥2000$m^3/m^3$, is set to shut-in in the simulation runs. The results to this process is presented in Fig. 6.39-A, where it can be seen that at the year 2033, the abandonment stage sets in. The cumulative oil recovered at this time is about 1.29E+06 (recovery factor of 43.45% OOIP). There is also a remarkable decrease in the observed 9,2E+08 $m^3$ of cumulative gas injected and 4.11E+08 $m^3$ cumulative gas produced as opposed to the high cumulative gas production seen in the initial $CO_2$ injection scenario without high gas production wells shut in (Fig. 6.26-C) which is about 5.68E+08 $m^3$.

The $N_2$ injection shut-in case also has the same GOR limit as the air and $CO_2$ injection, i.e. 2000$m^3/m^3$. The results for this process is presented in Fig. 6.39-C The abandonment stage was observed to be at year 2030, which is 18 years after the start of the injection operation. The cumulative oil produced is 1.24E+06 $m^3$ (recovery factor of about 41.76% OOIP), and also showed a reduced 7.89E+08 $m^3$ and 4.55E+08 $m^3$ cumulative gas injected and produced respectively when compared with that of the initial $N_2$ injection scenario (without high GOR production wells shut-in) presented in Fig. 6.34-C.

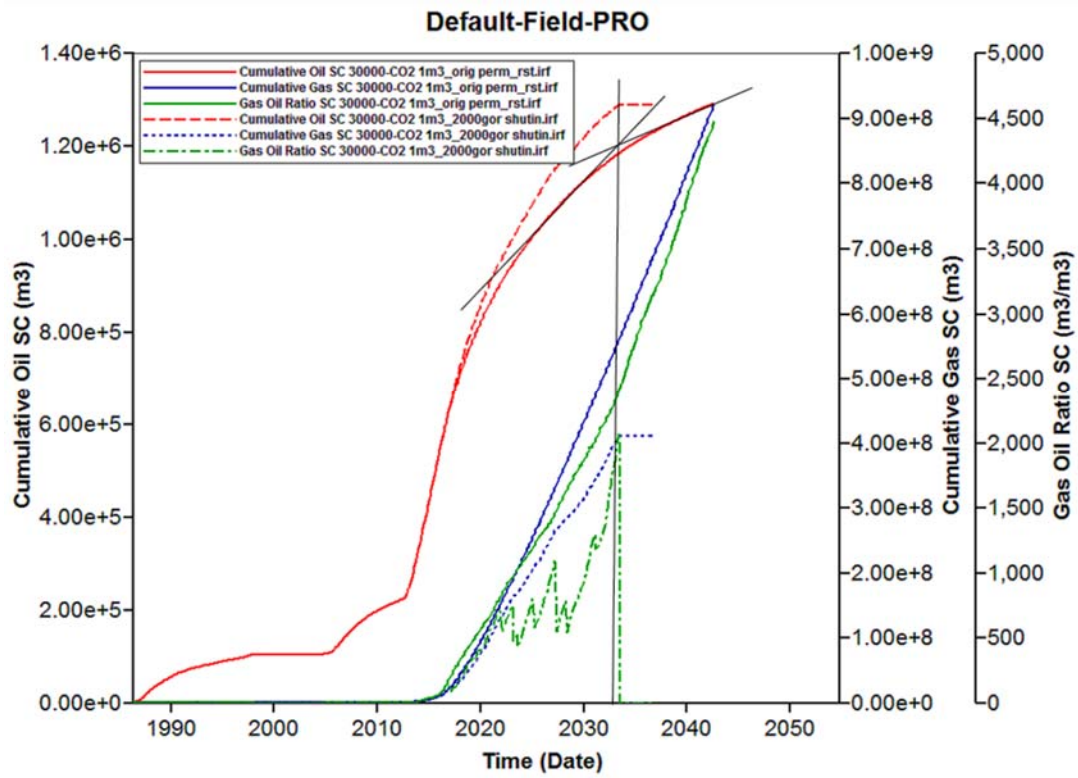


**Fig. 6.39-B: Simulation Results of the two (2) optimization scenarios for $CO_2$ Injection**

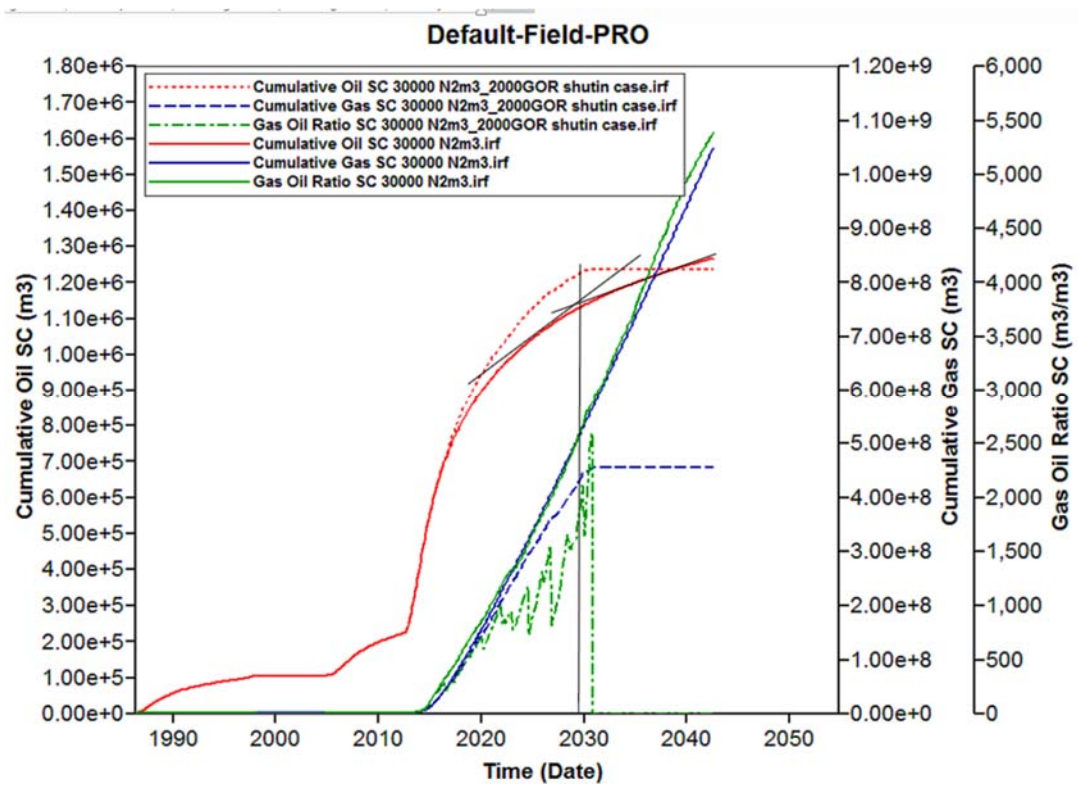


**Fig. 6.39-C: Simulation Results of the two (2) optimization scenarios for $N_2$ Injection**

The summary of this case is presented in Table 6.6 shown below.

**Table 6.6: Summary of the Simulation Results of the Two Optimization Scenarios**

| Case 1: High GOR production well(s) shut-in | | | |
|---|---|---|---|
| | **Air** | **$CO_2$** | **$N_2$** |
| **Abandonment Time (Year)** | **2029** | **2033** | **2030** |
| **Cumulative Oil Produced, $10^6$ $m^3$** | **1.212** | **1.290** | **1.237** |
| **Recovery Factor, %** | **40.89** | **43.45** | **41.76** |
| **Cumulative Gas Produced, $10^8$ $m^3$** | **3.67** | **4.11** | **4.55** |
| **Cumulative Gas Injected, $10^8$ $m^3$** | **7.45** | **9.2** | **7.89** |

| Case 2: Best Stop time without well(s) shut-in | | | |
|---|---|---|---|
| | **Air** | **$CO_2$** | **$N_2$** |
| **Abandonment Time (Year)** | **2029** | **2033** | **2029** |
| **Cumulative Oil Produced, $10^6$ $m^3$** | **1.125** | **1.188** | **1.132** |
| **Recovery Factor, %** | **38.25** | **40.4** | **38.48** |
| **Cumulative Gas Produced, $10^8$ $m^3$** | **4.68** | **5.68** | **5.19** |
| **Cumulative Gas Injected, $10^8$ $m^3$** | **7.45** | **9.2** | **7.89** |

### 6.3.2 Best Injection Stop Time without Well(s) Shut-In Case

In a crude (manual) way to determine when it is the best time to stop gas injection operations in the field, another method was employed to determine the best stop time for each of the gas injection techniques by drawing two tangents lines at the lower and upper curved parts of the cumulative oil produced line. The corresponding time of injection (in years) of intersections of these two tangent lines are is deduced to be the best stop time for the injection operation. From Figs. 6.39-A, Band C, we have that the best stop times for air, $CO_2$ and $N_2$ injections are 2029, 2033 , 2029 respectively. The cumulative oil produced at these times are 1.21E+6 $m^3$, 1.29E+6$m^3$, and 1.23E+6$m^3$.

The summary of the results and comparison of the two methods are presented in Table 6.6. It is quite interesting to note that the two methods showed that the best time to stop the any of the gas injection operations for the oil block matches themselves i.e. 2029 for air injection, 2033 for $CO_2$ injection, and 2029 or 2030 for $N_2$ injection. But the shut-in high gas production wells scenario gives higher oil recovery than the second method of just abandoning the field without any well shut-in.

# CHAPTER 7: ECONOMICS, SAFETY AND RISK ASSESSMENTS

## 7.1 Preliminary Economic Assessment

The simulation results have shown that injecting air, $CO_2$, and $N_2$ into Q131 oil reservoir has potentials to extend the life of the field, accelerate oil production and increase the ultimate recovery. However, the economics of the project depends on many factors, such as availability of the gas sources and its proximity to the oil field, investment on infrastructure for gas injection, separation and transportation, and operational cost. In this study, a generalized economic assessment of gas injection IOR projects based on the simulation results presented above was carried out to ascertain the profitability margin of each of the gas injection techniques studies in the case of Q131 reservoir. To facilitate this task, field capital and operational costs is computed, evaluated the cumulative incremental oil produced and calculate the revenue generated which will be compared with the individual total costs of the different injection techniques within the injection period.

Table 7.1 summarizes the economic parameters used in the economic assessment study for the different gas injection techniques screened for application in the Q131 oil block. The default currency used is the American dollars, $. All the cost data is expressed in real terms and an inflation rate of 3% is assumed. It is seen that no tax evaluation was used, this is because the project is a government funded business and this study is focused on the technical aspects and the revenue generated from the application of the gas injection techniques, not the policies behind the management, and regulations of the operation. So having this in mind, we ignored taxation in this study's preliminary economic evaluation. It will be added and discussed in subsequent studies.

**Table 7.1: Economic Parameter Used on the Economic Assessment**

| | |
|---|---|
| **Cost of Air Capture and Compression** | $0.08/m$^3$ |
| **Cost of $CO_2$, transportation and separation** | $81.40/ton of $CO_2$ (approximately $0.146/m3) |
| **Cost of $N_2$, transportation and separation** | $0.147/m$^3$ |
| **Exchange Rate** | 6.14元/$ (Year 2014) |
| **Capex for injection/separation units** | $1.335 Million |
| **Cum. Gas injected (maximum)** | 1.32x10$^9$ sm$^3$ (the same for the 3 gases) |
| **Gas injection Rate** | 30000m$^3$/day (base case scenario) |
| **Taxation** | Ignored (Government-owned enterprise) |

Note: 1 ton of $CO_2$ = 556.2m$^3$ (Appendix C)

### 7.1.1 Major Expenditure Costs

The expenditure for the studied gas injection is divided into 2: the Capital expenditure (Capex) and the operational expenditure (Opex) as shown in details in Tables 7.2, 7.3 and 7.4 below.

**Capital/Equipment Investment (Capex):** include 4 new wellheads for the injectors, 2 air compressor units, gas injection pipelines and installation costs, produced gas detecting equipment and the costs for research and plan of the gas injection project, replacement of anticorrosion oil tubes for air injection, etc. The Capex items are the same for the different gas injection techniques studied.

**The Operational Cost (Opex):** include the costs of the gas purchase, separation, and injection including the electricity cost, gas compressor maintenance, and greasing, injection well with oxygen corrosion inhibitors (anticorrosion tubing, preservatives) in injection and production wells, which is only applied to the costs of air injection and $CO_2$ and not in $N_2$ injection, injection and production wells $CO_2$ corrosion prevention (anticorrosion tubing, preservatives), gas handling and other unexpected (contingencies) expenses which can include labor wages, decommissioning units' costs etc. are also considered in the Opex. The detailed costing of these items are shown in Tables 7.2, 7.3 and 7.4 for air, $N_2$ and $CO_2$ respectively.

**Note that especially for $CO_2$ injection** use in IOR and geological storage, the main cost factors and restrictions of field implementation include gas separation, transportation, gas compression, retardation of corrosion, processing and/or recycling of produced gas. Gas separation includes $CO_2$ capture or $N_2$ separation from air. **Also for $N_2$ gas injections,** the above costs applies and extra costs of gas separation, transportation should be added. It is also noted that for **air injection**, the current cost to purchase an air compressor (air flow rate of 7 sm3/min) is $137,000. Based on the field experience of air injection using a similar air compressor in ZhongYuan Oilfield China (Hongmin et al., 2008), the average air compression cost (electricity) is around $0.052/Sm$^3$ of air at 30MPa. The additional cost for safety and corrosion control per well is estimated as $12,000. Other costs, including installation, facility maintenance and operation are estimated based on field experience and the industry standards. The cost of $N_2$ at a similar condition from air separation is more than double of that for the air.

Besides of technical factors, also the combination of reservoir parameters and economic factors such as flood performance, oil price, final deliverable of injected gas price, operational, drilling and recycling costs, project discount rate, etc. have great impact on the project economics as well as type of economic incentives which might be needed to encourage gas injection EOR (Ghomian Y. et al, 2007).

### 7.1.2 Calculations of Economic Evaluation Parameters

#### 7.1.2.1 Capex, Opex, Total Costs and Cost of Unit Oil Produced

Table 7.5 showed the cost of unit oil produced for the gas injection techniques increased from the case of air injection ($116/m$^3$) to $N_2$ ($191/m$^3$) and highest for $CO_2$ at $230/ m$^3$. This indicates that $CO_2$ injection has the highest operational costs because of its unavailability of the source close to the oilfield, safety and corrosion issues, more money will be spent to prevent or minimize the negative effects of these factors, thus leading to high cost. $CO_2$ costs also rises from the high cost of $CO_2$ separation from produced gas after gas breakthrough, which is almost about 30% the cost of its injection. The detailed total costs of $CO_2$ injection for the 30 years period studied is seen in Table 7.4. The main challenges for a successful $CO_2$ process are the availability of $CO_2$, corrosion in the well and surface facilities, environmental constraints, and the high cost of $CO_2$ for use in remote fields. In general, four economic elements (i.e., $CO_2$ capture and compression cost, $CO_2$ transportation cost, $CO_2$ storage cost and revenue from incremental oil production) should be used to evaluate the economic efficiency (Algharaib, 2008).

$N_2$ injection also showed relative high Opex even though there was not any costs of $O_2$ and $CO_2$ corrosions prevention. This high cost observed in $N_2$ injection is basically because $N_2$ gas is very expensive to obtain and transported to the oilfield but a cheaper method is used in the oil field to generate nitrogen (95-98% volume) from air using the cryogenic plants, separate it and ready for injection. This process usually requires more amount of money to achieve commercial quantity of nitrogen for injection on a daily basis. The detailed total costs of $N_2$ injection for the 30 years period studied is seen in Table 7.3.

For air injection, the Opex is very low compared to the other two gases, because it is readily availability and cheap to obtain and compressed and injected. Corrosion prevention is also seen to add to the costs of air injection (Table 7.2).

Table 7.5 summarized the economic assessment evaluation and showed that the total cost showed from highest to lowest cost in the order of $CO_2$, $N_2$ and air with approximate total costs (addition of Capex and Opex) of $211.7, $199.7, and $119.1 million respectively.

#### 7.1.2.2 Revenue

From the numerical simulation results we have discussed above in Chapter 7, we used the cumulative oil production records of the 3 different gas injection techniques from 2012 to 2042 (30years period) to calculate the revenue that will be generated from the oil production using three scenarios of oil price ranging from $70/barrel (low case), $100/barrel (base case) to $150/barrel (high case). High oil price

is a positive driver of gas injection IOR, and oil prices have been known to always change with time, so we considered the acquired revenue with low, normal and high oil prices to accommodate all circumstances that surrounds the unsteady oil price for the 30 years period being studied.

Tables 7.2 to 7.4 show the different revenue generated by the different gas injection techniques (at base case, 30000m$^3$/day injection rate) under the different oil prices sampled. This is gotten by multiplying the incremental oil produced in barrels by the oil price. $CO_2$ had the highest cumulative oil produced and thus had the highest the oil revenue of the 3 gases (Table 7.5), with a $100/barrel oil price generating a revenue of approximately $672 million. This is followed by $N_2$ with the second largest cumulative oil produced and an approximate $656 million revenue. The least is air injection which generated a revenue $646 million in the 30 years of injection.

#### 7.1.2.3 Cost-Benefit Ratio

Tables 7.2 to 7.4 showed a parameter known as the cost-benefit ratio. It is the ratio of the generated revenue to the total costs (Capex and Opex). It can be used to determine how much of the money invested in the applying any of the gas injection techniques will yield more profit i.e. the profitability of the operations. When we focus on one case scenario of oil price, say the base case of $100/barrel, we observe that air injection has the highest cost-benefit ratio of 1:5.4, followed by $N_2$ injection with 1:1.33 and finally $CO_2$ injection with 1:2.7. This means that the air injection will give the most return for money invested in the project, and $N_2$ will also do better economically more than $CO_2$ injection.

## Table 7.2: 30years air injection economic benefit evaluation: 30000m$^3$/day (Base Case injection rate scenario)

| | Equipment Investment (Capex) | | | | Operating Cost (Opex) | |
|---|---|---|---|---|---|---|
| | **Description** | **Amount, $10^6$ USD** | | | **Description** | **Amount, $10^6$ USD** |
| **Cost Estimation** | Air Compressor Unit(s) | 0.261 | | | Cost of air injection @ 30000m$^3$/day | 105.60 |
| | 4 High Pressure well head (Conversion) | 0.130 | | | Air compressor maintenance | 0.782 |
| | Gas injection pipeline and installation | 0.098 | | | Injection well $O_2$ corrosion prevention | 1.95 |
| | Produced gas testing equipment | 0.032 | | | Production well $CO_2$ corrosion prevention | 4.56 |
| | Engineering design, planning and outsourcing research | 0.977 | | | Produced Gas handling Cost and other Unexpected expenses | 4.886 |
| | **Subtotal** | **1.335** | | | **Subtotal** | **117.778** |
| | **Total Cost, Million USD 119.113** | | | | | |
| **Oil Revenue** | Cum. Oil Produced, $10^6$ sm$^3$ | 1.252 | | | | |
| | Incremental Cum. Oil Produced, $10^6$ sm$^3$ | 1.027 | | | | |
| | Incremental Cum. Oil Produced, $10^6$ barrel | 6.460 | | | | |
| | Oil prices (3scenarios), USD/barrel | 70 (Low); | 100 (Base); | 150 (High) | | |
| | **Amount, Million USD** | **452.2** | **646.0** | **969.0** | | |
| **Cost-Benefit ratio** | | **1:3.8** | **1:5.4** | **1:8.1** | | |

## Table 7.3: 30years $N_2$ injection economic benefit e valuation: 30000m$^3$/day (Base Case injection rate scenario)

| | Equipment Investment (Capex) | | | | Operating Cost (Opex) | |
|---|---|---|---|---|---|---|
| | **Description** | **Amount, $10^6$ USD** | | | **Description** | **Amount, $10^6$ USD** |
| **Cost Estimation** | Gas Compressor Unit(s) | 0.261 | | | Cost of $N_2$ injection @ 30000m$^3$/day | 194.04 |
| | 4 High Pressure well head (Conversion) | 0.130 | | | $N_2$ compressor maintenance | 0.782 |
| | Gas injection pipeline and installation | 0.098 | | | Produced Gas handling cost and other Unexpected expenses | 3.5 |
| | Produced gas testing equipment gas testing equipment | 0.032 | | | | |
| | Engineering design, planning and outsourcing research | 0.977 | | | | |
| | **Subtotal** | **1.335** | | | **Subtotal** | **198.322** |
| | **Total Cost, Million USD 199.657** | | | | | |
| **Oil Revenue** | Cum. Oil Produced, $10^6$ sm$^3$ | 1.268 | | | | |
| | Incremental Cum. Oil Produced, $10^6$ sm$^3$ | 1.043 | | | | |
| | Incremental Cum. Oil Produced, $10^6$ barrel | 6.561 | | | | |
| | Oil prices (3scenarios), USD/barrel | 70 (Low); | 100 (Base); | 150 (High) | | |
| | **Amount, Million USD** | **459.2** | **656.05** | **984.1** | | |
| **Cost-Benefit ratio** | | **1:2.3** | **1:3.3** | **4.9** | | |

## Table 7.4: 30years $CO_2$ injection economic benefit evaluation: 30000m$^3$/day (Base Case injection rate scenario)

| | Equipment Investment (Capex) | | | | Operating Cost (Opex) | |
|---|---|---|---|---|---|---|
| | **Description** | **Amount, $10^6$ USD** | | | **Description** | **Amount, $10^6$ USD** |
| **Cost Estimation** | $CO_2$ Compressor Unit(s) | 0.261 | | | Cost of $CO_2$ injection @ 30000m$^3$/day | 231.913 |
| | 4 High Pressure well head (Conversion) | 0.130 | | | $CO_2$ compressor maintenance | 0.782 |
| | Gas injection pipeline and installation | 0.098 | | | Injection well $O_2$ corrosion prevention (precaution measures) | 1.95 |
| | Produced gas testing equipment gas testing equipment | 0.032 | | | Production well $CO_2$ corrosion prevention | 4.56 |
| | Engineering design, planning and outsourcing research | 0.977 | | | Produced Gas separation and handling costs, and other Unexpected expenses | 5.1 |
| | **Subtotal** | **1.335** | | | **Subtotal** | **244.305** |
| | **Total Cost, Million USD 245.64** | | | | | |
| **Oil Revenue** | Cum. Oil Produced, $10^6$ sm$^3$ | 1.293 | | | | |
| | Incremental Cum. Oil Produced, $10^6$ sm$^3$ | 1.068 | | | | |
| | Incremental Cum. Oil Produced, $10^6$ barrel | 6.718 | | | | |
| | Oil prices (3scenarios), USD/barrel | 70 (Low); | 100 (Base); | 150 (High) | | |
| | **Amount, Million USD** | **470.2** | **671.8** | **1007.7** | | |
| **Cost-Benefit ratio** | | **`1:1.9** | **1:2.7** | **1:4.1** | | |

**Table 7.5: Summary of the economic evaluation of the 3 gas injection techniques studied**

| Gas | Cum. gas injected, $10^9$ $m^3$ | Incr. Cum. oil produced, $10^6$ $m^3$ | Incr. Cum. oil produced, $10^6$ bbl | Revenue (@$100/ bbl), Million $ | Basic capital expenditure (CAPEX), Million $ | OPEX (including corrosion control cost), Million $ | Total Cost, Million $ | Cost of unit oil produced, $/sm$^3$ oil | Cum. NCF, $ [2014] | Cum. NCF, $ [mod]. @ 3% inflation rate | DCF [0.10], Million $[2014] | DPI |
|---|---|---|---|---|---|---|---|---|---|---|---|---|
| Air | 1.32 | 1.027 | 6.46 | 646.0 | 1.335 | 117.778 | 119.113 | 115.98 | 526.9 | 1201.3 | 30.033 | 22.496 |
| $CO_2$ | 1.32 | 1.068 | 6.718 | 671.8 | 1.335 | 244.305 | 245.64 | 230.00 | 426.2 | 971.6 | 24.291 | 18.196 |
| $N_2$ | 1.32 | 1.043 | 6.561 | 656.05 | 1.335 | 198.322 | 199.657 | 191.43 | 456.4 | 1040.6 | 26.014 | 19.486 |

#### 7.1.2.4 NPV Evaluation

Another economic yardstick used to identify projects that will be profitability and can help to screen proposed projects is called the Net Profit Value (NPV). NPV is the sum of all project cash flows, discounted back to a common point in time, in this case 2012. Oil companies mostly use 10% discount rate on nominal cash flows. Therefore, NPV [0.10] indicates a discount rate of 10% in which the value of an investment in relation to an investment with a return of 10% per annum. If 10% represents the corporate target, a positive NPV [0.10] indicates a worthwhile investment from a financial point of view, i.e. if NPV is positive, the project is viable. NPV, which is also known as cumulative discounted net cash flow (DNCF) can be calculated by multiplying cumulative net cash flow (NCF) by the discount factor (DF) i.e. $NCF*(1+i)^{-n}$, where i is the discount rate and n is the number of years of injection. Cumulative discounted net cash flow curves are demonstrated for the case scenarios to achieve a comprehensive understanding of the project financially. Even though, the model is subject to sensitivity analysis, still associated with high degree of uncertainty, for example, reservoir evaluation (volume), capital and operation costs, current and future prices of gas and interest rate, etc. Table 7.5 shows the NPV computation using a real discount of NPV with real discount of 10% and 3% inflation rate at $100/barrel oil price, resulted in all 3 injection techniques having a positive NPV in the decreasing order of $30, 26 and 24 x$10^6$ for air, $N_2$ and $CO_2$ respectively, expressed in real value terms [$2014]. This also shows that the air injection is the most favorable project followed by the $N_2$ and the least is $CO_2$ based on the profit that is generated at the end of the project life.

Discounted profitability index is another DPI used by oil companies in order to assess the profitability of the projects. It is calculated by dividing NPV by the present value of CAPEX. Table 7.5 showed a

DPI of 22.5, 19.5 and 18.2 for air, $N_2$ and $CO_2$ injection respectively. This also confirms the order of profitability in embarking on the gas injection project for the oil block being studied.

### 7.1.3 Discussion on Economic Evaluation Results

In this study, $CO_2$ injection is the lease favorite because, even though $CO_2$ had the highest cumulative oil produced and generated more money but very large amount of money is spent during $CO_2$ injection unlike in air injection. $CO_2$ is expensive to generate or purchase, the source is usually far from the oilfield and would need an expensive transportation system, corrosion prevention both in the injectors and producer wells have to be accounted for, when gas breakthrough at the producers $CO_2$ is mixed with the produced natural gas and it has to be separated (additional cost for separation) and re-injected into the reservoir or sequestrated or disposed depending on the plan of the oilfield. All these factors contribute to the high costs of $CO_2$ injection and thus greatly affect the profit made after the operations. Nitrogen also showed lesser profit margin than air due to the high cost in the generation and purchase of $N_2$. Nitrogen injection economics are very sensitive to injection and separation costs which made its profit value lesser than air injection. Air injection showed a cheap cost on its injection operations and thus have the highest profit margin.

Globally, $CO_2$ injection has been known to be an attractive venture producing billions of barrels of oil all over the world especially for large oil reserves, miscible displacement drive, and high injection rate operations. But in our study, in relation to the low permeability light oil Q131 reservoir block, it is the less attractive of the three gas injection techniques in terms of its high cost and less return (profit) on investment. $CO_2$ injection may not be attractive for an oil reservoir with little associated $CO_2$ on-going project. However, for specific $CO_2$ associated oil reservoirs, $CO_2$ separation and reinjection project for IOR is expected to be more feasible and attractive, because the processing and separation facilities are already in place thus no extra capital cost is incurred, while good IOR targets can be achieved as shown by the simulation. The main challenges for a successful $CO_2$ injection in this economics analysis are the availability of $CO_2$, corrosion in the well and surface facilities, environmental constraints, and the high cost of $CO_2$ for use in remote fields. In general, four economic elements (i.e., $CO_2$ capture and compression cost, $CO_2$ transportation cost, $CO_2$ storage cost and revenue from incremental oil production) is very important in every economic evaluation of the $CO_2$ injection. Refer to Appendix D for more additional notes on economics and proposed advantages of $CO_2$ injection for IOR.

In summary, the economic assessment also reveals that for Q131 oil block, the 3 different gas injection IOR techniques yield a positive Net Present Value (NPV) at current West Texas Intermediate (WTI) oil prices at $100/day with air injection being the most profitable and $CO_2$ the least. The economic assessment is highly sensitive to oil prices, reservoir performance, choice of injection rate and project facilities. Also, multiple barriers could jeopardize commercial viability of these projects. These include weak incentives and uncertainties around gas storage liabilities, oil price, oil recovery levels, infrastructure requirements and costs, gas supply, gas storage capacity, and future regulation. The produced gases can be separated, compressed and re-injected into the reservoir after compression to save cost.

## 7.2 Safety, Corrosion Control and Risk Assessment

The major safety associated with the gas injection techniques are mainly related to air injection's oxygen breakthrough, corrosion problems of air and $CO_2$ injection, the management and separation of injected and gas that breakthrough at the production wells, oil field production facilities and other problems in the oil field that could endanger lives and sabotage the millions invested in the acquisition, planning and operations in the oilfield. So safety and risk assessment is an important aspect in planning and screening of the gas injection techniques selected for the IOR application in the Q131 oil block.

### 7.2.1 Safety and Process Facilities of Air injection

Air injection has been used successfully in onshore field operations but with more difficulties coming from the offshore operations since the application of gas injection techniques for an offshore installation is innovatory. The risk of explosion that could be caused by HC gases mixed with unconsumed oxygen in the production system is the main concern for air injection projects. The safety issues always considered include the risks of explosion in air compressor system and lines, explosion in the injector wellbore owing to hydrocarbon backflow, explosion in the producer well owing to oxygen breakthrough, and also the oxygen corrosion in both wells. Also another major safety consideration for the injection well is to prevent oil and gas flow back into the injector wellbore to mix with air in the case of compressor system failures. There are many effective safety precautions reported in on-going air injection projects (Gutierrez, D et al 2008b), such as injection of high temperature synthetic lubricants into injection lines to prevent corrosion and auto ignition; isolation of the annulus with a permanent packer and corrosion inhibitors. The experiences gained from ongoing air injection projects and reports provide requisite guidelines for the application of air injection for IOR (Germain et al., 1997; Watts et al., 1997,; Gilham et al., 1997).

**Air Compressor System.**

A high-temperature synthetic lubricant are usually used to prevent explosion in the air compressor and injection lines. For high-pressure air compression, inter-stage cooling of the compressed air and scrubbers are required to keep the discharge temperature below 150°C, remove water and excess lubricants, and to reduce the risks of explosion and corrosion. An air dryer can be installed after the final stage of compression to eliminate moisture accumulation in the lines, but this has an adverse economic effect (Gutiérrez et al., 2008).

**Production Wells.**

The primary problems with production wells have been gas interference, carbon dioxide corrosion, emulsions, and casing collapse. The gas interference is caused by the increasing production of combustion gases. The primary corrosion problem with production wells is the corrosion caused by carbon dioxide and un-consumed oxygen and can cause several tubing failures, though it may take place in a later stage of the project after gas breakthrough. Using coated tubing or stainless steel tubing can solve a part of the problem, and corrosion inhibitors should be used for scheduled annular treatments to control the corrosion of casing and external tubing surface. The emulsion problem usually occur during the gas interference and flowing stages due to inadequate gas separation. The emulsion problem can be minimized by separating the majority of the gas at the wellhead, increasing emulsion chemical rates at the wellhead, and increasing the gas separator sizes at the centralized production facilities.

To prevent wellbore explosion by backflow, wellhead controls and dual compressors are advisable to be installed. An additional water purge system, or a nitrogen blanket, can be designed and employed in these air injection field projects. Maintenance of a positive air pressure in the injector well is an essential requirement for safe operation to prevent hydrocarbon backflow. Monitoring and warning systems are needed to be installed to measure the injection pressure. Oxygen breakthrough into the producer is unlikely in a properly selected, well-designed, and managed project. Cautionary procedures should, however, be taken to detect the oxygen level in the produced gas. Current field project experience adopts a policy that the producer should be shut in when the oxygen mole fraction reaches 5%. Oxygen and/or $CO_2$ contents can set to be monitored by on-line gas analyzers to ensure safety and corrosion precautions can be effectively taken. They are also important parameters to be used for injection and production control. Increasing oxygen content in the producers always indicates some problems with the process, which may arise from an improper air injection rate, less effective LTO reaction in the oil zone, fault, fracture or high-permeable layers near an offset injection well. If

there is a presence of a fault, or fracture near an offset injection well, oxygen content increase can occur in production well. The geo-mechanics of the reservoir should be well studied to avoid this scenario.

**Injection Wells.**

Air is injected into the oil layers through production tubes. The main safety consideration for the injection well is to prevent oil and gas flow back into the injector wellbore to mix with air in the case of compressor system failures. The annulus between injector tube and casing should be sealed using a gas-tight packer to prevent formation fluids leak into the annulus. This is also important to protect the upper casing from corrosion. One or two one-way valves can be installed downhole to prevent the back flow. This is also important to protect the upper casing from corrosion. One or two one-way valves can be installed downhole to prevent the back flow. The tubing corrosion can be eliminated by replacing the steel tubing with plastic coated or stainless steel tubing. For low permeability reservoirs, there could be problems of near well formation being plugged by compressor lubricant and/or iron oxide in the injector. Low air injectivity may be observed from the damaged injection well, and generally this can be fixed by allowing a controlled backflow to the atmosphere for 15 to 30 minutes to release the plugging. In some cases, the wells need to be acidized or re-perforated to eliminate the damage problem. In some cases, the wells can be acidized to eliminate the damage.

The main facilities involved in an air injection project are air compression and produced oil/gas separation facilities. Larger gas separators and heater treaters should be installed to handle the increased production when the produced gas and fluid volumes start increasing due to the HPAI enhanced recovery process.

Economics and environmental regulations are always considered in the treatment of produced gases. Flaring of produced gas has been a common resort previously, but this is restricted in China and most parts of the world because of environmental regulations. If the LTO process is not operated beyond gas breakthrough, then obviously there will not be a gas handling problem. However, when there is layer channeling, gas treatment will be necessary. If the energy content of a produced gas is low, the resultant $CO_2$ emissions will present less of a problem. However, if the hydrocarbon gas content is high and important for field economics, then more sophisticated gas separation facilities will be required.

### 7.2.2 Air and CO2 Flooding Corrosion Problems and Control Measures

Corrosion is found to be a serious problem during the air and $CO_2$ injection, which mainly includes corrosion caused by oxygen in air injection wells at the early stage of the project while gas has not

broken through to the producers. Corrosion in $CO_2$ injection is caused by the mixing of injected or produced $CO_2$ with water at the injection and production wells. For nitrogen pipeline or facility, no special treatment is needed to prevent corrosion effect as nitrogen is chemically inert. Selective methods to reduce corrosion problems in air and $CO_2$ flooding are:

•Use of corrosion inhibitors

•Separate $CO_2$ injection lines

•Stainless steel wellheads

•Fiber glass gathering systems

#### 7.2.2.1 $CO_2$ Flooding Corrosion Control Measures

**Injection Wells**

$CO_2$ and water will occasionally mix and present a potential corrosion problem. Since $CO_2$ is not corrosive in the absence of water, a common principle is to keep the fluids separate nearly right up to the injection well, so very little lined steel or stainless steel pipe is needed on the surface. Only short sections downstream of the merging of the $CO_2$ and water lines, where the choke and meter are located, need to be protected.

Another common practice is to insert blind flanges to block backflow of fluid into the line for a different fluid should a check valve failure occur. If this section is designed and operated properly, and with sufficient flow velocity the time in which both $CO_2$ and water are both present is short since, one will transport the other into the well and to the formation. Building this short section out of stainless steel does not present significant cost, and this has become common practice. Wellheads are typically constructed out of 410 stainless steel. There are several elastomers that are available for use in $CO_2$ service (Newton et al., 1977).

Corrosion abatement in the injection packer and tubing is a problem with multiple solutions; the best of which will depend on injection scheme. In some floods, bare carbon steel injection tubing can be successfully used where continuous $CO_2$ injection was employed. Plastic-coated, fiberglass-lined, and cement-lined tubing were used but all had inconsistent performance. Plastic coating also had problems with holidays at the connection caused by handling, and often got damaged by wireline runs. Cement lined tubing worked in some cases but the cement failed if the tubing was subject to tension (i.e. pulling stuck tubing).

Most operators have now switched to fiberglass-lined tubing. The main problem with fiberglass used to be at the connection. Fiberglass lining is much more durable than the plastic or cement. Acid can

be pumped through it an unlimited number of times, wireline or coiled tubing will not damage it, and it provides 100% protection for the metal. The only drawbacks to the fiberglass are slightly higher cost and more restriction of the tubing inside diameter than the alternatives.

Packers are protected by nickel-plating internally and either nickel plating or plastic coating externally. If on-off tools are run they are nickel plated as well. The casing below the packer is an unprotected area. This is the case with nearly all $CO_2$ injection wells, but the corrosion may not be much worse than for water injectors. If existing wells are to be used as $CO_2$ injectors, it is best to manage this problem by flooding the deepest zone first in multi-pay fields and therefore avoiding having to recomplete below a corroded section. If the corroded casing below the packer turns out to be severe and results in out-of-zone injection losses, it may be necessary to run a liner made of a corrosion-resistant alloy (CRA) such as Incoloy 826, or possibly fiberglass-lined steel casing. If a new well is drilled the lower section of the casing across the pay zone may also include CRA casing. Open-hole completions, where applicable, could limit the amount of CRA casing needed to 2-3 joints across the interval where the packer seat would be.

**Production Wells**

In producing wells, there are numerous approaches to corrosion inhibition. In the Permian Basin most wells have packerless completions and are pumped either with sucker rod pumps or electric submersible pumps ($CO_2$ flooding Report on some field in Permian basin, 2012). The wells are pumped down until the fluid level gets as close to the pump intake as practical. For the formations that have low permeability, reducing producing BHP as low as possible is necessary to maximize throughput. Corrosion inhibitors are pumped down the annulus, flushed (usually with produced water), and pumped back up the tubing, coating metal surfaces along the way. If the proper inhibitor is used this method is highly effective at controlling corrosion. Most corrosion that does occur is the result of erosion of the inhibitor film. In sucker-rod pumps erosion is caused by contact between the rods and tubing during the pump stroke. Abrasive solids passing through the pump, especially in submersible pumps, can also cause erosion (Newton et al., 1984).

Once fluids reach the surface, the fluids are typically produced into fiberglass flow lines to a stainless steel header, and then to separators that are glass-flake or epoxy-lined. The gas from the separator then should be immediately dehydrated. Before any $CO_2$ operations in the field are initiated, some testing needs to be done at expected operating temperatures and pressures to see what an acceptable water content is.

In summary, corrosion is an issue that must be taken into account when designing any $CO_2$ flood. With proper design specifications and project engineering, monitoring of corrosion to check results, and proper follow-up, there is no reason for it to cause a catastrophe or a $CO_2$ flood failure.

### 7.2.3 $N_2$ Injection Field Implementation Practice

Nitrogen injection is selected so as maintain reservoir pressure and displace liquid phase hydrocarbon immiscibly under the basis of availability, cost, handling infrastructure, environmental, does not have any noxious effect on the reservoir, and safety issues. Nitrogen is an inert fluid, so it is not expected any environmental damage, it is not flammable and it is not corrosive. Nitrogen can be extracted from air in unlimited volumes, is an inert gas, costs less than the other gases considered, and there is commercial value for the oxygen which will be produced as a by-product. The nitrogen will be separated from air using membrane and cryogenic plants in tandem at a 99.98 mole percent purity.

Nitrogen would be injected at the top of the reservoir in the gas cap and pressure would be maintained within the oil column. Nitrogen will be injected into the gas cap through 3 wells, drilled and completed at the top of Q131. The response of the fields will be followed up through a program designed and implemented to monitor pressure, nitrogen concentration and the gas-oil contact movement. A carefully designed program should be planned and implemented to monitor the pressure response, oil recovery and produced GOR of the fields to nitrogen injection, the distribution of nitrogen in the gas cap of Q131, gas-oil contact movement, and composition of the produced gas during nitrogen injection. From reservoir management and well workover experience, the following practices have been proposed to help achieve high production rate while keep the nitrogen cut in check.

a. Maintain the injection and withdrawal ratio (IWR) close to 1.0 at early stage of nitrogen injection to pressure the reservoir for high liquid production rate. With a maintained reservoir pressure, the in-fill drilling activities would have less operation risk.

b. Horizontal wells and workovers were helpful in managing production decline. Simulation works and production history have demonstrated that horizontal well sidetrack or workover had a positive effect on nitrogen cut at the producers and delaying production decline (Xingru et al., 2013). At low hydrocarbon pore volume (HCPV), a few key producers can be re-perforated, and these workovers can flatten the nitrogen cut in the gas stream. At a higher HCPV, horizontal wells can be drilled and completed in the oil column and by this, oil production rate can increase tangibly and achieve late gas breakthrough. In summary, horizontal wells and well workover program have produced prolific wells with sustained high production rates, and reportedly increased field reserve extended field life (Clancy

et al, 1983). The produced gases can be separated, compressed and re-injected into the reservoir after compression to save cost.

### 7.2.4 Management of $N_2$ Injection Problems and Risk Factors

$N_2$ injection does not offer severe safety issues, but still at this point, I will like to highlight some development management strategies and risk evaluation for $N_2$ injection for IOR. Nitrogen injection into an oil field exhibits many unique features of reservoir development, and field development is an integrated process involving subsurface engineering, production engineering, and process/facility engineering. Pilot testing cab be designed to solve some issues, along with other key reservoir management issues identified at the outset of the project that could potentially impact its success, include: nitrogen channeling (usually countered by injecting at the top, far away from the gas-oil contact); asphaltene aggregation; number of required injection wells; gas breakthrough time and evolution of its concentration with time (nitrogen effluents depend on the position of the production platforms relative to the gas-oil contact and injection point); monitoring nitrogen injection; and impact of nitrogen injection on neighboring fields assuming there is hydraulic communication and production interference of Q131 in Liaohe oilfield through a regional aquifer or aquifers.

Reservoir uncertainties directly affect field depletion plan, resource deliverability, production forecast, and facility design. Identification of these uncertainties is an important step in analyzing reservoir performance forecast and risk management. When nitrogen is considered for reservoir pressure maintenance and IOR, the following key uncertainties need to be taken into account.

**A. Reservoir energy from aquifer influx:** Water encroaching a producing well bore due to pressure drop would lead to liquid loading problem or even premature well abandonment. This has been observed few fields in Rocky Mountains fields (Xingru, et al. 2013). Also water advancement traps hydrocarbon behind and lowers the hydrocarbon recovery.

**B. Reservoir heterogeneity and fracturing:** The mobility contrast between oil and nitrogen is very large. Premature nitrogen breakthrough through high permeable layers or fractures would lower the sweep efficiency and results in low reservoir factor. This is not particularly obvious in the case of Q131 $N_2$ injection IOR study, because a reasonable injection rate was used, therefore higher recoveries were obtained in the simulation results. Reservoir heterogeneity is exhibited from core and well logging information, and fractures are also prevalent in some reservoirs.

**C. Near-well bore condensate blockage:** From radial flow theory, the pressure changes dramatically nearby the wellbore. When the reservoir pressure is below the dew point, liquid would drop out. Liquid drop out near the well bore would result in production rate loss because of low gas relative

permeability. Coning effects from bottom water and crest gas cap should also be considered. When oil zone is extracted, if extract rate is too high, the bottom water and/or crest gas would come into the perforation because water and gas usually have high mobility than the oil phase. The coning effect can be mitigated by choosing a right depletion rate. When the flow rate is high, the rate dependent skin could also contribute to low productivity of a gas well.

**D. Some reservoir uncertainties** associated with geological settings such as fracture properties, low manageability. However, some uncertainties can be mitigated by taking proactive approaches though a rigorous surveillance plan. In the early stage of the reservoir development, a large amount of reservoir surveillance data such as well logging, coring, and pressure transient testing are usually used to identify specific uncertainties and challenges for the field development. For example, if the natural energy of a reservoir has a large uncertainty and oil column is high, water injection can be used as contingency in the design stage. If the gas have a high dew point, early injection can be used to mitigate the problem. In the production stage, because of the reservoir heterogeneity, the injected nitrogen may not distribute evenly across the field even through injected into the crest of the field. Nitrogen breakthrough timing could be used as a chemical tracer signal which indicates the conductivity between the injector and producers. With further data collection and interpretation, the tracer signal can potential yield the reservoir volume between the injector and producer pair with a quantitative analysis of the nitrogen production returns.

# CONCLUSIONS

The Q131 block meets all the criteria required for gas injection IOR and is expected to achieve better oil recovery via the gravity stabilized gas injection mechanisms.

1) The reservoir characteristics, dipping and thick oil layers of the block, will facilitate gravity segregation which is important for IOR in low permeability reservoirs.
2) The actual oil recovered will depend on the amount of injected gas, reservoir structure and properties, and the oil field management. Oil recovery increases with the increase in injection rate, if the gas breakthrough can be minimized.
3) The laboratory and numerical simulation results confirmed the feasibility of the 3 gas injection techniques for IOR application in the low permeable Q131 oil reservoir, under a safe operating environment.
4) For a 30 years period of injection using a base case 30000m3/day of gas injection rate, an incremental oil recovery factors of about 35%, 36.5%, 35.5% of OOIP were achieved in air, $CO_2$ and $N_2$ injection simulations respectively. $CO_2$ injection produces the best performance in terms of oil production because of its miscibility effect, followed by $N_2$ and then air injection.
5) A sensitivity study to shut-in wells with high GOR showed a decrease in the cumulative injected gas produced, the required injection time, and a better reservoir performance of incremental oil recovery factors. This is very favorable to the project economics because the operating cost and time are reduced.
6) Preliminary economic assessment showed that the 3 injection techniques are all profitable (positive NPV), but Air injection is the most attractive due to its availability and low Opex, followed by the $N_2$ injection and finally the $CO_2$ injection is the least economic attractive option due to its high costs of purchase and operations.

# RECOMMENDATIONS

1) Especially for low permeability sandstone reservoir with high heterogeneity and gas displacement mobility ratio, gas channeling plugging and fracturing cracks must be controlled and sealed, to avoid oxygen breakthrough (air injection) in the production wells. The well gas-oil ratio control or shut-in high gas-oil ratio setup are newly developing sealing technology of gas channeling layers to minimize the amount of gas produced and increase gas breakthrough time. Some key supporting technology in use to control high GOR level in gas injection can further be researched and applied in this case of gas injection for IOR in Q131 to optimize recovery.
2) Some significant uncertainties are identified during the course of the simulation studies e.g. pressure stabilization and maintenance, high GOR, large volumes of produced gas, etc., so it recommended that pilot projects can be designed and implemented to address these uncertainties before large scale field application.
3) Once a gas injection project has been selected and implemented, ongoing surveillance programs and optimization studies are to be performed to ensure that maximum value is obtained from the resource such as the use of reservoir flow modeling to understand performance expectations and to develop reservoir management strategies to optimize oil recovery.
4) An integrated flood management system need to created and used to a) Recognize areas of higher remaining oil saturation; b) Identify areas where reservoir intervals (or layers) have been swept by the injected gas; c) Prioritize a list of wells with these mature intervals that need to be closed off to redirect the injected gas to the layers that have not been effectively flooded; etc.
5) Proper field management of the produced gases ($CO_2$ and $N_2$) in all injection cases should be set in place to collect, separate and dispose of the produced gases or may be re-injected back into the reservoir through the gas injection wells located high on structure to reduce costs incurred during gas handling and disposal. $CO_2$ sequestration can be practiced to reduce the effects of greenhouse disadvantage of disposing $CO_2$ to the atmosphere.

# REFERENCES

Adetunji L.A., Teigland R., Kleppe J. (2005) Light-Oil Air-Injection Performance: Sensitivity to Critical Parameters. SPE 96844 presented at the 2005 SPE Annual Technical Conference and Exhibition held in Dallas, Texas, U.S.A., 9 – 12 October 2005.

Algharaib, M., Economic Modeling of $CO_2$ Capturing and Storage Project, paper SPE 120815, presented at SPE Saudi Arabia Section Technical Symposium, Al-Khobar, Saudi Arabia, 12 May 2008.

Allen, M.B., Macdonald, D.I.M., Zhao Xun, Vincent, S.J., and Brouet-Menzies, C., 1997, Early Cenozoic two-phase exten¬sion and late Cenozoic thermal subsidence and inversion of the Bohai Basin, northern China: Marine and Petroleum Geology, v. 14, nos. 7−8, p. 951−972.

Akkutla, I. Y., Yortsos, Y. C. The Effect of Heterogeneity on In-Situ Combustion: The Propagation of Combustion Fronts in Layered Porous Media. SPE 75128 presented at the SPE/DOE Improved Oil Recovery Symposium, Tulsa, Oklahoma, 13-17 April (2002).

Arshad, A., Al-Majed, A.A., Maneouar, H., Muhammadain, A. and Mtawaa, B. 2009. Carbon Dioxide Miscible Flooding in Tight Oil Reservoirs: A Case Study. Paper SPE 127616 presented at the 2009 Kuwait International Petroleum Conference and Exhibition held in Kuwait City, Kuwait, 14-16 December.

Bardon, C., Longeron, D.G., Baudoin, F., Delhomme, A. and Naili, N. 1994. Gas/Oil Permeability and Residual Oil Saturations in a Field Case of a Very Light Oil, in the Near-Miscibility Conditions. Paper SPE 28625 presented at the 1994 SPE Annual Technical Conference and Exhibition, New Orleans, USA, 25-28 September.

Bauer, M. Near-Term Opportunities and Emerging Economies: A view from Mexico. Presentation at the G8/IEA/CSFL Workshop on Near Term Opportunities for Carbon Capture and Storage, San Francisco, California, August 22-23, 2006.

Bin, G.; Qing, Y. Y.; Hui, J. W.; Xin, Z.; Yao, L. Effects of Low Temperature oxidation on the Chemical Composition of a Light Crude Oil. Energy Fuels; 2010, 24, 1139−1145.

Campbell, B.T. and Orr, F.M. Jr., Flow Visualization for $CO_2$/Crude-Oil Displacements. 1985. 25(5): p. 665-678.

Castanier, L. M., Baena, C. J., Holt, R. J., Brigham, W. E., and Tavares, C., "In-situ Combustion with Metallic A ; Paper 23708 Presented at the SPE Latin American Petroleum Engineering Conference, Venezuela, 8-11 March (1992).

Celius, H.K., Ingeberg, K., The Impact of $CO_2$ Taxation on Oil and Gas Production in Norway; SPE Paper 35961, presented at the International Conference on Health, Safety & Environment held in New Orleans, 9-12 June 1996.

Chang Cheng-yong, 1991, Geological characteristics and distribution patterns of hydrocarbon deposits in the Bohai Bay Basin, east China: Marine and Petroleum Geology, v. 8, no. 1, p. 98−106.

Chen, B.L. et al. 2013: Improvement of the $CO_2$ minimum miscible pressure calculation model of crude oil. Journal of Oil and Gas Technology (J.JPI) Vol. 35 No. 2, Feb. 2013.

Chen, Z.; Wang, L.; Duan, Q.; Zhang, L.; Ren S.R. High-Pressure Air Injection for Improved Oil Recovery: Low Temperature Oxidation Models and Thermal Effect. Energy Fuels; 2013, 27, 780-786.

Chengyao Song and Daoyong Yang: Optimization of $CO_2$ flooding schemes for unlocking resources from tight oil formations. SPE 162549 presented at the SPE Canadian Unconventional Resources Conference held in Calgary, Alberta. Canada 30 Oct-1 Nov 2012.

Christopher, C.A, "Air Injection for Light and Medium Gravity Reservoirs", Presented at DTI Share Meeting (1), London, 20 July 1995.

Clancy, J.P., and Gilchrist, R.E. 1983. Nitrogen Injection Applications Emerge in the Rockies. Paper SPE-11848-MS presented at SPE Rocky Mountain Regional Meeting, Salt Lake City, Utah, 22-25 May.

Clancy, J.P., Gilchrist, R.E., Cheng, L.H.K., & Bywater, D.R. "Analysis of Nitrogen-Injection Projects to Develop Screening Guides and Offshore Design Criteria." SPE 11902, 1985: Journal of Petroleum Technology, Volume 37 Number 6, June 1985, Pages 1097-1104.

Clara, C. et al. Appraisal of the HORSE CREEK Air Injection Project Performa29-30nce. Proceedings of the SPE 8th Abu Dhabi International Petroleum Exhibition & Conference; Abu Dhabi, UAE, Oct. 11-14, 1998; SPE 49519

Cobb, LaVerne B. and Raymond Marlow. Reservoirs for $CO_2$ Miscible Flooding. U.S. Department of Energy (DOE/MC/08341-35, January, 1982.

Compiling Group of Petroleum Geology of Liaohe Oilfield (1993) Petroleum Geology of China (Vol. 3) [M]. pp. 138 -174. Petroleum Industry Press, Beijing (in Chinese).

Dake, LP 2004. The Practice of Reservoir Engineering, developments of petroleum science 36. Oxford, England: Elsevier.

Davies, R.J., "The Thin Flame Technique for In-Situ Combustion Simulation", SPE paper no. 19647 presented at the SPE 64th Annual Technical Conference and Exhibition, San Antonio, Texas, October 8-11(1989).

De Zwart, A. H., Batenburg, D. W.,Van Blom, C. P. A., Tsolakidis, A., Glandt, C. A., and Boerrigter, P., "The Modeling Challenges of High Pressure Air Injection"; SPE 113917 Presented at the 2008 SPE/DOE Improved Oil Recovery Symposium held in Tulsa, Oklahoma, U.S.A., 19 23 April (2008).

Dicharry, M.R., Perryman T.L., Ronquille, J.D. (1973): Evalation and Design of a $CO_2$ Miscible Flood Project – SACROC Unit, Kelly-Snyder Field. SPE 4083.

Dong, M., Huang, S.S. and Srivastava, R. 2001. A Laboratory Study on Near-miscible $CO_2$ Injection in Steelman Reservoir. J Can Pet Technol 40 (2): 53-61.

Douglas, J.L., and Weiss, M.: "Wizard Lake: Reservoir Quality as a Key to Successful Miscible Displacement," Proceedings of the 13th World Petroleum Congress, Buenos Aires, Argentina; J. Can. Petrol. Technol. (March-April 1991) Vol 30, No. 2, 86.

Duiveman, M.W.; et al. Integrated Management of Water, Lean Gas and Air Injection: The Successful Ingredients to EOR Projects on the Mature Handil Field. Proceedings of the SPE APOGCE; Jakarta, Indonesia, April 5-7, 2005; SPE 93858.

Elsayed, S. A., Baker, R., Churcher, P. L., and Edmunds, A. S., "A Multidisciplinary reservoir Characterization and simulator Study of the Weyburn Unit, Saskatchewan, Canada," paper SPE 25852 presented at the SPE Rocky Mountain Regional/ Low permeability Reservoirs Symposium, Denver, Colorado, April 12-14, 1993.

Fassihi, M.R. and Gillham, T.H. The Use of Air Injection to Improve the Double Displacement Processes. SPE 26374, presented at the SPE Annual Technical Conference and Exhibition, 3-6 October 1993, Houston, Texas

Fassihi, M. R., Meyers, K. O., & Baslie, P. F. (1990). Low-Temperature Oxidation of Viscous Crude Oils. Society of Petroleum Engineers. doi:10.2118/15648-PA

Fassihi, M.R.; Yannimaras, D.V.; Kumar, V.K. Estimation of Recovery Factor in Light-Oil Air-Injection Projects. SPE Reservoir Engineering (SPERE); August, 1997, 173-178; SPE 28733.

Fassihi, M.R.; Yannimaras, D.V.; Westfall, E.E.; Gillham, T.H. Economics of Light Oil Air Injection Projects. Proceeding of the SPE/Department of Energy (DOE) Improved Oil Recovery Symposium; Tulsa, Oklahoma, 21-24 April, 1996; SPE-35393-MS

Fraim, M. L., Moffitt, P. D.,Yannimaras, D. V.. 'Laboratory Testing and Simulation Results for High-Pressure Air Injection in a Waterflooded North Sea Oil Reservoir"; SPE 38905 presented at the SPE Annual Technical Conference & Exhibition, San Antonio, U.S.A, 5-8 October,(1997).

Gas-IOR team in-house report on Q131 production history and history matching design program. China University of Petroleum (2012).

Germain, P. and Geyelin, J.L. "Air Injection Into a Light Oil Reservoirs: The Horse Creek Project", paper SPE 37782 presented at the 1997 Middle East Oil Show in Bahrain, 15-18 March 1997

Ghomian, Y., Pope, G. A., and Sepehrnoori, K., "Economical Co-optimization of $CO_2$ Sequestration and Enhanced Oil Recovery," Sixth Annual Conference on Carbon Capture & Sequestration Proceeding, Pittsburgh, PA, May 7-10, 2007.

Ghomian, Y., Sepehrnoori, K., and Pope, G. A., 2008. "Reservoir Simulation of $CO_2$ Sequestration Pilot in Frio Brine, Formation, USA Gulf Coast," Energy Journal, Elsevier publications.

Gillham, T.H., Cerveny, B.W., Fornea, M.A. and Bassiouni, D.Z. 1998a. Low Cost IOR: An Update on the W. Hackberry Air Injection Project. Paper SPE 39642 presented at the SPE/DOE Improved Oil Recovery Symposium, Tulsa, Oklahoma, 19-22 April.

Gillham, T.H.; et al. (1998b). Low Cost IOR: An Update on the W. Hackberry Air Injection Project. Proceeding of the SPE DOE Improved Oil Recovery Symposium; Tulsa, OK, April 19-22 1998; SPE 39642.

Gillham, T.H.; Cerveny, B.W.; Turek, E.A.; Yannimaras, D.V. Keys to Increasing Production via Air Injection in Gulf Coast Light Oil Reservoirs, Proceeding of the SPE Annual Technical Conference and Exhibition; San Antonio, Texas, October 5-8, 1997; SPE 38848.

Glasco, O. Generalized Minimum Miscibility Pressure Correlation. SPE Journal (Dec. 1985) 927-34.

Glasco, O. Miscible Displacement: Recovery Tests with Nitrogen. SPERE February 1990.

Glandt, C.A.; Pieterson, R.; Dombrowski, A; Balzarini, M.A. Coral Creek Field Study: A Comprehensive Assessment of the Potential of High-Pressure Air Injection in a Mature Waterflood Project. Proceeding of the SPE Mid-Continent Operations Symposium, Oklahoma City, Oklahoma; March 28-31, 1999; SPE 52198.

Greaves, M., Ren, S.R. and Rathbone, R.R., "Air Injection Technique (LTO Process) for IOR from Light Oil Reservoirs: Oxidation Rate and Displacement Studies", SPE Paper 40062, presented at the 1998 SPE/DOE IOR Symposium, Tulsa, Oklahoma, 19-22 April 1998.

Greaves M., Rathbone R., Ren S. R, Chawla-Duggan S.R. (1999a). Air Injection Technique (LTO Process) for IOR from Light Oil Reservoirs – Final Project Report, IOR Research Group, Dept. of Chemical Engineering, University of Bath UK.

Greaves, M, Ren, S.R and Xia, T.X. (1999b). New Air Injection Technology for IOR Operations in Light and Heavy Oil Reservoirs, SPE Paper 57295, presented at the 1999 SPE Asia Pacific Improved Oil Recovery Conference, Kuala Lumpur, Malaysia, 25–26 October.

Greaves, M.; Ren, S. R.; Rathbone, R. R.; Fishlock, T.; Ireland, R. (2000a). Improved residual light oil recovery by air injection (LTO process). J. Can. Pet. Technol. 2000, 39 (1), 57−61

Greaves, M.; Young, T. J.; El-Usta, S.; et al. (200b). Air injection into light and medium heavy oil reservoirs: Combustion tube studies on West of Shetlands Clair oil and Light Australian oil. Trans. Inst. Chem. Eng., Part A, Chem. Eng. Res Des, 2000, 78: 721-730.

Guo, X., Du, Z., Sun, L., Fu, Y., Huang, W. and Zhang, C. 2006. Optimization of Tertiary Water-Alternate-$CO_2$ Flood in Jilin Oil Field of China: Laboratory and Simulation Studies. Paper SPE 99616 presented at the 2006 SPE/DOE Symposium on Improved Oil Recovery held in Tulsa, Oklahoma, USA, 22-26 April.

Gutierrez, D., Miller, R.J., Taylor, A.R., Thies, B.P. et al. (2006a). Buffalo Field High-Pressure Air Injection Projects (1977 to 2007): Technical Performance and Operational Challenges, SPE 113254, presented at the SPE/DOE Symposium on Improved Oil Recovery, Tulsa, 20-23 April.

Gutierrez, D.; Taylor, A. R.; Kumar, V. et al. (2008b). Recovery Factors in High-Pressure Air Injection Projects Revisited. SPE Reservoir Evaluation & Engineering. 2008; SPE 108429.

Hadlow, R.E. 1992. Update of Industry Experience with $CO_2$ Injection. Paper SPE 24928 presented at the 1992 SPE Annual Technical Conference and Exhibition, Washington, D.C., USA, 4-7 October.

Herzog, H., Eliasson, B., and Karstad, O., "Capturing Greenhouse Gases," Scientific American, p.72–79, 2000.

Holm, L.W. Carbon Dioxide Solvent Flooding for Increased Oil Recovery," Trans., AIME (1959) 216, 225-231.

Hongmin Yu et al. "Air Foam Injection for IOR: from Laboratory to Field Implementation in Zhongyuan Oilfield China" SPE 113913 presented at the 2008 SPE/DOE Improved Oil Recovery Symposium held in Tulsa, Oklahoma, U.S.A., 19-23 April 2008.

Hossein, A.A., Esmaiel, T.E.H., van Kruijsdijk, C.P.J.W. 2005. Exploring Dispersion Effects and Crossflow Mechanism in the Nearly Miscible Gas Drives. Paper SPE 97557 presented at the SPE International Improved Oil Recovery Conference in Asia Pacific held in Kuala Lumpur, Malaysia, 5-6 December.

Hou, S.M.; Ren, S.R.; et al. Feasibility study of air injection for IOR in low permeability oil reservoirs of Xinjiang oilfield China. Proceedings of the Chinese Petroleum Society (CPS)/Society of Petroleum Engineers (SPE) International Oil and Gas Conference and Exhibition; China; Beijing, China, June 8-10, 2010; SPE 131087.

Hu, J. et al. Recent Progress of High-Pressure Air Injection (HPAI) Process in Light Oil Reservoir: Laboratory Investigation and Field Application. Proceeding of the SPE Heavy Oil Conference; Calgary, Alberta, Canada, June 12 14, 2012; SPE 156974.

Hudgins, D.A., Llave, F.M., and Chung, F.T.H. 1990. Nitrogen Miscible Displacement of Light Crude Oil: A Laboratory Study. SPE Res Eval. & Eng. 5 (1): 100–106.

Hughes, B.L. and Sarma, H.K. Burning Reserves for Greater Recovery? Air Injection Potential in Australian Light Oil Reservoirs. Paper SPE 101099, presented at the SPE Asia Pacific Oil & Gas Conference and Exhibition. Adelaide, Australia, 11-13 September 2006.

Ibukunoluwa, A.O. and Onyekonwu, M.O.: Prospects and Economics of Miscible-$CO_2$ Enhanced Oil Recovery in Some Nigerian Reservoirs, SPE paper 140673, presented at the 34th Annual SPE International Conference and Exhibition held in Tinapa, Calabar, Nigeria, 31 July - 7 August 2010.

Jeschke, P.A., Schoeling, L. and Morgan, K. 2000. $CO_2$ Flood Potential of California Oil Reservoirs and Possible $CO_2$ Source. Paper SPE 63305 presented at the 2000 SPE/AAPG Western Regional Meeting, Long Beach, CA, USA, 19-23 June.

Jessen, K., Kovscek, A. R., and Orr, F. M., "Increasing $CO_2$ Storage in Oil recovery," Energy Conversion Management, No.46, p. 293–311, 2005.

Ji Ya-juan, Zhou Le-ping, Ren Shao-ran, et al. Experimental Study of Gas Explosion in Oil Field Air Injection Process. China Safety Science Journal (in Chinese), Feb 2008: 87-92.

Jia, H., Zhao, J. Z., Pu, W. F., Liao, R., Wang, L. L., "The influence of Clay Mineral Types on the Oxidation Thermo kinetics of Crude Oil"; Energy Sources, Part A: Recovery, Utilization, and Environmental Effects, 34;877-886 (2012).

Jiang, Y. W., Zhang, Y. T., Liu, S. Q., Guan, W. L., Chen, Y. P., Liu, S. M., "Displacement Mechanisms of Air Injection in Low Permeability Rerservoirs"; Petroleum Exploration and Development; 37:471-476 (2010).

Johns, R.T., Sah, P. and Solano, R. 2002. Effect of Dispersion on Local Displacement Efficiency for Multi-component Enriched-Gas Floods above the Minimum Miscibility Enrichment. Paper SPE 64725 Presented at the 2000 SPE International Oil and Gas Conference and Exhibition in Beijing, China, 7–10 November.

Johnson, J.P., Pollin, JS. Measurement and correlation of $CO_2$ miscibility pressures. Presented in SPE/DOE enhanced oil recovery symposium. Tulsa, Oklahoma: Society of Petroleum Engineers; 1981.

Johnston, J.R., "Weeks Island Gravity Stable $CO_2$ Pilot," paper SPE/DOE 17351, presented at the SPE/DOE Symposium on Enhanced Oil Recovery, Tulsa, Oklahoma, April 17-20, 1988.

Klett, T.R., Schmoker, J.W., Charpentier, R.R., Ahlbrandt, T.S., and Ulmishek, G.F., 2000, Glossary, chap. GL of U.S. Geological Survey World Energy Assessment Team, U.S. Geological Survey World Petroleum Assessment 2000—Description and results: U.S. Geological Survey Digital Data Series DDS–60, 8 p. Entire report is available on 4 CD-ROMs and at http://pubs.usgs.gov/dds/dds-060.

Kuhlman, M. L., "Simulation of Light-oil Air Injection into Viscous-Dominated and Gravity-Stable Reservoirs" ; SPE 59331 Presented at the SPE/DOE Symposium on Improved Oil Recovery, Tulsa (OK), April (2000).

Kumar, V.K.; Fassihi, M.R; Yannimaras, D.V. Case History and Appraisal of the Medicine Pole Hills Unit Air-Injection Project. SPE Reservoir Engineering; August 1996, 198-202; SPE 27792

Kumar, V. K.; Gutierrez, D.; Moore R. G.; et al. Case History and Appraisal of the West Buffalo Red River Unit High-Pressure Air Injection Project, Proceeding of the 2007 Society of Petroleum Engineers (SPE) Hydrocarbon Economics and Evaluation Symposium; Dallas, Texas, U.S.A., April 1–3, 2007; SPE 107715.

Kumar, V.K.; Gutierrez, D.; Moore, R.G.; Mehta, S.A. Air Injection and Waterflood Performance Comparison of Two Adjacent Units in Buffalo Field: Technical Analysis., Proceeding of the SPE/DOE Symposium on Improved Oil Recovery; Tulsa, Oklahoma, U.S.A., April 22–26, 2006; SPE 99454.

Kumar, V. K.; Gutierrez, D.; Thies, B.P.; Cantrell, C. 30 Years of Successful High-Pressure Air Injection: Performance Evaluation of Buffalo Field, South Dakota. Proceeding of the Society of Petroleum Engineers (SPE) Annual Technical Conference and Exhibition; Florence, Italy, September 19–22, 2010; SPE 133494.

Kumar, V.K. Simulation of West Heidelberg In-Situ Combustion Project. SPE 62nd Annual Technical Conference and Exhibition; Dallas, Texas, September 27-30, 1987, 283-294; SPE 16724.

Lake, L. W.: Enhanced Oil Recovery, Prentice Hall Englewood Cliffs, NJ, 1989.

Langenberg, M.A., Henry, D.M., and Chlebana, M.R.:"Performance and Expansion Plans for the Double Displacement Process in the Hawkins Field Unit," SPE Reservoir Engineering, p.301, November 1995.

Lee J. Effectiveness of carbon dioxide displacement under miscible and immiscible conditions. Report RR-40. Calgary: Petroleum Recovery Inst.; 1979.

Lim, M. T., Khan, S. A., Sepehrnoori, K., and Pope, G. A., "Simulation of Carbon Dioxide Flooding Using Horizontal Wells," paper SPE 24929 presented at the SPE Annual Technical Conference and Exhibition, Washington D.C., October 4-7, 1992.

Lim, M. T., Pope, G. A., and Sepehrnoori, K., Mechanistic Study of Carbon Dioxide Flooding Using Horizontal Wells, paper SPE/DOE 27807 presented at the SPE/DOE Ninth Symposium on Improved Oil Recovery, Tulsa, Oklahoma, April, 17-20, 1994.

Luo, R., Cheng, L.S., Peng, J.C. 2005. Feasibility Study of $CO_2$ Injection for Heavy Oil Reservoir after Cyclic Steam Stimulation: Liaohe Oil Field Test. Paper SPE/PS-CIM/CHOA 97462 presented at the 2005 SPE International Thermal Operations and Heavy Oil Symposium held in Calgary, Alberta, Canada, 1-3 November.

Lv L.H. and Liu, B.G. 1998. A Feasibility Research Method and Project Design on $CO_2$ Miscible Flooding for a Small Complex Fault Block Field. Paper SPE 50930 presented at 1998 SPE International Conference and Exhibition in China held in Beijing, 2-6 November.

Malik, Q. M., and Islam, M. R., "$CO_2$ Injection in the Weyburn Field of Canada: Optimization of Enhanced Oil Recovery and Greenhouse Gas Storage With Horizontal Wells," paper SPE 59327 presented at the SPE/DOE eighth Symposium on Improved Oil Recovery, Tulsa, Oklahoma, April 3-5, 2000.

Manrique, E., Araya, A. Capture and Geologic Sequestration: What it is and its Implications. Coal Preparation Society of America (CPSA) Journal, V. 6, No. 4, February 2008.

Manrique, E., Thomas C., Ravikiran, R., Izadi, M., Lantz, M., Romero, J., and Alvarado, V., "EOR: Current Status and Opportunities" SPE 130113 presented at the SPE Improved Oil Recovery Symposium held in Tulsa, Oklahoma, USA, 24–28 April 2010.

Moore, R.G., Mehta, S.A., Ursenbach, M.G. et al. 1998. Strategies for Successful Air Injection-Based IOR Processes. Paper No. 1998.235 in Heavy Oil- A Major Energy Source for the 21st Century: Proceedings of the 7th UNITAR International Conference on Heavy Crude and Tar Sands, 27-30 October, 1998 Beijing, China, ed. R.F. Meyer and D.K. Olsen.

Moore, R. G., Mehta, S. A., Ursenbach, M. G. A Guide to High Pressure Air Injection (HPAI) Based Oil Recovery (SPE-75207). SPE/DOE Improved Oil Recovery Symposium, Tulsa, Oklahoma, April 13-17, 2002.

Moore, R.G., Mehta, S.A., Ursenbach, M.G. et al. 2012. Potential for In Situ Combustion in Depleted Conventional Oil Reservoirs: SPE Paper 154299, presented at the Eighteenth SPE Improved Oil Recovery Symposium held in Tulsa, Oklahoma, USA, 14–18 April 2012.

Mungan N. Carbon dioxide flooding – fundamentals. J. Can. Petrol. Technol. 1981; 20, 87 – 92.

Mungan, N. Enhanced Oil Recovery with High Pressure Nitrogen Injection (SPE-62547). SPE/AAPG Western Regional Meeting, Long Beach, California, June 19-22, 2000.

Muro, H. G., Campos, S. B., Alcazar, L. O., Rodríguez , J. A. Quebrache-A Natural CO2 Reservoir: A New Source for EOR Projects in Mexico (SPE-107445). Latin American & Caribbean Petroleum Engineering Conference, Buenos Aires, Argentina, April 15-18, 2007.

National Petroleum Council (NPC). Enhanced oil recovery – an analysis of the potential for enhanced oil recovery from known fields in the United States – 1976–2000, Washington, DC; 1976.

Newton L., "SACROC CO2 Project – Corrosion Problems and Solutions", Advances in $CO_2$ Corrosion, paper 67 presented at Corrosion/84 Conference, National Association of Corrosion Engineers", April 2-6, 1984, New Orleans, Louisiana.

Newton L. and R.A. McClay, "Corrosion and Operational Problems, Project, SACROC Unit", SPE Permian Basin Oil and Gas Recovery Conference, Midland, Texas, March 10-11, 1977, SPE-6391.

Niu, B.; Ren, S.; Liu, Y.; Wang, D.; Tang, L.; Chen, B. Low temperature oxidation of oil components in an Air Injection Process for Improved Oil Recovery. Energy Fuels; 2011, 25 (10), 4299−4304.

Nouar, A. and Flock, D.L.: "Parametric Analysis on the Determination of the Minimum Miscibility Pressure in Slim Tube Displacements," J. Cdn. Pet. Tech. (Oct. 1984) 23, No.5, 80-88.

Nute, A. J., "Design and Evaluation of a Gravity-Stable, Miscible $CO_2$-Solvent Flood, Bay St. Elaine Filed," SPE paper 11506 presented at the SPE Middle East Oil Technical Conference, Manama, Bahrain, March, 14-17, 1983.

Orr, F.M. Jr. et al.: "Laboratory Experiments to Evaluate Field Prospects for $CO_2$ Flooding," JPT (April 1982) 888-898.

Orr, F.M. Jr., Yu, A.D. and Lien, C.L. 1981. Phase Behavior of $CO_2$ and Crude Oil in Low-Temperature Reservoir. SPE J 480-492.

Parrish, D.R.; Pollock, C.B; Craig Jr., F.F. Evaluation of COFCAW as a Tertiary Recovery Method, Sloss Field, Nebraska. Journal of Petroleum Technology; June 1974, 676-686; SPE-3777.

Pascual, M.; et al. Air Injection into a Mature Water flooded Light Oil Reservoir: Laboratory and Simulation Results for Barrancas Field Argentina. Proceedings of the SPE Europec/EAGE Annual Conference, Madrid, Spain, June 13-16, 2005; SPE 94092.

Perry, G. A., "Weeks Island "S" Sand Reservoir B Gravity Stable Miscible $CO_2$ Displacement, Iberia Parish, Louisiana," SPE/DOE paper 10695 presented at the SPE/DOE Third Joint Symposium on Enhanced Oil Recovery, Tulsa, Oklahoma, April 4-7, 1982.

Prieditis, J., and Paulett, G. S., "$CO_2$ Foam Mobility Tests at Reservoir Conditions in San Andres Cores," paper SPE/DOE 24178 presented at the SPE/DOE Eighth Symposium on Enhanced Oil Recovery, Tulsa, Oklahoma, April, 22-24, 1992.

Ren Minyan, Wang Zhen, Xu Yang, Niu Baolun, et al. 2012. An Improved Relative Permeability Model and Its Application for $CO_2$ Injection EOR Process, Journal of the University of Petroleum, China.

Ren, S.R., Greaves, M., Rathbone, R.R., Air Injection LTO Process: A Feasible IOR Technique for Light Oil Reservoirs; SPE Journal, pp.90-99, March 2002.

Ren, S. R.; Niu, B. L.; Hou, S. M.; Zhang, L.; Gu, H.J. Screening of Gas Injection for IOR in a Low Permeability Reservoir of Xinjiang Oilfield. Journal of China University of Petroleum; April 2011, 35, 2.

Ryder, R.T; Qiang, J., McCabe, P., et al., 2012. Shahejie−Shahejie/Guantao/Wumishan and Carboniferous/Permian Coal−Paleozoic Total Petroleum Systems in the Bohaiwan Basin, China (based on geologic studies for the 2000 World Energy Assessment Project of the U.S. Geological Survey). U.S. Geological Survey, Reston, Virginia.

Sakthikumar, S., Madaoui, K., Chastanf, J., "Air Investigation of the Feasibility of Air-Injection into a Waterflooded Light Oil Rerservoir"; SPE 29806, Presented at the SPE Middle East Oil Show, Bahrain, March (1995).

Sanchez B., et al. (2005). Nitrogen Injection in the Cantarell Complex: Results after Four Years of Operation. SPE-97385 presented at the SPE Latin American and Caribbean Petroleum Engineering Conference, 20-23 June, Rio de Janeiro, Brazil

Schneider, G., Alwani, Z., Heim, W., Horvath E., and Franck, E. U.: "Phasengleichgewichte und kritische Erschemungen in binaren Mischsystemen bis 1,500 bar: CO, mit n-Octan, n-Undecan, n-Tridecan und n-Hexadeca@" (1967) 39, 649.

Shokir EME-M. CO2–oil minimum miscibility pressure model for impure and pure CO2 streams. J Petrol. Sci. Engr. 2007; 58: 173–85.

Shyeh-Yung and J-G, J. 1991. Mechanism of miscible oil recovery: Effects of pressure on miscible and near-miscible displacement of oil by carbon dioxide. Paper SPE 22651 presented at the SPE Annual Technical Conference and Exhibition, Dallas, Texas, USA, 6-9 October.

Sinanan, B., and Budri, M. 2012. Nitrogen Injection Application for Oil Recovery in Trinidad. Paper SPE-156924-MS presented at SPETT 2012 Energy Conference and Exhibition, Port-of-Spain, Trinidad, 11-13 June.

Sohrabi, M., Danesh, A. and Tehrani, D.H. 2005. Oil Recovery by Near-miscible SWAG Injection. Paper SPE 94073 presented at the SPE Europe/EAGE Annual Conference held in Madrid, Spain, 13-16 June.

Stalkup, F. I.: Miscible Flooding Fundamentals, Society of Petroleum Engineers Monograph Series, 1983.

STARS User Manual, 2003.10, Computer Modelling Group, Calgry, Canada.

Taber, J., and Orr, M. F. Jr., "Contracts for EOR and Improved Drilling Technology," U.S. DOE Progress Review No. 37, BERC, Bartlesville, December 1983.

Taber, J. J., Martin, F. D., Seright, R. S., EOR Screening Criteria Revisited- Part 1: "Introduction to Screening Criteria and Enhanced Recovery Field Projects; SPE 35387, (1997a).

Taber J.J., F.D. Martin and R.S. Seright, "EOR Screening Criteria Revisited – Part 2: Application and Impact on Oil Prices", SPERE, August 1997b, p199-205

Thomas, F.B., Holowach, N., Zhou, X.L., Bennion, D.B. and Bennion, D.W. 1994. Miscible or near-miscible gas injection, which is better? Paper SPE 27811 presented at the 1994 SPE/DOE Ninth Symposium on Improved Oil Recovery at Tulsa, Oklahoma, USA, 17-20 April.

Thomas, S., 2008. Enhanced oil recovery: An overview. Oil Gas Sci. Technol., 63: No. 1, 9-19.

Tian Zai-Yi, Han Ping, and Xu Ke-Ding, 1992, The Mesozoic-Cenozoic East China rift system: Tectonophysics, v. 208, no. 1−3, p. 341−363.

Tsau, J.S., Bui, L.H. and Willhite, G.P. 2010. Laboratory Investigation of $CO_2$ Near-miscible Application in Arbuckle Reservoir. Paper SPE 129710 presented at the 2010 SPE Improved Oil Recovery Symposium, Tulsa, USA, 24-28 April.

Turta, A. T., Singhal, A. K., Reservoir Engineering Aspects of Light-Oil Recovery by Air injection; SPE Reservoir Evaluation & Engineering. 4: 336-344, (2001).

Turta, A.T., Singhal, A.K., "Reservoir Engineering Aspects of Oil Recovery from Low Permeability Reservoirs by Air Injection", SPE paper no. 48841 presented at the SPE International Conference and Exhibition, Beijing, China, November 2-6 (1998).

Van Batenburg, D. W., Bosch, M., Boerrigter P. M., de Zwart, A. H., Vink, J. C., "Application of Dynamic Gridding Techniques to IOR/EOR-Process ; SPE 141711 Presented at the SPE Reservoir Simulation Symposium Held in The Woodlands, Texas, USA, 21-23 February (2011).

Vossoughi, S., Willhite, G.P., Shoubary, Y.EI. and Bartlett, G., Study of the Clay Effect on Crude Oil Combustion by Thermogravimetry and Differenial Scanning Calorimetry; J. Therm.Anal. 27:17 36, (1983).

Watts, B.T.; et al. The Horse Creek Air Injection Project: An Overview. Proceedings of the SPE Rocky Mountain Regional Meeting; Casper, Wyoming, May 18-21, 1997; SPE 38359.

Xingru W., Kegang L., Dexin L., (2013). Nitrogen Injection Experience to Development Gas and Gas Condensate Fields in Rocky Mountains. International Petroleum Technology Conference, 26-28 March, Beijing, China.

Xuan, Z. and He, S.L. 2010. Potential and Early Opportunity-Analysis on $CO_2$ Geo-Sequestration in China. Paper SPE 130358 presented at the SPE EUROPEC/EAGE Annual Conference and Exhibition Held in Barcelona, Spain, 14-17 June.

Yelling WF, Metcalfe RS. Determination and prediction of $CO_2$ minimum miscibility pressures (Includes associated paper 8876). SPE J Petrol Technol. 1980; 32:160–8.

Zhang, J.C., Xie S.X., Han, P.H., Chen, J.B., Zhang, Z.H. and Guo, E.C. 1995. Field Test of Immiscible $CO_2$ Drive in Daqing Oilfield. SPE Advanced Technology Series 5 (1): 49-55.

Zhang, Y.P., Sayegh, S.G., Luo, P. and Huang, S. 2010. Experimental Investigation of Immiscible Gas Process Performance for Medium Oil. J. Can. Pet. Technol. 49 (2): 32-39.

Zekri, A.Y., Almehaideb R.A., and Shedid S.A., Displacement Efficiency of Supercritical $CO_2$ Flooding in Tight Carbonate Rocks under Immiscible and Miscible Conditions (SPE 98911). SPE Europec/EAGE Annual Conference and Exhibition held in Vienna, Austria, 12–15 June 2006.

# APPENDIX

## Appendix A: Reservoir Fluid Composition and Calculations

| Gas composition | | | |
|---|---|---|---|
| Sample No. | Depth sampled (m) | | Layer |
| 2012-04012 | 3067.73-3130.17 | | S3 |
| Component | Content % mol | | |
| O2 | | | |
| N2 | 0.58 | | |
| C1 | 71.48 | Average molecular weight : MO | 23.68 |
| C2 | 10.80 | | |
| C3 | 9.10 | | |
| iC4 | 1.54 | | |
| nC4 | 2.70 | Relative density : RD | 0.8253 |
| iC5 | 0.67 | | |
| nC5 | 0.68 | | |
| nC6 | 0.29 | | |
| nC7 | 0.15 | | |
| nC8 | 0.09 | | |
| nC9 | | | |
| nC10 | | | |
| nC11 | | | |
| nC12 | | | |
| CO | | | |
| CO2 | 1.92 | | |

| Oil Composition | |
|---|---|
| Component | Concentration %mol |
| nC1 | / |
| nC2 | / |
| nC3 | 0.1 |
| nC4 | 0.39 |
| nC5 | 0.95 |
| nC6 | 1.76 |
| nC7 | 2.84 |
| nC8 | 3.07 |
| nC9 | 3.31 |
| nC10 | 3.32 |
| nC11 | 3.61 |
| nC12 | 3.56 |
| nC13 | 4.24 |
| nC14 | 3.87 |
| nC15 | 4.17 |
| nC16 | 3.61 |
| nC17 | 3.79 |
| nC18 | 3.4 |
| nC19 | 3.74 |
| nC20 | 3.45 |
| nC21 | 3.53 |
| nC22 | 3.33 |
| nC23 | 3.42 |
| nC24 | 3 |
| nC25 | 3.1 |
| nC26 | 2.6 |
| nC27 | 2.46 |
| nC28 | 1.91 |
| nC29 | 1.73 |
| nC30 | 1.21 |
| nC31 | 1.15 |
| nC32 | 0.77 |
| nC33 | 0.72 |
| nC34 | 0.42 |
| nC35 | 0.29 |
| nC36 | 0.24 |
| nC37 | 0.19 |
| nC38 | 0.18 |
| iC5 | 0.14 |
| iC5 | 0.65 |

**Table A.1: Gas and Oil composition and mol. fraction of the sampled Q131 light oil**

To calculate the live reservoir fluid composition, i.e. recombine the reservoir fluid, we will follow these simple steps:

**Step 1:** Determine lb moles gas produced per lb mols liquid

| | Gas | | Liquid | | mol. wt; lb/lb.mol | Weight; lb | Liquid density ; lb/cu.ft | Liquid vol.; cu.ft |
|---|---|---|---|---|---|---|---|---|
| **Component** | **mol %** | **mol fraction** | **mol %** | **mol fraction; lb.mol** | | | | |
| | | **lb.mol** | | **A** | **B** | **C=A*B** | **D** | **C/D** |
| O2 | | | | | | | | |
| N2 | 0.58 | 0.0058 | | | | | | |
| C1 | 71.48 | 0.7148 | | | | | | |
| C2 | 10.8 | 0.108 | | | | | | |
| C3 | 9.1 | 0.091 | 0.13 | 0.0013 | 44.09 | 0.057317 | 31.66 | 0.0018 |
| n & iC4 | 4.24 | 0.0424 | 0.9 | 0.009 | 58.12 | 0.52308 | 35.78 | 0.0146 |
| n & iC5 | 1.35 | 0.0135 | 2.41 | 0.0241 | 72.15 | 1.738815 | 39.16 | 0.0444 |
| nC6 | 0.29 | 0.0029 | 2.25 | 0.0225 | 86.17 | 1.938825 | 41.43 | 0.0468 |
| nC7 | 0.15 | 0.0015 | 2.88 | 0.0288 | 100.2 | 2.88576 | 42.92 | 0.0672 |
| nC8 | 0.09 | 0.0009 | 4.36 | 0.0436 | 114.2 | 4.97912 | 44.09 | 0.1129 |
| nC9 | | 0 | 3.41 | 0.0341 | 128.3 | 4.37503 | 45.02 | 0.0972 |
| nC10-38 | | 0 | 83.66 | 0.8366 | 317.34 | 265.486644 | 70 | 3.7927 |
| CO2 | 1.92 | 0.0192 | | | | | | |
| **Total** | **100** | **1** | **100** | **1** | | **281.984591** | | **4.1776** |

$$\text{Density of Liquid } = \frac{281.98459}{4.1776} = 67.4985\, lb/cu.ft * 5.615\, stb/cuft = 379.004\, lb/cu.ft$$

$$n_o = \frac{379.004}{281.985} = 1.344 \ lbmol$$

$$n_g = \frac{533.425}{379.4} = 1.4075 \ lbmol$$

The lb moles gas produced per lb mols liquid: $ng/nl = \frac{1.4075}{1.344} = 1.047\, lbmo\lg as/lbmolliqui\ d$

**Step 2:** Recombination of Gas and Liquid with the ratio 1.047 lbmol gas/lbmol liquid:

| Component | Mol fraction | Mol fraction | ng/nl | Res. Fluid | Comp. Res. Fluid |
|---|---|---|---|---|---|
| | **lb.mol** | **lb.mol** | **1.047** | | **mol. Fraction** |
| | **y** | **x** | **1.047y** | **1.047y+x** | |
| | **Gas** | **Oil** | | | |
| **$O_2$** | ~ | ~ | ~ | ~ | ~ |
| **$N_2$** | 0.0058 | | 0.006 | 0.006 | **0.003** |
| **$C_1$** | 0.7148 | | 0.748 | 0.748 | **0.366** |
| **$C_2$** | 0.108 | | 0.113 | 0.113 | **0.055** |
| **$C_3$** | 0.091 | 0.0013 | 0.095 | 0.097 | **0.047** |
| **n & $iC_4$** | 0.0424 | 0.009 | 0.044 | 0.053 | **0.026** |
| **n & $iC_5$** | 0.0135 | 0.0241 | 0.014 | 0.038 | **0.019** |
| **$nC_6$** | 0.0029 | 0.0225 | 0.003 | 0.026 | **0.012** |
| **$nC_7$** | 0.0015 | 0.0288 | 0.002 | 0.030 | **0.015** |
| **$nC_8$** | 0.0009 | 0.0436 | 0.001 | 0.045 | **0.022** |
| **$nC_9$** | | 0.0341 | 0.000 | 0.034 | **0.017** |
| **nC10-38** | | 0.8366 | 0.000 | 0.837 | **0.409** |
| **$CO_2$** | 0.0192 | | 0.020 | 0.020 | **0.010** |
| **Total** | 1 | 1 | 1.047 | 2.047 | **1.000** |

**Table A.2: The recombined reservoir fluid composition used in the study**

## Appendix B: Volume Calculation of One Ton $CO_2$ to Cubic Meters

One ton = 1000kg
One cubic meter = 1000liters
One mole $CO_2$ = 44.0g ($CO_2$ = 12.0g + 32.0g = 44.0g)
One ton contains 22730 moles of $CO_2$ (1,000,000g / 44.0g/mole)
One mole is 24.47L (Boyle's law at 25°C and 1 atmosphere pressure)
Volume of one ton $CO_2$ = 22730moles × 24.47L/mole = 556200L = 556.2m³
***Therefore, One ton of $CO_2$ occupies 556.2m³ of volume***

## Appendix C: Simulation Results for Air Injection using 100000m$^3$/day

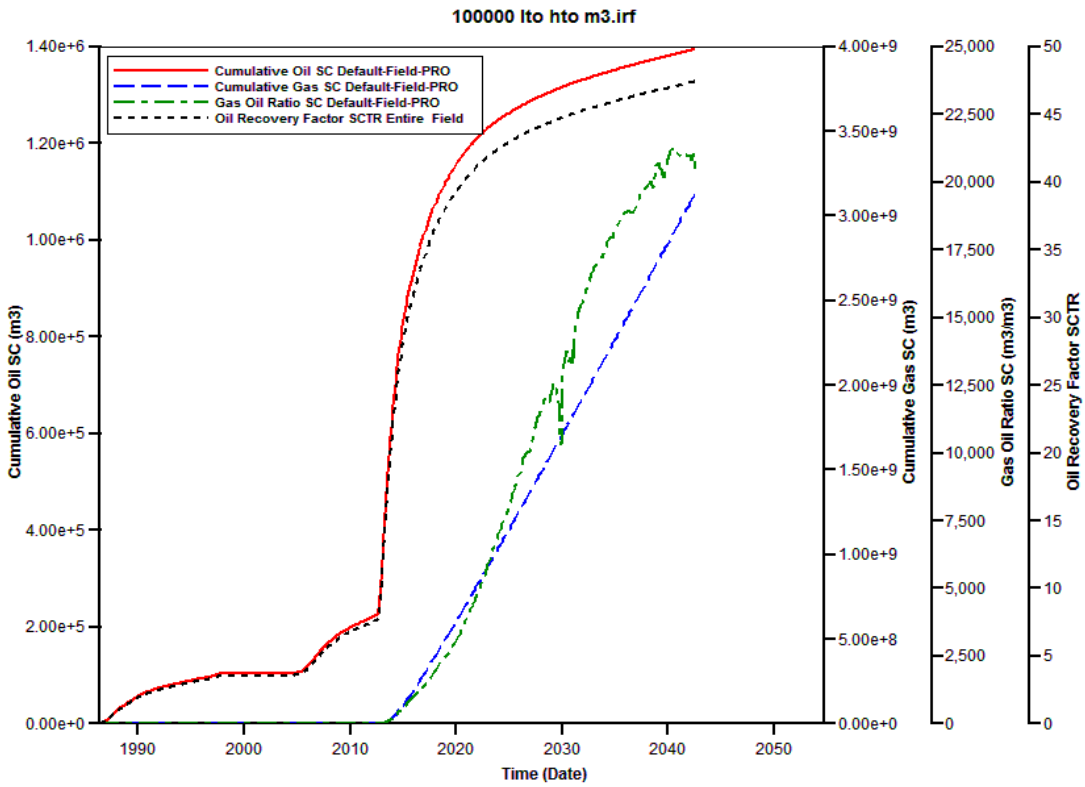


**Fig. C-1: Cumulative oil produced, Cum. gas produced, GOR and Oil recovery factor of 100000m$^3$ of air injection**

## Appendix D: Additional Notes on $CO_2$ Injection for IOR: Economics Evaluation

Implementing a $CO_2$-EOR project is a capital-intensive undertaking, even though generally the single largest project expense is the purchase of $CO_2$. Total $CO_2$ costs (both purchase price and recycle costs) can amount to 25% to 50% of the cost per barrel of oil produced. As such, operators have historically strived to optimize and reduce the cost of its purchase and injection wherever possible. However, $CO_2$ costs are not the only costs affecting the economics of $CO_2$-EOR projects. Up front expenditures also include mechanical integrity reviews of well bores and surface production facilities; pressure testing casing and replacing old tubing; installing new wellheads, flow lines, as well as addressing any potential local environmental concerns. In addition, large $CO_2$ separation facilities must be built to separate, recycle, and compress $CO_2$ recovered from produced oil for subsequent reinjection. New injection and production wells (to reduce pattern spacing) may need to also be drilled, and $CO_2$ (and possibly water) distribution lines will need to be installed. Once injection begins, it can be a number

of months before sufficient oil field pressure is reached and oil production can be realized (Taber et al., 1997a and b).

However, these costs are comparable to conducting secondary oil recovery operations. In geologically and geographically favorable settings, and the cost increase specific to $CO_2$-EOR operations would be relatively modest, especially relative to the total costs of the full CCS stream from capture to storage. Importantly, when the $CO_2$ flood is started while secondary oil recovery operations are still underway, there could be the opportunity of sharing some field operating costs and utilizing water injection wells for $CO_2$ injection, reducing capital costs. Moreover, incremental development costs associated with $CO_2$-EOR in an existing field would be substantially less than in a new development.

The key factors influencing the various categories of costs for a $CO_2$-EOR project are summarized below (Taber et al., 1997b)

1. Well Drilling and Completion. New wells may need to be drilled to configure a $CO_2$-EOR project into an injection/production pattern amenable for $CO_2$-EOR production. Well drilling and completion costs are generally a function of location and the depth of the producing formations.
2. Lease Equipment for New Producing Wells. The costs for equipping new production wells consists of a fixed costs for common items, such as free water knock-out, water disposal and electrification, and a variable cost component to capture depth-related costs such as pumping equipment.
3. Lease Equipment for New Injection Wells. The costs associated with equipping new $CO_2$ injection wells include gathering lines, a header, electrical service, and a water pumping system. These costs also include a fixed cost component and a depth-related cost component, which varies based on surface pressure requirements.
4. Converting Existing Production Wells into Injection Wells. To implement a $CO_2$-EOR project, it is generally necessary to convert some existing oil production wells into $CO_2$ and water injection wells, which requires replacing the tubing string and adding distribution lines and headers. For existing fields, it can be assumed that all surface equipment necessary for water injection are already in place on the lease. Again, existing well conversion costs include a fixed cost component and a depth-related cost component, which varies based on the required surface pressure and tubing length.
5. Annual operations and maintenance (O&M) including Periodic Well Workovers. The annual O&M costs associated with $CO_2$-EOR projects include both normal oil field O&M costs along with additional costs specific to the application of $CO_2$-EOR. To account for the O&M cost differences between traditional water flooding and $CO_2$-EOR, two adjustments are usually considered. First, workover costs are, on average, about double for $CO_2$-EOR because of the need for more frequent

remedial well work. Second, traditional lifting costs should be subtracted from annual waterflood O&M costs to allow for the more rigorous accounting of liquid lifting volumes and costs for $CO_2$-EOR.

6. $CO_2$ Recycle Plant Investment. Operation of $CO_2$-EOR requires a recycling plant to capture, separate, and re-inject the produced $CO_2$. The size of the recycle plant is based on peak $CO_2$ production and recycling requirements. The O&M costs of $CO_2$ recycling are a function of energy costs.

7. Fluid Lifting for $CO_2$-EOR. Liquid (oil and water) lifting costs are calculated based on total liquid production. This cost includes liquid lifting, transportation and re-injection.

8. $CO_2$ Distribution. The $CO_2$ distribution system is similar to the gathering systems used for natural gas. A distribution "hub" is constructed with smaller pipelines delivering purchased $CO_2$ to the project site. The distribution pipeline cost is dependent on the injection requirements for the project, and the distance of the $CO_2$-EOR project from the $CO_2$ source.

In today's market, with oil prices in excess of $100 per barrel, delivered $CO_2$ costs where some $CO_2$-EOR projects remain economically viable could be as high as $70 to $90 per metric ton including transportation cost or construction costs of pipelines from the $CO_2$ source to the oil-field, and the separation costs. On the other hand, under a market where $CO_2$ emission reductions have value, "gas-on-gas" competition for new $CO_2$ sources entering the market may put downward pressure on $CO_2$ prices. If increasingly strict requirements are implemented for limiting $CO_2$ emissions, particularly for new energy sources, producers/emitters of $CO_2$ may become increasingly willing to provide $CO_2$ supplies to $CO_2$-EOR projects at competitive or even lower delivered $CO_2$ costs. Assuming that such policies serve to reduce prices for delivered $CO_2$ to merely the cost of compression and transportation, costs of $CO_2$ on the order of $15 per metric ton are conceivable.

The causes of less than optimum performance of $CO_2$-EOR/IOR include the following:

1. Low injection volumes. Due to the high cost of $CO_2$ relative to oil prices and the inability to control the $CO_2$ flow through the reservoir, if injected volumes were limited, sweep efficiency will be restricted.
2. Poor sweep efficiency. Gravity override, viscous fingering and channeling in heterogeneous reservoirs can lead to limited contact with the residual oil.
3. Poor displacement efficiency with only a small portion of the residual oil mobilized often due to lack of effective miscibility.
4. Lack of $CO_2$ contact with the residual oil due to inefficient targeting, bypassing more highly saturated layers.
5. Poor operation management and control due to lack of real time process and performance data.

Culled from *Economic impacts of $CO_2$-enhanced oil recovery for Scotland,* Final report for Scottish Enterprise, 2012. Led by Element Energy Limited and Heriot Watt University.

# ACADEMIC ACHIEVEMENTS DURING THE PERIOD OF MASTER'S DEGREE STUDY

[1] Liang Zhang, Justin Ezekiel, Dexiang Li, Jingjing Pei, Shaoran Ren. Potential Assessment of $CO_2$ Injection for Heat Mining and Geological Storage in Geothermal Reservoirs of China [J]. Applied Energy, Volume 122, 1 June 2014, Pages 237-246, ISSN 0306-2619.

http://dx.doi.org/10.1016/j.apenergy.2014.02.027.

[2] Jianhua Ren, Liang Zhang, Justin Ezekiel, Shaoran Ren, Shangzhi Meng, Reservoir Characteristics and Productivity Analysis of Tight Sand Gas in Upper Paleozoic Ordos Basin China [J]. Journal of Natural Gas Science and Engineering, Volume 19, July 2014, Pages 244-250, ISSN 1875-5100. http://dx.doi.org/10.1016/j.jngse.2014.05.014.

[3] Ezekiel, J., Wang, Y., Liu, Y., Zhang, L., Deng, J., & Ren, S. (2014, November 12). Case Study of Air Injection IOR Process for a Low Permeability Light Oil Reservoir in Eastern China (English and Russian). Society of Petroleum Engineers Technical Conference Paper (SPE Paper 172292). DOI 10.2118/172292-MS.

[4] Liang Zhang, Dexiang Li, Justin Ezekiel, et al. $CO_2$ Geological Storage into a lateral aquifer of an Offshore Gas Field in the South China Sea: Storage Safety and Project Design [J]. Frontiers of Earth Science. 2014. DOI 10.1007/s11707-014-0462-7. (Accepted for publication but not yet published).

[5] Justin Ezekiel, Liang Zhang, Shaoran Ren. Displacement Mechanisms of Air Injection for IOR in Low Permeability Light Oil Reservoirs [J]. International Journal of Oil, Gas and Coal Technology. (Still under review).

# ACKNOWLEDGEMENTS

Support for this work was provided by Petrochina, the Changjiang Scholar and Innovation Team Program (IRT1086 and IRT1294). Also special thanks to China Scholarship Council and Bilateral Education Agreement (BEA) for funding my Master's degree program in the China University of Petroleum (Huadong).

I would like to thank my advisor Prof. Ren Shaoran first and foremost for accepting me as his student and always have the time and patience in his daily busy schedule to guide me in the course of my studies and while writing this thesis. He is always kind to me and treated me nicely, never complained about my too many questions to him about whatever I don't understand and needed clarifications. He also helped me to be able to finish my thesis on time, publish some academic technical papers in good journals, and above all helped me in different ways that made it possible for me to be able to finish my Master's degree program 6 months earlier than normal time. I would also I would also like to thank Prof. Zhang Zhiying, who was always there to listen to my academic problems, and did her very best to always assist me in any way possible. She also taught me some courses which really made me easily understand Petroleum reservoir engineering. In fact, she is like my mother (younger version though) in China. I would thank Dr. Liang Zhang, who assisted my advisor to see that my study here was less stressful and tried to assist in diverse ways so that I can finish the program on time. Also thanks to my officemates and other colleagues, whose friendship, useful comments on my work, and helpful advices saw me through in some tough days in China. Also I will not forget all the teachers that taught me and helped me grasp the rudimentary and detailed understanding of reservoir engineering during my years in China.

On a personal level there are many people to thank: my classmates and foreign and Chinese friends, without u guys, life would be a lot less interesting. I want to specially thank a special person to me who helped me to adjust to living in China and showed me love, dear Cristal thank you very much for everything, even for helping me with the formatting of this thesis.

My final acknowledgements are to the very important people in my life. My parents, Victor and Joy, my siblings Victor (Jnr.), Precious and Favor, and my Uncle P, who taught me that hard work will get you wherever you want to go in life. Without my parents support I wouldn't be where I am today.